1986

Some reactions of norcaranylidene with polar solvents

I-Shan Chu
Iowa State University

INFORMATION TO USERS

This reproduction was made from a copy of a manuscript sent to us for publication and microfilming. While the most advanced technology has been used to photograph and reproduce this manuscript, the quality of the reproduction is heavily dependent upon the quality of the material submitted. Pages in any manuscript may have indistinct print. In all cases the best available copy has been filmed.

The following explanation of techniques is provided to help clarify notations which may appear on this reproduction.

1. Manuscripts may not always be complete. When it is not possible to obtain missing pages, a note appears to indicate this.

2. When copyrighted materials are removed from the manuscript, a note appears to indicate this.

3. Oversize materials (maps, drawings, and charts) are photographed by sectioning the original, beginning at the upper left hand corner and continuing from left to right in equal sections with small overlaps. Each oversize page is also filmed as one exposure and is available, for an additional charge, as a standard 35mm slide or in black and white paper format.*

4. Most photographs reproduce acceptably on positive microfilm or microfiche but lack clarity on xerographic copies made from the microfilm. For an additional charge, all photographs are available in black and white standard 35mm slide format.*

***For more information about black and white slides or enlarged paper reproductions, please contact the Dissertations Customer Services Department.**

U·M·I Dissertation Information Service

University Microfilms International
A Bell & Howell Information Company
300 N. Zeeb Road, Ann Arbor, Michigan 48106

Chu, I-Shan

SOME REACTIONS OF NORCARANYLIDENE WITH POLAR SOLVENTS

Iowa State University PH.D. 1986

Some reactions of norcaranylidene with polar solvents

by

I-Shan Chu

A Dissertation Submitted to the

Graduate Faculty in Partial Fulfillment of the

Requirements for the Degree of

DOCTOR OF PHILOSOPHY

Department: Chemistry
Major: Organic Chemistry

Approved:

Signature was redacted for privacy.

In Charge of Major Work

Signature was redacted for privacy.

For the Major Department

Signature was redacted for privacy.

For the Graduate College

Iowa State University
Ames, Iowa

1986

TABLE OF CONTENTS

ABSTRACT

As part of our efforts to understand the chemistry of cyclopropylidenes in solution, the reactions of norcaranylidene in alcohols and nitriles have been studied.

In alcohols (methanol or t-butanol), the partitioning of norcaranylidene between intramolecular insertion and intermolecular reaction with alcohols is a function of alcohol concentration. In methanol, an ylide intermediate is transformed into the product ether in a stepwise manner. However, in t-butanol, the corresponding ylide intermediate releases the t-butanol molecule to give the intramolecular insertion product, in competition with protonation to form the ether product.

Methanol was found to react with norcaranylidene 2.5 times faster than t-butanol, irrespective of the total alcohol concentrations. A reasonable interpretation of the activation parameters is that norcaranylidene is solvated preferentially by t-butanol monomers at "high" alcohol concentration, but is solvated essentially equally by either methanol or t-butanol at "low" alcohol concentration. Thus at either "low" or "high" alcohol concentrations, the "starting carbene" is a single, albeit differently, solvated species.

When nitriles are present in methanol, the nitrile ylide intermediate from the reaction of norcaranylidene with nitriles reacts with methanol to yield a mixture of epimeric methanol insertion products. In acrylonitrile, the ylide is also captured by another molecule of acrylonitrile

to give [3 + 2] cycloadduct. And dipolarophiles also capture the diazo-precursor to norcaranylidene in acrylonitrile and methacrylonitrile.

Pyrolysis of anti-7-bromo-syn-7-trimethylstannylbicyclo[4.1.0]heptane also generates norcaranylidene. This allows the high temperature study of the kinetic deuterium isotope effects for the reaction of norcaranylidene with methanol and t-butanol. Mechanisms to account for the isotope effects at low (diazo-precursor) and high (tin bromide precursor) temperatures are discussed. Two changes in mechanism are seen as the temperature is changed from -78° to 160°C.

CHAPTER I. TEMPERATURE AND SOLVENT EFFECTS ON THE REACTIONS OF NORCARANYLIDENE IN METHANOL AND t-BUTANOL

Introduction

The insertion reactions of carbenes into the O-H bonds of alcohols have received considerable attention (1, 2). While a greater number of mechanisms are possible in principle, three mechanisms have been chiefly discussed for this reaction (3). The first mechanism [equation (1)], which we shall refer to as the ylide mechanism, involves attack by the carbene, behaving as an electrophile, on the oxygen atom of the alcohol. Then the ylide is transformed into the product ether in a subsequent step (4). The second mechanism [equation (2)], which we shall refer to as the carbonium ion mechanism, suggests that proton transfer from the alcohol to the carbene is the controlling step in ether formation (5). The third mechanism to be considered is direct insertion [equation (3)]. No intermediates are involved, and the transition state is represented by (I) in equation (3).

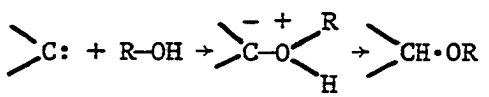

(1)

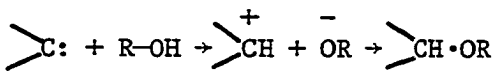

(2)

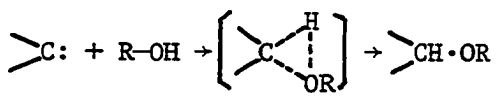

(3)

(I)

In 1969, Bethell et al. (6) demonstrated that the reaction of diphenylmethylene with water to form diphenylmethanol occurred by way of an ylide [equation (4)]. But the available evidence did not enable a

$$Ph_2C: \xrightarrow{H_2O} Ph_2\overset{-}{C}\cdot\overset{+}{O}H_2 \rightarrow Ph_2CH\cdot OH \qquad (4)$$

firm conclusion concerning the reaction mechanism for ether formation at that time. Later, in 1971, they again studied the thermal decomposition of diphenyldiazomethane in acetonitrile containing methyl and t-butyl alcohols (4). Evidence had already been presented that the reactivity of alcohols towards diarylmethylenes showed a rough parallelism with the acidity of the alcoholic hydroxyl group. Thus towards 4.4'-disubstituted diphenylmethylenes, methyl alcohol was found to be 3-9 times more reactive than t-butyl alcohol. The relative reactivities are given in Table 1. In accordance with the kinetic hydrogen isotope effects, they concluded that the ylide mechanism was the most likely route for the formation of ether in these experiments.

Although Bethell observed first-order kinetics for thermal decomposition of diaryldiazomethanes in acetonitrile and alcohols, Griller et al. (7) reported nonlinear plots (Figure 1) when $k_{obs.}$ was plotted against [alcohol] in the reactions of carbenes 1a and 1b with methanol and t-butanol. For methanol, the curvature in the kinetic plots implied that this substrate was in some way becoming disproportionately more reactive as its concentration was increased, while, for t-butyl alcohol, the opposite was true.

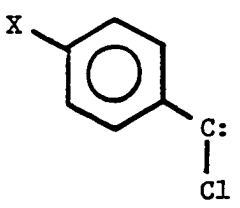

1a, X = H

1b, X = CH_3O

Table 1. Relative reactivities of methyl and t-butyl alcohols towards diarylmethylenes, $(p\text{-}X\cdot C_6H_4)_2C:$, in acetonitrile at 85°C from competition experiments

Substnt. X	$[Ar_2N_2]_0$ (M)	$\frac{[MeOH]}{[t\text{-}BuOH]}$	$\frac{[Ar_2CHOME]^a}{[Ar_2CHOBU]}$	$\frac{k_{MeOH}}{k_{t\text{-}BuOH}}$
H	0.049	0.374	3.05 ± 0.16	8.2 ± 0.4
H	0.132	0.387	3.06 ± 0.16	7.9 ± 0.4
Me	0.052	0.554	3.16 ± 0.10	5.6 ± 0.1
Me	0.052	0.554	3.33 ± 0.20	5.9 ± 0.4
MeO	0.049	0.554	1.57 ± 0.04	2.9 ± 0.1
Cl	0.010	0.127	1.19	9.4
Cl	0.010	0.088	0.795	9.0

[a]Analysis by NMR.

The interpretation offered by Griller was that the hydrogen-bonded oligomers of methanol, the concentration of which increased as the methanol concentration was increased, were substantially more reactive than methanol monomer towards carbenes. For t-butyl alcohol, the converse was proposed and was explained with the suggestion that the t-butyl groups sterically protected the hydrogen-bonded hydroxyl groups in the oligomers from attack.

When $k_{obs.}$ was plotted against the total concentration of methanol oligomers or the free monomer concentration of t-butyl alcohol, plots of excellent linearity were obtained. Thus to a good approximation, the reactions of 1a and 1b with methanol were first order with respect to methanol oligomers. By contrast, the reactions were first order with respect to t-butanol monomer. The rate constants for the reactions of 1a

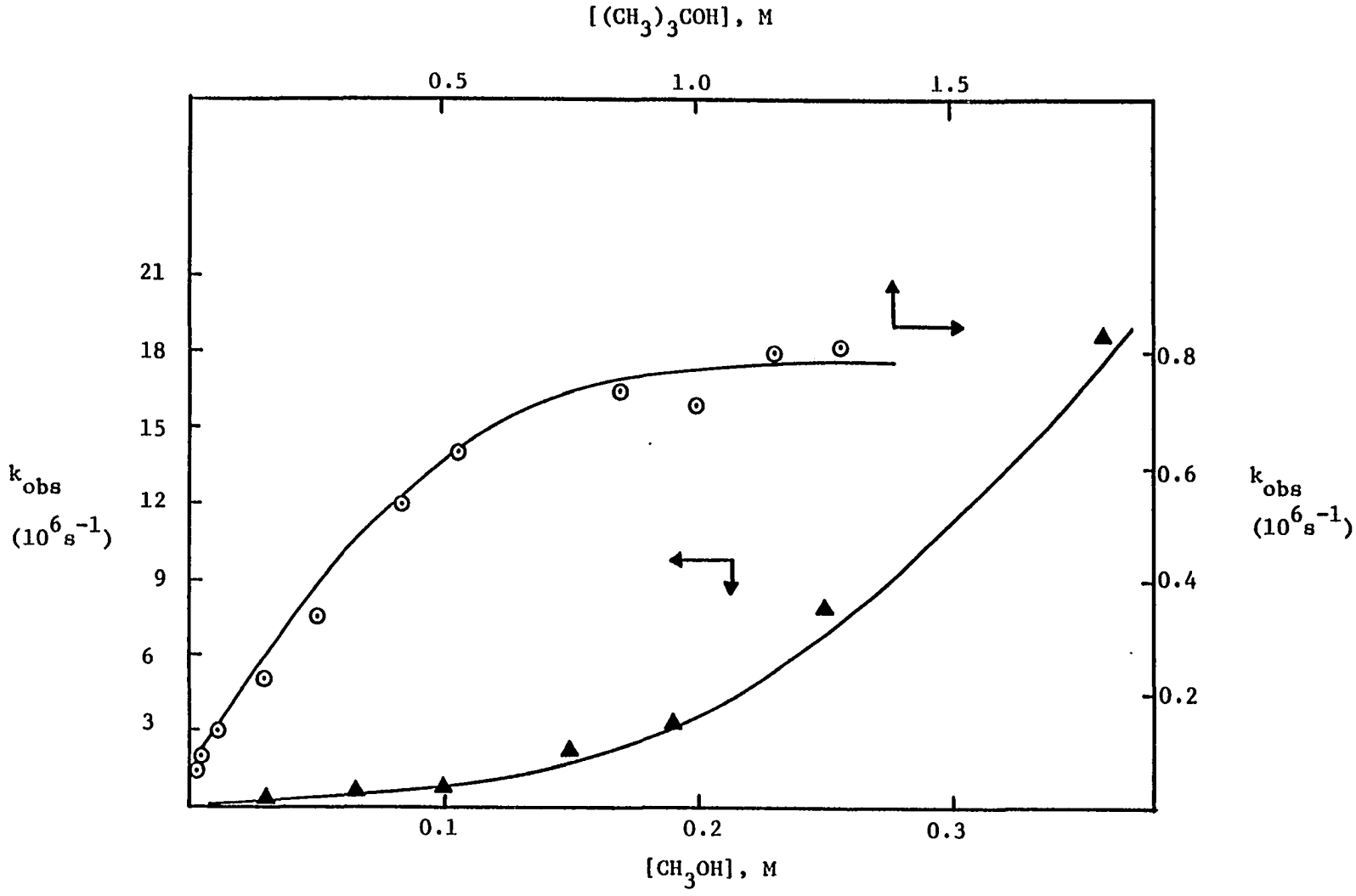

Figure 1. Quenching of p-anisylchlorocarbene by alcohols at 300K

and 1b with methanol oligomers were (2.9 ± 0.2) x 10^9 and (4.3 ± 0.4) x 10^9 $M^{-1}s^{-1}$ in isooctane, which implied the reaction was close to diffusion-controlled. The corresponding rate constant for the reaction with t-butyl alcohol monomer was (2.52 ± 0.15) x 10^6 $M^{-1}s^{-1}$. These results indicated a much stronger discrimination in the reactivities of 1a and 1b towards various alcohols ($k_{MeOH}/k_{t\text{-}BuOH} \simeq 1000$) than Bethell's observations.

Although it has long been held that ether formation from carbenes and alcohols is characteristic of carbenes in their singlet state (4, 8, 9), the suggestion that triplet carbenes may react with alcohols directly to give ethers has recently been challenged (10). However, Zupancic et al. (11) studied the kinetic and product isotope effects for the trapping of fluorenylidene 2 with nucleophiles, and concluded that these reactions were not a one-step process. They directly measured the rate constants in protio and deuterated nucleophiles to get the kinetic isotope effects. If there were an intermediate between the carbene and the eventual trap product, then the kinetic isotope effect need not be identical to the product isotope effect. The data for the series of nucleophiles examined are summarized in Table 2.

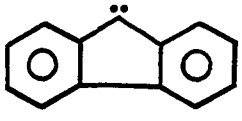

2

For both t-butylamine and t-butylthiol, inverse secondary kinetic isotope effects were observed, as were primary product isotope effects. These results meant that in each case there was a product-determining intermediate formed after the rate-determining step in the reaction sequence. For alcohols, it was possible that the large kinetic isotope

Table 2. Data for reaction of fluorenylidene with heteroatom nucleophiles

Nucleophile	Concentration (M)	$K_{nuc}^{obs}(M^{-1}s^{-1})$	K_{nuc}^{H}/K_{nuc}^{D}	P_H/P_D
CH_3OH	0.05 (0.5)	8.6×10^8	1.8 ± 0.04	2.4 ± 0.1 (1.4)
CH_3OD	0.1 (0.1)	4.7×10^8		
$(CH_3)_3COH$	0.4	1.6×10^8	3.8 ± 0.5	3.5 ± 0.3
$(CH_3)_3COD$	1.6	0.42×10^8		
$(CH_3)_3CNH_2$	3.5	6.3×10^7	0.94 ± 0.2	2.5 ± 0.3
$(CH_3)_3CND_2$	3.8	7.0×10^7		
$(CH_3)_3CSH$	0.56	1.1×10^9	0.92 ± 0.13	2.3 ± 0.2
$(CH_3)_3CSD$	0.55	1.2×10^9		
CH_3OH	0.1			
CH_3OD	0.4	---		2.4 ± 0.2
$(CH_3)_3COH$	0.4			
$(CH_3)_3COD$	1.6			

effects might arise from changes in solvation or association equilibria of the alcohol (amines and thiols are known to be less associated than alcohols). To test this possibility, the effects of adding methanol to t-butanol on the product isotope effect for ether formation from fluorenylidene and t-butanol were examined. The reduction in the t-butanol isotope effect (P_H/P_D = 2.4) indicated that there must be some "communication" from one alcohol to another in the reaction sequence.

Moreover, they also examined the ratio of t-butylether to methylether products at a constant ratio of methyl and t-butyl alcohol, but over a

Table 3. Competition reaction between methyl and t-butyl alcohols

MeOH (M)	t-BuOH (M)	$P_{MeOH}/P_{t\text{-}BuOH}$
0.08	0.08	5.6
0.1	0.1	5.3
0.2	0.2	4.2
0.5	0.5	2.8
1.0	1.0	2.5

range of total alcohol concentration. The results indicated the ratio changed with total alcohol concentration and reached a constant value when the concentration was greater than 0.5 M (Table 3). These findings also ruled out a simple one-step mechanism and required the reversible formation of an intermediate in the reaction sequence.

Liu and Subramanian (12) have reported the termolecular trapping of singlet benzylchlorocarbene 3 by methanol. When 3 was generated photochemically (13), 4 and 5 were afforded by two competing reactions (intramolecular 1,2 shift and reaction with methanol). The results could be interpreted in terms of a kinetic model in which a complex is formed reversibly by the reaction of the carbene with two methanol molecules contained in the oligomer chain, as shown in Scheme I. The Arrhenius relationship led to $E_i - E_t = 10.9 \pm 0.3$ Kcal/mol.

Tomioka et al. (14) then studied temperature and matrix effects on competitive intermolecular and intramolecular reactions of 3 in ethanol (Scheme II). The irradiations were carried out at various temperatures ranging from 0° to -196°C, and the results indicated that reaction patterns

Scheme I

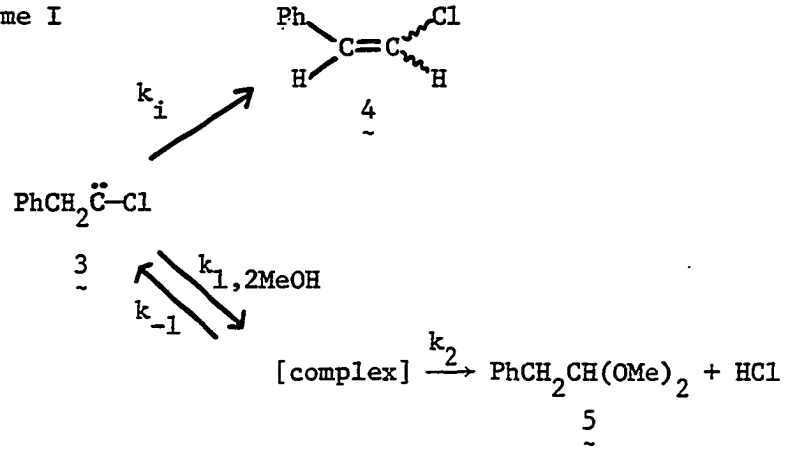

Scheme II

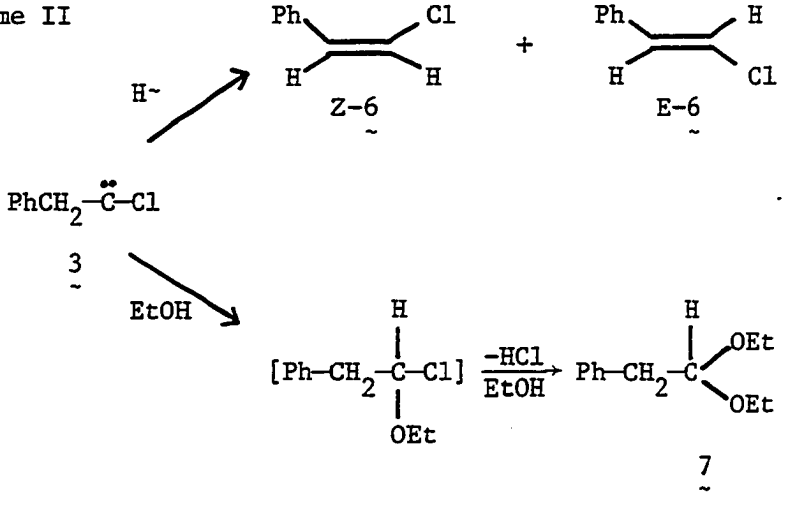

were markedly influenced by temperature. The yields of 6 decreased as reaction temperatures were lowered (0° → -110°C). Analysis of the 6/7 ratios gave a ΔE_a between 1,2-H shift and O-H insertion of 0.7 Kcal/mol. However, the temperature-dependent trends reversed once the environment became solid (-150° ∿ -196°C). In the matrix (8, 15-17), the carbene was trapped in an EtOH framework, and hence mobility was severely restricted. Thus, intermolecular insertion was reduced relative to intramolecular rearrangement.

Eisenthal et al. (18) have recently demonstrated the absolute reactivity of diphenylmethylene (DPM) towards a series of alcohols from time-resolved and steady-state studies. Photolysis of diphenyldiazomethane in the presence of equimolar methanol and one of the other alcohols led to two major products, 8 and 9 [equation (5)]. The ratios of 8 : 9, which were assumed to be equal to the relative rates of reaction for the alcohols, are listed in Table 4 for R = H, CH_3.

$$Ph_2CN_2 + CH_3OH + RC(CH_3)_2OH \rightarrow \underset{8}{Ph_2CHOCH_3} + \underset{9}{Ph_2CHO(CH_3)_2CR} \qquad (5)$$

It appeared that the reaction of ^{1}DPM with alcohols was very fast and was at or near the diffusion controlled rate expected for a bimolecular reaction. Furthermore, the relative rates of alcohol quenching of ^{1}DPM could be correlated with the acidity of the O-H bond of the alcohol, which was also observed by Bethell et al. (4) in their studies.

More recently, Turro et al. (19) have reported the temperature dependence of the reaction of singlet diphenylcarbene 10 with methanol and t-butanol. In both cases, non-linear plots of the ratio of the quantum yields for triplet (Q_3) and singlet (Q_1) products vs. temperature were obtained (Figure 2). And methanol and t-butanol showed essentially the same behavior in these experiments even though they were known to have very different aggregation properties (20). These results were interpreted in terms of reversible ylide formation (Scheme III). At low temperatures, the reaction rate was determined by the competition between reversion to starting materials and reaction from the intermediate ylide. These

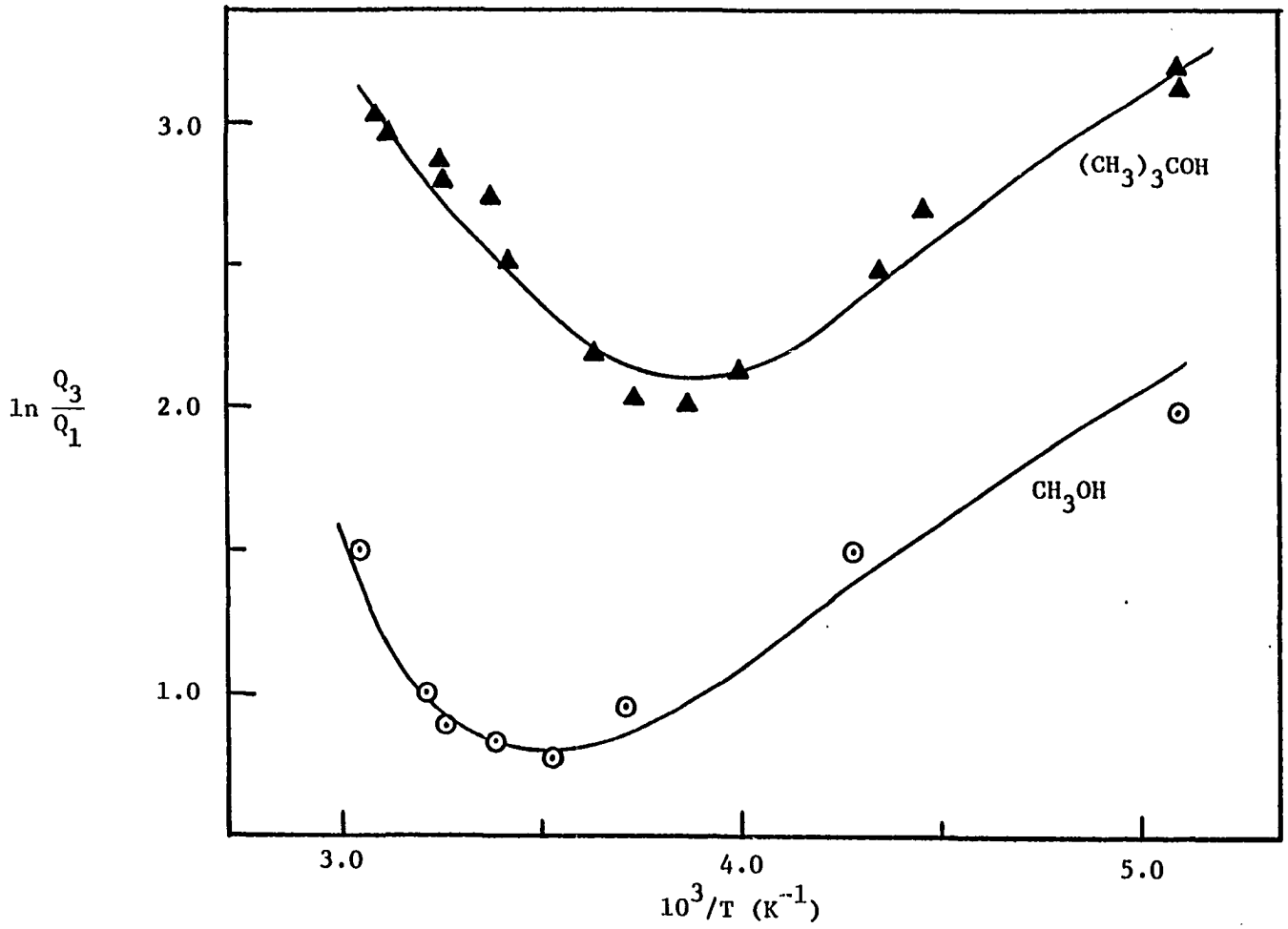

Figure 2. Plots of temperature dependence of the reaction of DPC with alcohols

Table 4. Relative yield of ether products from the photolysis of diphenyldiazomethane in N_2 saturated acetonitrile containing methanol and either isopropanol or t-butanol and relative rate values from time-resolved studies

Quencher	8/9	K, $M^{-1}s^{-1}$
Methanol	1.0	5.6×10^9
i-propanol	1.65	3.5×10^9
t-butanol	3.40	1.5×10^9

Scheme III

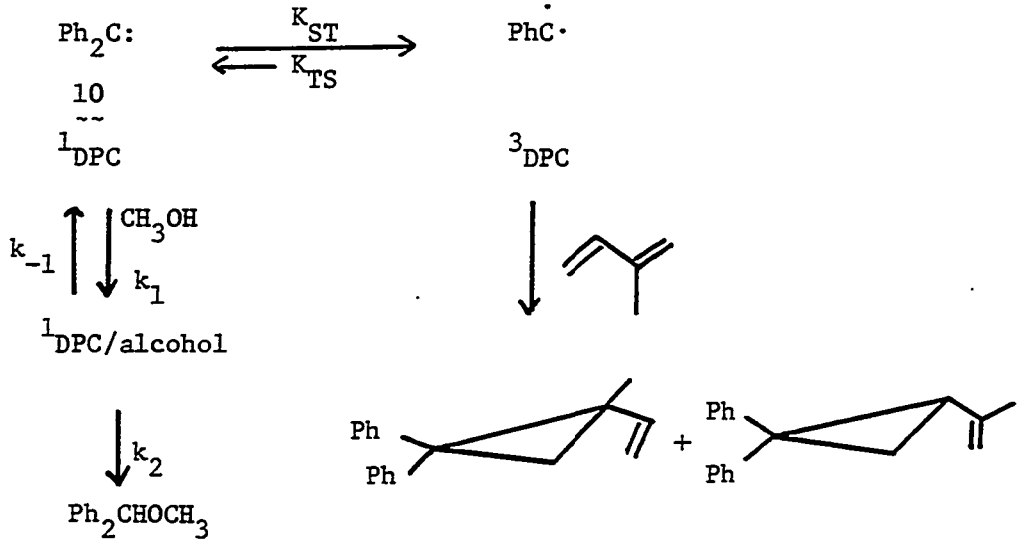

findings are similar to our previous observations for bicyclopropylidene 11 in methanol at low temperatures (Scheme IV, Table 5, and Figure 3) (21, 22). The reversible formation of 12 provided a chance for 15 to form via carbene-carbene rearrangement at low temperatures. Moreover, the primary kinetic isotope effects for 13 at low temperatures also supported reversible ylide formation in the reaction of 11 with methanol.

Table 5. Temperature effects upon 15/13 ratios

T (K)	$10^3/T$ (K^{-1})	15/13	ln 15/13
195	5.1	2.58	0.95
214	4.7	2.51	0.92
226	4.4	2.72	1.00
245	4.1	3.00	1.10
283	3.5	5.31	1.67
297	3.4	6.36	1.85
313	3.2	10.38	2.34

Scheme IV

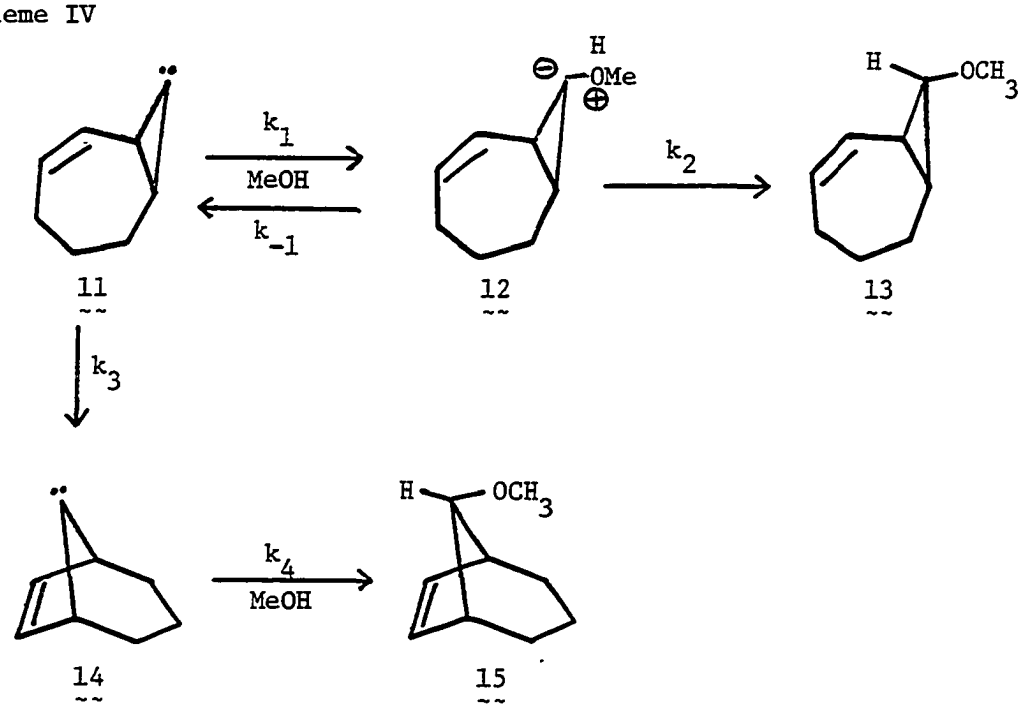

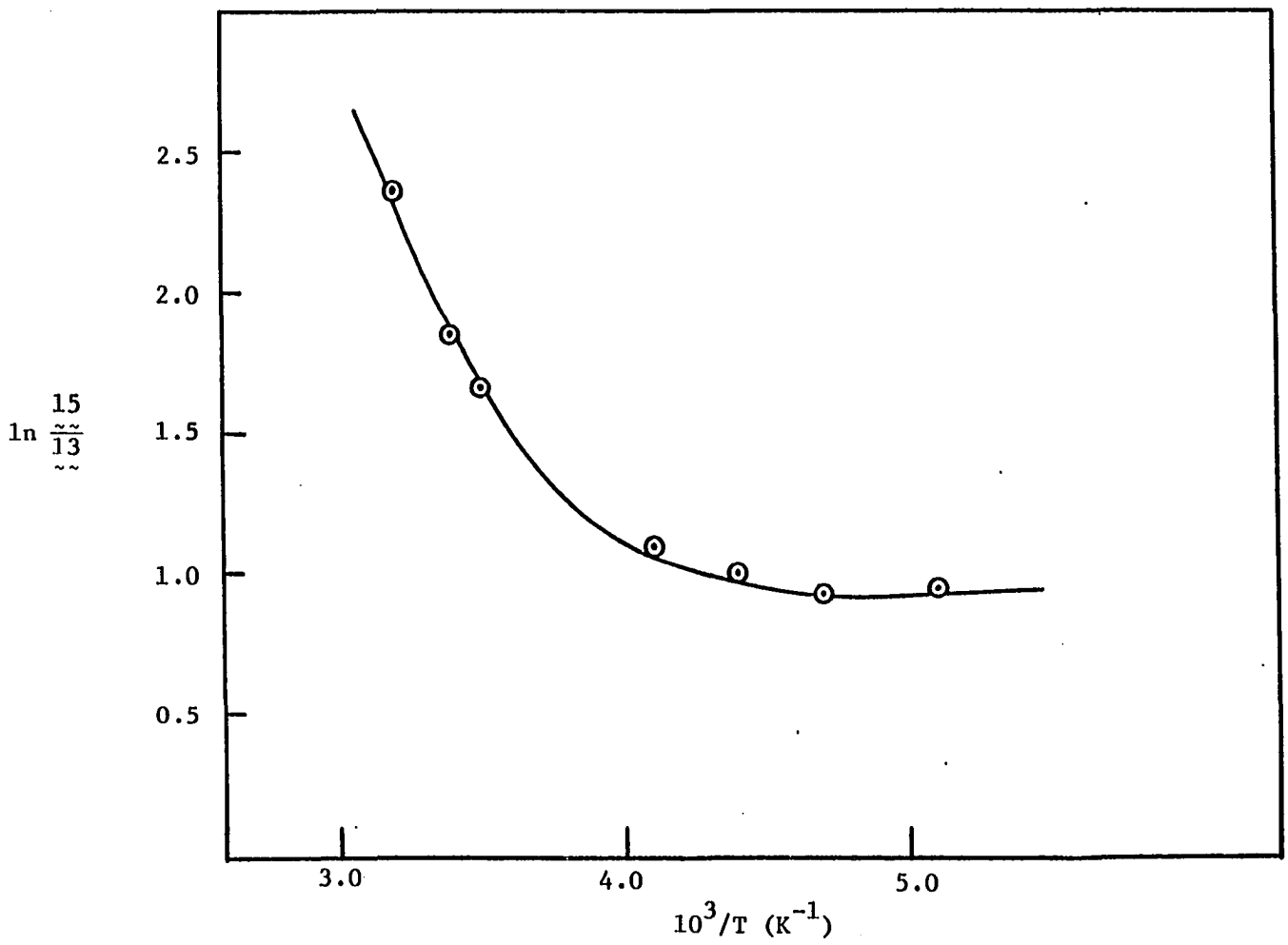

Figure 3. Plot of temperature dependence of the reaction of carbene 11 in methanol

Gilbert et al. (23) recently demonstrated the relationship between structure and the energy separation between the triplet and singlet states of diarylcarbenes. The series of carbenes diphenyl, mesityl-phenyl, mesityl-o-tolyl and dimesityl (10, 16-18) were used for kinetic and product studies. Electron paramagnetic resonance (EPR) spectra of the triplet states of these carbenes showed that increasing ortho substitution led to an expansion of the C-C-C angle (24-27). And kinetic studies indicated that this angle expansion also led to an enhanced triplet-singlet energy gap, which was consistent with theoretical calculations (28, 29). For diphenylcarbene 10 (a central C-C-C angle of 148°), the small energy gap provided small concentrations of the singlet,

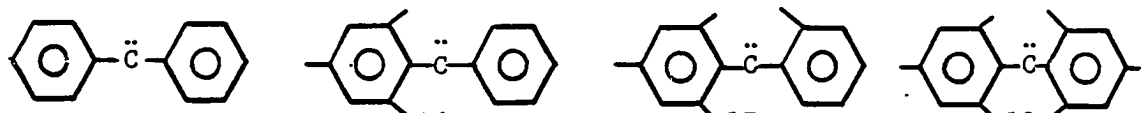

10 16 17 18

in thermal equilibrium with the triplet, the singlet was responsible for the insertion reaction into alcohols (Scheme V) (30, 31).

Scheme V

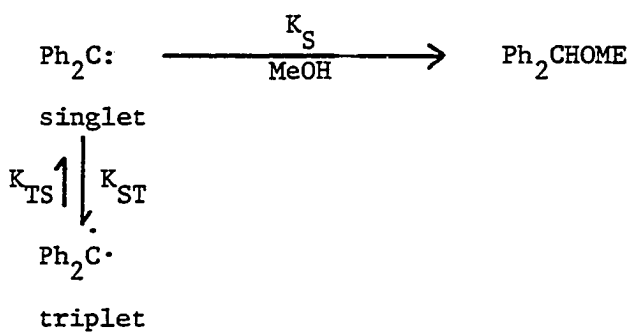

As part of our continuing efforts to understand the chemistry of bicyclopropylidenes generated from nitrosoureas 19 under basic conditions

[equation (6)], it was of interest to study the reactions of norcaranylidene (20, n = 4), in various alcohols to compare the reactivities. Kirmse and Jendralla (32) have reported that treatment of 19 (n = 4) with sodium methoxide (1M) in methanol afforded 25 and 26 in a 24:1 ratio. However,

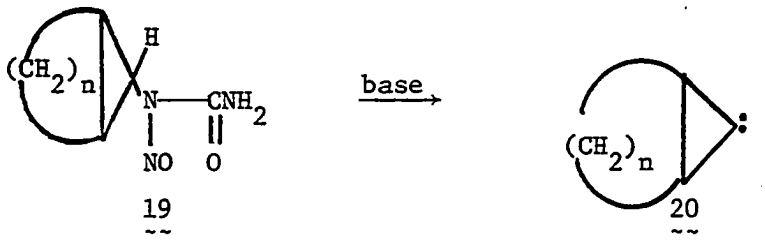

19 20 (6)

when the base concentration was lowered, the ring-opening product 27 was also formed. They proposed the mechanism shown in Scheme VI.

As noted in Scheme VI, the partitioning of 20' between intramolecular insertion and intermolecular reaction with methanol should be a function of methanol concentration at high [NaOMe] (where no 23 is formed). It should be feasible to carry out the reaction of 20' in various alcohols at different temperatures under the proper base concentrations.

Results and Discussion

Preparation of N-(7-exo-bicyclo[4.1.0]heptyl)-N-nitrosourea (19') was affected by the method of Kirmse and Jendralla (32). Reaction of 19' with NaOMe ([NaOMe]/[19'] $\geq$ 7) in methanol/benzene at room temperature afforded a mixture consisting chiefly of 25 and 26. However, when the ratio of [NaOMe]/[19'] was lowered, a significant amount of 27 was formed through a cationic ring-opening process from cation 23. Additionally, 23 gave some 25 by collapse with methanol, which increased the ratio of 25/26. (Based on Scheme VI, the ratio of 25/26 should be a constant at same

Scheme VI

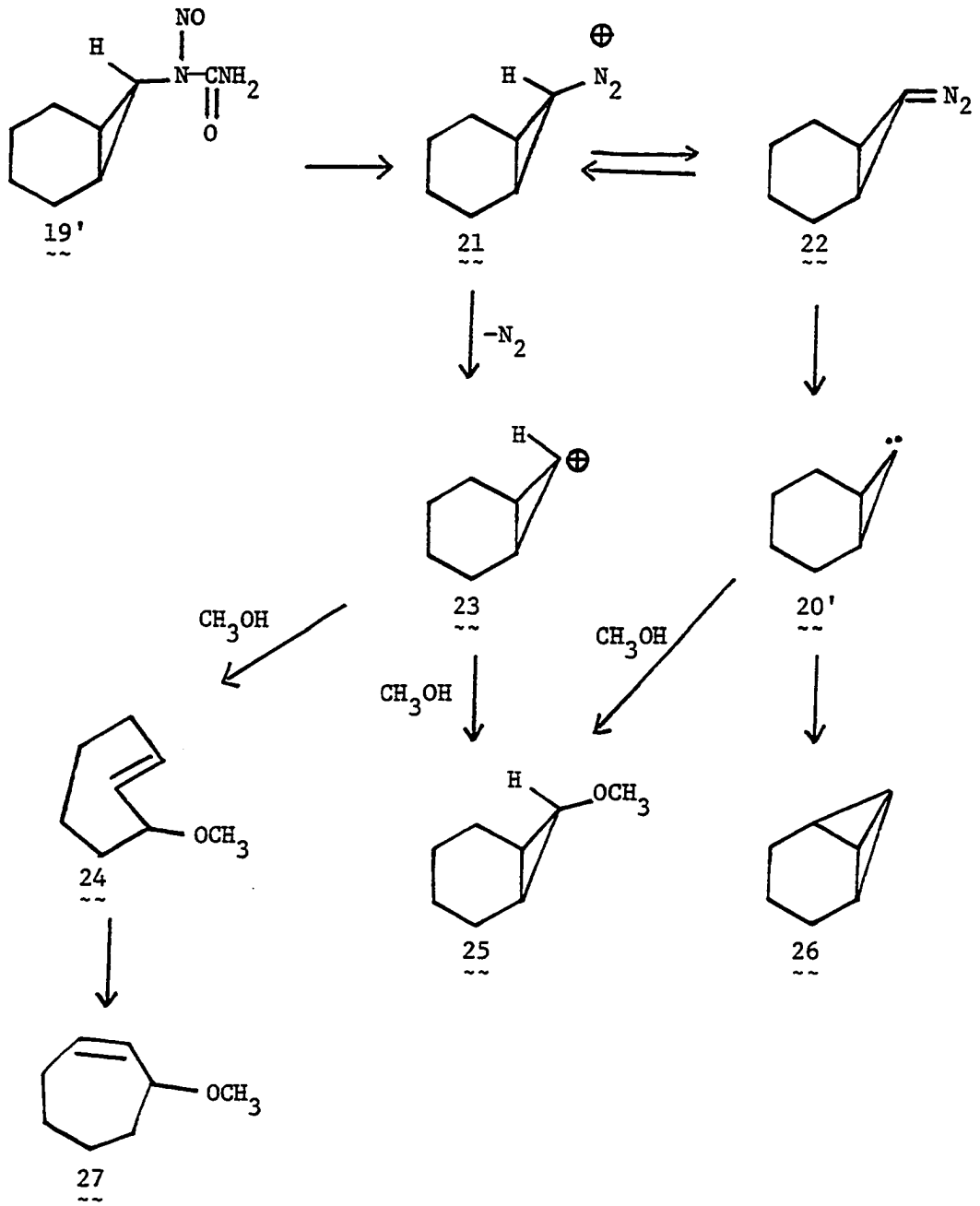
NO
H
N—CNH2
O
19'
H
⊕
N2
21
N2
22
-N2
H
⊕
23
20'
CH3OH
CH3OH
CH3OH
OCH3
24
H
OCH3
25
26
OCH3
27

[MeOH], so that some 25 must be from cation 23 by attack of MeOH as well.) Table 6 lists the product ratios at different [NaOMe]. The assignments

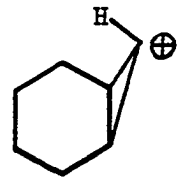

23

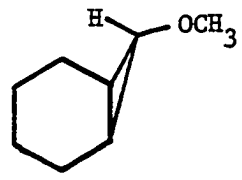

25

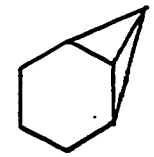

26

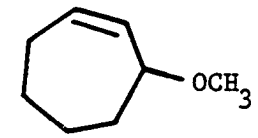

27

of 25, 26 and 27 were based on independent syntheses of these compounds, and comparison of their GC retention times.

We also examined the effect of changing the concentration of nitrosourea 19' at constant [NaOMe]; the results are shown in Table 7. The ratios of 25/26 at [NaOMe]/[19'] $\geq$ 6 were not constant. This discrepancy was suggested to be the "dilution effect" (33) of starting material employed in different experiments. Again, we found that more 25 was formed when [NaOMe]/[19'] was lowered.

Tricyclo[4.1.0.$0^{2,7}$]heptane (26) was prepared via the reaction of 7.7-dibromobicyclo[4.1.0]heptane (28) with methyl lithium in ether at room temperature; also formed were minor products 29 and 30 [equation (7)] (34-39). Compound 26 was isolated as a colorless liquid by preparative

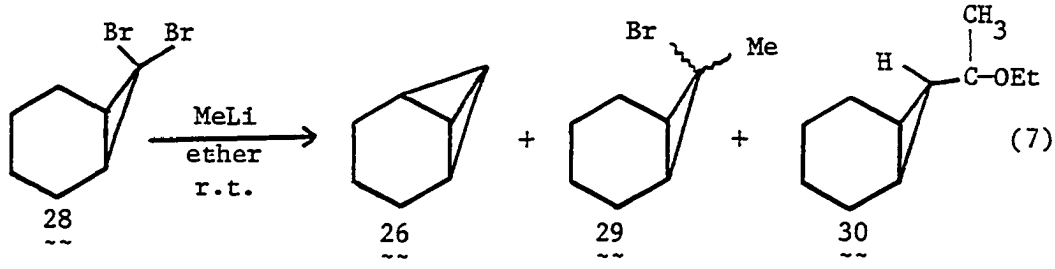

28 → 26 + 29 + 30 (7)

gas chromatography (SE-30 column, 40°C), along with small amounts of the rearranged isomer, 1.3-cycloheptadiene (40, 41). It was noted that 26

Table 6. Product ratios at different [NaOMe] for the reaction of 19' in 80% methanol and 20% benzene

[19'] (M)	[NaOMe] (M)	[NaOMe]/[19']	25/26	27/25
0.15	2.00	13.3	11.81	0
0.15	1.45	9.7	11.56	0.01
0.15	1.00	6.7	11.19	0.01
0.15	0.54	3.6	27.21	1.12
0.15	0.36	2.4	31.96	1.25

Table 7. Product ratios of 25/26 at different [19']

[19'] (M)	[NaOMe] (M)	[NaOMe]/[19']	25/26
0.12	1.0	8.3	7.96
0.15	1.0	6.6	11.19
0.24	1.0	4.2	19.66[a]
0.15	2.0	13.3	11.81
0.24	2.0	8.3	9.60
0.36	2.0	5.5	9.00
0.45	2.0	4.4	19.44[a]

[a]In these cases, 25 was also formed via cation 23 by attack of methanol.

was quite stable in the absence of acids and isomerized to 2-norcarene upon contact with acids (42).

anti-7-Methoxybicyclo[4.1.0]heptane (25) was synthesized by treating cyclohexene with α,α-dichloromethyl methyl ether in ether in the presence of methyl lithium/lithium iodide complex (43). Purification via preparative TLC on silica gel afforded both 25 and its epimer 31 in pure form. Compound 27 was locally available thanks to Herold (44).

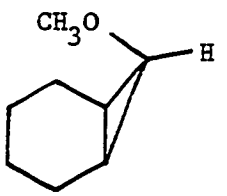

31

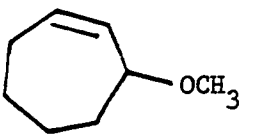

27

The initial study was to conduct the reaction of 19' with sodium methoxide in various mixtures of methanol and benzene at room temperature. The product ratios of 26/25 were obtained by GC analysis (with correction factors) in the presence of an internal standard. It was also determined that 26 didn't convert to 25 under the reaction conditions. However, the yield of 26 decreased after standing in the reaction mixture at room temperature for more than one hour. Therefore, all analyses were done immediately after each reaction. Table 8 lists the results at 25°C.

The results can be interpreted in terms of a kinetic model in which the ylide 32 is formed by the reaction of carbene 20' with methanol, as shown in Scheme VII.

Application of the steady-state treatment to Scheme VII leads to expression (8), where $k_t = k_1k_3/(k_2 + k_3)$.

Table 8. Product distribution as a function of [MeOH] from the reaction of 19' in methanol/benzene at 25°C

% MeOH	[MeOH] (M)	$\frac{1}{[MeOH]}$ (M^{-1})	% 26[a]	% 25[a]	25/26	26/25
1.0	0.25	4.00	36.7	8.6	0.24	4.25
2.0	0.49	2.03	32.1	16.0	0.50	2.01
3.0	0.74	1.35	21.4	22.3	1.04	0.96
10.0	2.47	0.41	9.5	17.3	1.82	0.55
20.0	5.00	0.20	5.5	13.3	2.40	0.42
25.0	6.25	0.16	13.9	39.1	2.80	0.36
40.0	10.0	0.10	7.1	29.5	4.15	0.24
50.0	12.5	0.08	6.4	34.7	5.46	0.18
70.0	16.7	0.06	3.8	28.3	7.41	0.13

[a]The somewhat low yields of 25 and 26 are partially due to the unpurified nature of starting material 19' (which was used as produced from the pure urea). However, the same bath of 19' was used throughout, so the product ratios should be internally accurate.

Scheme VII

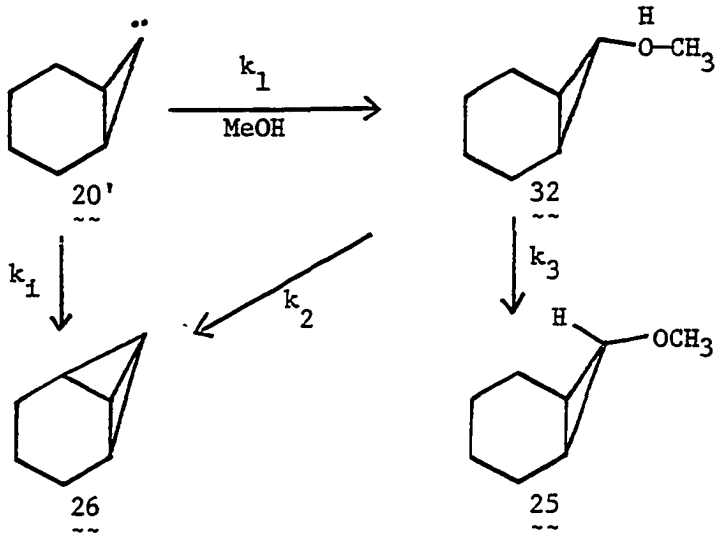

$$\frac{26}{25} = \frac{k_2}{k_3} + \frac{k_i(k_2 + k_3)}{k_1 k_3} \cdot \frac{1}{[MeOH]}$$

$$= \frac{k_2}{k_3} + \frac{k_i}{k_t} \cdot \frac{1}{[MeOH]} \qquad (8)$$

If the mechanism shown in Scheme VII is operative, the ratio of products from intramolecular and intermolecular reactions should vary linearly with the reciprocal of methanol concentration. But plots of the observed change in the ratio 26/25 vs. 1/[MeOH] and 25/26 vs. [MeOH] show pronounced deviations from linearity (Figures 4 and 5). However, linear regression analysis of the ratio 26/25 vs. 1/[MeOH] gives satisfactory correlation coefficients for separate lines A and B, where the data have been bisected into low (1-3%) and high (25-70%) methanol

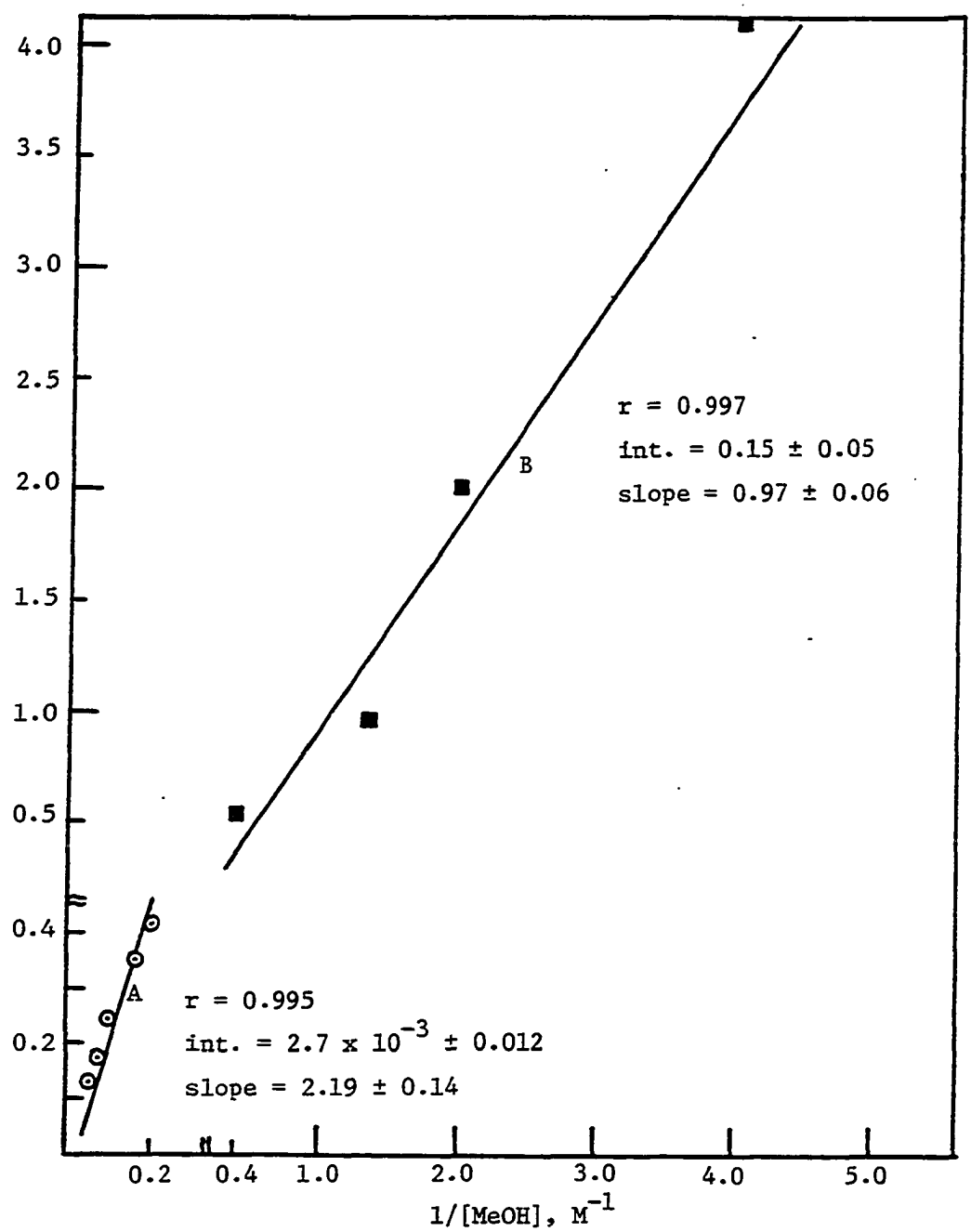

Figure 4. Plot of 26/25 vs. 1/[MeOH] at 25°C

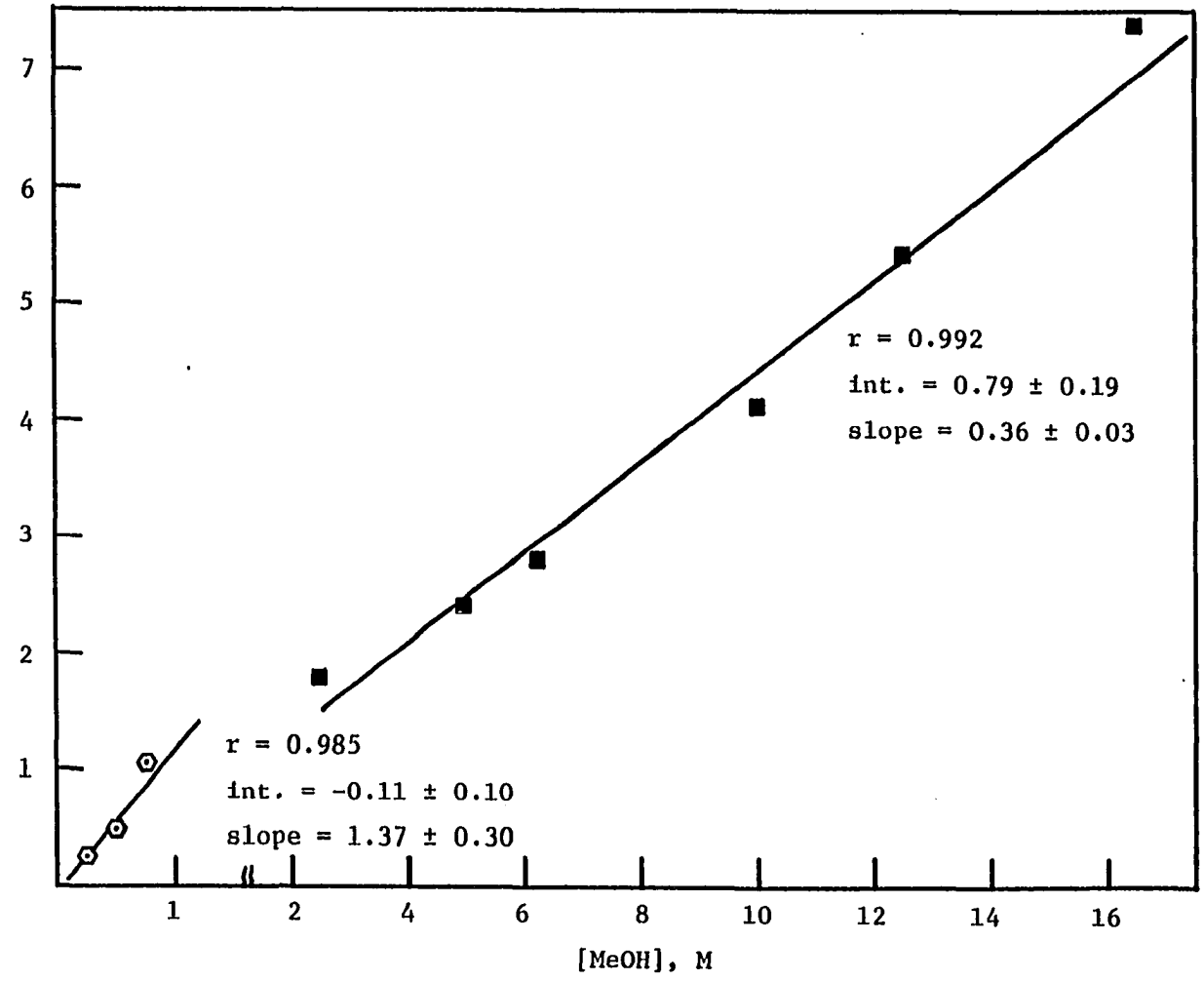

Figure 5. Plot of $\frac{25}{26}$ vs. [MeOH] at 25°C

concentration ranges. At high [MeOH], the term k_2/k_3 is very small, wherefore it is appropriate to use k_i/k_1 instead of k_i/k_t.

When t-butanol was used in place of methanol, the plot of $\underset{\sim\sim}{26}/\underset{\sim\sim}{33}$ vs. 1/[t-butanol] was again nonlinear (Figure 6). Table 9 lists the results at 42°C.

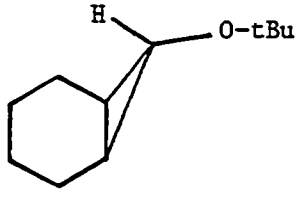

$\underset{\sim\sim}{33}$

Again, the plotted data (Figure 6) could be divided into two straight lines, C and D, each of which gave correlation coefficients >0.99 in the linear regression analysis.

Since Griller et al. (7) have reported that oligomers of methanol react faster with phenylchlorocarbenes than the monomer, while the converse was found for t-butanol, the curvature shown in Figures 4 and 6 might be related to the increasing concentration of oligomers at high [ROH] (R = Me, t-Butyl). To probe this possibility, the distributions of monomer, dimer and oligomers were calculated by using data obtained in the analysis of vapor-pressure experiments (7, 20, 45, 46). In

$$(CH_3OH)_{i-1} + (CH_3OH) \rightleftharpoons (CH_3OH)_i \qquad i = 2, 3$$

this model the equilibria are described by two equilibrium constants. The first, K_2, represents the monomer-dimer equilibrium, while K_3 is used for all oligomer equilibria.

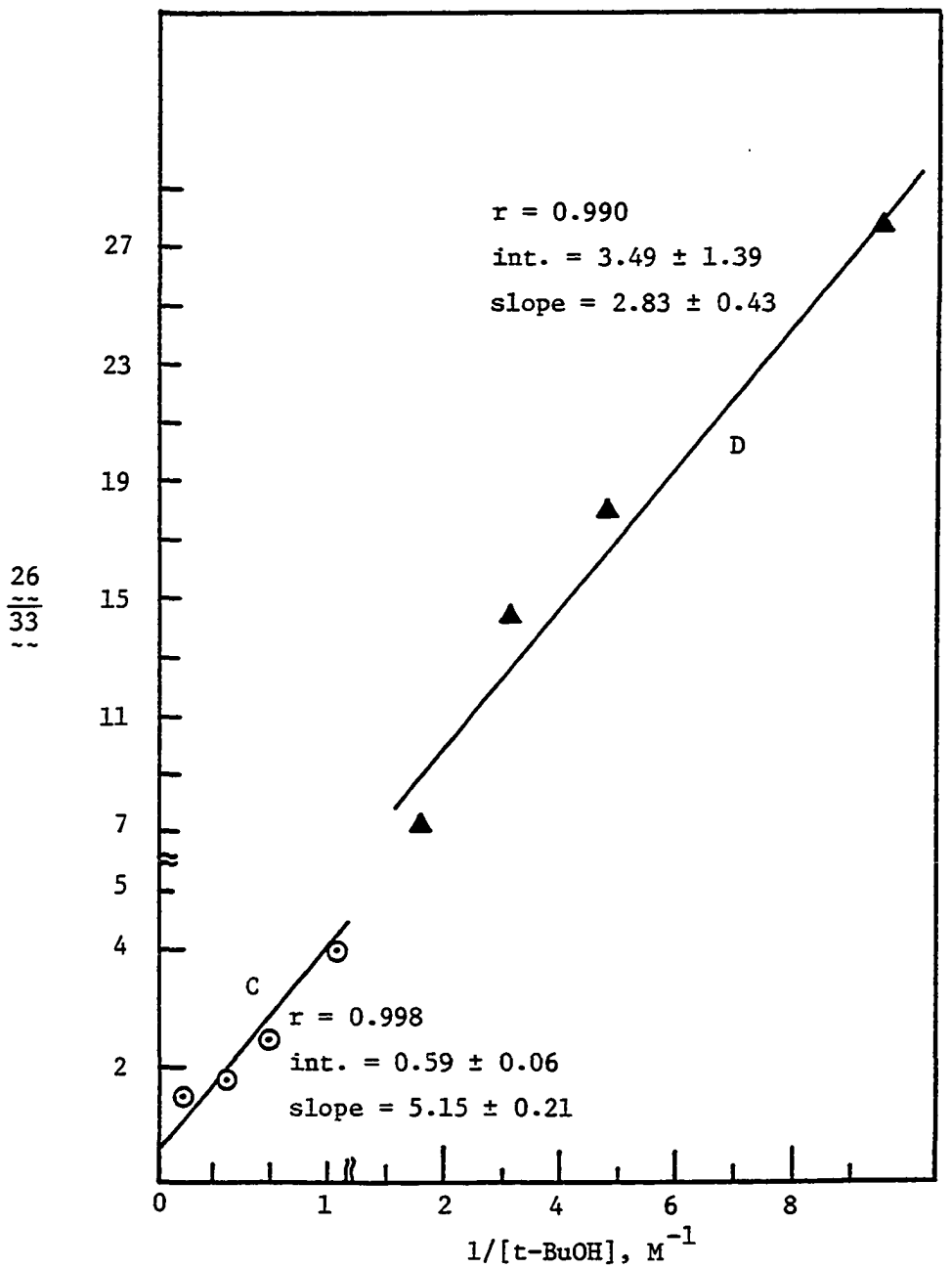

Figure 6. Plot of 26/33 vs. 1/[t-BuOH]

Table 9. Product distribution as a function of [t-BuOH] from the reaction of 19' in t-butanol/benzene at 42°C

% t-BuOH	[t-BuOH] (M)	$\frac{1}{[\text{t-BuOH}]}$ (M^{-1})	% 26	% 33	26/33
1.0	0.11	9.43	50.9	1.8	27.6
2.0	0.21	4.72	66.8	3.7	18.1
3.0	0.32	3.14	74.5	5.2	14.3
6.0	0.64	1.57	54.9	7.4	7.4
15.0	1.59	0.63	44.8	11.5	3.9
25.0	2.65	0.38	43.8	17.6	2.5
40.0	4.24	0.24	46.5	25.2	1.8
50.0	5.29	0.19	32.5	19.7	1.6

The mole fraction of monomer, X_1, in a given mole fraction of total alcohol, X_A, is given by equation (9) (20).

$$X_1^3(K_3^2 - K_2K_3) - X_1^2(2[K_3 - K_2] + X_A[K_3^2 + K_2]) + X_1(1 + 2K_3X_A) - X_A = 0 \quad (9)$$

where $K_2 = 31.6$, $K_3 = 80.0$ for methanol

$K_2 = 7.5$, $K_3 = 12.77$ for t-butanol.

Under the restrictions X_1 real, $K_3X_1 < 1$, $X_1 \leq X_A$, equation (9) was solved to give X_1 in each [ROH] (R = Me, t-Bu). The results are listed in Tables 10 and 11.

In Figures 7 to 9, product ratios $\underset{\sim\sim}{26}/\underset{\sim\sim}{25}$ and $\underset{\sim\sim}{26}/\underset{\sim\sim}{33}$, respectively, are plotted against the total concentration of methanol oligomers and the free methanol and t-butanol monomer concentration, respectively. Non-linearity is still seen for both cases. We have so far been unable to develop a single mechanism which unites the high and low concentration data. We have considered dielectric constant effects (the product ratios are reasonably linear with calculated $[(MeOH)_1] \cdot \varepsilon$(correction), although it is not obvious why this should be so), specific solvation by different alcohol oligomers, and variants thereof. No simple adjustment, which might be interpretable, appears to be effective. Therefore we decided to study the temperature-dependent behavior of norcaranylidene in methanol and t-butanol at low concentrations ($\leq$6%) and high concentrations ($\geq$25%) separately.

Tables 12-15 list four sets of data in methanol and t-butanol at different temperatures and concentrations.

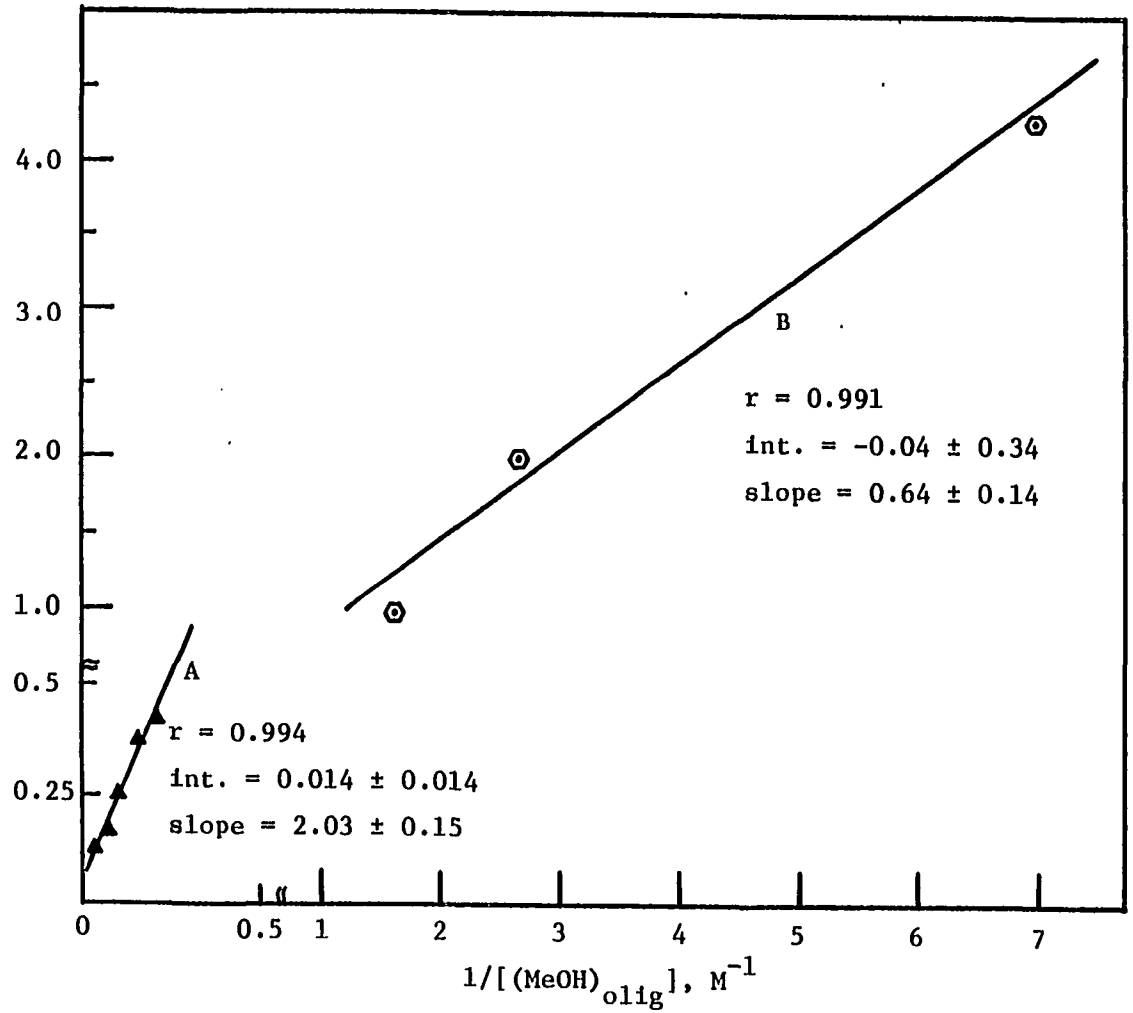

Figure 7. The ratio 26/25 plotted as a function of the methanol oligomer concentration

$\frac{26}{25}$

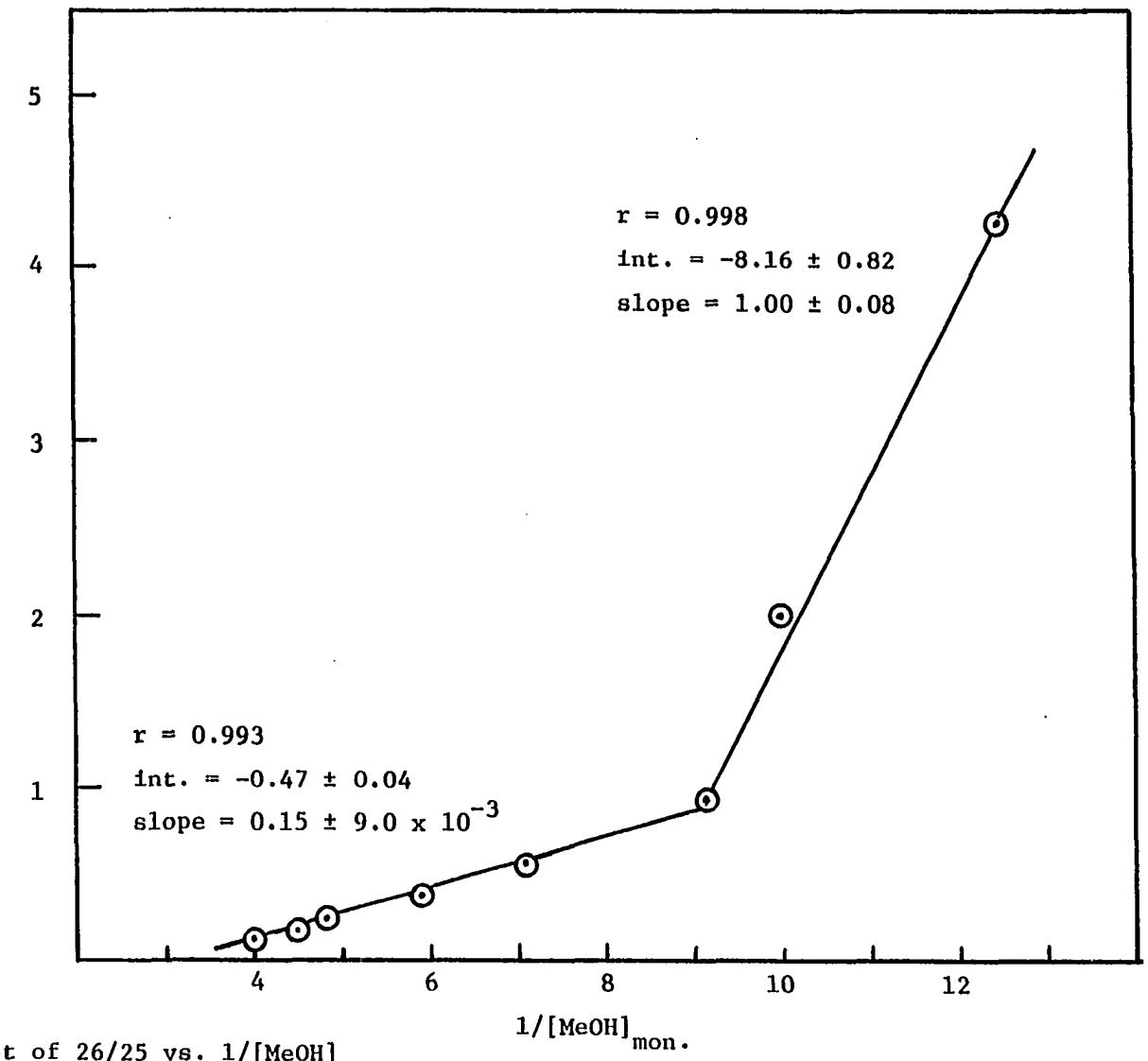

Figure 8. Plot of $\frac{26}{25}$ vs. $1/[MeOH]_{mon.}$

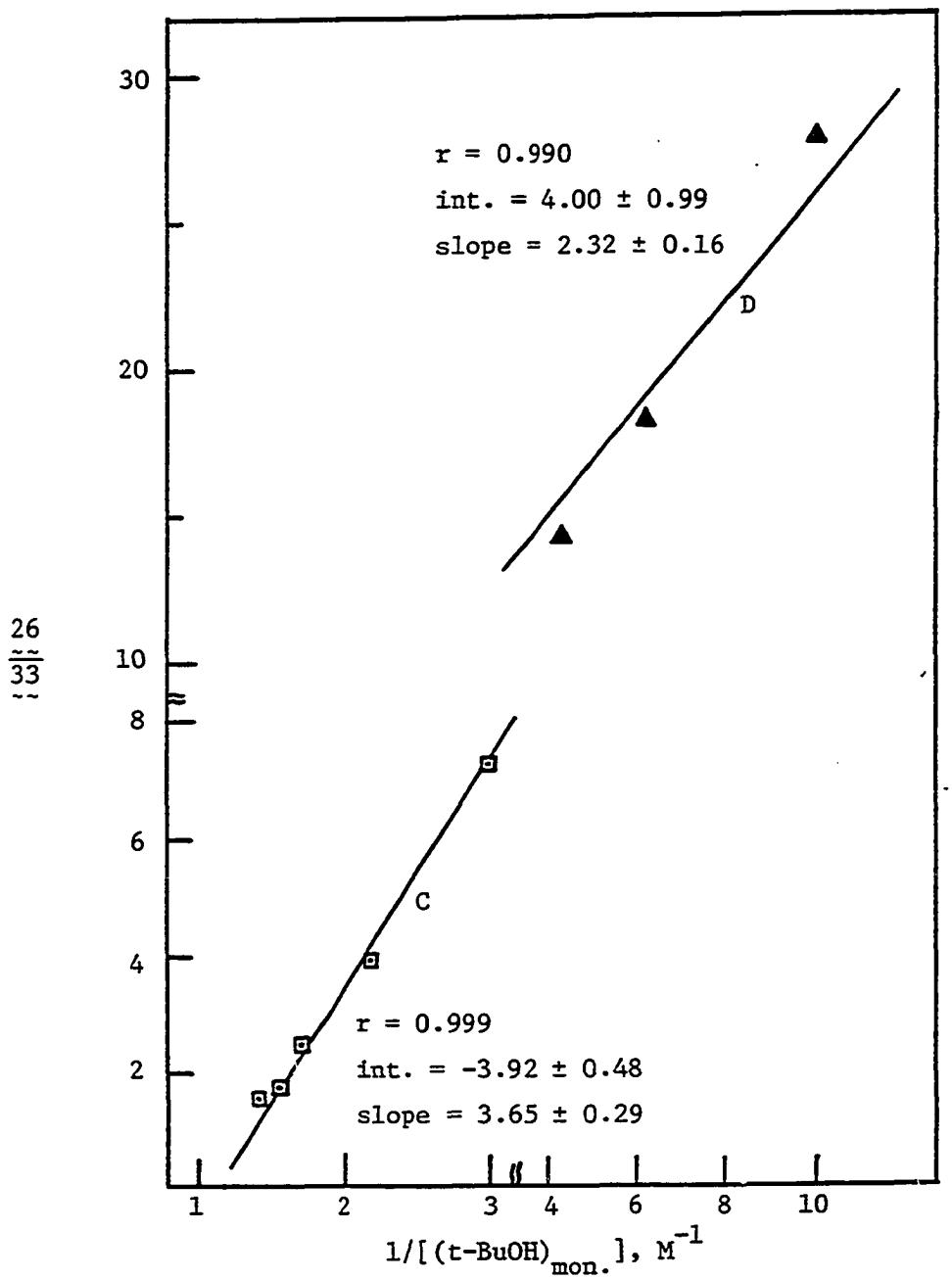

Figure 9. The product ratio 26/33 plotted as a function of t-butanol monomer concentration

Table 10. Calculated distributions of monomer, dimer and oligomer at different bulk [MeOH]; benzene cosolvent

% Bulk MeOH (by volume)	Bulk [MeOH], M	$10^2 \cdot X_A$ [a]	$10^2 \cdot X_1$ [b]	$10^2 \cdot X_d$ [c]	$10^2 \cdot X_o$ [d]	% monomer [e]	[monomer] M	[oligomers] M
1.0	0.25	2.2	0.75	0.17	1.3	34	0.08	0.14
2.0	0.49	4.3	0.85	0.23	3.2	20	0.10	0.37
3.0	0.74	6.4	0.93	0.27	5.2	15	0.11	0.60
10.0	2.47	19.7	1.08	0.37	18.2	5.5	0.14	2.29
20.0	4.94	35.5	1.23	0.48	33.8	3.5	0.17	4.70
25.0	6.17	42.4	1.18	0.44	40.8	2.8	0.17	5.93
40.0	9.88	59.5	1.25	0.49	57.8	2.1	0.21	9.59
50.0	12.3	68.8	1.21	0.46	67.1	1.8	0.22	12.05
70.0	17.3	83.7	1.21	0.46	82.1	1.4	0.25	16.94

[a] X_A = mole fraction of bulk MeOH (remainder is benzene).

[b] X_1 = mole fraction monomeric MeOH.

[c] X_d = mole fraction $(MeOH)_2$.

[d] X_o = mole fraction oligomeric MeOH.

[e] Relative to total bulk [MeOH].

Table 11. Calculated distributions of monomer, dimer and oligomer at different bulk [t-BuOH]; benzene cosolvent

% bulk t-BuOH (by volume)	Bulk [t-BuOH] M	$10^2 \cdot X_A$ [a]	$10^2 \cdot X_1$ [b]	$10^2 \cdot X_d$ [c]	$10^2 \cdot X_o$ [d]	% monomer [e]	[monomer] M	[oligomers] M
1.0	0.11	0.95	0.85	0.05	0.04	90	0.10	0.005
2.0	0.22	1.90	1.40	0.15	0.35	74	0.16	0.04
3.0	0.33	2.85	2.00	0.29	0.60	69	0.23	0.07
6.0	0.65	5.71	2.99	0.67	2.04	52	0.34	0.23
15.0	1.59	14.2	4.10	1.23	8.96	28	0.45	1.00
25.0	2.65	24.0	5.13	1.97	16.9	21	0.57	1.87
40.0	4.24	28.7	5.77	2.49	30.5	15	0.63	3.34
50.0	5.30	48.7	6.12	2.81	39.7	13	0.67	4.33

[a] X_A = mole fraction of bulk t-BuOH (remainder is benzene).

[b] X_1 = mole fraction monomeric t-BuOH.

[c] X_d = mole fraction $(t\text{-BuOH})_2$.

[d] X_o = mole fraction oligomeric t-BuOH.

[e] Relative to total [t-BuOH].

Table 12. Product distribution as a function of methanol concentration and temperature. S.M. = 0.027 mmole, MeOH $\geq$ 0.305 mmole. [NaOMe]/[S.M.] = 7:1, total solvent volume = 1.2 ml, benzene cosolvent

T (°C)	% MeOH	$\frac{1}{[MeOH]}$ (M^{-1})	% 26	% 25	26/25
20	1.0	4.0	54.7	11.9	4.59
20	2.0	2.0	38.7	24.2	1.60
20	3.0	1.4	45.5	32.4	1.40
20	6.0	0.7	22.3	34.9	0.64
40	1.0	4.0	55.1	8.3	6.65
40	2.0	2.0	29.9	8.0	3.73
40	3.0	1.4	30.0	19.4	1.54
40	6.0	0.7	23.7	28.4	0.83
55	1.0	4.0	45.6	5.1	9.01
55	2.0	2.0	26.6	9.5	2.79
55	3.0	1.4	24.4	9.9	2.48
55	6.0	0.7	22.2	20.0	1.11
62	1.0	4.0	53.2	4.2	12.54
62	2.0	2.0	30.3	8.1	3.72
62	3.0	1.4	33.6	12.4	2.70
62	6.0	0.7	15.3	12.3	1.23

Table 13. Product distribution as a function of methanol concentration and temperature. S.M. = 0.027 mmole, [NaOMe]/[S.M.] = 7:1, total solvent volume = 0.4 ml, benzene cosolvent

T (°C)	% MeOH	$\frac{1}{[MeOH]}$ (M^{-1})	% 26	% 25	26/25
15	25.0	0.16	14.9	48.8	0.31
15	40.0	0.10	7.3	36.3	0.20
15	50.0	0.08	5.1	31.4	0.16
20	25.0	0.16	14.3	36.1	0.40
20	40.0	0.10	11.5	41.6	0.28
20	50.0	0.08	6.4	27.6	0.23
25	25.0	0.16	13.9	39.1	0.36
25	40.0	0.10	7.1	29.5	0.24
25	50.0	0.08	6.4	34.7	0.18
30	25.0	0.16	8.4	26.7	0.31
30	40.0	0.10	5.5	29.5	0.19
30	50.0	0.08	5.5	41.1	0.13
35	25.0	0.16	10.9	28.3	0.39
35	40.0	0.10	5.2	20.7	0.25
35	50.0	0.08	5.9	33.0	0.18
40	25.0	0.16	8.4	21.1	0.40
40	40.0	0.10	8.3	37.9	0.22
40	50.0	0.08	6.2	33.2	0.19
50	25.0	0.16	11.5	27.6	0.41
50	40.0	0.10	6.6	27.7	0.24
50	50.0	0.08	8.5	44.4	0.19
55	25.0	0.16	17.9	43.8	0.41
55	40.0	0.10	5.9	27.1	0.22
55	50.0	0.08	4.0	26.0	0.16

Table 14. Product distribution as a function of t-butanol concentration and temperature. S.M. = 0.027 mmole, t-BuOH $\geq$ 0.276 mmole, [t-BuOH]/[S.M.] = 7:1, total solvent volume = 2.6 ml, benzene cosolvent

T (°C)	% t-BuOH	$\frac{1}{[\text{t-BuOH}]}$ (M^{-1})	% 26	% 33	26/33
20	1.0	9.4	69.2	3.4	20.2
20	2.0	4.7	48.9	4.6	10.5
20	3.0	3.1	71.4	8.4	8.5
20	6.0	1.6	48.2	11.4	4.2
42	1.0	9.4	50.9	1.8	27.7
42	2.0	4.7	66.8	4.0	18.1
42	3.0	3.1	74.5	5.2	14.4
42	6.0	1.6	54.9	7.4	7.4
55	1.0	9.4	77.6	2.5	31.4
55	2.0	4.7	71.7	3.9	18.2
55	3.0	3.1	56.8	3.8	15.0
55	6.0	1.6	58.6	7.0	8.4

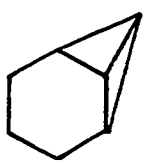

26

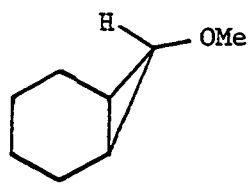

25

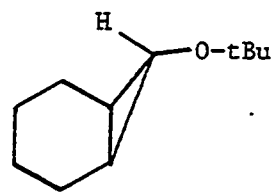

33

Table 15. Product distribution as a function of t-butanol concentration and temperature. S.M. = 0.027 mmole, [t-BuOH]/[S.M.] = 7:1, total solvent volume = 0.4 ml, benzene cosolvent

T (°C)	% t-BuOH	$\frac{1}{[\text{t-BuOH}]}$ (M^{-1})	% 26	% 33	26/33
25	25.0	0.38	24.3	11.4	2.13
25	40.0	0.24	37.4	21.8	1.71
25	50.0	0.19	31.6	20.6	1.53
32	25.0	0.38	39.0	18.4	2.12
32	40.0	0.24	34.6	20.2	1.71
32	50.0	0.19	27.2	18.9	1.44
37	25.0	0.38	58.9	25.2	2.33
37	40.0	0.24	40.4	23.3	1.74
37	50.0	0.19	28.9	18.9	1.53
42	25.0	0.38	43.7	17.6	2.48
42	40.0	0.24	46.5	25.2	1.84
42	50.0	0.19	32.5	19.7	1.65
50	25.0	0.38	33.5	13.3	2.51
50	40.0	0.24	31.7	16.9	1.88
50	50.0	0.19	33.0	19.8	1.67
65	25.0	0.38	23.8	7.4	3.24
65	40.0	0.24	27.0	13.7	1.97
65	50.0	0.19	19.9	12.1	1.64
75	25.0	0.38	26.4	6.2	4.22
75	40.0	0.24	14.8	8.3	1.80
75	50.0	0.19	23.0	12.9	1.78

Based on Scheme VII and equation (8), the values of k_i/k_t were obtained by linear least-squares analysis. Tables 16-19 show the results.

The Arrhenius law was then used to determine $\Delta\Delta S^{\neq}(\Delta S_i^{\neq} - \Delta S_t^{\neq})$ and $\Delta\Delta H^{\neq}(\Delta H_i^{\neq} - \Delta H_t^{\neq})$ for the four different cases. These data are shown in Table 20.

There was concern that errors in the differential enthalpy and entropy in each case might be masked by the dual calculations (least-squares analysis of the concentration dependences and Arrhenius relationships). A better way to analyze the data might be to use a simultaneous computation method. Thus a NLLSQ (nonlinear least-squares) program was adapted to our systems to give the activation parameters directly in each case by treating equation (8) as follows:

$$\frac{\underset{\sim\sim}{26}}{\underset{\sim\sim}{25} \text{ or } \underset{\sim\sim}{33}} = \frac{k_2}{k_3} + \frac{k_i}{k_t} \cdot \frac{1}{[ROH]} \quad (R = Me,\ t\text{-}Bu) \tag{8}$$

Equation (8) can be written as

$$\frac{\underset{\sim\sim}{26}}{\underset{\sim\sim}{25} \text{ or } \underset{\sim\sim}{33}} = \frac{(RT/h)e^{\Delta S_2^{\neq}/R_e - \Delta H_2^{\neq}/RT}}{(RT/h)e^{\Delta S_3^{\neq}/R_e - \Delta H_3^{\neq}/RT}} + \frac{(RT/h)e^{\Delta S_i^{\neq}/R_e - \Delta H_i^{\neq}/RT}}{(RT/h)e^{\Delta S_t^{\neq}/R_e - \Delta H_t^{\neq}/RT}} \cdot \frac{1}{[ROH]} \tag{10}$$

Equation (10) can then be simplified as

Table 16. Rate constants as a function of temperature for the formation of 26 and 25 in methanol/benzene (25-50% methanol)

T (°C)	$10^3/T$ (K^{-1})	$\frac{k_2}{k_3}$	$\frac{k_1}{k_t}$	$\ln \frac{k_1}{k_t}$	R
15.0	3.47	0.010 ± 0.004	1.87 ± 0.04	0.63 ± 0.02	0.999
20.0	3.41	0.062 ± 0.013	2.12 ± 0.12	0.75 ± 0.05	0.999
25.0	3.56	0.026 ± 0.003	2.27 ± 0.26	0.82 ± 0.11	0.996
30.0	3.30	-0.050 ± 0.026	2.29 ± 0.27	0.83 ± 0.12	0.998
35.0	3.25	-0.028 ± 0.030	2.66 ± 0.31	0.98 ± 0.12	0.993
40.0	3.20	-0.024 ± 0.044	2.58 ± 0.44	0.95 ± 0.17	0.995
50.0	3.10	-0.031 ± 0.009	2.74 ± 0.09	1.01 ± 0.03	0.999
55.0	3.05	-0.090 ± 0.004	3.11 ± 0.05	1.13 ± 0.02	0.999

Table 17. Rate constants as a function of temperature for the formation of 26 and 25 in methanol/benzene (1-6% methanol)[a]

T (°C)	$10^3/T$ (K^{-1})	$\frac{k_i}{k_t}$	$\ln \frac{k_i}{k_t}$	R
20.0	3.41	0.97 ± 0.17	-0.03 ± 0.17	0.999
40.0	3.20	1.64 ± 0.35	0.49 ± 0.21	0.994
55.0	3.05	1.78 ± 0.39	0.58 ± 0.21	0.999
62.0	2.99	2.42 ± 0.50	0.88 ± 0.20	0.997

[a] k_2/k_3 ratios are meaningless since the intercept at 1/[MeOH] = 0 is out of the region being studied.

Table 18. Rate constants as a function of temperature for the formation of 26 and 33 in t-butanol/benzene (1-6% t-butanol)[a]

T (°C)	$10^3/T$ (K^{-1})	$\frac{k_i}{k_t}$	$\ln \frac{k_i}{k_t}$	R
20.0	3.41	2.10 ± 0.20	0.74 ± 0.09	0.997
42.0	3.18	2.87 ± 0.47	1.05 ± 0.16	0.990
55.0	3.05	3.06 ± 0.32	1.12 ± 0.10	0.996

[a] k_2/k_3 ratios are meaningless since the intercept at 1/[t-BuOH] = 0 is out of the region being studied.

Table 19. Rate constants as a function of temperature for the formation of 26 and 33 in t-butanol/benzene (25-50% t-butanol).

T (°C)	$10^3/T$ (K^{-1})	$\frac{k_2}{k_3}$	$\frac{k_i}{k_t}$	$\ln \frac{k_i}{k_t}$	R
25.0	3.35	0.941 ± 0.037	3.14 ± 0.14	1.14 ± 0.04	0.999
32.0	3.28	0.800 ± 0.150	3.54 ± 0.58	1.26 ± 0.16	0.990
37.0	3.23	0.730 ± 0.001	4.21 ± 0.01	1.44 ± 0.00	0.999
42.0	3.17	0.807 ± 0.049	4.37 ± 0.19	1.48 ± 0.04	0.999
50.0	3.10	0.825 ± 0.019	4.42 ± 0.07	1.49 ± 0.01	0.999
65.0	2.96	0.022 ± 0.169	8.35 ± 0.70	2.12 ± 0.08	0.999
75.0	2.87	-0.658 ± 1.38	11.60 ± 5.89	2.45 ± 0.51	0.970

Table 20. Activation parameters for the formation of 25, 26 and 33 in methanol and t-butanol from linear least-squares analyses

% ROH	$\Delta\Delta H^{\neq}$ ($\Delta H_i^{\neq} - \Delta H_t^{\neq}$) (kcal/mol)	$\Delta\Delta S^{\neq}$ ($\Delta S_i^{\neq} - \Delta S_t^{\neq}$) (e.u.)
1∿6% MeOH	3.98 ± 0.45	13.5 ± 1.5
1∿5% t-BuOH	2.22 ± 0.35	9.0 ± 1.1
25∿50% MeOH	1.58 ± 0.43	6.9 ± 1.4
25∿50% t-BuOH	4.73 ± 0.67	18.0 ± 2.1

$$\frac{26}{25 \text{ or } 33} = e^{(\Delta S_2^{\neq} - \Delta S_3^{\neq})/R} \, e^{-(\Delta H_2^{\neq} - \Delta H_3^{\neq})/RT} + \left\{ e^{(\Delta S_i^{\neq} - \Delta S_t^{\neq})/R} \, e^{-(\Delta H_i^{\neq} - \Delta H_t^{\neq})/RT} \right\} \cdot \frac{1}{[ROH]} \qquad (11)$$

In NLLSQ notation,

$B(1) = \Delta S_2^{\neq} - \Delta S_3^{\neq}$ $\qquad$ $B(4) = \Delta H_t^{\neq} - \Delta H_i^{\neq}$

$B(2) = \Delta H_3^{\neq} - \Delta H_2^{\neq}$ $\qquad$ $X(I,1) = T\ (K)$

$B(3) = \Delta S_i^{\neq} - \Delta S_t^{\neq}$ $\qquad$ $X(I,2) = 1/[ROH]$

Therefore, equation (11) can be written as

$$\frac{26}{25 \text{ or } 33} = \exp(B(1)/1.987) * \exp[B(2)/(1.987 * X(I,1))] + \exp(B(3)/1.987) * \exp[B(4)/(1.987 * X(I,1))] * (X(I,2)) \qquad (12)$$

By inputting the product ratios [26/(25 or 33)], temperatures (X(I,1)) and alcohol concentrations (X(I,2)), the activation parameters

(B(1)-B(4)) were calculated in an average of fifteen iterative cycles to reach the smallest standard deviation (Table 21). The product ratios were also "back-calculated" from the best calculated activation parameters. Tables 22-25 show the comparison between the experimental and computational results.

From the values of B(1)-B(4), the rate constant ratios k_i/k_t, k_i/k_1 and k_2/k_3 could be calculated. Tables 26-29 and Figures 10-13 show the comparison of rate ratios from least-squares analyses with those "back-calculated" from B(1)-B(4).

It was found that when the [MeOH] was $\geq$ 25%, a significant difference between the two methods was attained (Figure 10). This might be due to the fact that the NLLSQ program was forced to make the k_2/k_3 ratios linearly temperature-dependent. Since $k_2 \cong 0$ at all temperatures, small deviations around zero lead to large percentage errors when the k_2/k_3 ratio is taken as significant. Therefore, the least-squares analysis was taken as more reliable at high [MeOH].

It was of interest to compare the reactivity of norcaranylidene (20') with methanol and t-butanol, in as much as such has been done for some aromatic carbenes (e.g., Ph_2C:). Since we couldn't measure the rate constants $k_{t,MeOH}$ and $k_{t,t\text{-}BuOH}$ directly, the ratios of $k_{t,MeOH}/k_{t,t\text{-}BuOH}$ could only be obtained from competition experiments conducted in mixtures of methanol and t-butanol. Scheme VIII shows the reaction mechanism (32 does not give 26).

Table 21. Activation parameters for the formation of 26, 25 and 33 in methanol and t-butanol from NLLSQ analysis

% ROH	$\Delta H_1^{\neq} - \Delta H_t^{\neq}$ (Kcal/mol)	$\Delta S_1^{\neq} - \Delta S_t^{\neq}$ (cal/mol.K)	$\Delta H_2^{\neq} - \Delta H_3^{\neq}$ (Kcal/mol)	$\Delta S_2^{\neq} - \Delta S_3^{\neq}$ (cal/mol.K)
1∿6% MeOH	4.97 ± 1.13	17.13 ± 3.47	8.06 ± 8.27	24.94 ± 25.08
1∿6% t-BuOH	2.23 ± 0.86	8.90 ± 2.75	4.06 ± 3.27	15.70 ± 10.27
25∿50% MeOH	0.64 ± 0.65	3.75 ± 2.05	-11.43 ± 9.47	-49.80 ± 331.45
25∿50% t-BuOH	3.98 ± 0.70	15.90 ± 2.04	-6.24 ± 2.88	-21.20 ± 9.69

Table 22. Comparison of the experimental product ratios with those "calculated" by NLLSQ analysis in 25-50% methanol

T (K)	1/[MeOH] (M^{-1})	$\underset{\sim\sim}{26/25} \cdot 10^1$		$\Delta \cdot 10^1$
		experimental	NLLSQ	
288	0.16	3.07	3.47	-0.40
288	0.10	2.02	2.19	-0.17
288	0.08	1.62	1.77	-0.15
293	0.16	3.98	3.53	0.45
293	0.10	2.76	2.22	0.54
293	0.08	2.31	1.78	0.53
298	0.16	3.57	3.58	-0.01
298	0.10	2.41	2.25	0.16
298	0.08	1.83	1.81	0.02
303	0.16	3.14	3.63	-0.49
303	0.10	1.89	2.28	-0.39
303	0.08	1.34	1.82	-0.48
308	0.16	3.86	3.69	-0.17
308	0.10	2.53	2.31	0.22
308	0.08	1.80	1.85	-0.05
313	0.16	3.97	3.75	0.22
313	0.10	2.19	2.34	-0.15
313	0.08	1.87	1.88	-0.01
323	0.16	4.15	3.87	0.28
323	0.10	2.40	2.41	-0.01
323	0.08	1.92	1.93	-0.01
328	0.16	4.08	3.92	0.16
328	0.10	2.18	2.45	-0.27
328	0.08	1.55	1.96	-0.41

Table 23. Comparison of the experimental product ratios with those "calculated" by NLLSQ analysis in 1-6% methanol

T (K)	1/[MeOH] (M^{-1})	26/25 ratio		Δ
		experimental	NLLSQ	
293	4.05	4.59	4.09	0.50
293	2.03	1.60	1.91	-0.31
293	1.35	1.40	1.18	0.22
293	0.67	0.64	0.45	0.19
313	4.05	6.65	6.86	-0.21
313	2.03	3.73	3.11	0.62
313	1.35	1.54	1.84	-0.30
313	0.67	0.83	0.58	0.25
328	4.05	9.01	9.65	-0.64
328	2.03	2.79	4.24	-1.45
328	1.35	2.48	2.42	0.06
328	0.67	1.11	0.60	0.51
335	4.05	12.5	11.2	1.3
335	2.03	3.72	4.83	-1.11
335	1.35	2.70	2.69	0.01
335	0.67	1.23	0.55	0.67

Table 24. Comparison of the experimental product ratios with those "calculated" by NLLSQ analysis in 25-50% t-butanol

T (K)	1/[t-BuOH] (M^{-1})	26/33		Δ
		experimental	NLLSQ	
298	0.38	2.13	2.22	-0.09
298	0.24	1.71	1.72	-0.01
298	0.19	1.53	1.55	-0.02
305	0.38	2.12	2.25	-0.13
305	0.24	1.71	1.67	0.04
305	0.19	1.44	1.47	-0.03
310	0.38	2.33	2.32	0.01
310	0.24	1.74	1.67	0.07
310	0.19	1.53	1.45	0.08
315	0.38	2.48	2.42	0.06
315	0.24	1.84	1.70	0.14
315	0.19	1.65	1.46	0.19
323	0.38	2.52	2.64	-0.12
323	0.24	1.88	1.80	0.08
323	0.19	1.66	1.52	0.14
338	0.38	3.23	3.24	-0.01
338	0.24	1.97	2.11	-0.11
338	0.19	1.64	1.74	-0.10
348	0.38	4.22	3.70	0.52
348	0.24	1.80	2.39	-0.59
348	0.19	1.79	1.95	-0.16

Table 25. Comparison of the experimental product ratios with those "calculated" by NLLSQ analysis in 1-6% t-butanol

T (K)	1/[t-BuOH] (M^{-1})	26/33 experimental	26/33 NLLSQ	Δ
293	9.4	20.2	20.4	-0.2
293	4.7	10.5	11.4	-0.9
293	3.1	8.5	8.5	0
293	1.6	4.2	5.5	-1.3
315	9.4	27.7	27.5	0.2
315	4.7	18.1	15.8	2.3
315	3.1	14.3	11.9	2.4
315	1.6	7.4	8.0	-0.6
328	9.4	31.4	32.2	-0.8
328	4.7	18.2	18.8	-0.6
328	3.1	15.0	14.3	0.7
328	1.6	8.4	9.8	-1.4

Table 26. Comparison of rate constant ratios for the formation of 25 and 26 in 25-50% methanol from NLLSQ and least-squares analysis

T (K)	$10^3 \cdot \frac{k_2}{k_3}$ [a]	$\frac{k_i}{k_t} \cong \frac{k_i}{k_1}$	$10^3/T$ (K^{-1})	$\ln \frac{k_i}{k_t}$
288	6.2	2.13 (1.87 ± 0.04)[b]	3.47	0.76 (0.63 ± 0.02)[b]
293	4.4	2.17 (2.12 ± 0.12)	3.41	0.77 (0.75 ± 0.05)
298	3.2	2.21 (2.27 ± 0.26)	3.36	0.79 (0.82 ± 0.11)
303	2.3	2.26 (2.29 ± 0.27)	3.30	0.82 (0.83 ± 0.12)
308	1.7	2.30 (2.66 ± 0.31)	3.25	0.83 (0.98 ± 0.12)
313	1.3	2.34 (2.58 ± 0.44)	3.20	0.85 (0.95 ± 0.17)
323	0.7	2.41 (2.74 ± 0.09)	3.10	0.88 (1.01 ± 0.03)
328	0.5	2.45 (3.11 ± 0.05)	3.05	0.90 (1.13 ± 0.02)

[a] The value of k_2/k_3 is essentially zero at each temperature from least-squares analysis.

[b] The data in parentheses were obtained from least-squares analysis.

Table 27. Comparison of rate constant ratios for the formation of 26 and 33 in 25-50% t-butanol from NLLSQ and least-squares analyses

T (K)	$\frac{k_2}{k_3}$	$\frac{k_i}{k_t}$	$\frac{k_i}{k_1}$	$10^3/T$ (K^{-1})	$\ln \frac{k_i}{k_t}$
298	0.89 (0.941 ± 0.037)[a]	3.55 (3.14 ± 0.14)[a]	1.88 (1.62 ± 0.13)[a]	3.36	1.26 (1.14 ± 0.04)[a]
305	0.70 (0.800 ± 0.150)	4.14 (3.54 ± 0.58)	2.44 (1.97 ± 0.66)	3.28	1.42 (1.26 ± 0.16)
310	0.59 (0.730 ± 0.001)	4.60 (4.21 ± 0.01)	2.90 (2.43 ± 0.01)	3.23	1.53 (1.44 ± 0.00)
315	0.50 (0.807 ± 0.049)	5.10 (4.37 ± 0.19)	3.40 (2.41 ± 0.24)	3.18	1.63 (1.48 ± 0.04)
323	0.39 (0.825 ± 0.019)	5.97 (4.42 ± 0.07)	4.29 (2.42 ± 0.09)	3.10	1.79 (1.49 ± 0.01)
338	0.25 (0.022 ± 0.169)	7.86 (8.35 ± 0.70)	6.27 8.17[b]	2.96	2.06 (2.12 ± 0.08)
348	0.19(-0.658 ± 1.380)	9.32(11.60 ± 5.89)	7.80 ——[b]	2.87	2.23 (2.45 ± 0.51)

[a]Values in parentheses are from least-squares analysis.

[b]The error in k_2/k_3 is too large to calculate the error in k_i/k_1.

Table 28. Comparison of rate constant ratios for the formation of 26 and 25 in 1-6% methanol from NLLSQ and least-squares analyses

T (K)	$\frac{k_i}{k_t}$	$10^3/T$ (K^{-1})	$\ln \frac{k_i}{k_t}$
293	1.07 (0.97 ± 0.17)[a]	3.41	0.067(-0.03 ± 0.17)[a]
313	1.85 (1.54 ± 0.35)	3.20	0.615 (0.49 ± 0.21)
328	2.67 (1.78 ± 0.39)	3.05	0.982 (0.58 ± 0.21)
335	3.14 (2.42 ± 0.50)	2.99	1.144 (0.88 ± 0.20)

[a]Values in parentheses are from least-squares analyses.

Table 29. Comparison of rate constant ratios for the formation of 26 and 33 in 1-6% t-butanol from NLLSQ and least-squares analyses

T (K)	$\frac{k_i}{k_t}$	$10^3/T$ (K^{-1})	$\ln \frac{k_i}{k_t}$
293	1.89 (2.10 ± 0.20)[a]	3.41	0.64 (0.74 ± 0.09)[a]
315	2.48 (2.87 ± 0.47)	3.18	0.91 (1.05 ± 0.16)
328	2.85 (3.06 ± 0.32)	3.05	1.05 (1.12 ± 0.10)

[a]Values in parentheses are from least-squares analyses.

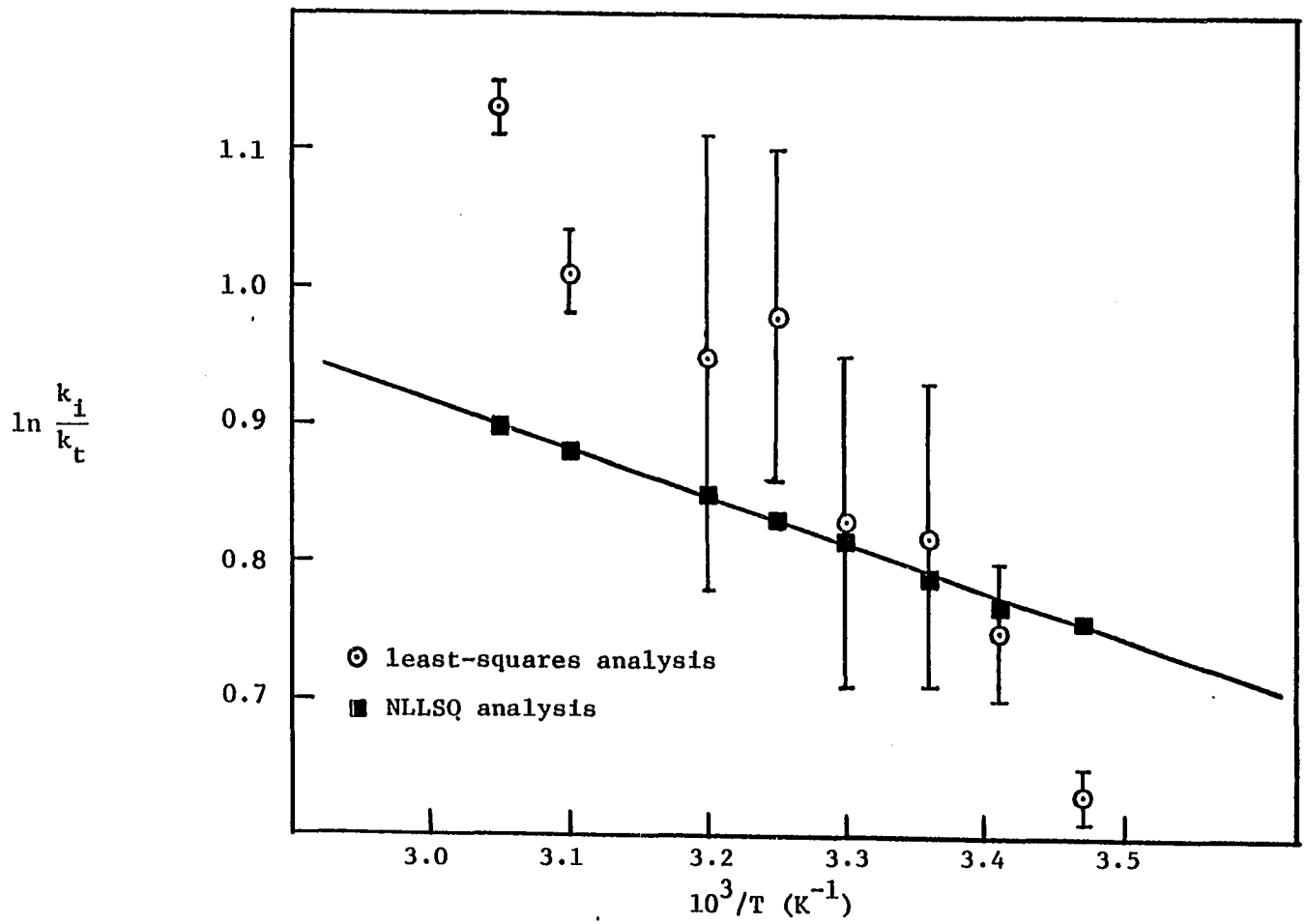

Figure 10. Plot of ln k_i/k_t vs. 1/T in 25-50% methanol in benzene

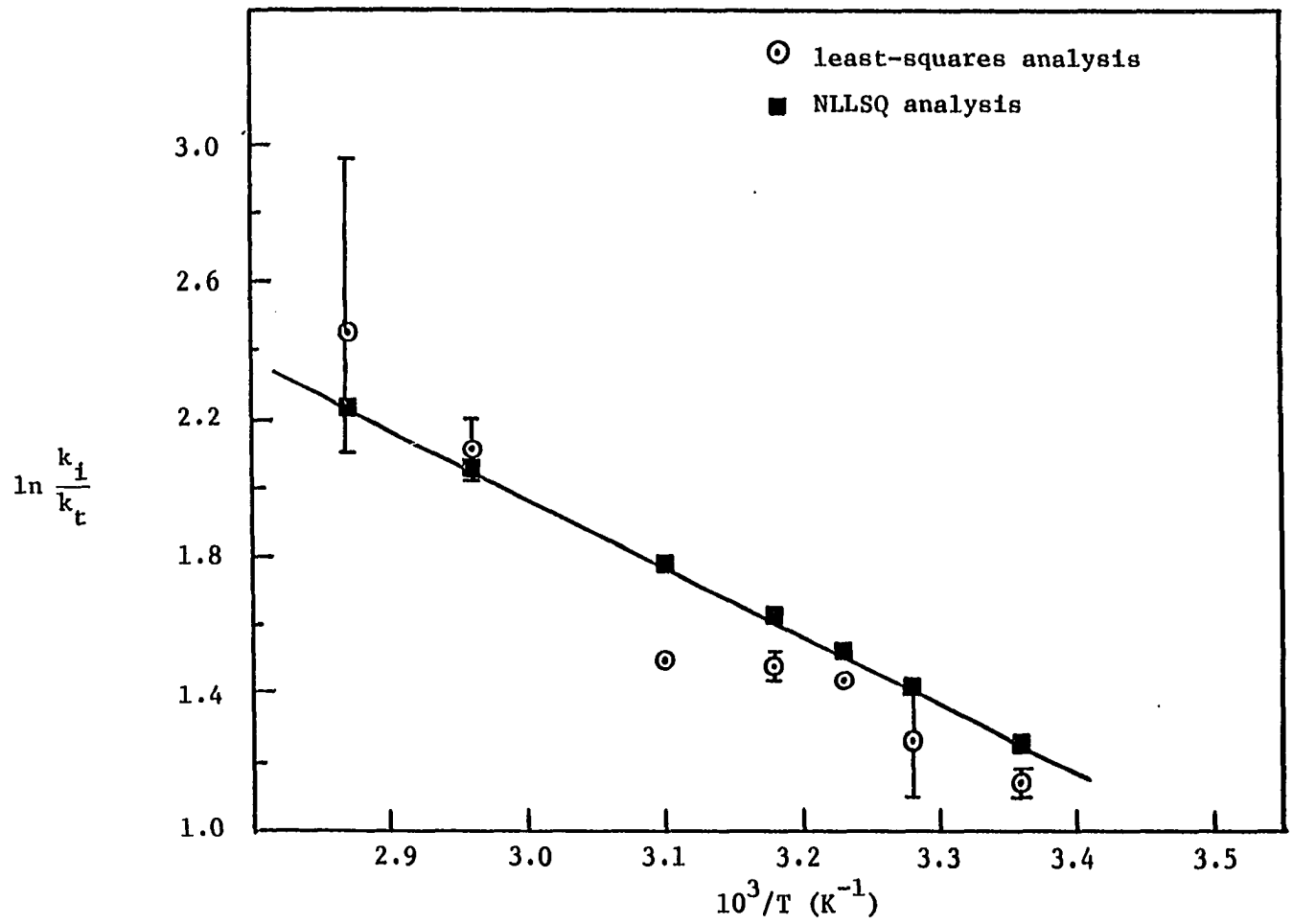

Figure 11. Plot of ln k_i/k_t vs. 1/T in 25-50% t-butanol in benzene

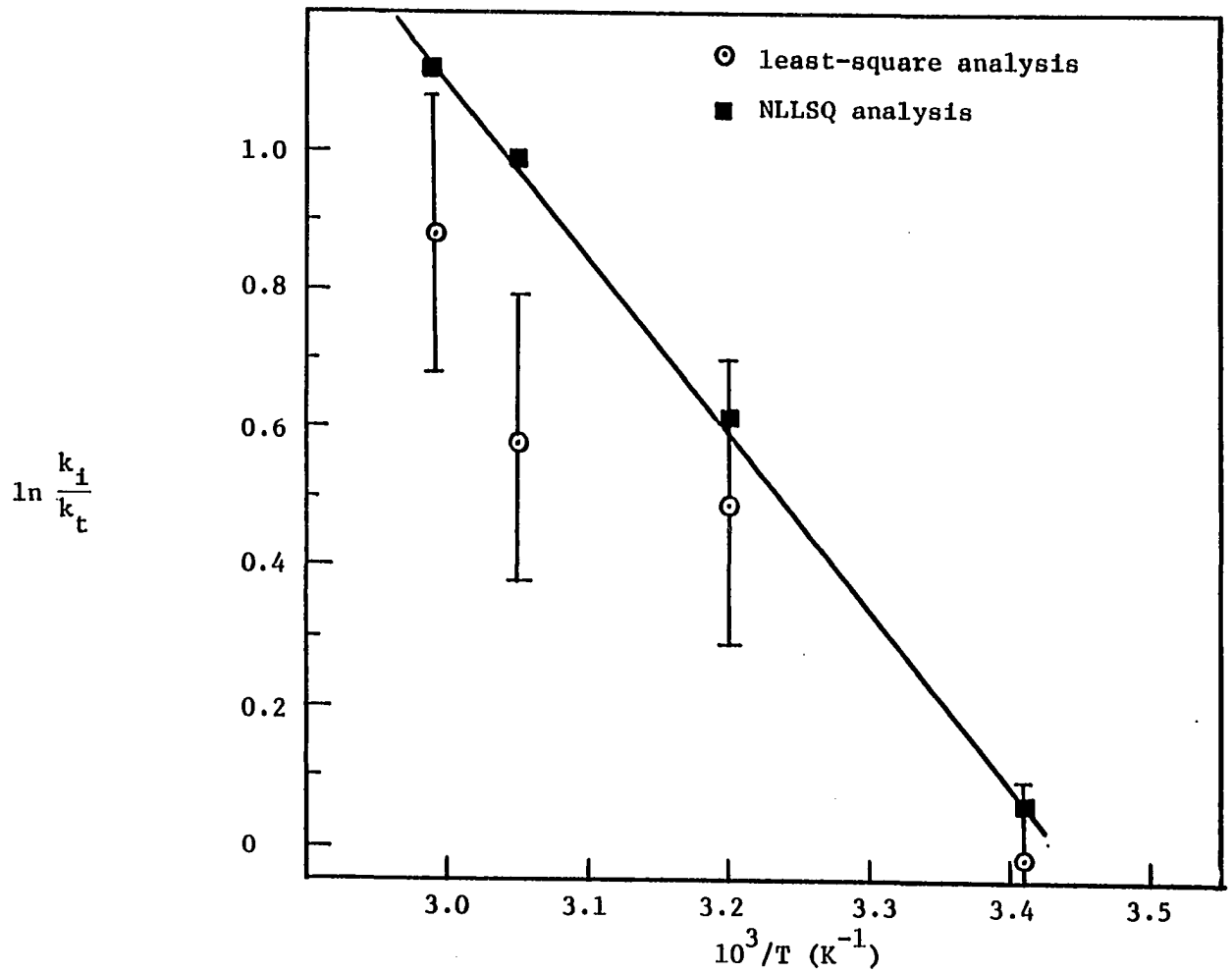

Figure 12. Plot of $\ln k_i/k_t$ vs. 1/T in 1-6% methanol in benzene

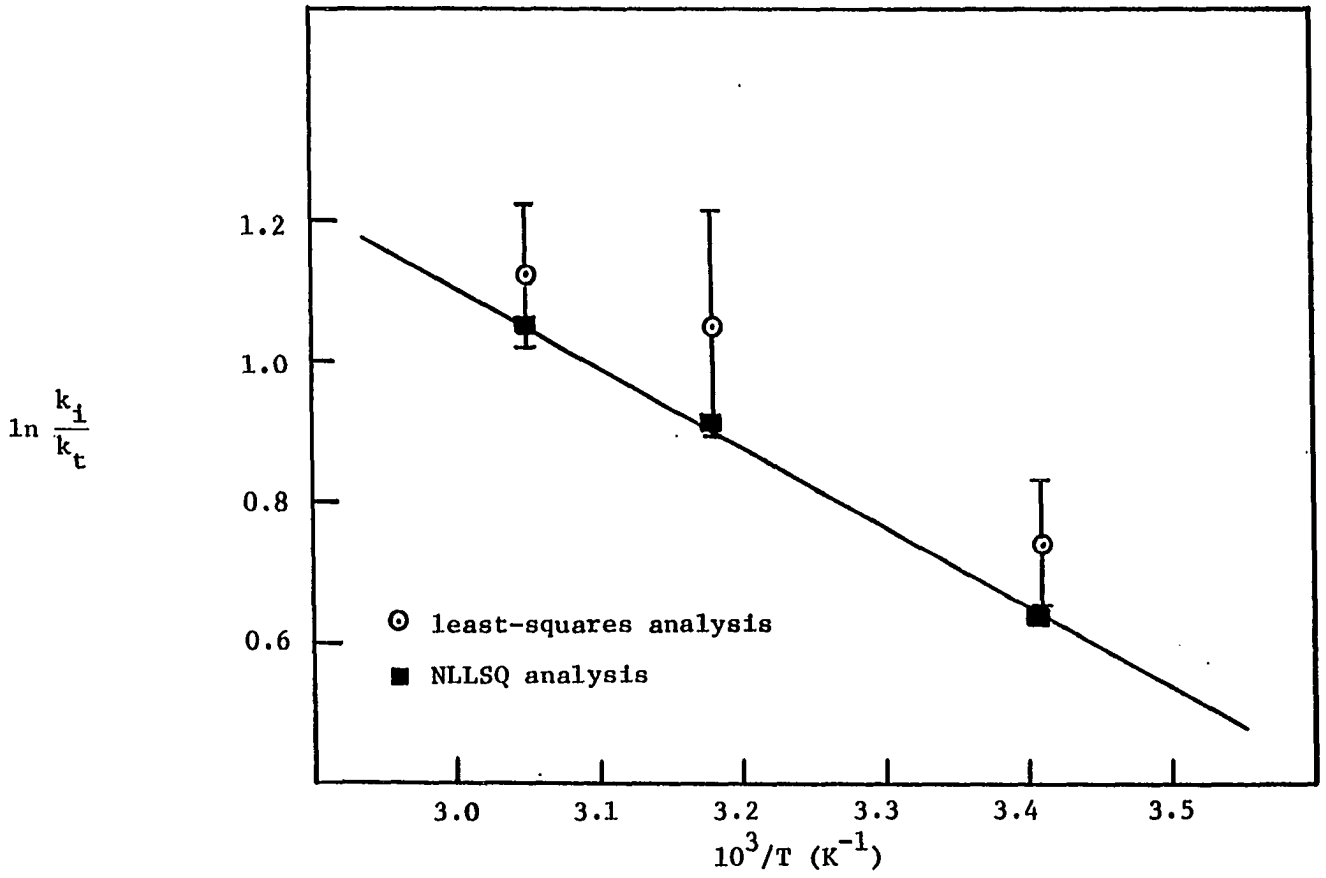

Figure 13. Plot of ln k_i/k_t vs. 1/T in 1-6% t-butanol in benzene

Scheme VIII

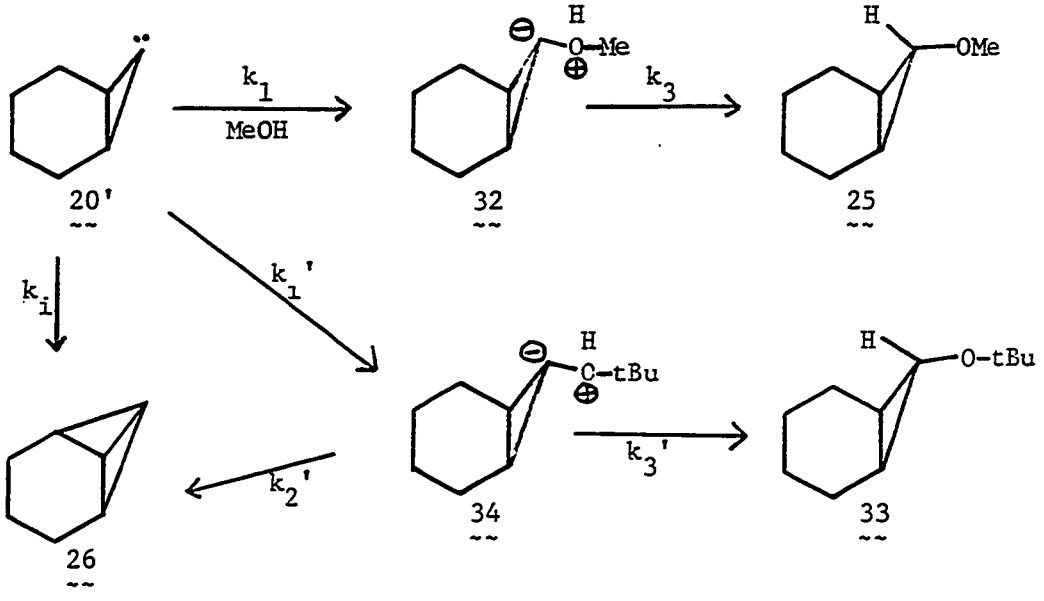

Based on Scheme VIII, equations (13) and (14) were derived as follows:

For competition experiments in mixtures of methanol and t-butanol:

$$\frac{d[25]}{dt} = k_1[MeOH][20']$$

$$\frac{d[33]}{dt} = \frac{k_1'k_3'}{k_2' + k_3'}[t\text{-BuOH}][20']$$

$$\frac{[25]}{[33]} = \frac{k_1(k_2' + k_3')}{k_1'k_3'} \cdot \frac{[MeOH]}{[t\text{-BuOH}]} = \frac{k_{t,MeOH}}{k_{t,t\text{-BuOH}}} \cdot \frac{[MeOH]}{[t\text{-BuOH}]} \qquad (13)$$

where $k_1 = k_{t,MeOH} \cdot \frac{k_1' k_3'}{k_2' + k_3'} = k_{t,t\text{-BuOH}}$.

For separate experiments in methanol of t-butanol:

$$\frac{[25]}{[26]} = \frac{k_1}{k_i} \cdot [MeOH]$$

$$\frac{[26]}{[33]} = \frac{k_2'}{k_3'} + \frac{k_i'(k_2' + k_3')}{k_1' k_3'} \cdot \frac{1}{[t\text{-BuOH}]}$$

(k_i' = rate constant for insertion in t-butanol)

Now, $[25]/[26] \cdot [26]/[33] = [25]/[33]$

$$\frac{[25]}{[33]} = \frac{k_1 k_2'}{k_i k_3'} \cdot [MeOH] + \frac{k_1 k_i'(k_2' + k_3')}{k_i k_1' k_3'} \cdot \frac{[MeOH]}{[t\text{-BuOH}]}$$

and

$$\frac{[25]}{[33]} \cdot \frac{1}{[MeOH]} = \frac{k_{t,MeOH}}{k_i} \cdot \frac{k_2'}{k_3'} + \frac{k_{t,MeOH}}{k_{t,t\text{-BuOH}}} \cdot \frac{k_i'}{k_i} \cdot \frac{1}{[t\text{-BuOH}]} \qquad (14)$$

The competition experiments were carried out in mixtures of methanol and t-butanol with different volume ratios. Tables 30 and 31 list the results.

When product ratios of 25/33 were plotted against the concentration ratios of [MeOH]/[t-BuOH], the relative reactivity of norcaranylidene in two different alcohols was obtained (by Apple computer least-squares analysis) based on equation (13) (Figure 14). In both cases, the plots were linear and methanol apparently reacted ∿2.5 times faster with

Table 30. Product distribution as a function of [MeOH]/[t-BuOH] from the reaction of 19' in 30% MeOH/t-BuOH in benzene at 30°C. S.M. = 0.027 mmole, [NaOMe]/[S.M.] = 7:1, total solvent volume = 0.4 ml

(V/V) MeOH/t-BuOH	$\frac{[MeOH]}{[t\text{-}BuOH]}$	% 26	% 25	% 33	25/33
1:1	2.33	35.1	48.0	7.1	6.71
1:2	1.16	42.6	44.9	11.6	3.86
1:5	0.46	50.1	32.8	15.2	2.16
1:9	0.26	56.3	22.9	20.5	1.12

Table 31. Product distribution as a function of [MeOH]/[t-BuOH] from the reaction of 19' in 3% MeOH/t-BuOH in benzene at 30°C. S.M. = 0.027 mmole, [NaOMe]/[S.M.] = 7:1, total solvent volume = 1.2 ml

(V/V) MeOH/t-BuOH	$\frac{[MeOH]}{[t\text{-}BuOH]}$	% 26	% 25	% 33	25/33
1:1	2.33	46.7	18.2	2.8	6.49
1:2	1.16	56.0	20.9	5.3	3.93
1:5	0.46	63.5	12.4	5.6	2.21
1:9	0.26	72.3	7.1	6.2	1.15

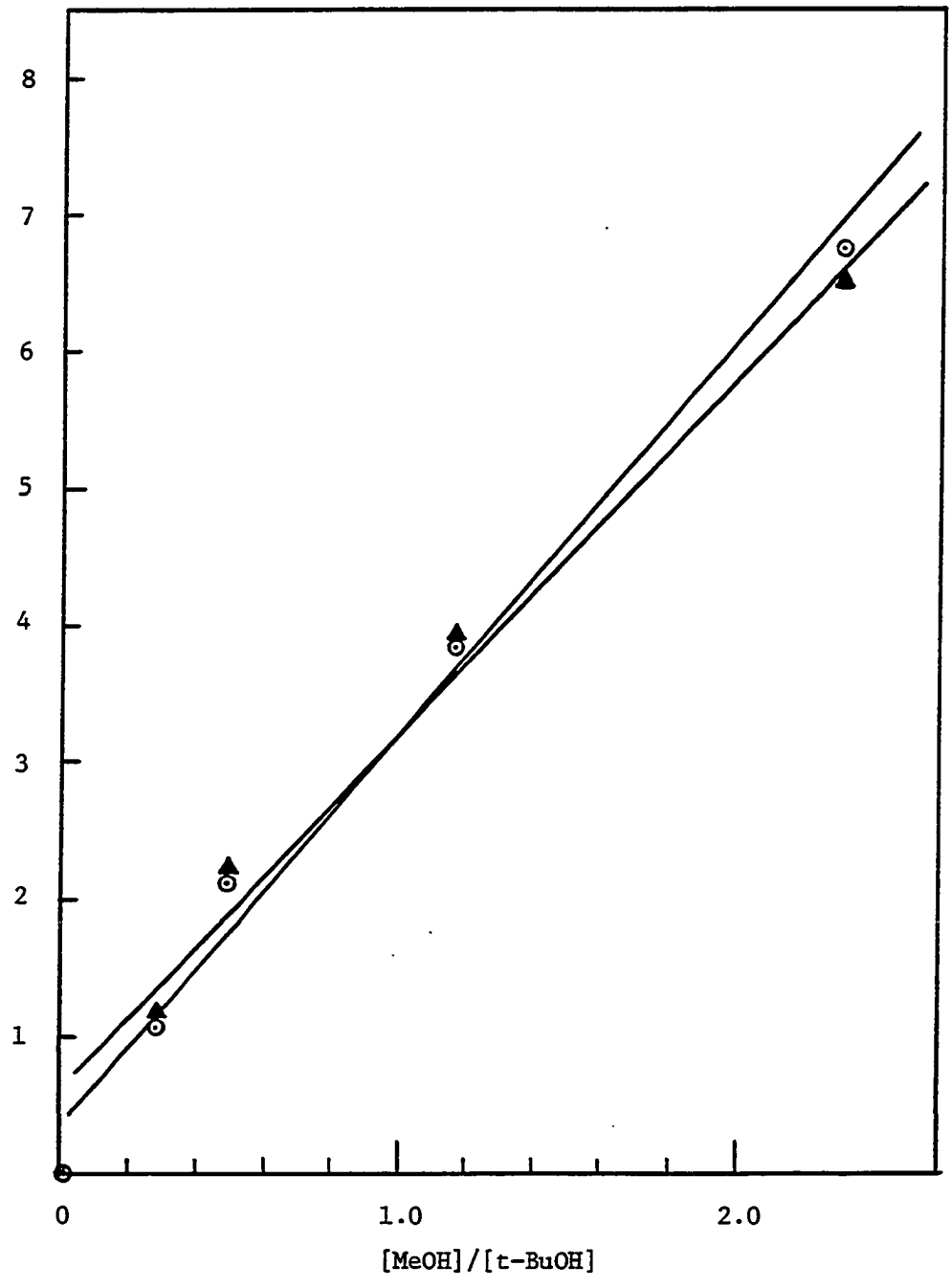

Figure 14. Plot of 25/33 vs. [MeOH]/[t-BuOH], 30°C

⊙ 30% alcohol, int. = 0.47 ± 0.20, slope = 2.86 ± 0.38

▲ 3% alcohol, int. = 0.53 ± 0.23, slope = 2.78 ± 0.42

carbene 20' than did t-butanol, regardless of the total alcohol concentrations (3% or 30%). However, the real carbenic reactivity rate (k_1/k_1', Scheme VIII) is 5.1-5.2 (slope of lines in Figure 14 times $(1 + k_2/k_3)$ -- see Table 19). These findings indicated that differential specific solvation effects did not need to be considered under these competition conditions. (Zupancic: the relative reactivity of F1 to methanol vs. t-butanol changed with total alcohol concentration (11), see Table 3).

Additionally, based on equation (14), the ratio of k_i'/k_i ($= k_{i,t\text{-BuOH}}/k_{i,MeOH}$) could be calculated using the values of $k_{t,MeOH}/k_{t,t\text{-BuOH}}$ derived from the competition experiments and the slope ($= (k_{t,MeOH} \cdot k_i')/(k_i \cdot k_{t\text{-BuOH}})$) of the plot of [(25]/[33]) · (1/[MeOH])] vs. 1/[t-BuOH] from the "separate" experimental data. Tables 32-37 list the data at different temperatures from "separate" experiments.

Figures 15-20 show the plots of [([25]/[33]) · (1/[MeOH])] vs. 1/[t-BuOH] at different temperatures. Table 38 lists the intercepts and slopes from those plots.

Since it was observed that the ratio of 25/33 increased linearly with [MeOH]/[t-BuOH] (Figure 14), values for $k_{t,MeOH}/k_{t,t\text{-BuOH}}$ could be obtained by applying equation (13) to the competition experiments' results (where one multiplies [25/33] by [t-BuOH]/[MeOH]). Table 39 lists the data from the reaction of 19' in 30% and 3% 1:2 (V/V) ([t-BuOH]/[MeOH] = 0.859) methanol/t-butanol in benzene at 25° and 45°C.

From the ratios of $k_{t,MeOH}/k_{t,t\text{-BuOH}}$, the activation parameters were obtained at "high" and "low" alcohol concentrations in the competition

Table 32. Product ratios from the reaction of 19' in 25-50% methanol or t-butanol at 25°C

$\frac{25}{26}$	$\frac{26}{33}$	$\frac{25}{33} = \frac{25}{26} \cdot \frac{26}{33}$	$\frac{1}{[MeOH]}$ (M^{-1})	$\frac{25}{33} \cdot \frac{1}{[MeOH]}$ (M^{-1})	$\frac{1}{[t\text{-}BuOH]}$ (M^{-1})
2.78	2.13	5.92	0.16	0.95	0.38
4.17	2.13	8.88	0.10	0.89	0.38
5.55	2.13	11.82	0.08	0.95	0.38
				(avg. 0.93 ± 0.03)	
2.78	1.71	4.75	0.16	0.76	0.24
4.17	1.71	7.13	0.10	0.71	0.24
5.55	1.71	9.49	0.08	0.76	0.24
				(avg. 0.74 ± 0.02)	
2.78	1.53	4.25	0.16	0.68	0.19
4.17	1.53	6.38	0.10	0.64	0.19
5.55	1.53	8.49	0.08	0.68	0.19
				(avg. 0.66 ± 0.02)	

Table 33. Product ratios from the reaction of 19' in 25-50% methanol or t-butanol at 35°C

$\frac{25}{26}$	$\frac{26}{33}$ [a]	$\frac{25}{33} = \frac{25}{26} \cdot \frac{26}{33}$	$\frac{1}{[MeOH]}$ (M^{-1})	$\frac{25}{33} \cdot \frac{1}{[MeOH]}$ (M^{-1})	$\frac{1}{[t\text{-}BuOH]}$ (M^{-1})
2.56	2.22	5.68	0.16	0.91	0.38
4.00	2.22	8.88	0.10	0.88	0.38
5.55	2.22	12.32	0.08	0.98	0.38
				(avg. 0.92 ± 0.04)	
2.56	1.73	4.43	0.16	0.71	0.24
4.00	1.73	6.92	0.10	0.69	0.24
5.55	1.73	9.60	0.08	0.77	0.24
				(avg. 0.72 ± 0.03)	
2.56	1.49	3.81	0.16	0.61	0.19
4.00	1.49	5.96	0.10	0.60	0.19
5.55	1.49	8.27	0.08	0.66	0.19
				(avg. 0.62 ± 0.02)	

[a]The average value (32°C and 37°C) was used in this column.

Table 34. Product ratios from the reaction of 19' in 25-50% methanol or t-butanol at 50°C

$\frac{25}{26}$	$\frac{26}{33}$	$\frac{25}{33} = \frac{25}{26} \cdot \frac{26}{33}$	$\frac{1}{[MeOH]}$ (M^{-1})	$\frac{25}{33} \cdot \frac{1}{[MeOH]}$ (M^{-1})	$\frac{1}{[t\text{-}BuOH]}$ (M^{-1})
2.44	2.51	6.12	0.16	0.98	0.38
4.71	2.51	10.47	0.10	1.04	0.38
5.26	2.51	13.20	0.08	1.05	0.38
				(avg. 1.02 ± 0.03)	
2.44	1.88	4.59	0.16	0.73	0.24
4.17	1.88	7.84	0.10	0.78	0.24
5.26	1.88	9.89	0.08	0.79	0.24
				(avg. 0.77 ± 0.02)	
2.44	1.67	4.07	0.16	0.65	0.19
4.17	1.67	6.96	0.10	0.69	0.19
5.26	1.67	8.78	0.08	0.70	0.19
				(avg. 0.68 ± 0.02)	

Table 35. Product ratios from the reaction of 19' in 1-6% methanol or t-butanol at 20°C

$\frac{25}{26}$	$\frac{26}{33}$	$\frac{25}{33} = \frac{25}{26} \cdot \frac{26}{33}$	$\frac{1}{[MeOH]}$ (M^{-1})	$\frac{25}{33} \cdot \frac{1}{[MeOH]}$ (M^{-1})	$\frac{1}{[t\text{-}BuOH]}$ (M^{-1})
0.22	20.2	4.44	4.0	17.76	9.4
0.63	20.2	12.73	2.0	25.46	9.4
0.71	20.2	14.34	1.4	20.08	9.4
1.56	20.2	31.51	0.7	22.06	9.4
				(avg. 21.34 ± 2.42)	
0.22	10.5	2.31	4.0	9.24	4.7
0.63	10.5	6.61	2.0	13.22	4.7
0.71	10.5	7.45	1.4	10.43	4.7
1.56	10.5	16.38	0.7	11.47	4.7
				(avg. 11.09 ± 1.26)	
0.22	8.5	1.87	4.0	7.48	3.1
0.63	8.5	5.36	2.0	10.72	3.1
0.71	8.5	6.03	1.4	8.44	3.1
1.56	8.5	13.26	0.7	9.28	3.1
				(avg. 8.98 ± 1.10)	
0.22	4.2	0.92	4.0	3.68	1.6
0.63	4.2	2.65	2.0	5.30	1.6
0.71	4.2	2.98	1.4	4.17	1.6
1.56	4.2	6.55	0.7	4.58	1.6
				(avg. 4.43 ± 0.51)	

Table 36. Product ratios from the reaction of 19' in 1-6% methanol or t-butanol at 40°C

$\frac{25}{26}$	$\frac{26}{33}$	$\frac{25}{33} = \frac{25}{26} \cdot \frac{26}{33}$	$\frac{1}{[MeOH]}$ (M^{-1})	$\frac{25}{33} \cdot \frac{1}{[MeOH]}$ (M^{-1})	$\frac{1}{[t\text{-}BuOH]}$ (M^{-1})
0.15	27.7	4.15	4.0	16.6	9.4
0.27	27.7	7.48	2.0	15.0	9.4
0.65	27.7	18.00	1.4	25.2	9.4
1.20	27.7	33.24	0.7	23.3	9.4
				(avg. 20.0 ± 4.2)	
0.15	18.1	2.71	4.0	10.8	4.7
0.27	18.1	4.89	2.0	9.8	4.7
0.65	18.1	11.76	1.4	16.5	4.7
1.20	18.1	21.72	0.7	15.2	4.7
				(avg. 13.1 ± 2.8)	
0.15	14.4	2.16	4.0	8.6	3.1
0.27	14.4	3.89	2.0	7.8	3.1
0.65	14.4	9.36	1.4	13.1	3.1
1.20	14.4	17.28	0.7	12.1	3.1
				(avg. 10.4 ± 2.2)	
0.15	7.4	1.11	4.0	4.4	1.6
0.27	7.4	2.00	2.0	4.0	1.6
0.65	7.4	4.81	1.4	6.7	1.6
1.20	7.4	8.88	0.7	7.1	1.6
				(avg. 5.6 ± 1.4)	

Table 37. Product ratios from the reaction of 19' in 1-6% methanol or t-butanol at 55°C

$\frac{25}{26}$	$\frac{26}{33}$	$\frac{25}{33} = \frac{25}{26} \cdot \frac{26}{33}$	$\frac{1}{[MeOH]}$ (M^{-1})	$\frac{25}{33} \cdot \frac{1}{[MeOH]}$ (M^{-1})	$\frac{1}{[t\text{-}BuOH]}$ (M^{-1})
0.11	31.4	3.45	4.0	13.8	9.4
0.36	31.4	11.30	2.0	22.6	9.4
0.40	31.4	12.56	1.4	17.6	9.4
0.90	31.4	28.26	0.7	19.8	9.4
				(avg. 18.4 ± 2.8)	
0.11	18.2	2.00	4.0	8.0	4.7
0.36	18.2	6.55	2.0	13.1	4.7
0.40	18.2	7.28	1.4	10.2	4.7
0.90	18.2	16.38	0.7	11.5	4.7
				(avg. 10.7 ± 1.6)	
0.11	15.0	1.65	4.0	6.6	3.1
0.36	15.0	5.40	2.0	10.8	3.1
0.40	15.0	6.00	1.4	8.4	3.1
0.90	15.0	13.50	0.7	9.4	3.1
				(avg. 8.8 ± 1.3)	
0.11	8.4	0.92	4.0	3.8	1.6
0.36	8.4	3.02	2.0	6.0	1.6
0.40	8.4	3.36	1.4	4.7	1.6
0.90	8.4	7.56	0.7	5.3	1.6
				(avg. 4.9 ± 0.7)	

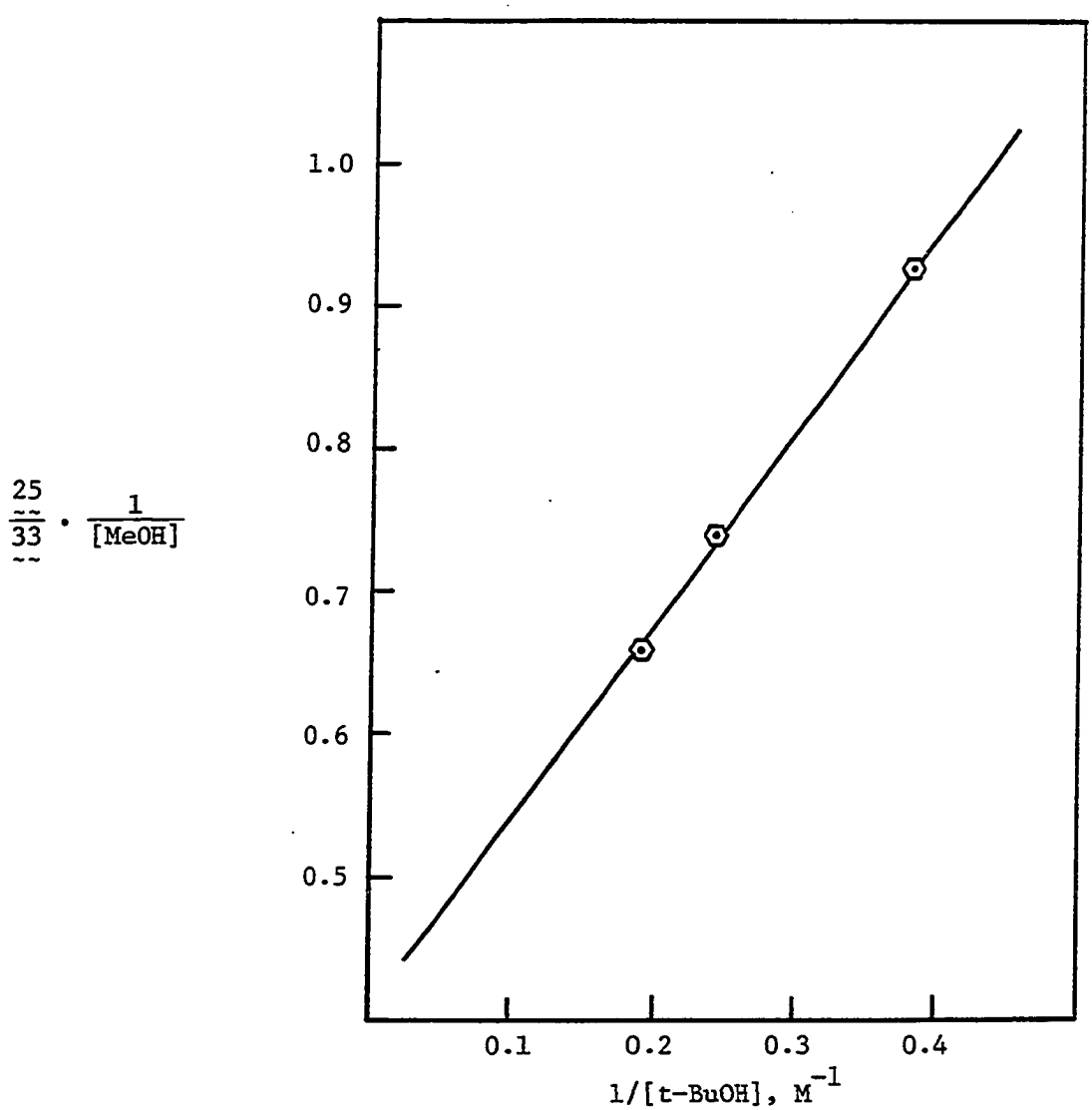

Figure 15. Plot of $[(\underset{\sim\sim}{25}/\underset{\sim\sim}{33}) \cdot (1/[MeOH])]$ vs. 1/[t-BuOH] at 25°C in 25-50% alcohols. r = 0.998, int. = 0.40 ± 0.02, slope = 1.36 ± 0.07

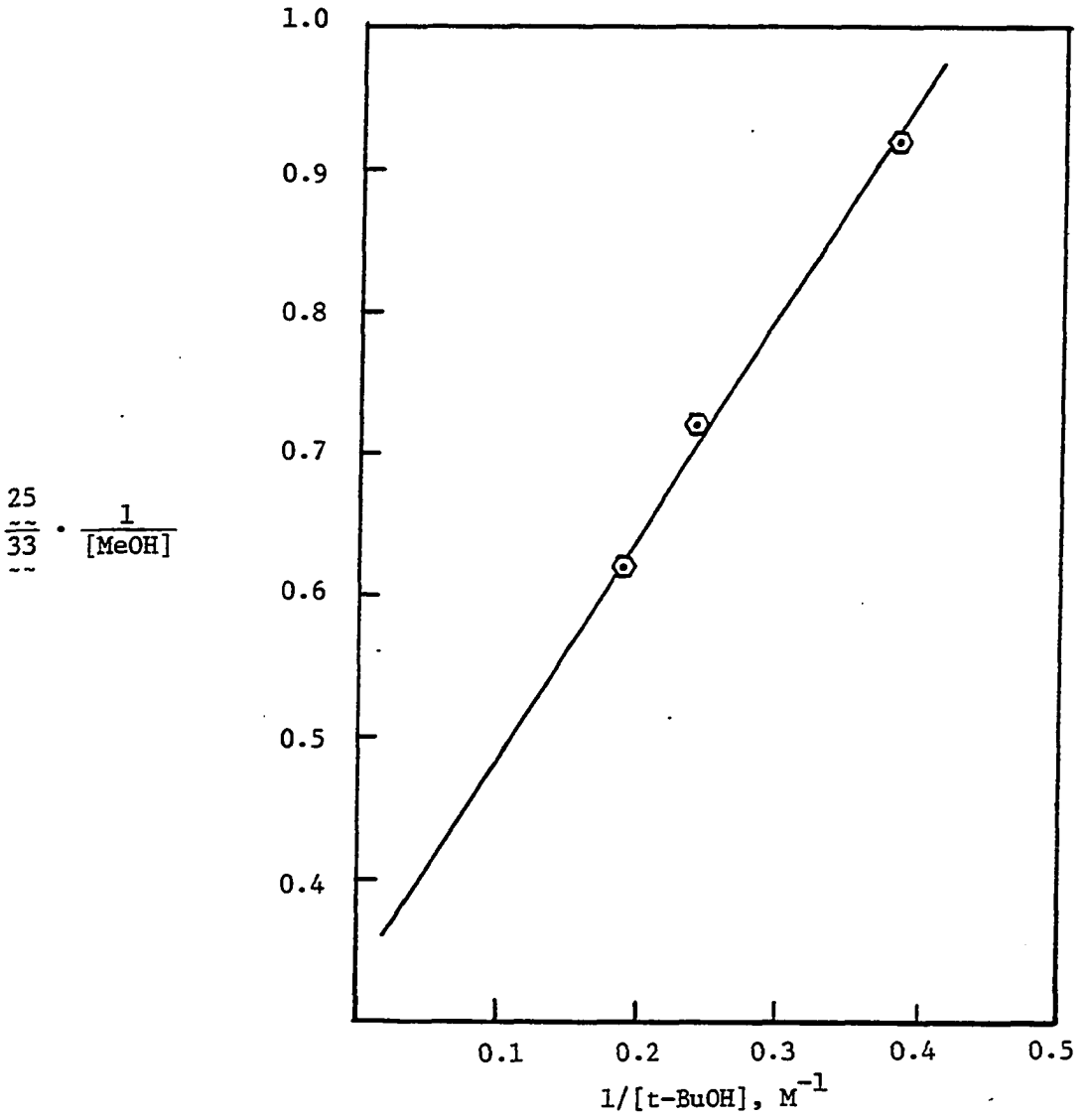

Figure 16. Plot of $[(\underset{\sim\sim}{25}/\underset{\sim\sim}{33}) \cdot (1/[MeOH])]$ vs. 1/[t-BuOH] at 35°C in 25-50% alcohols. r = 0.997, int. = 0.33 ± 0.03, slope = 1.57 ± 0.14

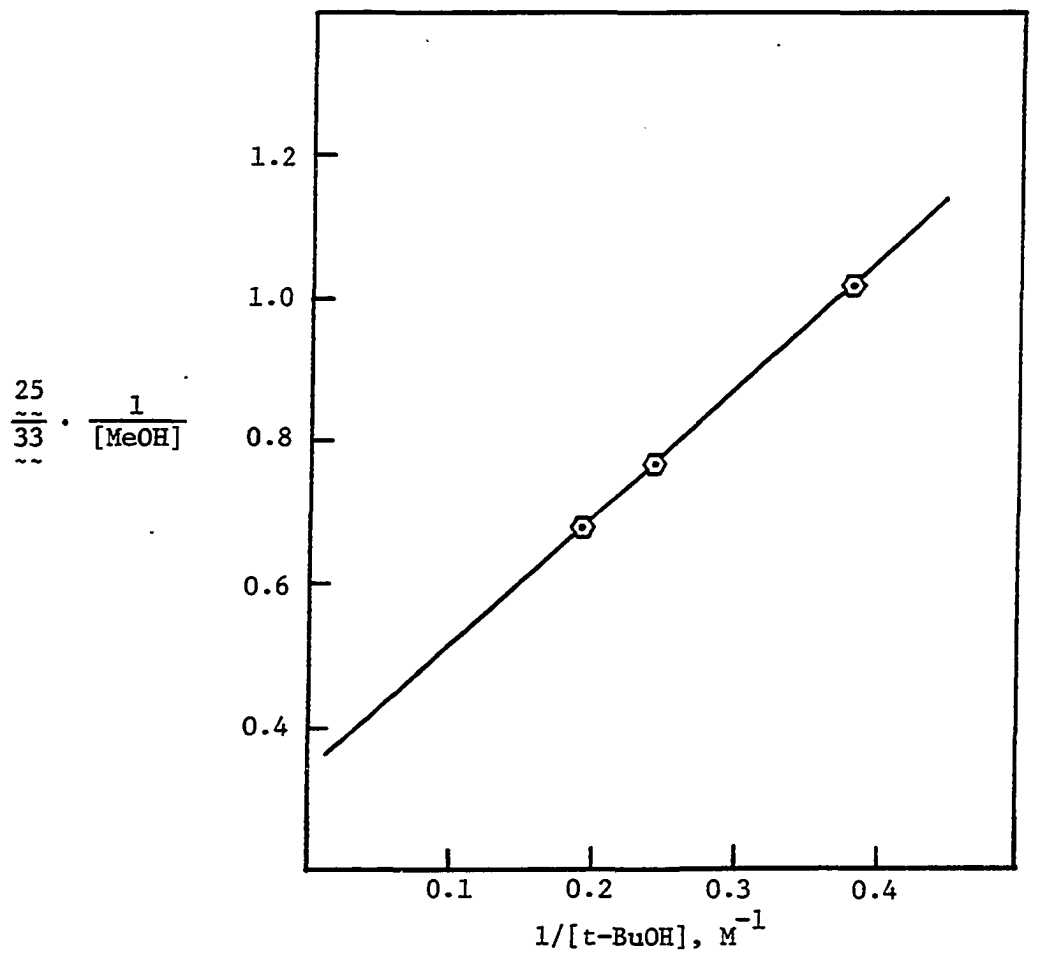

Figure 17. Plot of $[(\underset{\sim\sim}{25}/\underset{\sim\sim}{33}) \cdot (1/[MeOH])]$ vs. 1/[t-BuOH] at 50°C in 25-50% alcohols. r = 0.999, int. = 0.340 ± 0.001, slope = 1.790 ± 0.003

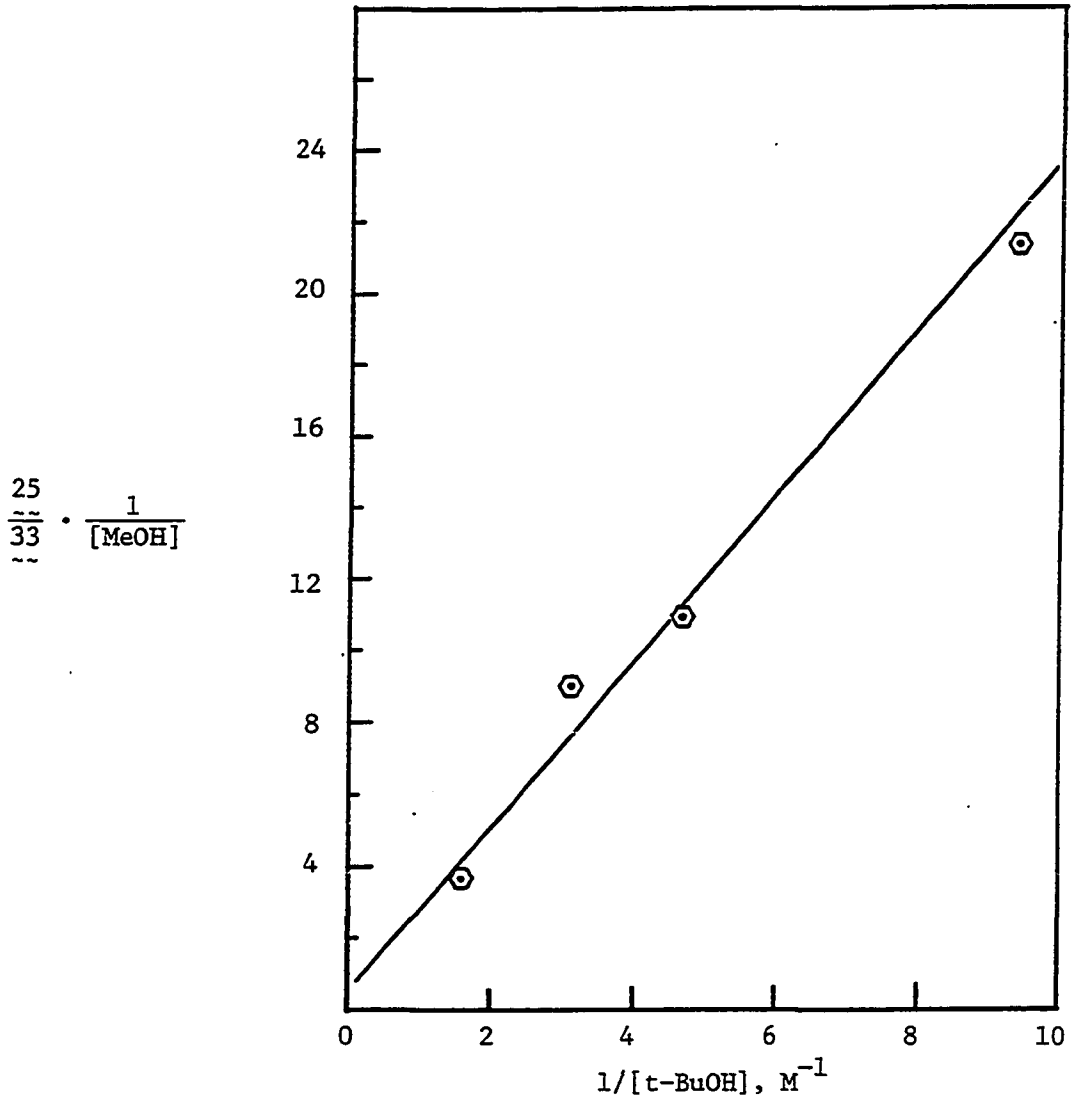

Figure 18. Plot of $[(\underset{\sim\sim}{25}/\underset{\sim\sim}{33}) \cdot (1/[MeOH])]$ vs. 1/[t-BuOH] in 1-6% alcohols at 20°C. $\underset{\sim\sim}{r} = 0.994$, int. = 0.12 ± 0.14, slope = 2.29 ± 0.05

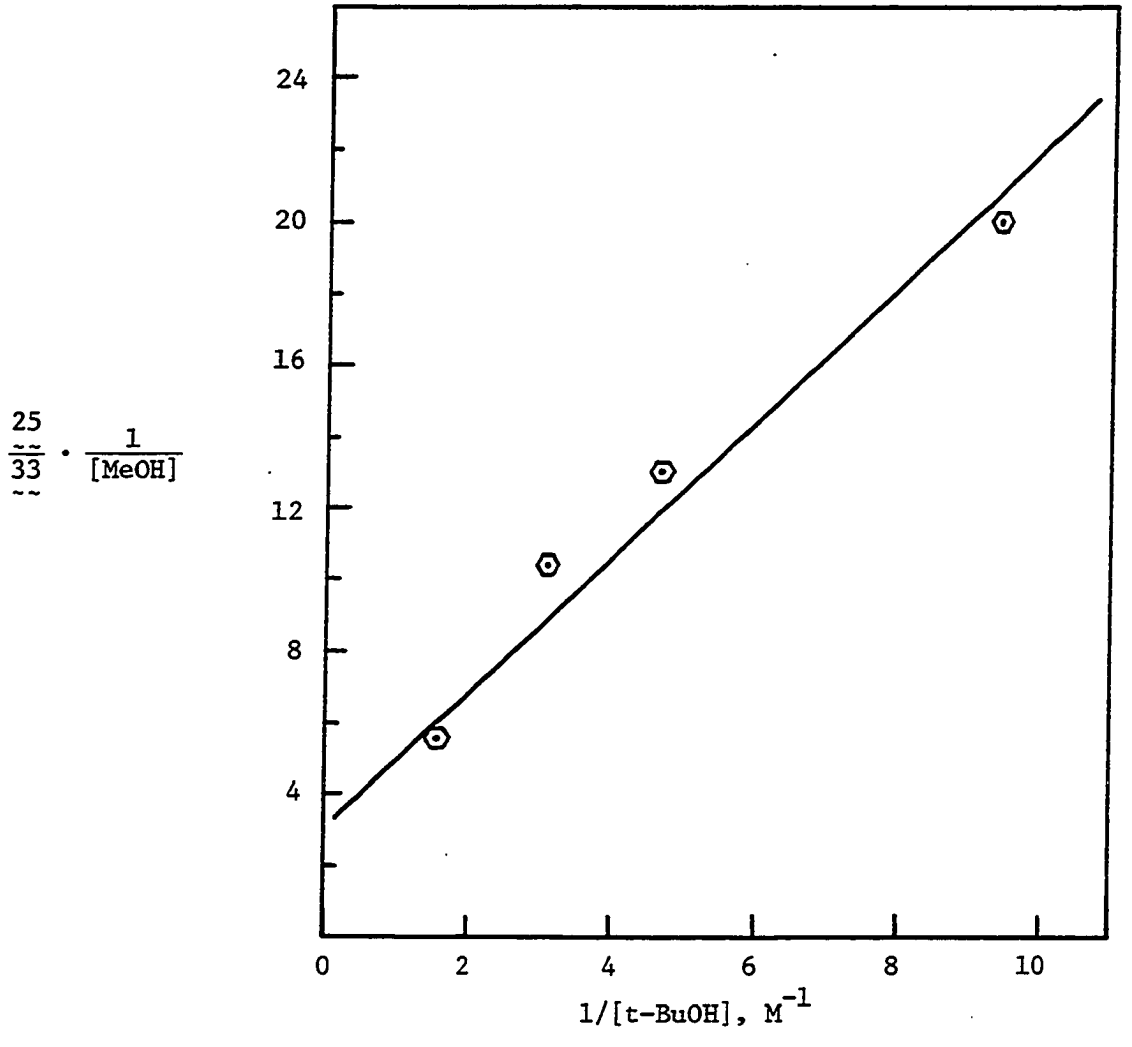

Figure 19. Plot of $[(\underset{\sim\sim}{25}/\underset{\sim\sim}{33}) \cdot (1/[MeOH])]$ vs. 1/[t-BuOH] in 1-6% alcohols at 40°C. $\underset{\sim\sim}{r} = 0.984$, int. = 2.74 ± 1.01, slope = 2.02 ± 0.31

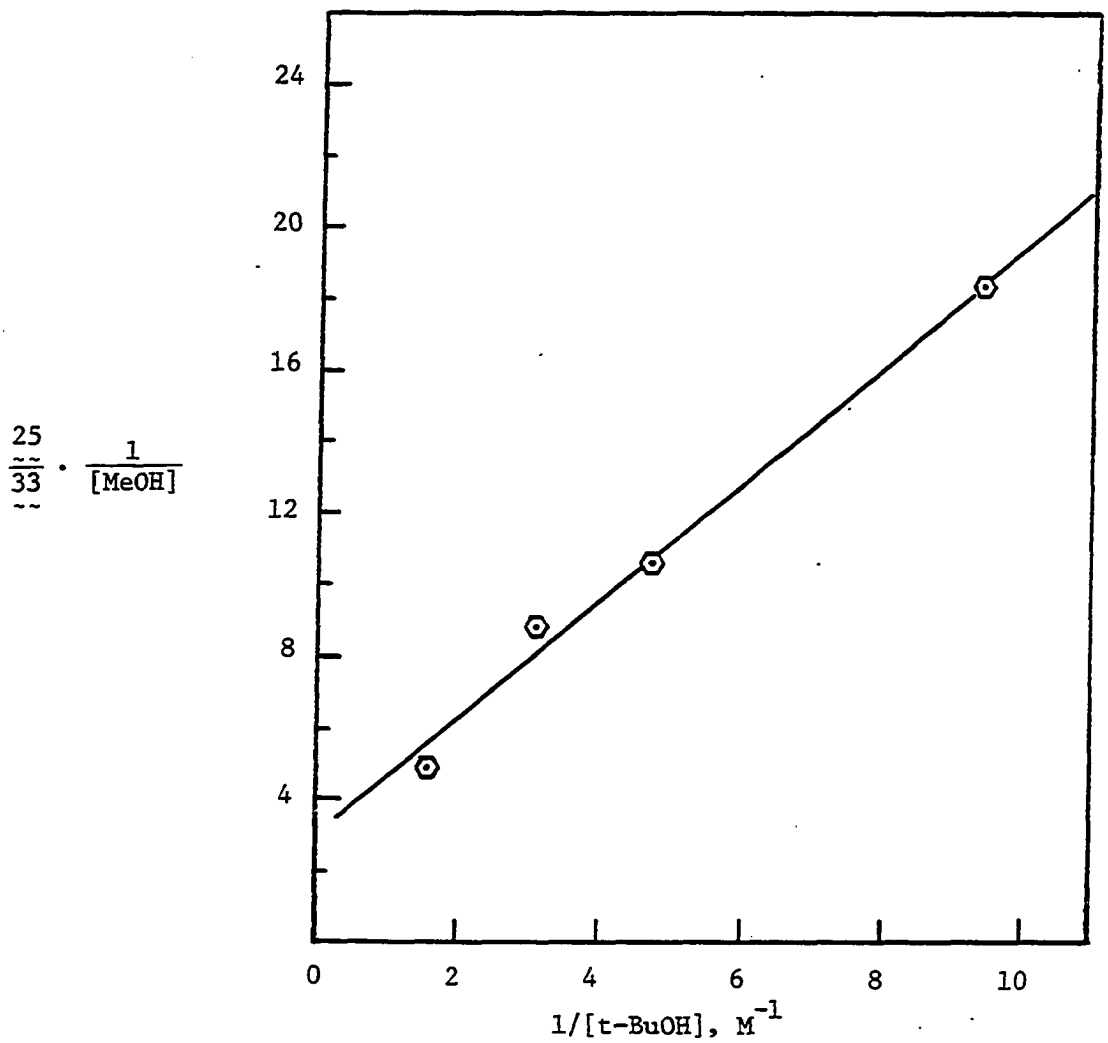

Figure 20. Plot of $[(25/33) \cdot (1/[MeOH])]$ vs. 1/[t-BuOH] in 1-6% alcohols at 55°C. $r = 0.995$, int. = 2.25 ± 0.61, slope = 1.80 ± 0.19

Table 38. Intercepts and slopes from Figures 15-20

T (°C)	% ROH	Int. = $\frac{k_{t,MeOH} \cdot k_2'}{k_i \cdot k_3'}$	Slope = $\frac{k_{t,MeOH} \cdot k_i'}{k_{t,t\text{-}BuOH} \cdot k_i}$
25	25-50	0.40 ± 0.02 (0.38)[a]	1.36 ± 0.07
35	25-50	0.33 ± 0.03 (0.31)[a]	1.57 ± 0.14
50	25-50	0.34 ± 0.01 (0.29)[a]	1.79 ± 0.01
20	1-6	0.12 ± 0.14[b]	2.29 ± 0.05
40	1-6	2.74 ± 1.01[b]	2.02 ± 0.31
55	1-6	2.25 ± 0.61[b]	1.80 ± 0.19

[a]Values in parentheses are from separate data in Tables 16 and 19.

[b]These data are meaningless since the intercepts at 1/[t-BuOH] = 0 are out of the region being studied.

Table 39. Product distribution from the reaction of 19' in 30% and 3% 1:2 (V/V) methanol/t-butanol in benzene

T (°C)	% ROH	% 25	% 33	% 26	25/33	$\frac{k_{t,\ MeOH}}{k_{t,t\text{-}BuOH}}$
25	30	27.9	8.35	18.9	3.34	2.86
45	30	23.2	7.87	25.8	2.95	2.53
25	3	11.7	3.86	48.0	3.03	2.60
45	3	6.2	2.35	39.8	2.64	2.25

experiments. Tables 40 and 41 give the kinetic parameters, Figures 21-22 show the Arrhenius plots, and Table 44 contains the derived activation parameters.

We next calculated the ratios of k_i/k_i' (= $k_{i,MeOH}/k_{i,t\text{-}BuOH}$) from the values of $k_{t,MeOH}/k_{t,t\text{-}BuOH}$ (data from competition experiments) and the slopes given in Table 38 (data from experiments in the separate alcohols). Tables 42 and 43, and Figures 23 and 24 give the results.

With the activation parameters from Figures 21 to 24 in hand, activation enthalpy and entropy diagrams at low or high alcohol concentrations were constructed (Figures 25-28). Table 44 lists the activation parameters associated with the combined MeOH/tBuOH experiments.

On the basis of these activation parameters, a reasonable interpretation is as follows. At "high" alochol concentration, carbene 20' is preferentially solvated by t-BuOH (methanol forms oligomers via H-bonding which are less nucleophilic than t-BuOH monomers present in the mixture). The necessity for desolvation in the transition state for insertion makes the insertion process entropically more favored in t-BuOH than in MeOH (where the oligomers must solvate 20'). However, when the alcohol concentration is "low", more methanol monomers are present in the solution, which increases the solvating ability of MeOH. Now carbene 20' may be solvated essentially equally by either MeOH or t-BuOH; in terms of solvation, it is as if there were only a single alcohol species present at "low" alcohol concentration. If the above is correct, then the ~2.5-fold reactivity advantage of MeOH over t-BuOH at both "high" and "low" alcohol concentrations can be understood -- no specific solvation

Table 40. The ratios of $k_{t,MeOH}/k_{t,t-BuOH}$ as a function of temperature in 30% alcohols

T (°C)	$10^3/T$ (K^{-1})	$\frac{k_{t,MeOH}}{k_{t,t-BuOH}} = A$	ln A
25	3.35	2.86	1.05
30	3.30	2.78[a]	1.02
45	3.14	2.53	0.93

[a]This value was obtained from Table 30 by least-squares analysis (r = 0.992) on a hand calculator.

Table 41. The ratios of $k_{t,MeOH}/k_{t,t-BuOH}$ as a function of temperature in 3% alcohols

T (°C)	$10^3/T$ (K^{-1})	$\frac{k_{t,MeOH}}{k_{t,t-BuOH}} = B$	ln B
25	3.35	2.60	0.96
30	3.30	2.48[a]	0.91
45	3.14	2.25	0.81

[a]This value was obtained from Table 31 by least-squares analysis (r = 0.994) on a hand calculator.

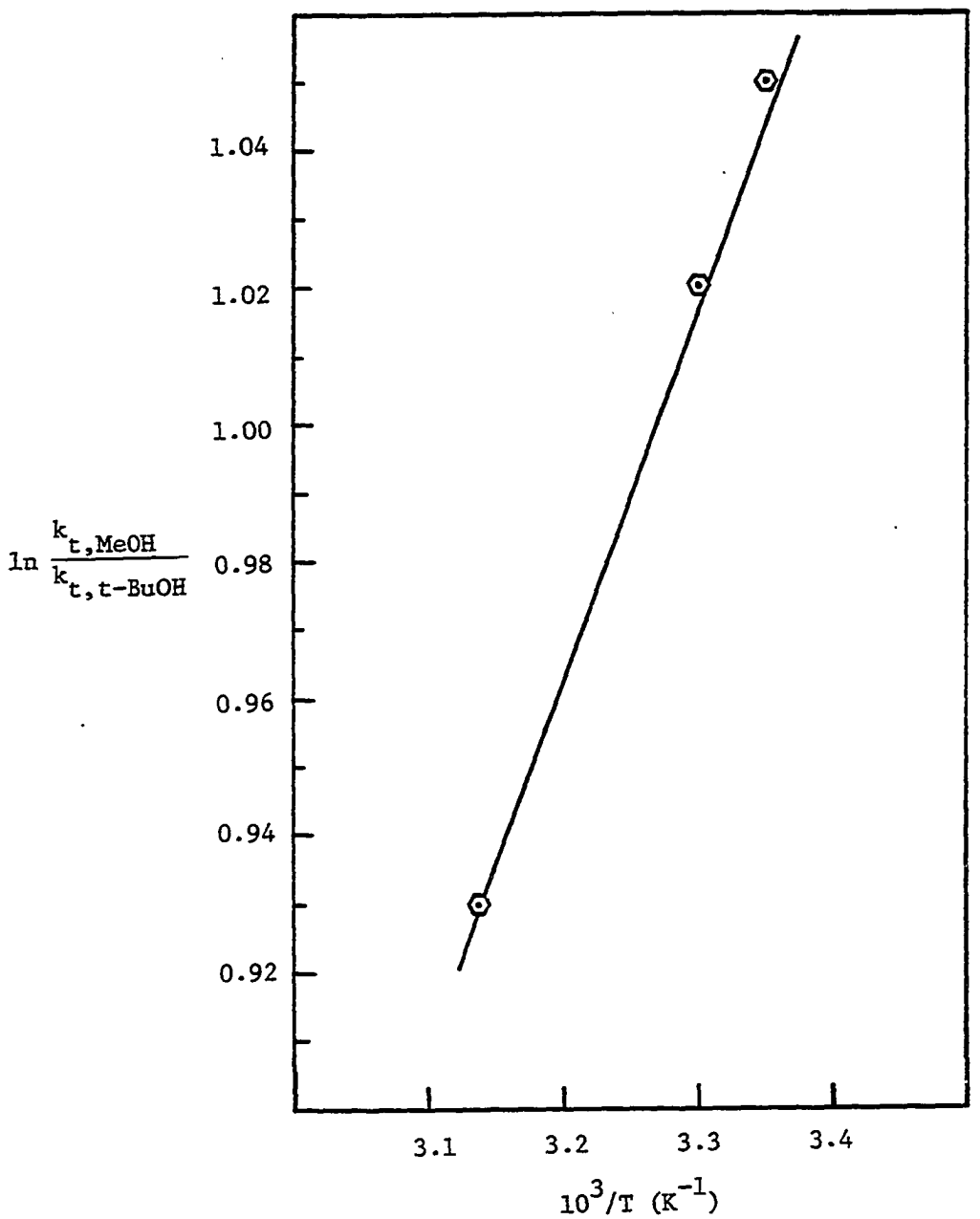

Figure 21. Plot of $\ln (k_{t,MeOH}/k_{t,t\text{-}BuOH})$ vs. 1/T in 30% alcohols. r = 0.999, int. = -0.85 ± 0.02, slope = 568.9 ± 6.8

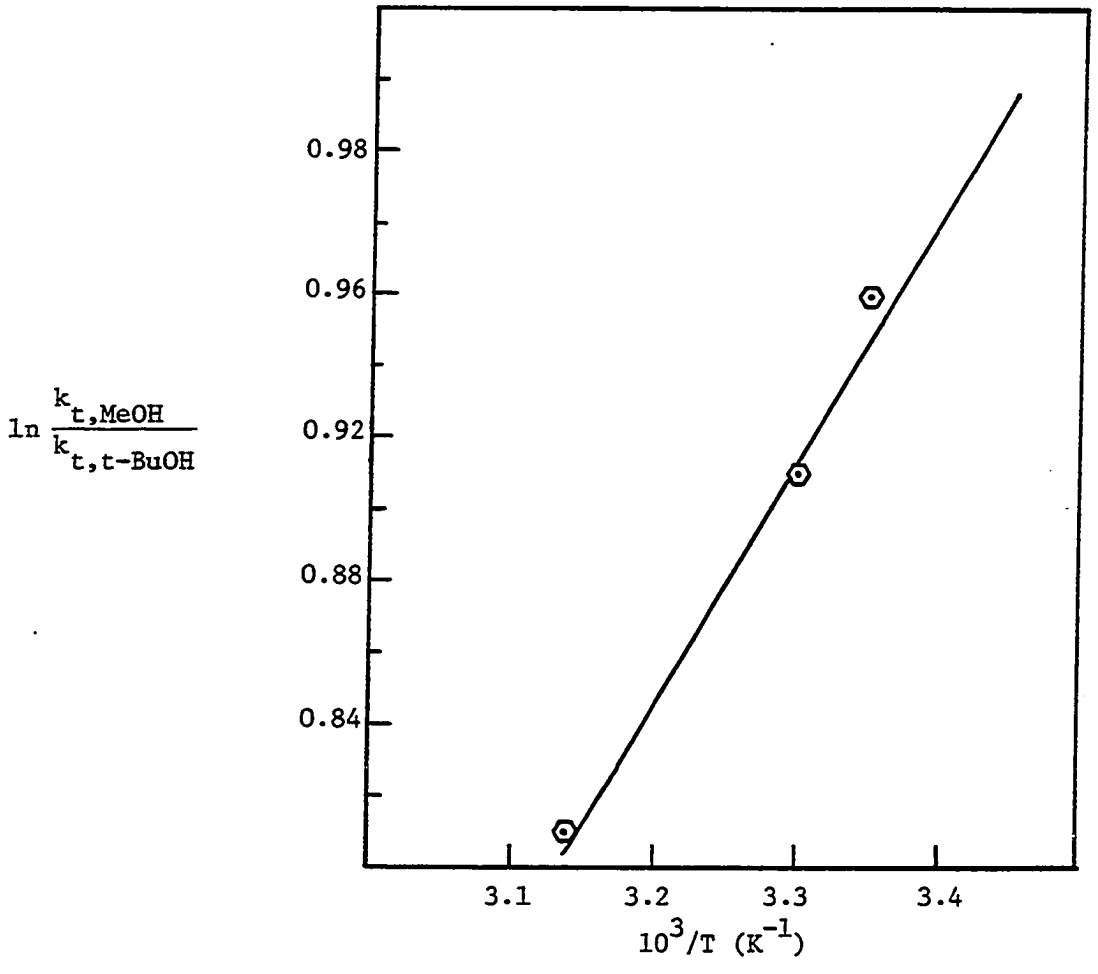

Figure 22. Plot of $\ln(k_{t,MeOH}/k_{t,t\text{-}BuOH})$ vs. 1/T in 3% alcohols. r = 0.995, int. = -1.35 ± 0.21, slope = 687.8 ± 67.2

Table 42. The ratios of $k_{i,MeOH}/k_{i,t\text{-}BuOH}$ as a function of temperature in 25-50% alcohols

T (°C)	$10^3/T$ (K^{-1})	$\frac{k_{t,MeOH}}{k_{t,t\text{-}BuOH}}$	$\frac{k_{i,MeOH}}{k_{i,t\text{-}BuOH}} = A$	ln A
25	3.35	2.86	2.10 ± 0.10	0.74 ± 0.04
35	3.25	2.70[a]	1.72 ± 0.15	0.54 ± 0.08
50	3.10	2.47[a]	1.38 ± 0.08	0.32 ± 0.05

[a]Values are interpolated from Figure 21.

Table 43. The ratios of $k_{i,MeOH}/k_{i,t\text{-}BuOH}$ as a function of temperature in 1-6% alcohols

T (°C)	$10^3/T$ (K^{-1})	$\frac{k_{t,MeOH}}{k_{t,t\text{-}BuOH}}$	$\frac{k_{i,MeOH}}{k_{i,t\text{-}BuOH}} = B$	ln B
20	3.41	2.69[a]	1.14 ± 0.02	0.13 ± 0.01
40	3.19	2.32[a]	1.23 ± 0.18	0.21 ± 0.14
55	3.05	2.11[a]	1.25 ± 0.13	0.22 ± 0.10

[a]Values are interpolated from Figure 22.

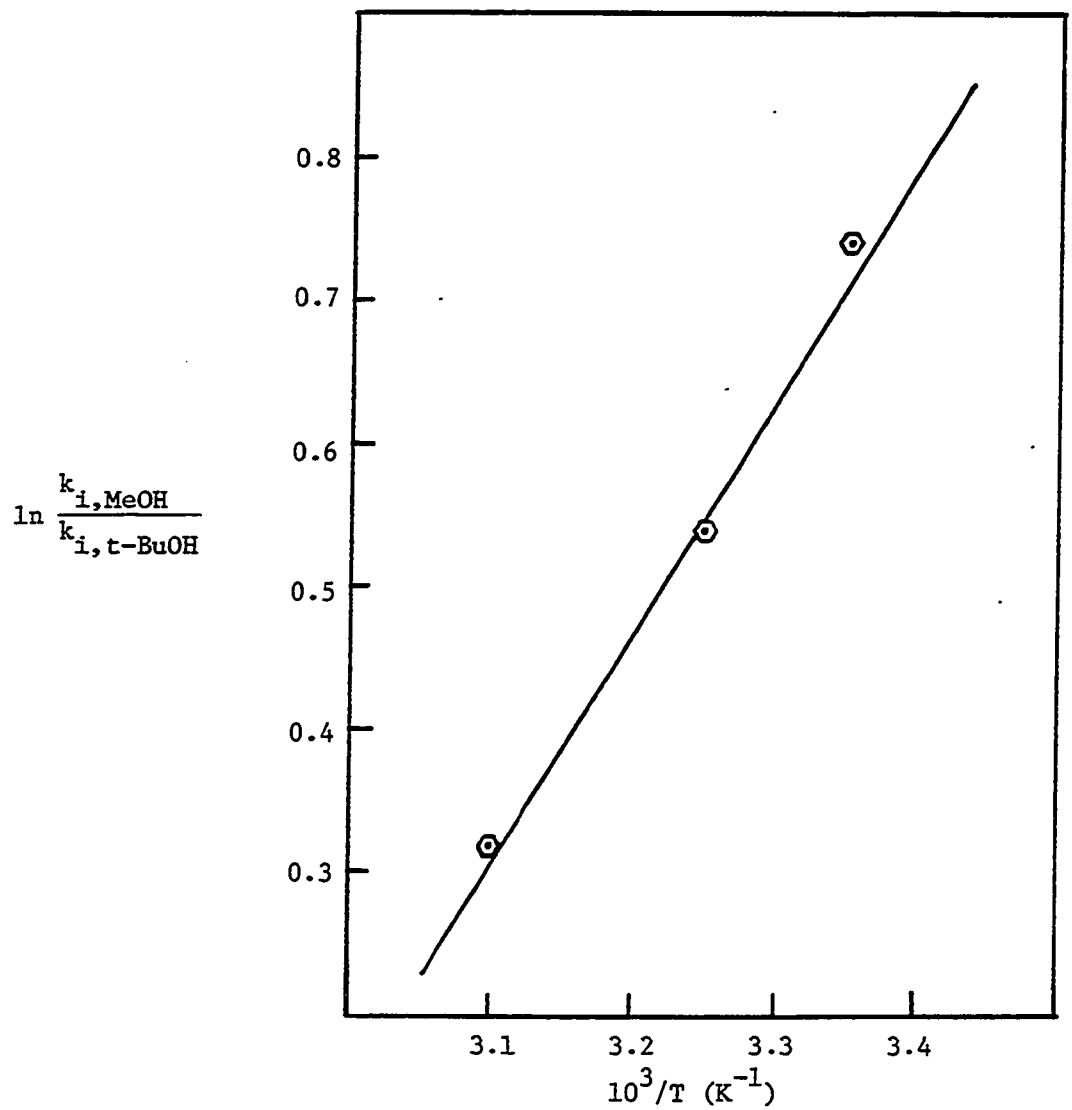

Figure 23. Plot of ln $(k_{i,MeOH})/k_{i,t\text{-}BuOH}$ vs. 1/T in 25-50% alcohols. r = 0.996, int. = -4.66 ± 0.39, slope = 1607.1 ± 125.6

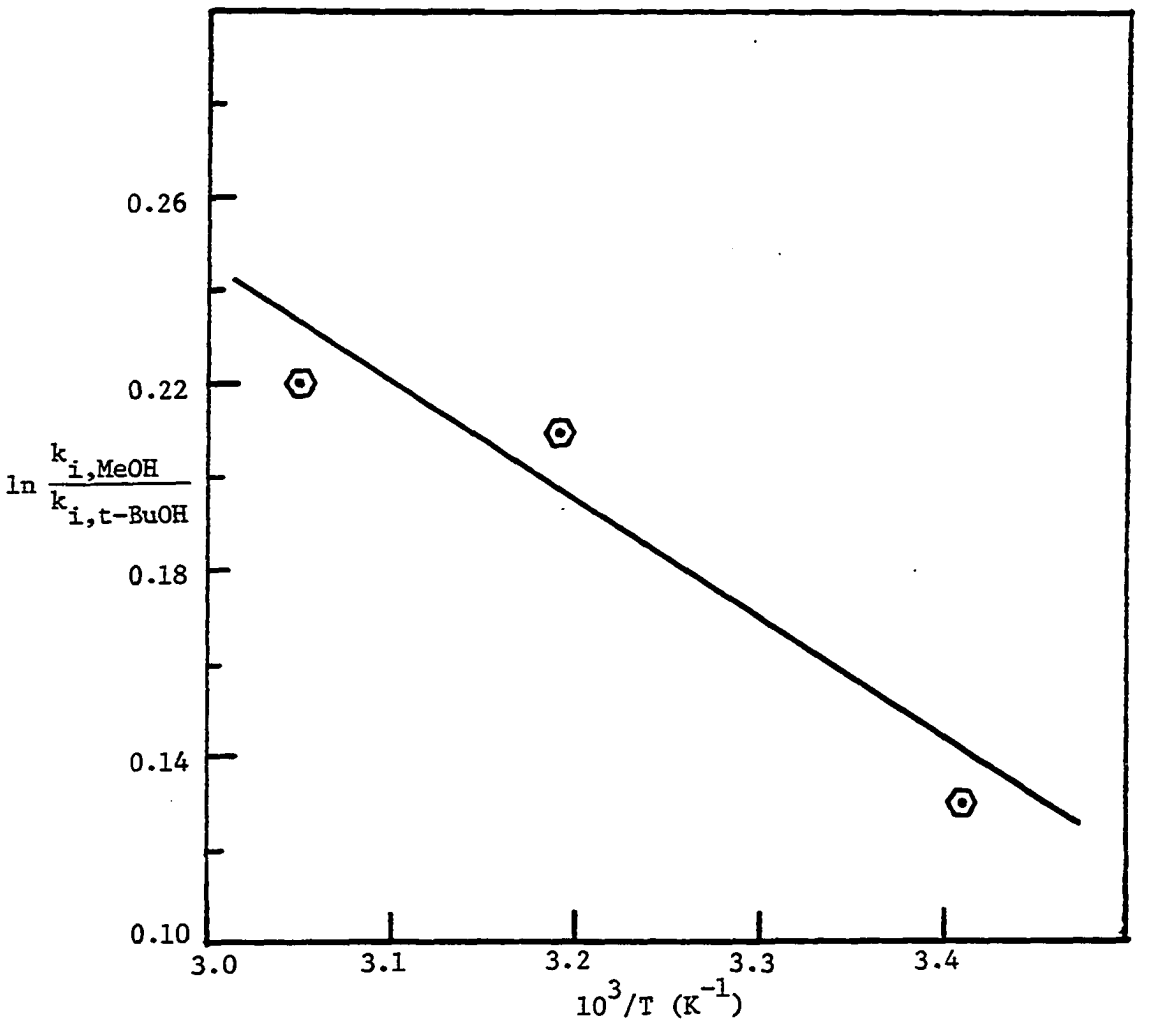

Figure 24. Plot of $\ln(k_{i,MeOH}/k_{i,t-BuOH})$ vs. 1/T in 1-6% alcohols. r = 0.960, int. = 1.06 ± 0.21, slope = -274.6 ± 65.2

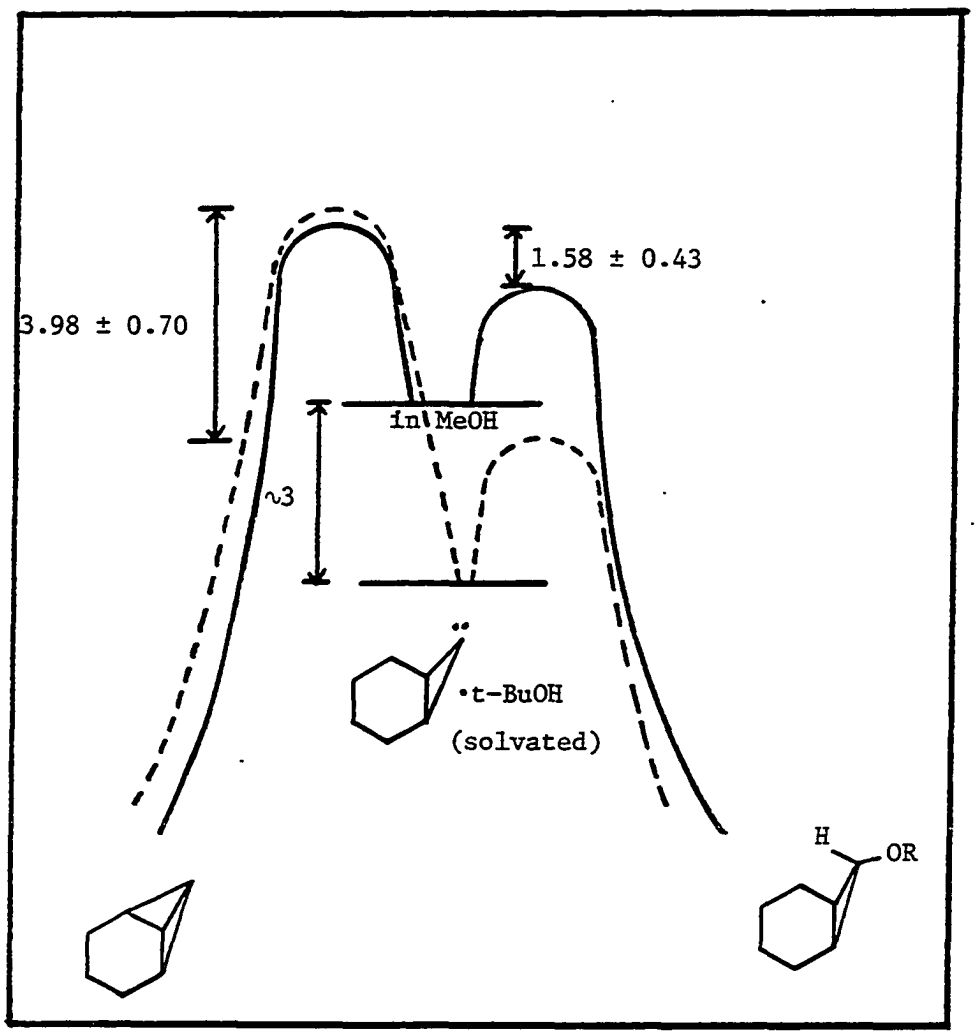

$\Delta H^{\neq}$

Figure 25. Enthalpy diagram in 30% alcohol

——— MeOH
- - - t-BuOH

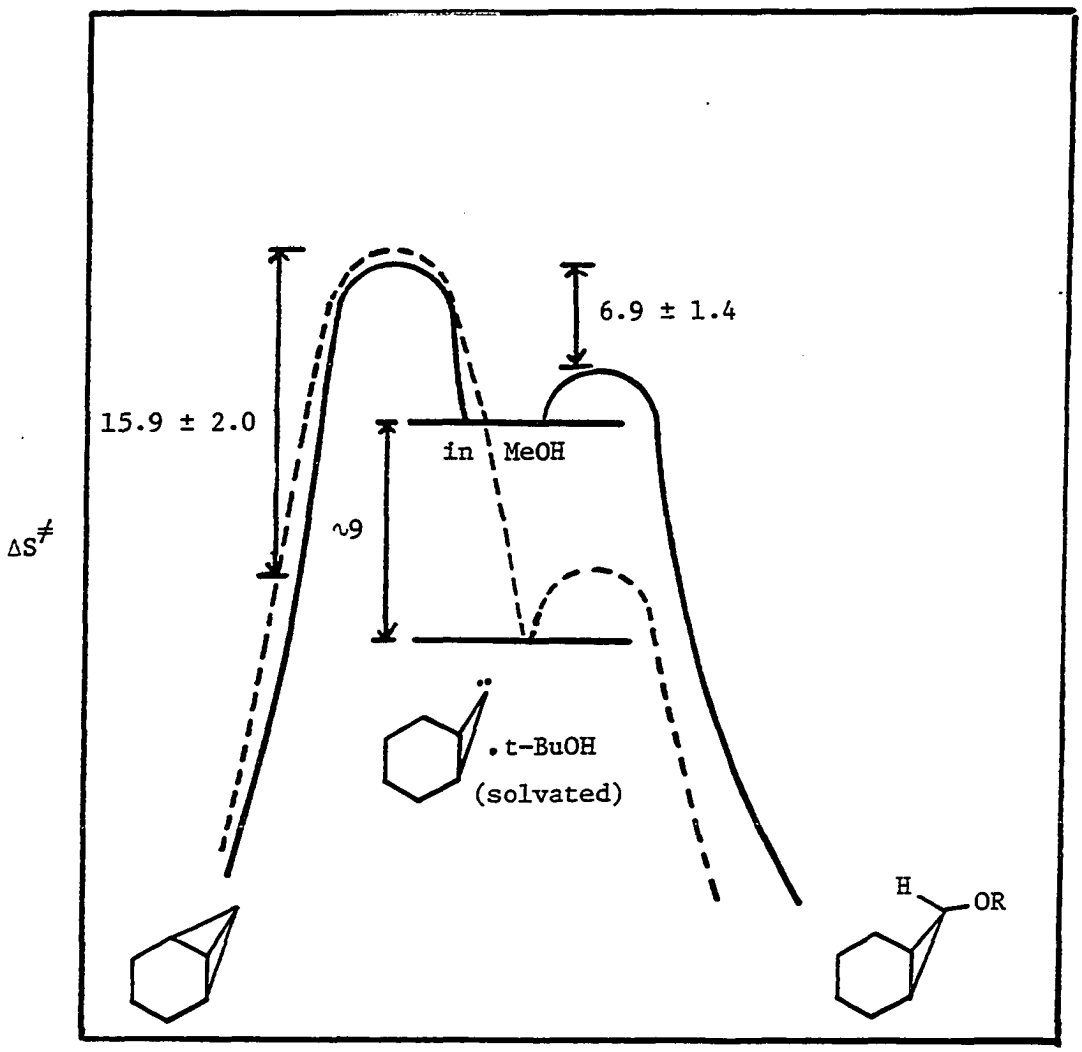

Figure 26. Entropy diagram in 30% alcohol

——— MeOH
- - - t-BuOH

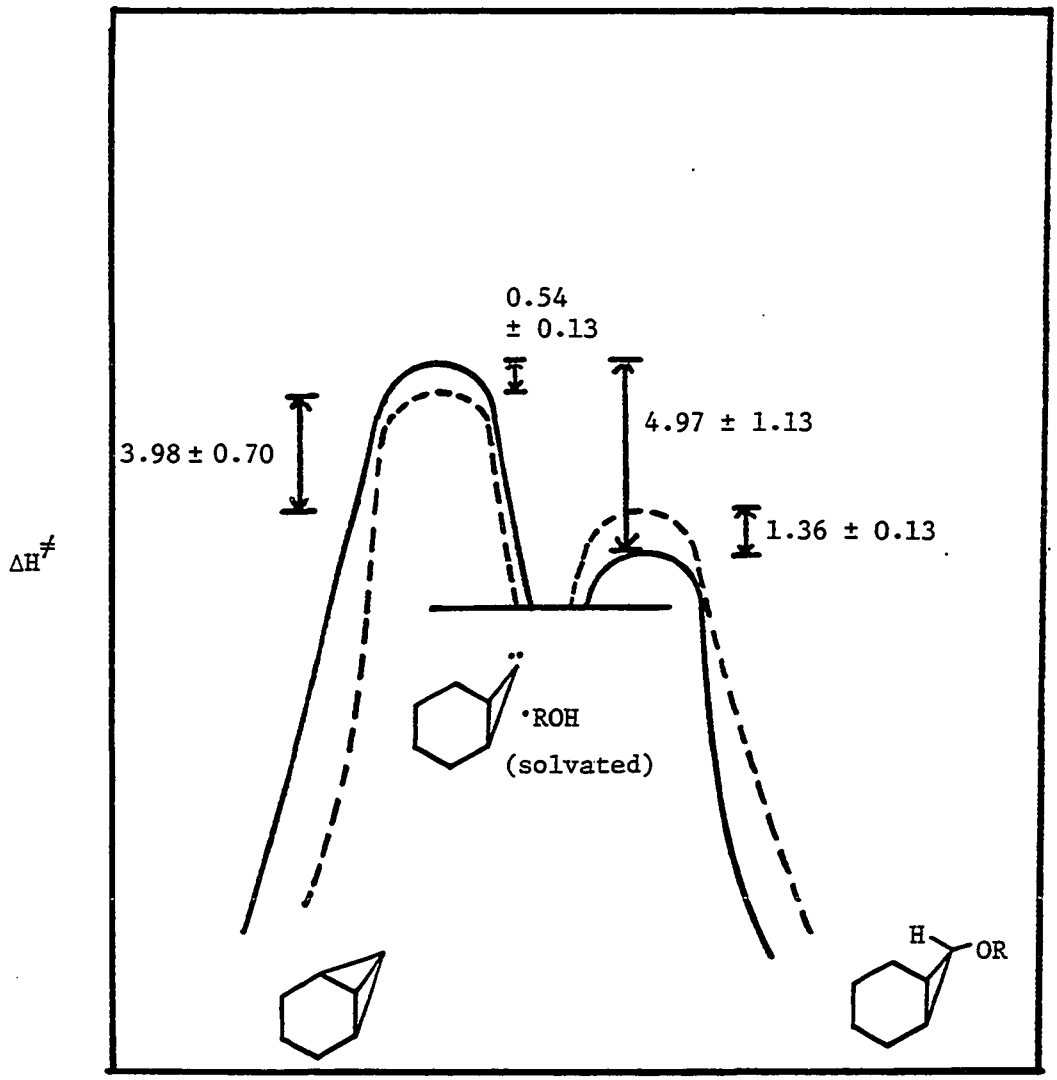

Figure 27. Enthalpy diagram in 3% alcohol

——— MeOH
- - - t-BuOH

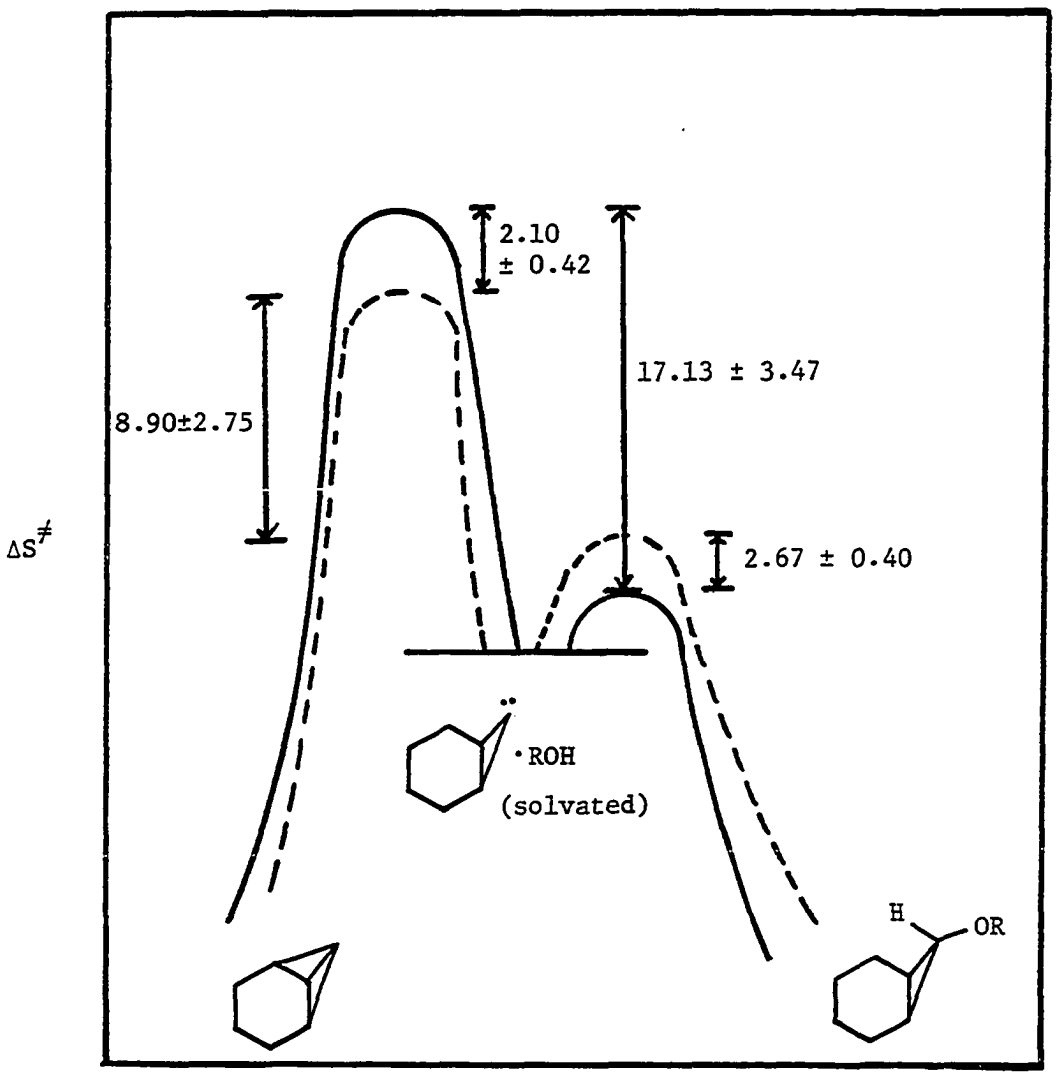

Figure 28. Entropy diagram in 3% alcohol

——— MeOH
- - - t-BuOH

Table 44. Activation parameters for the reaction of 19' in methanol/t-butanol

% ROH	$\Delta H^{\neq}_{i,t\text{-BuOH}}$ / $-\Delta H^{\neq}_{i,MeOH}$ (kcal/mol)	$\Delta S^{\neq}_{i,MeOH}$ / $-\Delta S^{\neq}_{i,t\text{-BuOH}}$ (e.u.)	$\Delta H^{\neq}_{t,t\text{-BuOH}}$ / $-\Delta H^{\neq}_{t,MeOH}$ (kcal/mole)	$\Delta S^{\neq}_{t,MeOH}$ / $-\Delta S^{\neq}_{t,t\text{-BuOH}}$ (e.u.)
1-6	-0.54 ± 0.13	2.10 ± 0.40	1.36 ± 0.13	-2.67 ± 0.40
25-50	3.18 ± 0.25	-9.23 ± 0.77	1.13 ± 0.01	-1.68 ± 0.03

equilibria need be considered vis a vis the relative alcohol reactivities. Thus irrespective of the total alcohol concentration, the "starting carbene" is a single species. Scheme IX shows the "solvated carbene" mechanism at "high" alcohol concentration. We see (equation (15)) that the ratio of 25/33 to [MeOH]/[t-BuOH] is still constant.

Scheme IX

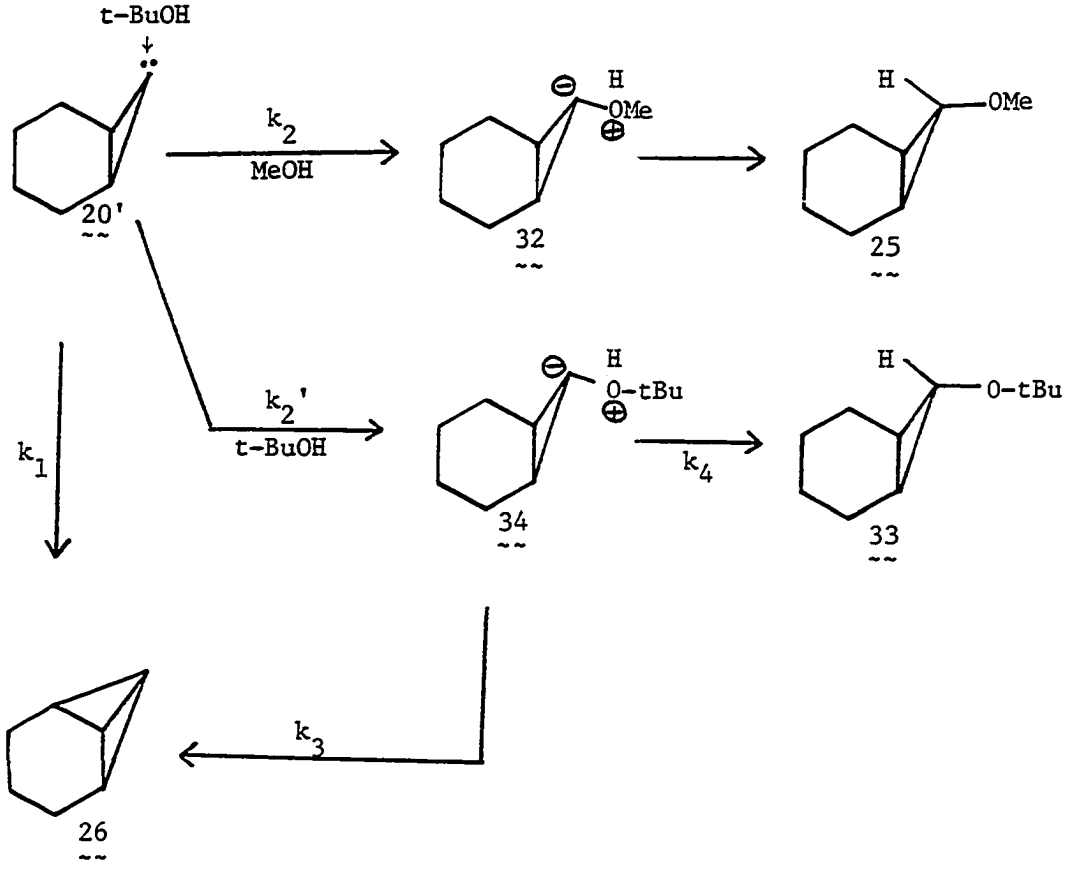

$$\frac{d[25]}{dt} = k_2[MeOH][20']$$

$$\frac{d[33]}{dt} = \frac{k_2'[t\text{-BuOH}][20'] \cdot k_4}{k_3 \cdot k_4}$$

$$\frac{[25]}{[33]} = \frac{k_2(k_3 + k_4)}{k_2'k_4} \cdot \frac{[MeOH]}{[t\text{-BuOH}]} \qquad (15)$$

So far we have considered only the "ylide" mechanism to interpret all the data. An alternative, if less likely, mechanism might also fit the data, and we now demonstrate its excludability. Scheme X and equation (16) illustrate the new mechanism (compare to equation (8)), where 26 is proposed to arise directly from diazo precursor 22.

Scheme X

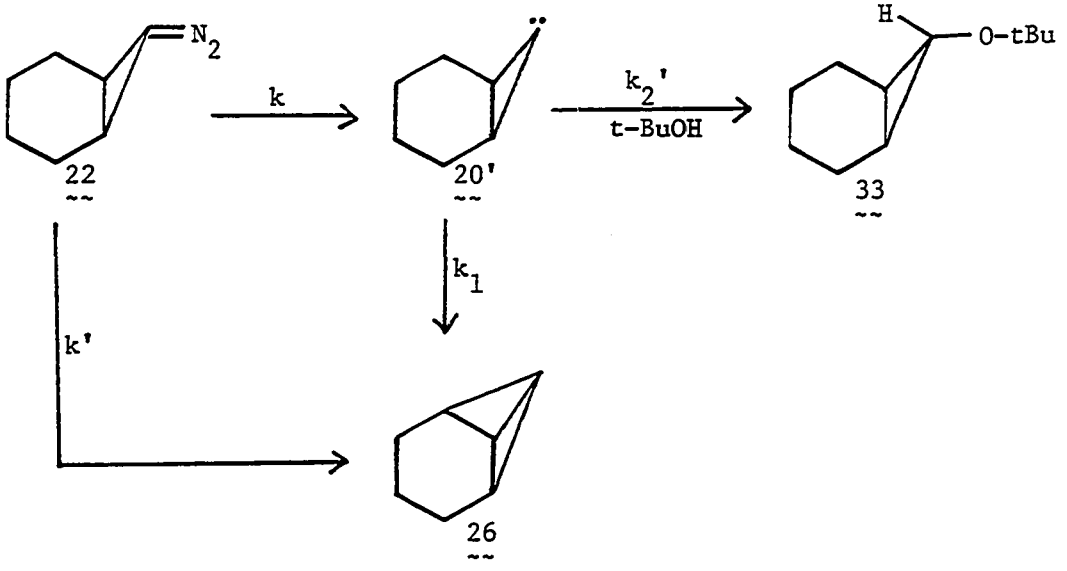

$$\frac{26}{33} = \frac{k'}{k} + \frac{k_1(k + k')}{kk_2'} \cdot \frac{1}{[t\text{-BuOH}]} \qquad (16)$$

A way to differentiate this "diazo" mechanism from the "ylide" mechanism is to study the product ratios of 26/33 in mixtures of methanol and t-butanol. For the ylide mechanism (see Scheme VIII), the ratio of 26/33 should be proportional to 1/[t-BuOH], as shown in equation (17). However, for the diazo mechanism (Scheme XI for competition experiments), equation (18) must represent the 26/33 ratio.

$$\frac{26}{33} = \frac{k_2'[34] + k_i[20']}{k_3'[34]}$$

$$= \frac{k_2'}{k_3'} + \frac{k_i[20']}{\dfrac{k_3' \cdot k_1'[20'][t\text{-BuOH}]}{k_2' + k_3'}}$$

$$= \frac{k_2'}{k_3'} + \frac{k_i(k_2' + k_3')}{k_1'k_3'} \cdot \frac{1}{[t\text{-BuOH}]} \qquad (17)$$

Figure 29 and Table 45 show the results of plotting 26/33 vs. 1/[t-BuOH]. The linearity ($r \geq 0.99$) in Figure 29 showed that the diazo mechanism was incorrect; the ylide mechanism remains valid (probably exclusively so) for our studies.

In order to probe the behavior of norcaranylidene at low temperatures ($\leq$ 0°C), experiments were then carried out in methanol/toluene (m.p. -93°C), since benzene has a m.p. of 5°C. To ensure that toluene behaved similarly to benzene, the kinetic studies of 19' in methanol/toluene

Scheme XI

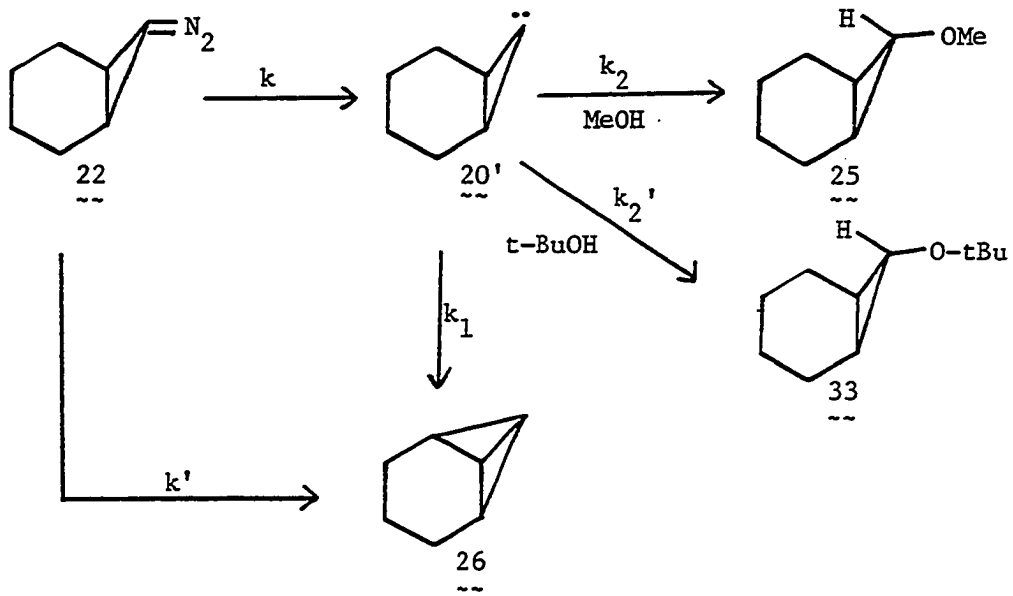

$$\frac{26}{33} = \frac{k_1[20'] + k'[22]}{k_2'[20'][t\text{-BuOH}]}$$

$$= \frac{k_1}{k_2'} \cdot \frac{1}{[t\text{-BuOH}]} + \frac{k'[22]}{\dfrac{k_2' \cdot k \cdot [22] \cdot [t\text{-BuOH}]}{k_1 + k_2[MeOH] + k_2'[t\text{-BuOH}]}}$$

$$= \frac{k_1}{k_2'}\left(1 + \frac{k'}{k}\right) \cdot \frac{1}{[t\text{-BuOH}]} + \left(\frac{k_2 \cdot k'}{k' \cdot k}\right) \cdot \frac{[MeOH]}{[t\text{-BuOH}]} + \frac{k'}{k} \qquad (18)$$

$\frac{26}{33}$

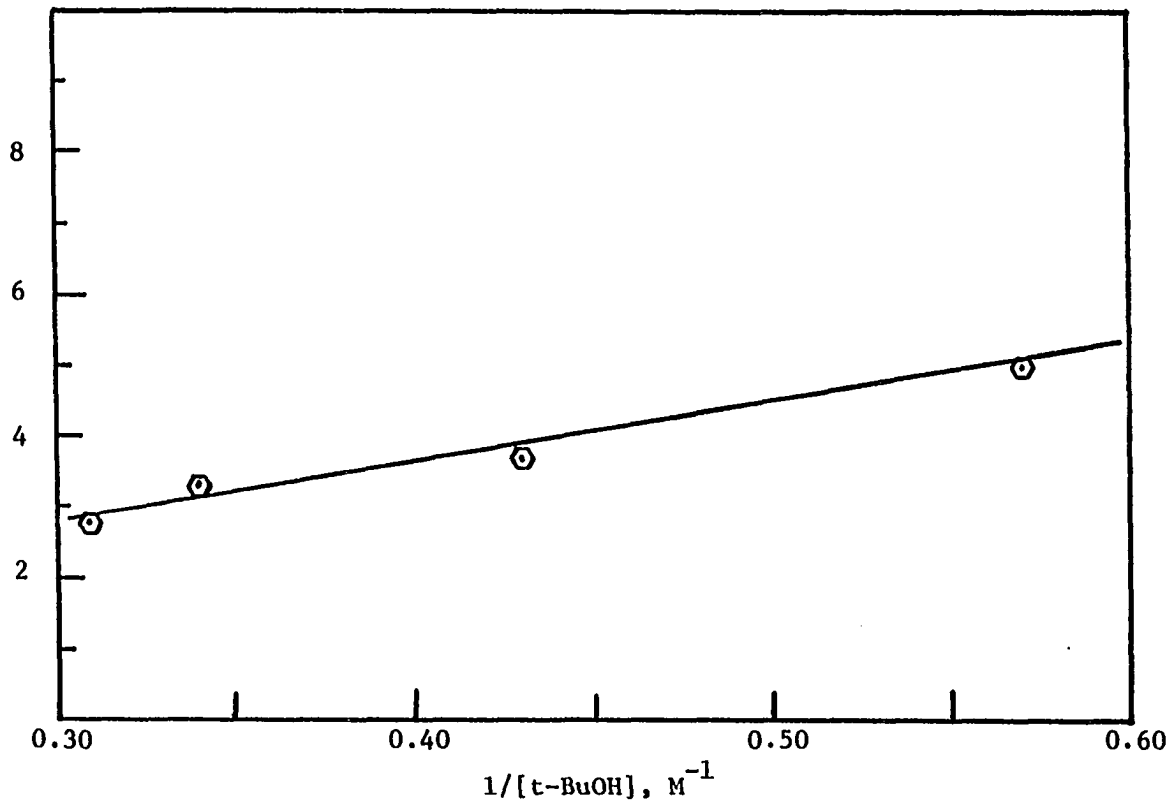

Figure 29. Plot of $\frac{26}{33}$ vs. 1/[t-BuOH]. r = 0.990, int. = 0.38 ± 0.44, slope = 7.92 ± 1.16

Table 45. Product ratios of 26/33 as a function of 1/[t-BuOH] in 30% MeOH/t-BuOH in benzene at 30°C

(V/V) MeOH/t-BuOH	$\frac{1}{[t\text{-BuOH}]}$ (M^{-1})	% 26	% 33	26/33
1:1	0.57	35.1	7.1	4.94
1:2	0.43	42.6	11.6	3.67
1:5	0.34	50.1	15.2	3.29
1:9	0.31	56.3	20.5	2.74

within the temperature range 0 to 62°C were also conducted. The results are tabulated in Tables 46 ($T < 0°C$) and 47 ($T > 0°C$).

Then all the data were analyzed by both nonlinear least squares (NLLSQ) and least squares methods (on an Apple computer). It was again found that the NLLSQ analyses gave larger errors due to problems (previously mentioned) with the k_2/k_3 ratios. Tables 48-54 and Figures 30 and 31 show the results and the comparison between the two analytical methods.

As is seen from the data in Tables 48 and 50, and in Figure 30, the results at low temperatures bear the opposite relationship between the two competition reactions (k_i/k_t became larger when the temperature was lowered) relative to temperatures above 0°C. This phenomenon is suggested to result from the reversibility of ylide formation (19, 21, 22). In other words, k_{-1} became competitive as the temperature was lowered (Scheme XII). Such an interpretation is also supported by the increased kinetic

Table 46. Product distribution as a function of methanol concentration and temperature in methanol/toluene at temperatures below 0°C; S.M. = 0.027 mmole, [NaOMe]/[S.M.] = 7:1, total solvent volume = 0.4 ml

T (°C)	% MeOH	$\frac{1}{[MeOH]}$ (M^{-1})	% 26	% 25	26/25
-15	25.0	0.16	1.68	8.4	0.20
-15	40.0	0.10	1.40	10.0	0.14
-15	50.0	0.08	0.77	7.5	0.10
-20	25.0	0.16	1.68	6.2	0.27
-20	40.0	0.10	3.06	14.5	0.21
-20	50.0	0.08	1.07	6.5	0.16
-30	25.0	0.16	1.55	3.3	0.47
-30	40.0	0.10	2.40	6.3	0.38
-30	50.0	0.08	1.01	2.8	0.35
-42	25.0	0.16	2.15	7.0	0.31
-42	40.0	0.10	3.49	17.5	0.20
-42	50.0	0.08	2.34	12.9	0.18
-50	25.0	0.16	7.59	11.3	0.67
-50	40.0	0.10	3.14	5.8	0.54
-50	50.0	0.08	3.73	7.2	0.51
-65	25.0	0.16	2.10	5.7	0.37
-65	40.0	0.10	1.40	5.6	0.25
-65	50.0	0.08	1.91	12.6	0.15
-69	25.0	0.16	2.00	5.6	0.35
-69	40.0	0.10	0.69	4.4	0.16
-69	50.0	0.08	1.31	10.3	0.13
-78	25.0	0.16	3.32	5.5	0.60
-78	40.0	0.10	1.53	3.9	0.40
-78	50.0	0.08	2.19	6.5	0.34

Table 47. Product distribution as a function of methanol concentration and temperature in 25-50% methanol in toluene at temperatures $\geq$ 0°C; S.M. = 0.027 mmole, [NaOMe]/[S.M.] = 7:1, total solvent volume = 0.4 ml

T (°C)	% MeOH	$\frac{1}{[MeOH]}$ (M^{-1})	% 26	% 25	26/25
0	25.0	0.16	4.38	18.3	0.24
0	40.0	0.10	3.22	17.2	0.19
0	50.0	0.08	2.74	18.5	0.15
4	25.0	0.16	5.81	19.1	0.30
4	40.0	0.10	4.33	18.2	0.24
4	50.0	0.08	3.29	15.5	0.21
5	25.0	0.16	5.84	16.6	0.35
5	40.0	0.10	4.52	17.0	0.27
5	50.0	0.08	4.63	18.4	0.25
6	25.0	0.16	4.00	14.4	0.28
6	40.0	0.10	2.52	13.8	0.18
6	50.0	0.08	2.61	16.6	0.16
8	25.0	0.16	7.90	19.3	0.41
8	40.0	0.10	3.74	12.4	0.30
8	50.0	0.08	4.08	15.5	0.26
10	25.0	0.16	8.26	19.8	0.42
10	40.0	0.10	7.93	25.7	0.31
10	50.0	0.08	5.05	19.4	0.26
12	25.0	0.16	4.87	14.9	0.33
12	40.0	0.10	3.96	17.5	0.23
12	50.0	0.08	3.82	23.2	0.16
13	25.0	0.16	4.89	15.6	0.31
13	40.0	0.10	3.02	15.6	0.19
13	50.0	0.08	2.59	15.8	0.16
15	25.0	0.16	4.55	14.9	0.31
15	40.0	0.10	3.25	14.3	0.23
15	50.0	0.08	4.33	24.5	0.18

Table 47. Continued

T (°C)	% MeOH	$\frac{1}{[MeOH]}$ (M^{-1})	% 26	% 25	26/33
18	25.0	0.16	5.06	10.2	0.49
18	40.0	0.10	6.48	18.7	0.35
18	50.0	0.08	4.57	16.3	0.28
20	25.0	0.16	7.04	17.3	0.41
20	40.0	0.10	7.16	21.9	0.33
20	50.0	0.08	5.65	22.2	0.25
23	25.0	0.16	5.43	14.1	0.38
23	40.0	0.10	3.96	14.8	0.27
23	50.0	0.08	2.51	12.8	0.19
25	25.0	0.16	7.84	17.7	0.44
25	40.0	0.10	4.92	19.8	0.25
25	50.0	0.08	5.17	23.1	0.22
27	25.0	0.16	4.20	9.5	0.44
27	40.0	0.10	5.25	17.9	0.29
27	50.0	0.08	4.87	17.6	0.28
29	25.0	0.16	12.79	20.2	0.63
29	40.0	0.10	4.90	12.1	0.40
29	50.0	0.08	6.33	18.7	0.34
30	25.0	0.16	11.98	21.7	0.55
30	40.0	0.10	7.72	21.6	0.36
30	50.0	0.08	7.95	25.8	0.31
42	25.0	0.16	8.26	17.2	0.48
42	40.0	0.10	5.30	17.5	0.30
42	50.0	0.08	4.06	19.1	0.21
62	25.0	0.16	6.99	13.7	0.51
62	40.0	0.10	4.68	17.1	0.27
62	50.0	0.08	2.35	11.7	0.20

Table 48. Rate constants as a function of temperature for the formation of 25 and 26 in 25-50% methanol in toluene at temperatures below 0°C (least-squares analyses)

T (°C)	$10^3/T$ (K^{-1})	$\frac{k_2}{k_3}$	$\frac{k_i}{k_t}$	$\ln \frac{k_i}{k_t}$	R
-15.0	3.87	$(2.70 \times 10^{-3}) \pm 0.02$	1.27 ± 0.25	0.24 ± 0.20	0.990
-20.0	3.95	0.057 ± 0.036	1.37 ± 0.35	0.32 ± 0.25	0.980
-30.0	4.11	$0.23 \pm 8.7 \times 10^{-7}$	$1.50 \pm 7.9 \times 10^{6}$	0.41 ± 0.00	0.999
-42.0	4.33	0.045 ± 0.022	1.62 ± 0.22	0.48 ± 0.13	0.995
-50.0	4.48	0.34 ± 0.01	2.02 ± 0.15	0.70 ± 0.07	0.998
-65.0	4.81	-0.07 ± 0.07	2.86 ± 0.76	1.05 ± 0.26	0.980
-69.0	4.90	-0.086 ± 0.052	2.62 ± 0.55	0.96 ± 0.21	0.993
-78.0	5.13	$0.078 \pm 8.95 \times 10^{-3}$	3.25 ± 0.08	1.18 ± 0.02	0.999

Table 49. Rate constants as a function of temperature for the formation of 25 and 26 in 25-50% methanol in toluene at temperatures $\geq$ 0°C (least-squares analyses)

T (°C)	$10^3/T$ (K^{-1})	$\frac{k_2}{k_3}$	$\frac{k_i}{k_t}$	$\ln \frac{k_i}{k_t}$	R
0	3.66	0.066 ± 0.028	1.11 ± 0.27	0.10 ± 0.24	0.981
4.0	3.61	0.123 ± 0.012	1.11 ± 0.11	0.10 ± 0.10	0.999
5.0	3.60	0.147 ± 8.54×10^{-3}	1.26 ± 0.07	0.23 ± 0.05	0.994
6.0	3.58	0.036 ± 0.018	1.50 ± 0.17	0.40 ± 0.11	0.999
8.0	3.56	0.011 ± 4.3×10^{-3}	1.87 ± 0.04	0.63 ± 0.02	0.999
10.0	3.53	0.104 ± 0.017	1.99 ± 0.16	0.69 ± 0.08	0.998
12.0	3.51	(-5.85×10^{-3}) ± 0.046	2.16 ± 0.46	0.77 ± 0.21	0.990
13.0	3.50	(8.09×10^{-3}) ± 0.013	1.87 ± 0.13	0.63 ± 0.07	0.998
15.0	3.47	0.055 ± 0.029	1.62 ± 0.28	0.48 ± 0.17	0.988
18.0	3.44	0.075 ± 0.030	2.62 ± 0.29	0.96 ± 0.11	0.998
20.0	3.41	0.103 ± 0.064	1.98 ± 0.61	0.68 ± 0.30	0.967
23.0	3.37	(5.74×10^{-3}) ± 0.054	2.41 ± 0.53	0.88 ± 0.22	0.990
25.0	3.36	(-5.94×10^{-3}) ± 0.048	2.71 ± 0.48	1.00 ± 0.18	0.990

Table 49. Continued

T (°C)	$10^3/T$ (K^{-1})	$\frac{k_2}{k_3}$	$\frac{k_i}{k_t}$	$\ln \frac{k_i}{k_t}$	R
27.0	3.33	0.105 ± 0.055	2.03 ± 0.52	0.71 ± 0.26	0.990
29.0	3.31	0.046 ± 0.022	3.61 ± 0.22	1.28 ± 0.06	0.999
30.0	3.30	0.066 ± 0.018	3.00 ± 0.17	1.10 ± 0.05	0.999
42.0	3.18	-0.058 ± 0.039	3.43 ± 0.41	1.23 ± 0.12	0.995
62.0	2.99	-0.109 ± 0.014	3.84 ± 0.15	1.35 ± 0.04	0.999

Table 50. Comparison of activation parameters for the formation of 25 and 26 in methanol/toluene obtained via NLLSQ and linear least-squares analyses

Condition	$\Delta H_i^{\neq} - \Delta H_t^{\neq}$ (NLLSQ) Kcal/mol	$\Delta H_i^{\neq} - \Delta H_t^{\neq}$ (least-squares) Kcal/mol
25-50% methanol in toluene at $T \geq 0°C$	1.58 ± 1.10	4.93 ± 0.63
25-50% methanol in toluene at $T < 0°C$	0.81 ± 1.80	-1.42 ± 0.10

$\Delta S_i^{\neq} - \Delta S_t^{\neq}$ (NLLSQ) cal/mol.k	$\Delta S_i^{\neq} - \Delta S_t^{\neq}$ (least-squares) cal/mol.k	$\Delta H_2^{\neq} - \Delta H_3^{\neq}$ (NLLSQ) Kcal/mol	$\Delta S_2^{\neq} - \Delta S_3^{\neq}$ (NLLSQ) cal/mol.k
6.99 ± 3.73	18.18 ± 2.26	0.31 ± 6.84	-4.98 ± 23.45
-2.20 ± 8.36	-5.03 ± 0.41	-0.15 ± 5.80	-5.78 ± 26.11

Table 51. Comparison of rate constant ratios for the formation of 25 and 26 in 25-50% methanol in toluene at temperatures below 0°C obtained from NLLSQ and least-squares analyses

T (K)	$10^2 \cdot \frac{k_2}{k_3}$	$\frac{k_i}{k_t}$	$10^3/T$ (K^{-1})	$\ln \frac{k_i}{k_t}$
258	7.3	1.62 (1.27 ± 0.25)[a]	3.87	0.48 (0.24 ± 0.20)[a]
253	7.3	1.67 (1.37 ± 0.35)	3.95	0.51 (0.32 ± 0.25)
243	7.4	1.78 (1.50 ± 7.9 x 10^{-6})	4.11	0.58 (0.41 ± 0.00)
231	7.5	1.94 (1.62 ± 0.22)	4.33	0.66 (0.48 ± 0.13)
223	7.6	2.07 (2.02 ± 0.15)	4.48	0.73 (0.70 ± 0.07)
208	7.8	2.36 (2.86 ± 0.76)	4.81	0.86 (1.05 ± 0.26)
204	7.9	2.45 (2.62 ± 0.55)	4.90	0.90 (0.96 ± 0.21)
195	8.0	2.69 (3.25 ± 0.08)	5.13	0.99 (1.18 ± 0.02)

[a]The data in parentheses were obtained from least-squares analyses.

Table 52. Comparison of rate constant ratios for the formation of 25 and 26 in 25-50% methanol in toluene at temperatures $\geq$ 0°C obtained from NLLSQ and least-squares analyses

T (K)	$\frac{k_2}{k_3}$ 10^2	$\frac{k_i}{k_t}$	$10^3/T$ (K^{-1})	$\ln \frac{k_i}{k_t}$
273	4.55	1.85 (1.11 ± 0.27)[a]	3.66	0.61 (0.10 ± 0.24)[a]
277	4.59	1.93 (1.11 ± 0.11)	3.61	0.66 (0.10 ± 0.10)
278	4.60	1.95 (1.26 ± 0.07)	3.60	0.67 (0.23 ± 0.05)
279	4.61	1.97 (1.50 ± 0.17)	3.58	0.68 (0.40 ± 0.11)
281	4.63	2.01 (1.87 ± 0.04)	3.56	0.70 (0.63 ± 0.02)
283	4.64	2.05 (1.99 ± 0.16)	3.53	0.27 (0.69 ± 0.08)
285	4.66	2.09 (2.16 ± 0.46)	3.51	0.74 (0.77 ± 0.21)
286	4.67	2.11 (1.87 ± 0.13)	3.50	0.75 (0.63 ± 0.07)
288	4.69	2.15 (1.62 ± 0.28	3.47	0.77 (0.48 ± 0.17)
291	4.71	2.21 (2.62 ± 0.29	3.44	0.79 (0.96 ± 0.11)
293	4.73	2.25 (1.98 ± 0.61)	3.41	0.81 (0.68 ± 0.30)
296	4.76	2.32 (2.41 ± 0.53)	3.37	0.84 (0.88 ± 0.22)
298	4.78	2.36 (2.71 ± 0.48)	3.36	0.86 (1.00 ± 0.18)

300	4.79	2.40 (2.03 ± 0.52)	3.33	0.88 (0.71 ± 0.26)
302	4.81	2.44 (3.61 ± 0.22)	3.31	0.89 (1.28 ± 0.06)
303	4.82	2.46 (3.00 ± 0.17)	3.30	0.90 (1.10 ± 0.05)
315	4.91	2.72 (3.43 ± 0.41)	3.18	1.00 (1.23 ± 0.12)
335	5.06	3.17 (3.84 ± 0.15)	2.99	1.15 (1.35 ± 0.04)

[a]The data in parentheses were obtained from least-squares analyses.

Table 53. Comparison of the experimental product ratios with those "calculated" by NLLSQ analysis in 25–50% methanol in toluene at temperatures below 0°C

T (K)	$\frac{1}{[MeOH]}$ (M^{-1})	$\frac{26/25}{\sim\sim\ \sim\sim} \cdot 10^{-1}$		$\Delta \cdot 10^{-1}$
		experimental	NLLSQ	
258	0.16	1.99	3.31	-1.32
258	0.10	1.40	2.34	-0.94
258	0.08	1.02	2.02	-1.00
253	0.16	2.71	3.39	-0.69
253	0.10	2.16	2.39	-0.23
253	0.08	1.63	2.06	-0.43
243	0.16	4.72	3.59	1.12
243	0.10	3.82	2.52	1.29
243	0.08	3.54	2.16	1.37
231	0.16	3.08	3.86	-0.78
231	0.10	2.00	2.69	-0.69
231	0.08	1.81	2.31	-0.49
223	0.16	6.72	4.07	2.64
223	0.10	5.45	2.83	2.61
223	0.08	5.14	2.42	2.72
208	0.16	3.70	4.56	-0.85
208	0.10	2.49	3.14	-0.65
208	0.08	1.54	2.67	-1.12
204	0.16	3.53	4.71	-1.18
204	0.10	1.57	3.24	-1.67
204	0.08	1.27	2.74	-1.48
195	0.16	5.99	5.10	0.88
195	0.10	3.96	3.49	0.47
195	0.08	3.39	2.95	0.43

Table 54. Comparison of the experimental product ratios with those "calculated" by NLSSQ analysis in 25-50% methanol in toluene at temperatures $\geq$ 0°C

T (K)	$\frac{1}{[MeOH]}$ (M^{-1})	$\underset{\sim\sim}{26/25} \cdot 10^{-1}$		$\Delta \cdot 10^{-1}$
		experimental	NLLSQ	
273	0.16	2.40	3.41	-1.01
273	0.10	1.87	2.31	-0.44
273	0.08	1.48	1.93	-0.46
277	0.16	3.05	3.54	-0.50
277	0.10	2.38	2.39	-0.01
277	0.08	2.12	2.00	0.11
278	0.16	3.51	3.58	-0.07
278	0.10	2.66	2.41	0.25
278	0.08	2.52	2.02	0.49
279	0.16	2.78	3.61	-0.83
279	0.10	1.83	2.43	-0.60
279	0.08	1.57	2.03	-0.47
281	0.16	4.09	3.68	0.41
281	0.10	3.01	2.47	0.53
281	0.08	2.63	2.07	0.55
283	0.16	4.17	3.74	0.42
283	0.10	3.09	2.51	0.57
283	0.08	2.60	2.09	0.51
285	0.16	3.27	3.81	-0.54
285	0.10	2.26	2.56	-0.30
285	0.08	1.65	2.14	-0.49
286	0.16	3.13	3.84	-0.71
286	0.10	1.93	2.58	-0.65
286	0.08	1.64	2.15	-0.51
288	0.16	3.06	3.91	-0.85
288	0.10	2.27	2.62	-0.35
288	0.08	1.76	2.19	-0.43

Table 54. Continued

T (K)	$\frac{1}{[MeOH]}$ (M^{-1})	$\frac{26}{\sim\sim}/\frac{25}{\sim\sim} \cdot 10^{-1}$		$\Delta \cdot 10^{-1}$
		experimental	NLLSQ	
291	0.16	4.94	4.01	0.93
291	0.10	3.46	2.68	0.77
291	0.08	2.80	2.24	0.55
293	0.16	4.06	4.08	-0.02
293	0.10	3.27	2.73	0.54
293	0.08	2.54	2.28	0.26
296	0.16	3.85	4.18	-0.34
296	0.10	2.67	2.79	-0.13
296	0.08	1.95	2.33	-0.38
298	0.16	4.42	4.25	0.17
298	0.10	2.48	2.84	-0.36
298	0.08	2.24	2.36	-0.12
300	0.16	4.42	4.32	0.10
300	0.10	2.94	2.88	0.05
300	0.08	2.76	2.40	0.36
302	0.16	6.32	4.39	1.93
302	0.10	4.03	2.93	1.10
302	0.08	3.38	2.44	0.94
303	0.16	5.53	4.43	1.10
303	0.10	3.58	2.95	0.63
303	0.08	3.08	2.45	0.63
315	0.16	4.81	4.85	-0.04
315	0.10	3.02	3.22	-0.20
315	0.08	2.10	2.67	-0.57
335	0.16	5.09	5.57	-0.48
335	0.10	2.73	3.67	-0.94
335	0.08	2.01	3.04	-1.03

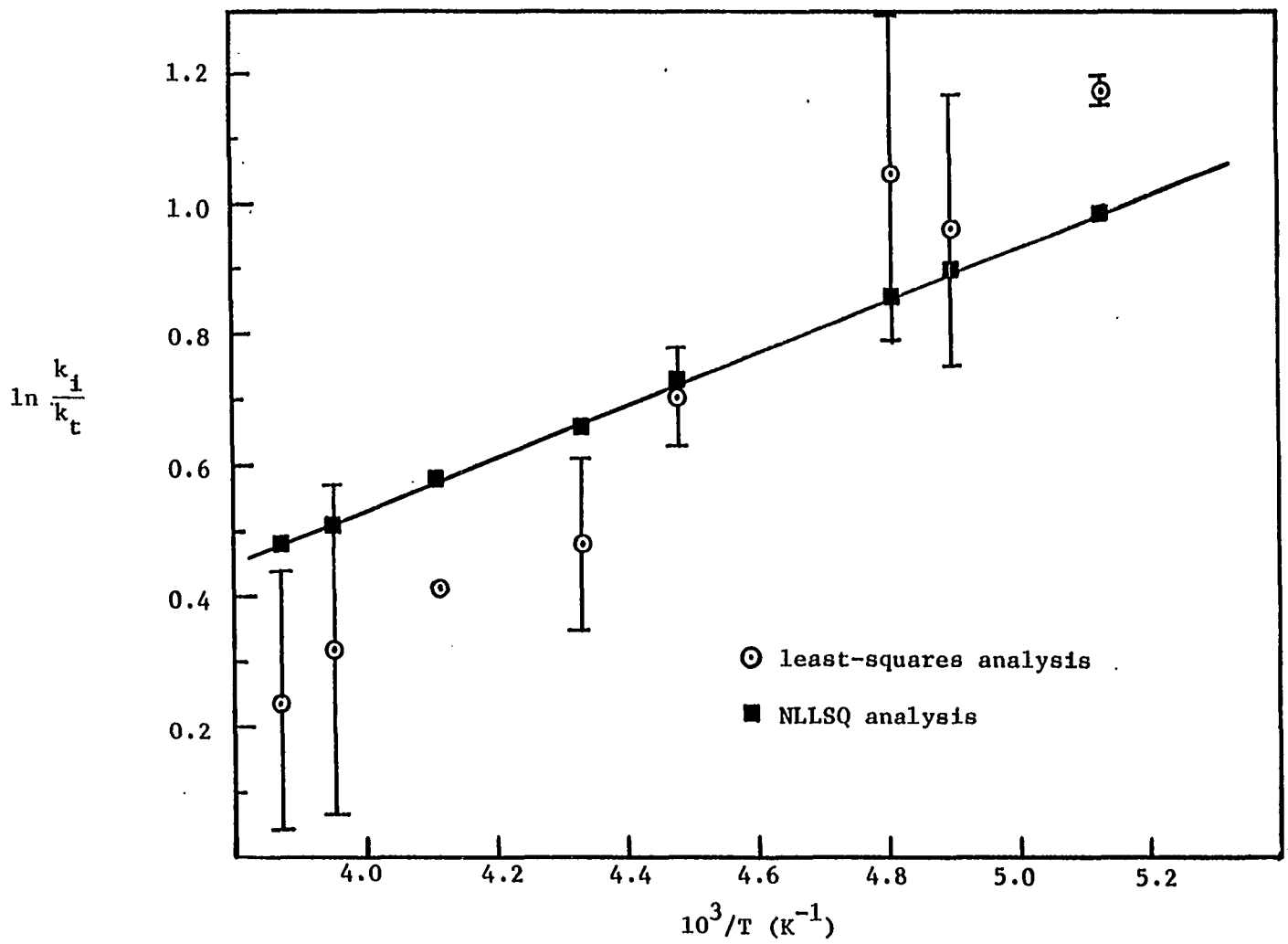

Figure 30. Plot of ln k_i/k_t vs. 1/T in 25-50% methanol in toluene at low temperatures

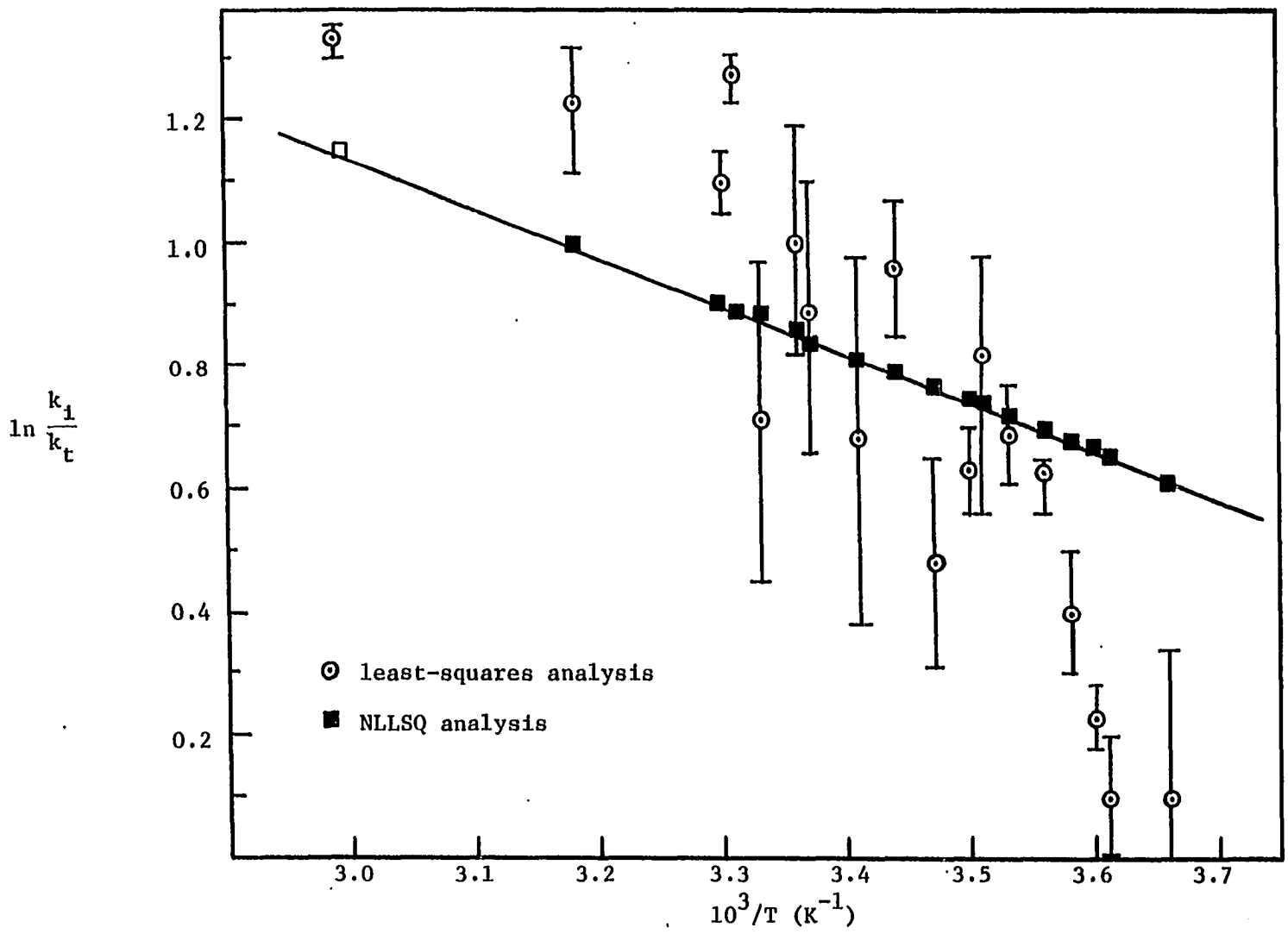

Figure 31. Plot of $\ln k_i/k_t$ vs. 1/T in 25-50% methanol in toluene

deuterium isotope effects for 25 at low temperatures (discussed in Chapter III).

Scheme XII

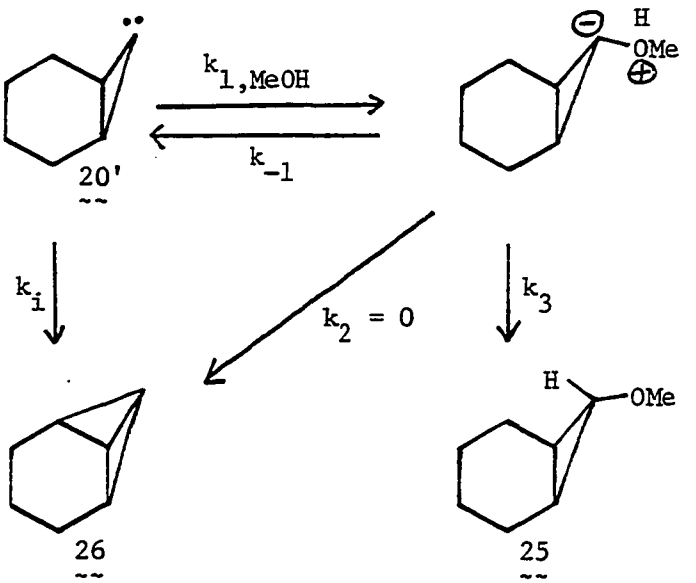

In summary, the following conclusions may be offered:

(i) The competitive intramolecular and intermolecular reactions of norcaranylidene in methanol or t-butanol can be interpreted by a kinetic model in which an ylide is found by the reaction of carbene 20' with alcohols (Scheme VII).

Scheme VII

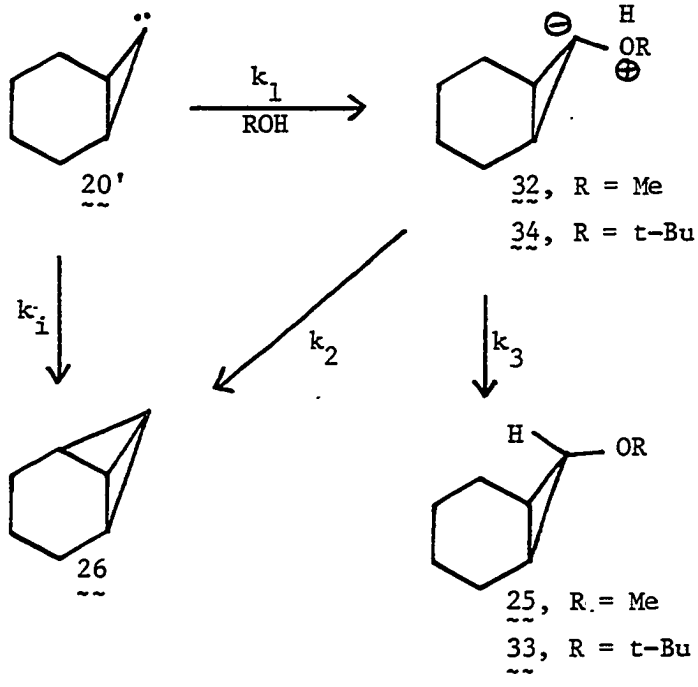

20' 32, R = Me 34, R = t-Bu

26 25, R = Me 33, R = t-Bu

(ii) In methanol, k_2/k_3 is close to zero at all the temperatures studied. However, in t-butanol, the ratio of k_2/k_3 is significant, since ylide 34 tends to release the t-butanol molecule to give insertion product 26. This may be due to the steric hindrance of the t-butyl group in the ylide structure 34.

(iii) Reversible ylide formation occurs only at low temperatures, which is consistent with our previous results (22) for carbene 11 and Turro's recent observations regarding diphenylcarbene (19).

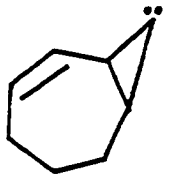

11

(iv) Methanol reacts with norcaranylidene 2.5 times faster than t-butanol (in 3% or 30% total alcohol concentration). This is closer to Bethell's results (k_{MeOH}/k_{t-BuOH} = 3-9 for diphenylcarbenes, depending on the substituents in the 4-position) than Griller's ($k_{MeOH}/k_{t-BuOH} \simeq 1000$ for phenylchlorocarbene).

Experimental

General

Infrared spectra were recorded on Beckman IR-18A, IR-4250 and IBM FT-IR 98 spectrophotometers. The proton magnetic resonance spectra were obtained on Varian EM 360 and Nicolet 300 spectrometers, using $CDCl_3$ as the solvent and tetramethylsilane as the internal standard. The mass spectra studies were conducted using High Resolution MS-902, MS-90 and Finnegan 4023 GLC-mass spectrometers. GLC analyses were conducted on an HP 5890 gas chromatograph. Melting points were taken on a Thomas-Hoover melting point apparatus and were uncorrected.

Syntheses and reactions

Preparation of ethyl bicyclo[4.1.0]hept-2-ene-7-carboxylates (35 and 36) (Figure 32) To a boiling mixture of 8 g of 1,3-cyclohexadiene (prepared by dehydrobromination of 1,2-dibromocyclohexane (48, 49) with lithium carbonate, lithium chloride in HMPTA at 160°C (50)), 0.1 g of powdered copper, and 0.8 g of ethyl diazoacetate was added dropwise,

under reflux, over forty minutes, the remainder of ethyl dizoacetate (total 3.8 g). After refluxing for an additional hour, gas evolution had ceased. The reaction mixture was then cooled, diluted with ether, filtered and distilled under vacuum to give 35 and 36 as a colorless oil in an 87:13 ratio in 60% yield, b.p. 95-96°C (5 mmHg).

GC-MS: P^+ at m/e 166

^{1}H NMR ($CDCl_3$): δ 5.5 ∿ 5.9 (m), δ 4.1 (q), δ 1.7 ∿ 2.1 (m)
δ 1.2 (doubly triplet).

IR (neat): 3040, 2980, 2920, 2850, 1740, 1640, 1440, 1360, 1330, 1285, 1250, 1170, 1040 cm^{-1}.

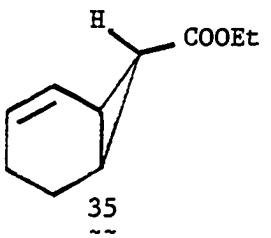

35

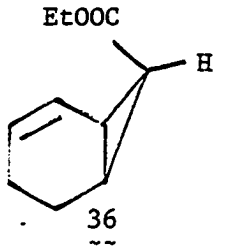

36

Preparation of bicyclo[4.1.0]hept-2-ene-7-carboxylic acids (37 and 38)

A 3.1 g mixture of 35 and 36 was stirred with 2.4 g of potassium hydroxide in 40 ml of 95% ethanol at room temperature for twenty-four hours. The ethanol was then evaporated on the steam bath, water added to the residue, and the mixture acidified with conc. HCl. The aqueous solution was then extracted with ether. The combined ether extracts were dried over anhydrous Na_2SO_4. Removal of ether gave 37 and 38 (2.45 g, 95% yield) as a white solid.

GC-MS: P^+ at m/e 138.

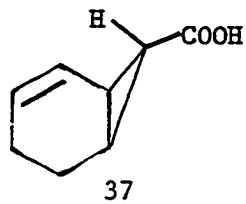

37

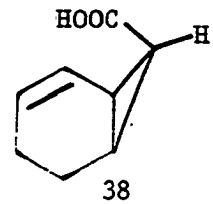

38

Isolation of exo-bicyclo[4.1.0]hept-2-ene-7-carboxylic acid (37)

(Figure 33) A solution of 1.46 g of acid mixture 37 and 38 in 15 ml of 10% Na_2CO_3 (aq) and 15 ml of saturated $NaHCO_3$ (aq) was shaken with ether. To the aqueous phase was then slowly added a solution of 0.3 g of I_2 and 1 g of KI in 5 ml of water. The resultant yellow precipitate was 39 (Figure 34), m.p. 138-139°C (0.2 g). Then the aqueous solution was acidified with conc. HCl, extracted with chloroform, and dried over anhydrous Na_2SO_4. Evaporation of solvent afforded 1.13 g of 37 as a white solid, m.p. 84-85°C.

GC-MS: P^+ at m/e 138.

^1H NMR ($CDCl_3$): δ 10.6 (s, broad), δ 5.5-6.3 (m), δ 1.8-2.4 (m).

IR ($CDCl_3$): 3200-2400 (br.), 1695, 1445, 1380, 1290, 1250, 1210, 1100 cm^{-1}.

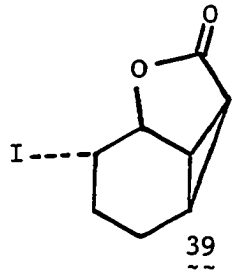

39

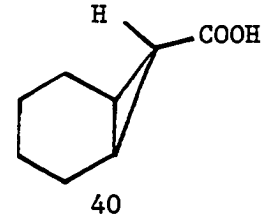

40

Preparation of exo-bicyclo[4.1.0]heptane-7-carboxylic acid (40)

(Figure 35) In the presence of a catalytic amount of platinum oxide, 400 mg of 37 in 30 ml of ethyl acetate was hydrogenated (40 psi H_2) overnight in a Parr shaker apparatus at room temperature. The PtO_2 was filtered off, and the solvent evaporated to give 380 mg of 40 as a white solid in 93% yield, m.p. 94-95°C.

HRMS: Calculated for $C_8H_{12}O_2$ - m/e 140.08373

found for $C_8H_{12}O_2$ - m/e 140.08358

IR ($CHCl_3$): 3400 ∿ 2400 (br.), 1695, 1450, 1380, 1310, 1220, 1180, 1090 cm^{-1}.

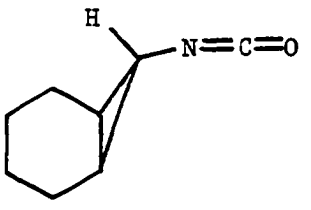

41

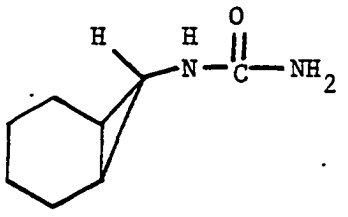

42

Preparation of 7-exo-bicyclo[4.1.0]heptylurea (42) (Figure 37) A 200 ml 3-necked round bottom flask equipped with a magnetic stirring bar, dropping funnel and low-temperature thermometer was charged with 750 mg of 40 and 40 ml of acetone. The mixture was stirred, and 0.8 ml of triethylamine was added dropwise. The solution was chilled to -5 to 0°C in an ice-salt bath, and 0.58 ml of ethyl chloroformate in 20 ml of acetone was added slowly so as to maintain the temperature between -5 to 0°C. After the addition was complete, the cold mixture was stirred for

an additional fifteen minutes. A solution of 700 mg of sodium azide in 20 ml of water was then added over a fifteen minute period. The mixture was stirred for another hour at this temperature, then poured into 50 ml of ice water, and extracted with toluene. The combined toluene extracts were dried over anhydrous Na_2SO_4. Then the solution was heated cautiously under reflux on a steam bath for one hour; N_2 evolution was observed. Removal of the toluene gave 600 mg of 41 (Figure 36) as a yellow oil.

Then a solution of 70 mg of 41 in 40 ml of toluene was cooled to 0°C. Ammonia was bubbled through slowly and a yellow precipitate was formed. Filtration gave 53 mg of 42 in 69% yield, m.p. 164-167°C.

HRMS: Calculated for $C_8H_{14}N_2O$ - m/e 154.11067

found for $C_8H_{14}N_2O$ - m/e 154.11010

^1H NMR ($CDCl_3$): δ 4.7 ∿ 5.2 (m), δ 2.0 ∿ 2.2 (m), δ 1.5 ∿ 1.9 (m), δ 1.0 ∿ 1.3 (m).

IR ($CDCl_3$): 3540, 3420, 3160, 2930, 2860, 1670, 1580, 1450, 1370, 1300, 1240, 1090 cm^{-1}.

Preparation of N-(7-exo-bicyclo[4.1.0]heptyl)-N-nitrosourea (19') (Figure 38) A solution of 100 mg of 42 in a mixture of HOAc (1 ml) and acetic anhydride (5 ml) was cooled to 0°C and 120 mg of sodium nitrite was added over thirty minutes. After stirring for another thirty minutes at 0°C, the mixture was poured into a mixture of ice and water. Filtration gave 95 mg of 19' as yellow crystals in 67% yield, m.p. 96-97°C. It was used without purification due to its thermal lability (51) (it is thermally stable only at or below room temperature).

HRMS: Calculated for $C_8H_{13}N_2O$ (M^+ - NO) - m/e 153.10279

found for $C_8H_{13}N_2O$ - m/e 153.10325

^1H NMR ($CDCl_3$): δ 6.75 (s, br), δ 5.88 (s, br), δ 1.98 (t,J = 3.9 Hz, 7-H), δ 1.2 ∿ 2.0 (m).

IR ($CDCl_3$): 3520, 3410, 3150, 2930, 2870, 1730, 1570, 1500, 1395, 1210, 1095 cm^{-1}.

^{13}C NMR ($CDCl_3$): δ 154.92 (rel. intens. 567), δ 33.77 (1184), δ 21.80 (3550), δ 21.08 (2457), δ 20.08 (2280).

Preparation of anti-7-t-butoxy-bicyclo[4.1.0]heptane (33) (Figure 39)

To a solution of 30 mg of N-(7-exo-bicyclo[4.1.0]heptyl)-N-nitrosourea (19') in 0.2 ml of t-butanol was added 60 mg of potassium t-butoxide at room temperature. An exothermic reaction ensued. Ether was added to the reaction mixture and the organic layer was washed with water, dried and concentrated to give the crude product. The resulting oil was then chromatographed (silica gel, ether) to give 11 mg of 33 as a colorless oil in 41% yield.

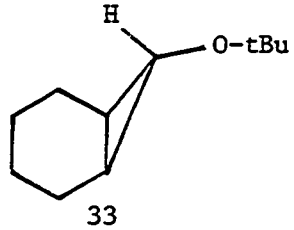

33

HRMS: Calculated for $C_{11}H_{22}O$ - m/e 168.15142

found for $C_{11}H_{22}O$ - m/e 168.15143

^1H NMR ($CDCl_3$): δ 2.81 (t,J = 2.74 Hz), δ 1.9 ∿ 1.5 (m), δ 1.25 (s), δ 1.15 ∿ 0.90 (m).

IR (CCl_4): 2920, 2860, 1550, 1450, 1260, 1100, 1020 cm^{-1}.

^{13}C NMR ($CDCl_3$): δ 57.56 (rel. intens. 773), δ 28.47 (2742), 22.18 (1788), 21.91 (1981), 17.85 (1198).

Kinetic experiments of 19' in methanol and t-butanol The experiments were carried out in 17 x 60 mm vials in which 5 mg of 19' was dissolved in a suitable amount of solvent (depending on the desired concentration) in the presence of a known amount of mesitylene as an internal standard. The vials were capped and clamped in the oil bath such that the oil level covered the solution. To the solution was added 11 mg of sodium methoxide (or 22 mg of potassium t-butoxide) at desired temperatures. The reaction took place immediately, and the solution became colorless. Except for the low-temperature runs (which were left in the cold bath for ten minutes), the vial was removed from the oil bath after two minutes, and the products were analyzed at once by capillary gas chromatography (DB-1 column in an HP 5890 gas chromatograph). From the peak areas and response factors (0.62 for 25, 0.68 for 26, 0.64 for 33), the yield of each product was calculated.

Figure 32. Ethyl bicyclo[4.1.0]hept-2-ene-7-carboxylates (35 and 36)

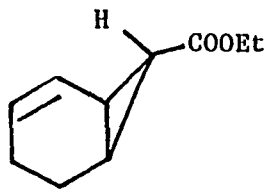

35

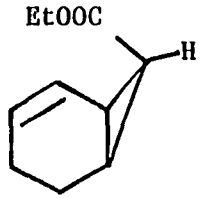

36

page 117: ^{1}HNMR in $CDCl_3$

page 118: IR (neat)

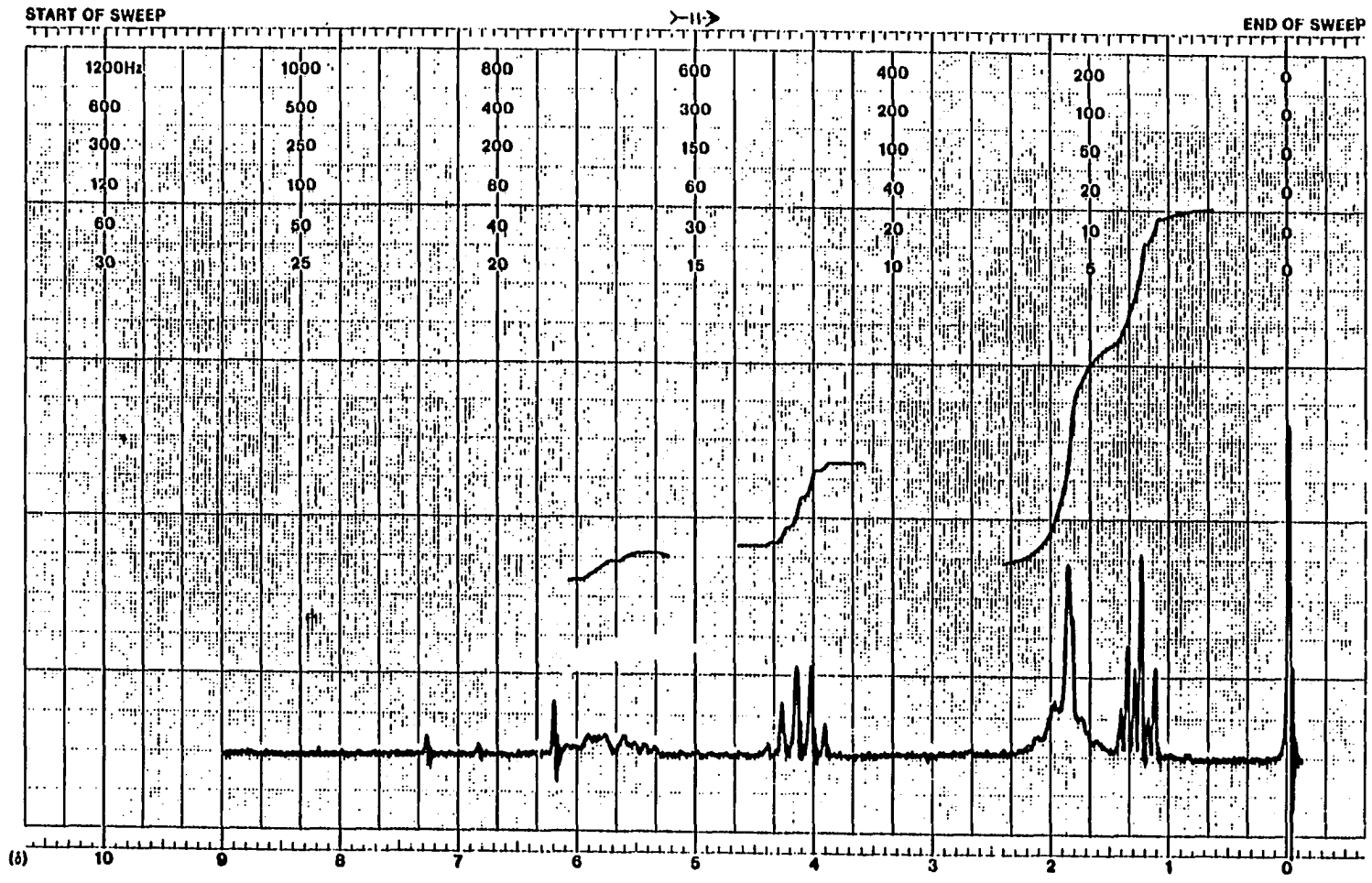
START OF SWEEP
END OF SWEEP
1200Hz
600
300
120
60
30
1000
500
250
100
50
25
800
400
200
80
40
20
600
300
150
60
30
15
400
200
100
40
20
10
200
100
50
20
10
5
0
0
0
0
0
0
(δ)
10
9
8
7
6
5
4
3
2
1
0

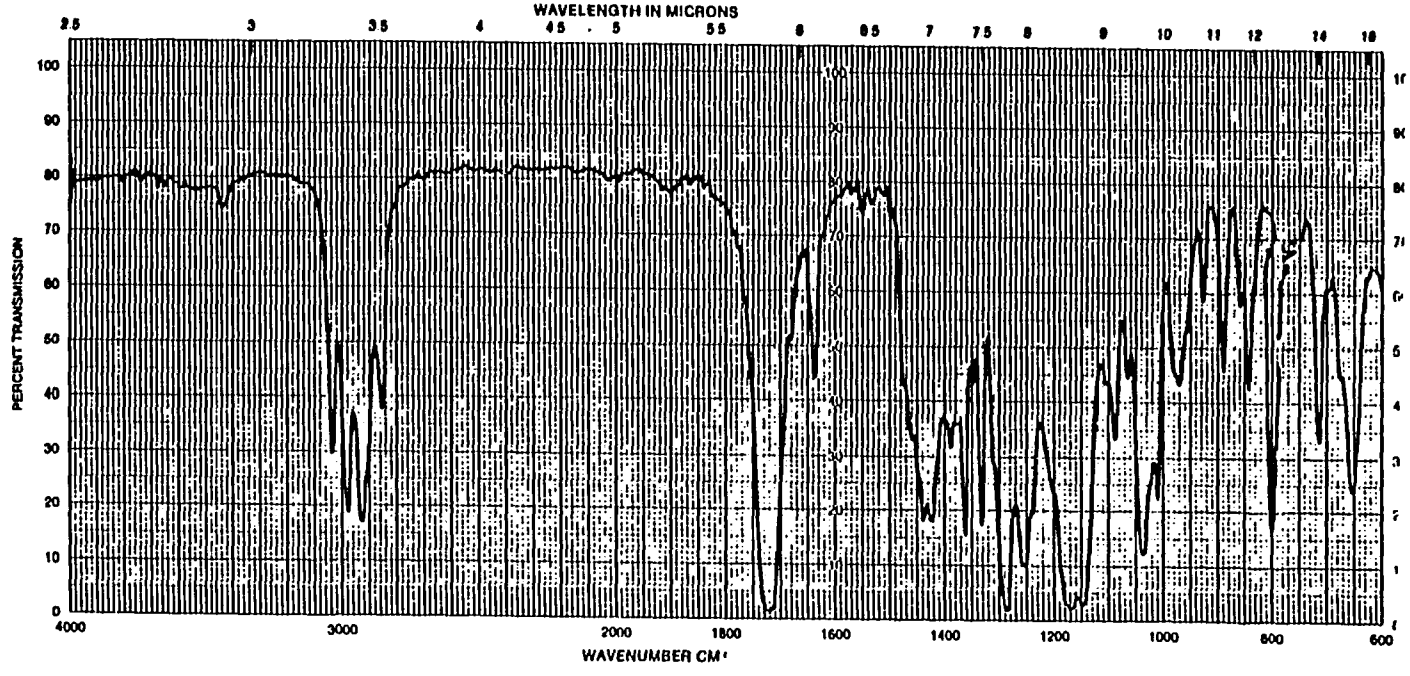

Figure 32. Continued

Figure 33. exo-Bicyclo[4.1.0]hept-2-ene-7-carboxylic acid (37)

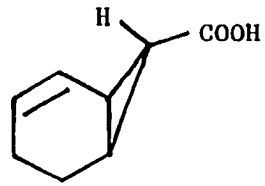

37

page 120: ^{1}H NMR in $CDCl_3$

page 121: IR in $CDCl_3$

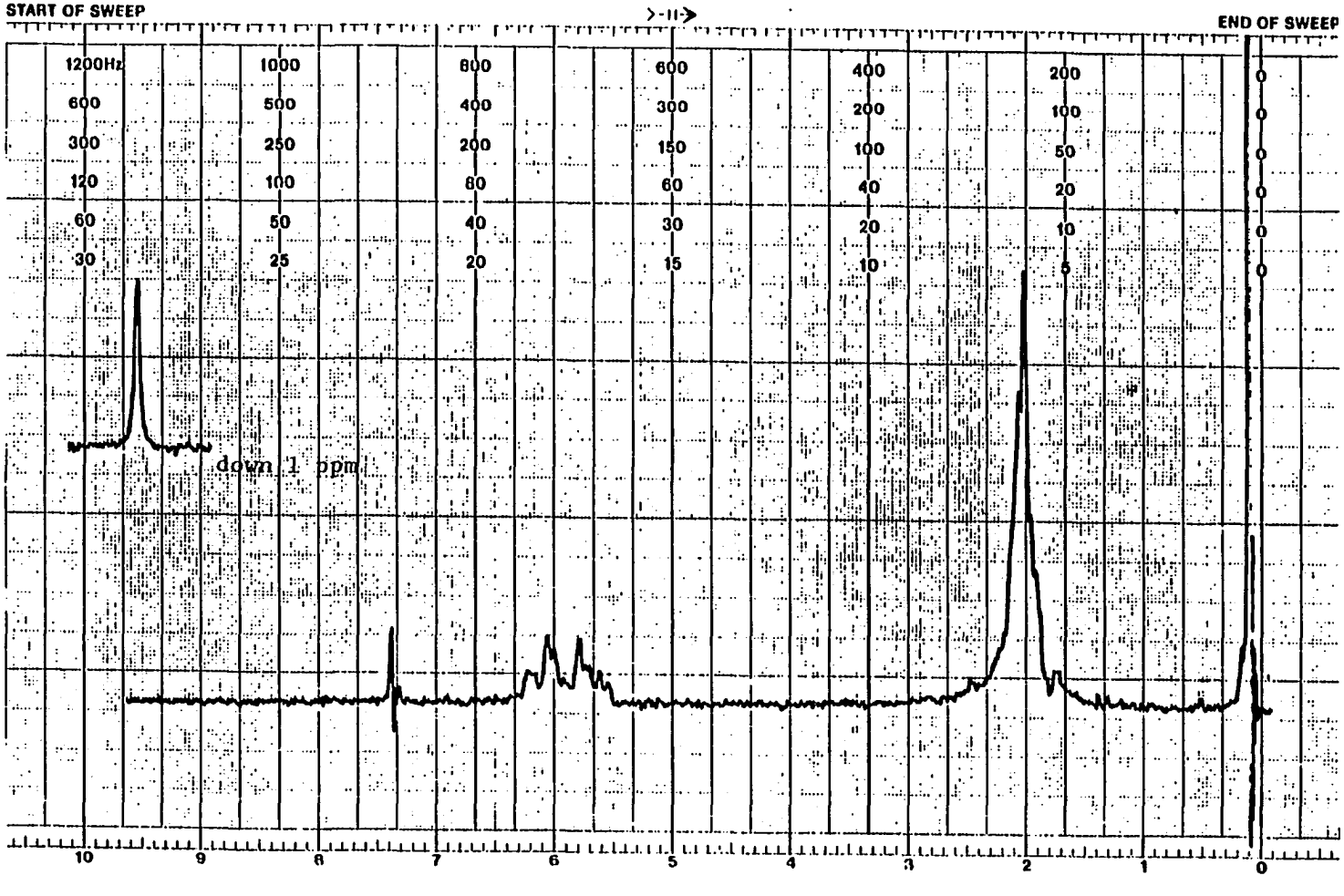
START OF SWEEP
END OF SWEEP
1200Hz
600
300
120
60
30
1000
500
250
100
50
25
800
400
200
80
40
20
600
300
150
60
30
15
400
200
100
40
20
10
200
100
50
20
10
5
0
0
0
0
0
0
down 1 ppm
10
9
8
7
6
5
4
3
2
1
0

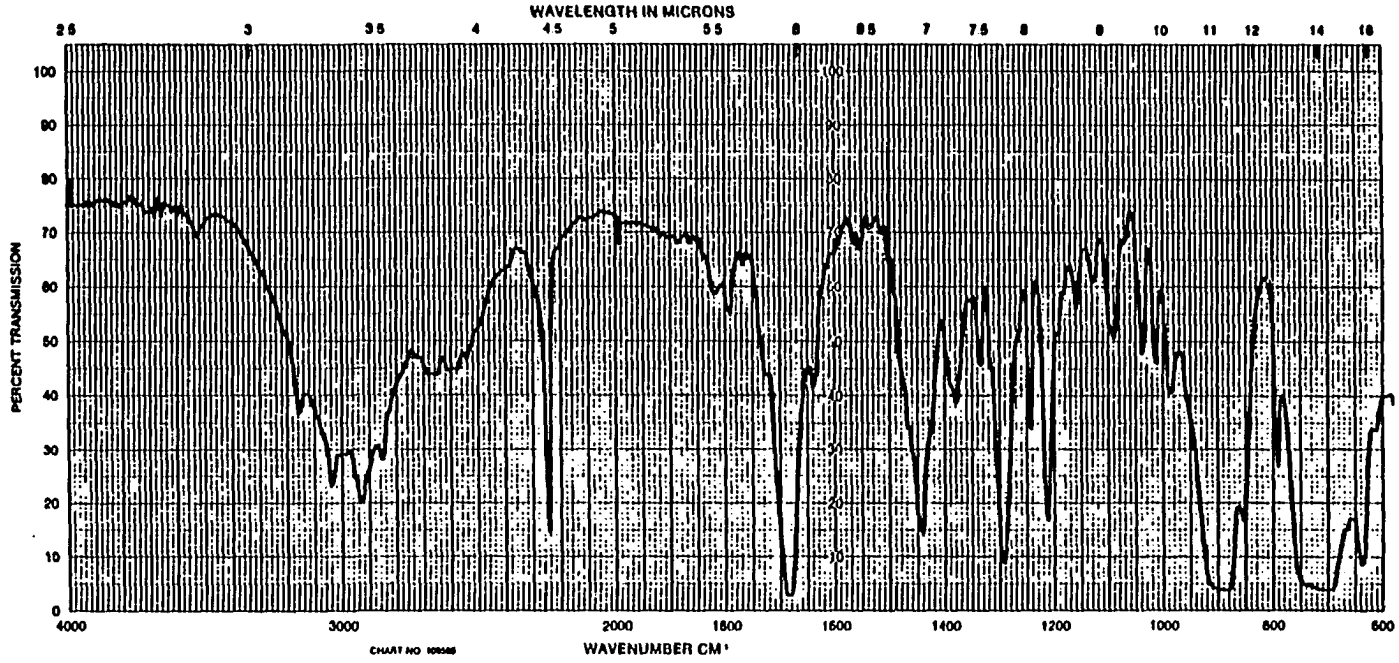

Figure 33. Continued

Figure 34. Iodolactone of acid 38 (39)

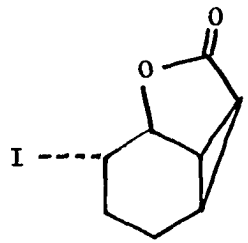

39

page 123: ^{1}H NMR in $CDCl_3$

page 124: IR in $CDCl_3$

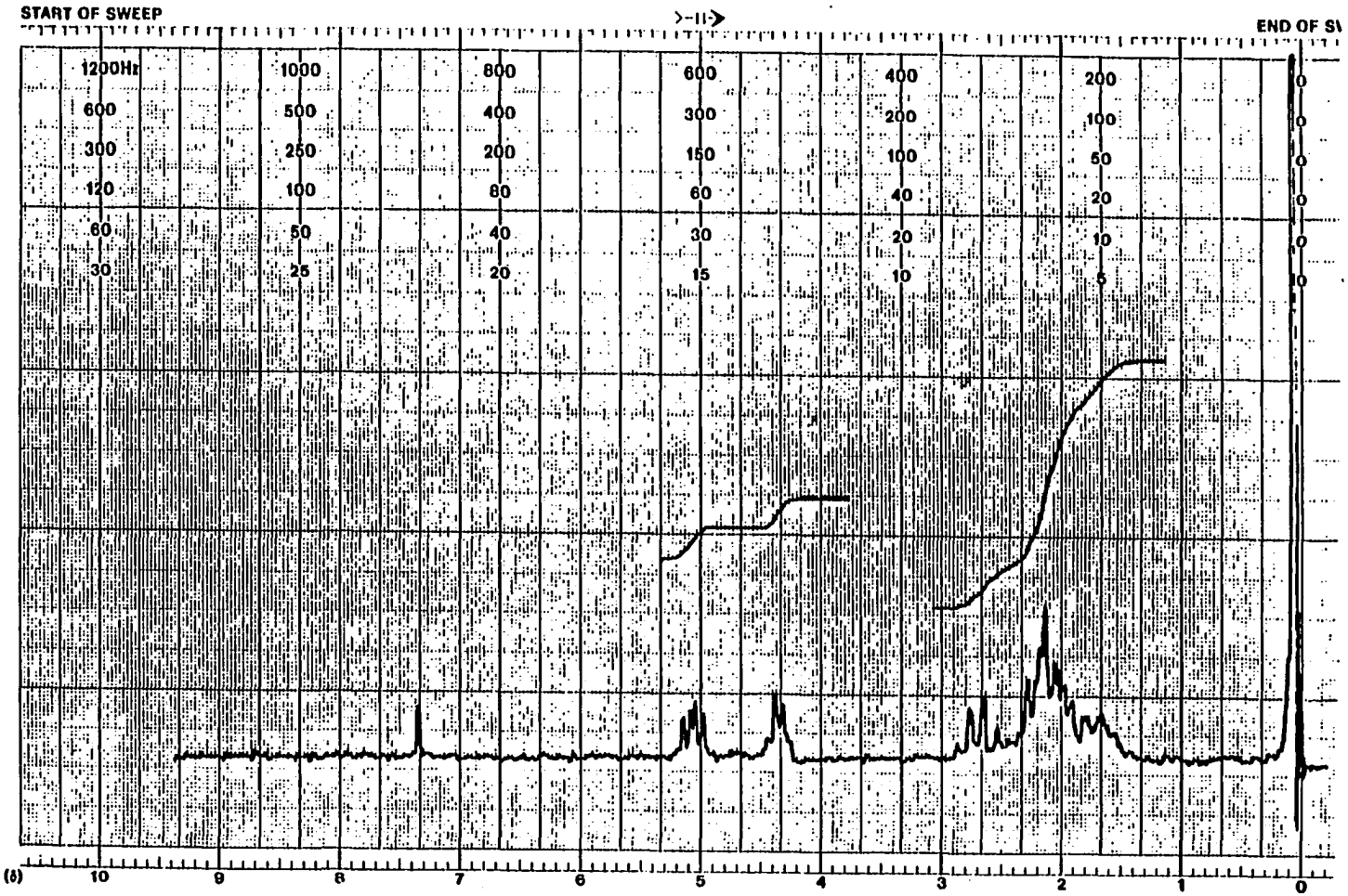
START OF SWEEP
END OF SW
1200Hz
600
300
120
60
30
1000
500
250
100
50
25
800
400
200
80
40
20
600
300
150
60
30
15
400
200
100
40
20
10
200
100
50
20
10
5
0
0
0
0
0
10
(δ)
10
9
8
7
6
5
4
3
2
1
0

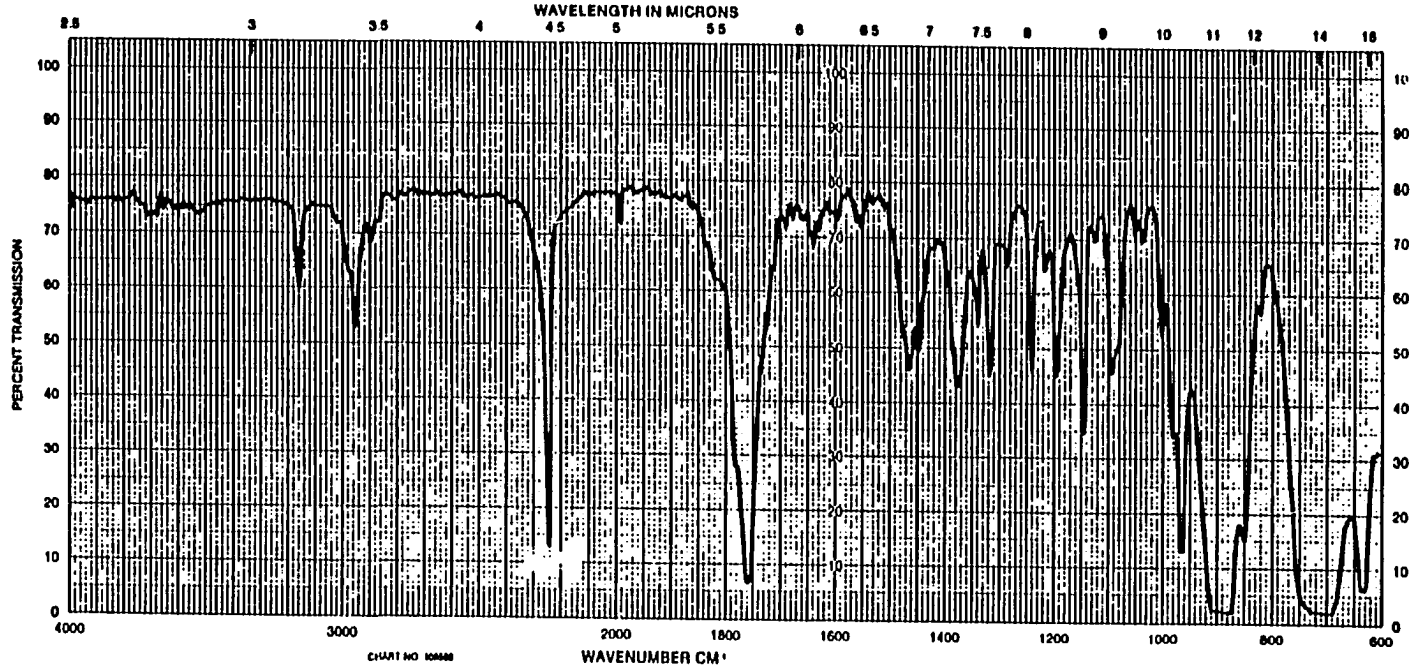

Figure 34. Continued

Figure 35. exo-Bicyclo[4.1.0]hept-7-carboxylic acid (40)
~~

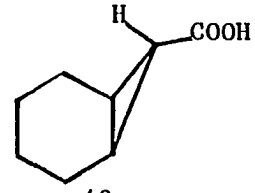

40
~~

page 126: ^{1}H NMR in $CDCl_3$

page 127: IR in $CDCl_3$

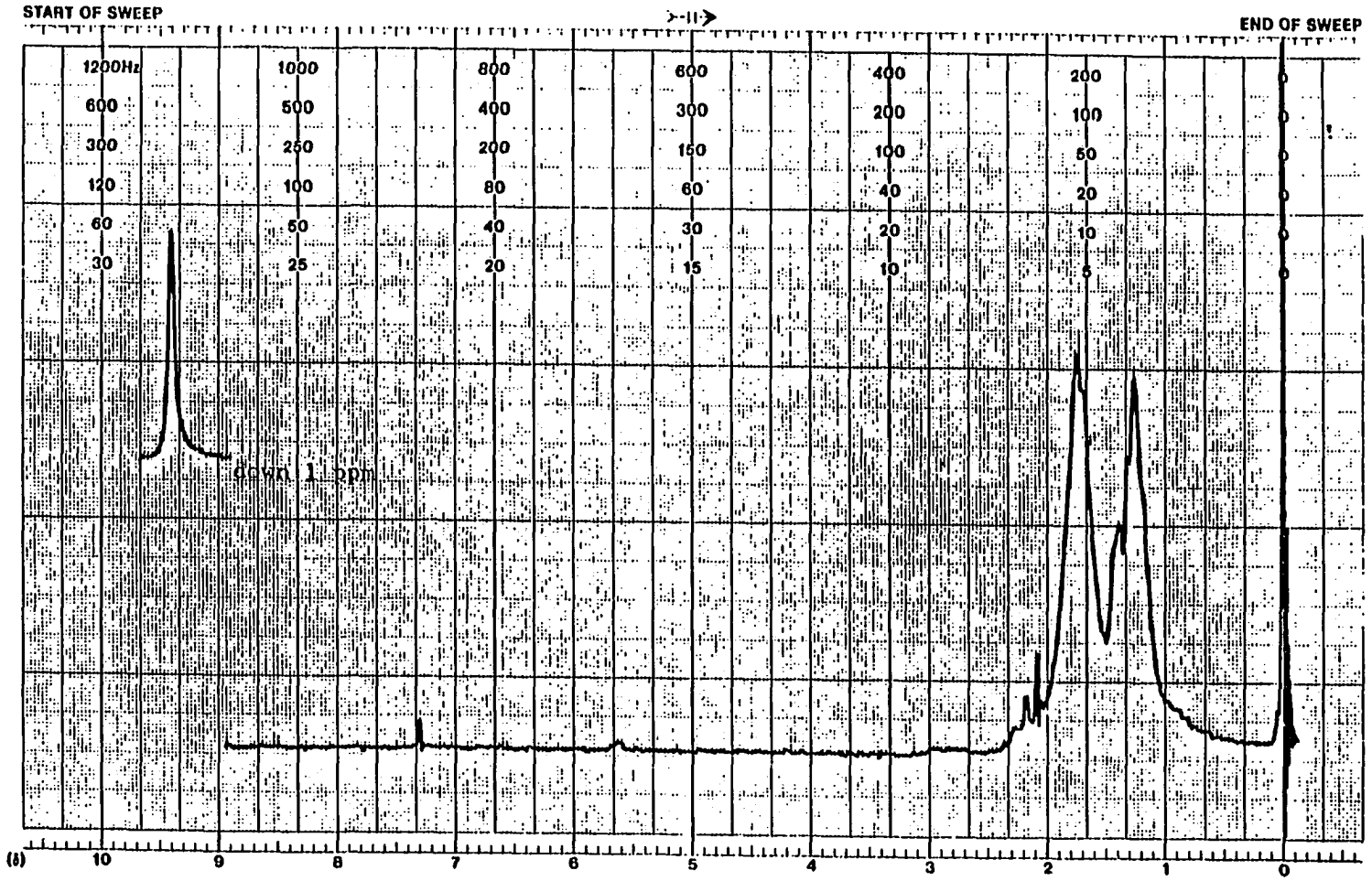
START OF SWEEP
END OF SWEEP
1200Hz
600
300
120
60
30
1000
500
250
100
50
25
800
400
200
80
40
20
600
300
150
60
30
15
400
200
100
40
20
10
200
100
50
20
10
6
down 1 bpm
(s)
10
9
8
7
6
5
4
3
2
1
0

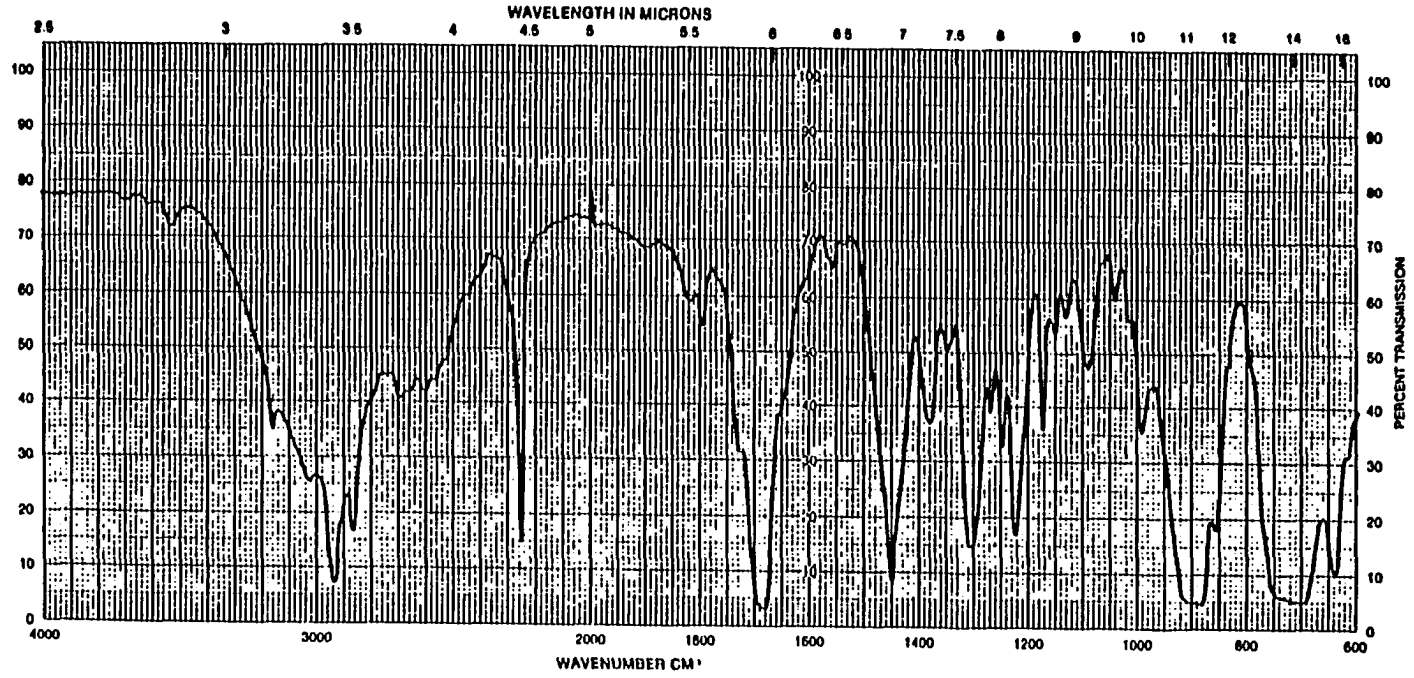

Figure 35. Continued

Figure 36. exo-Bicyclo[4.1.0]hept-7-ylisocyanate (41)
~~

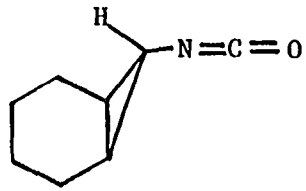

41
~~

page 129: IR (neat)

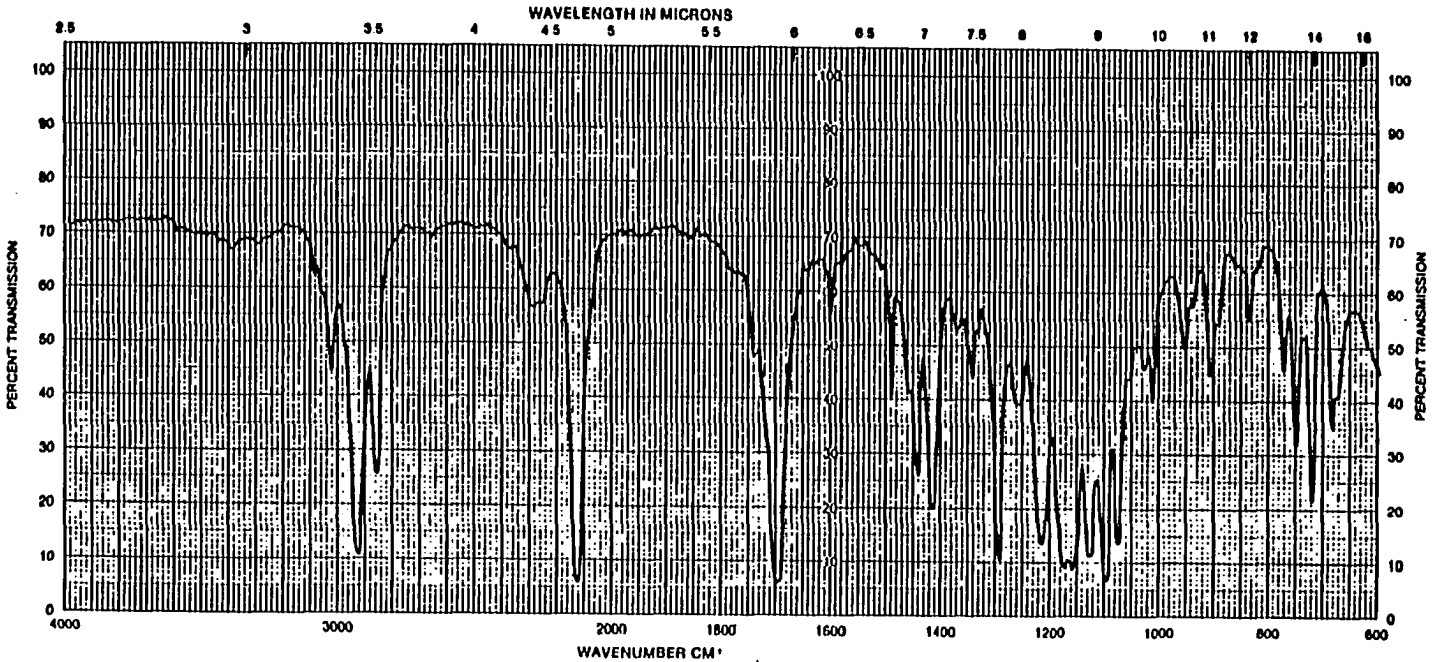
WAVELENGTH IN MICRONS
2.5
3
3.5
4
4.5
5
5.5
6
6.5
7
7.5
8
9
10
11
12
14
16
PERCENT TRANSMISSION
100
90
80
70
60
50
40
30
20
10
0
4000
3000
2000
1800
1600
1400
1200
1000
800
600
WAVENUMBER CM⁻¹

Figure 37. 7-exo-Bicyclo[4.1.0]heptylurea (42)

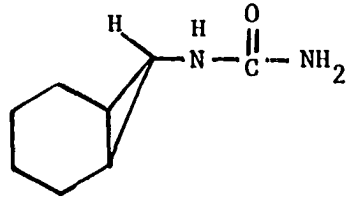

42

page 131: ^{1}H NMR in $CDCl_3$

page 132: IR in $CDCl_3$

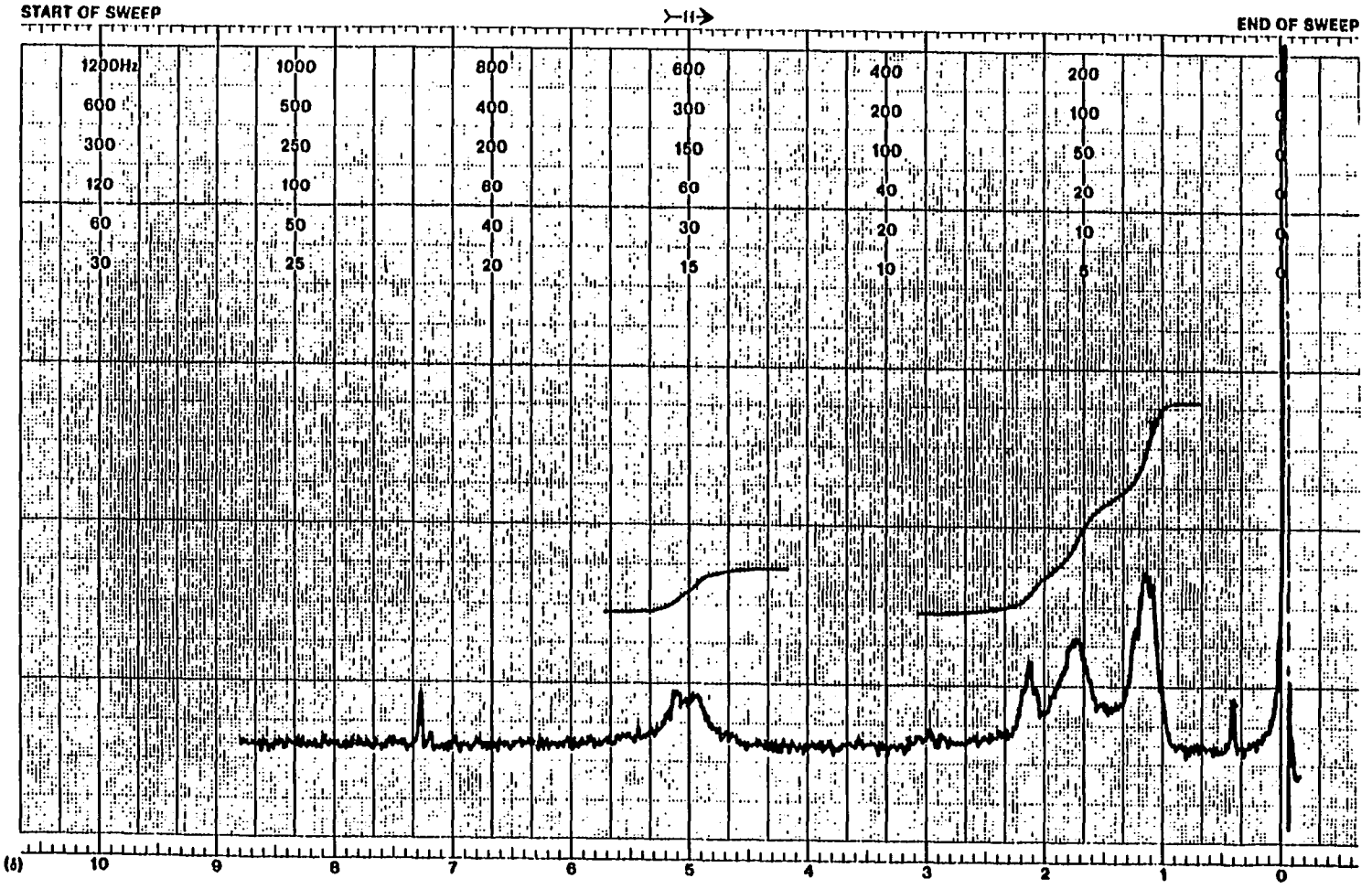
START OF SWEEP
END OF SWEEP
1200Hz
600
300
120
60
30
1000
500
250
100
50
25
800
400
200
60
40
20
600
300
150
60
30
15
400
200
100
40
20
10
200
100
50
20
10
5
(δ)
10
9
8
7
6
5
4
3
2
1
0

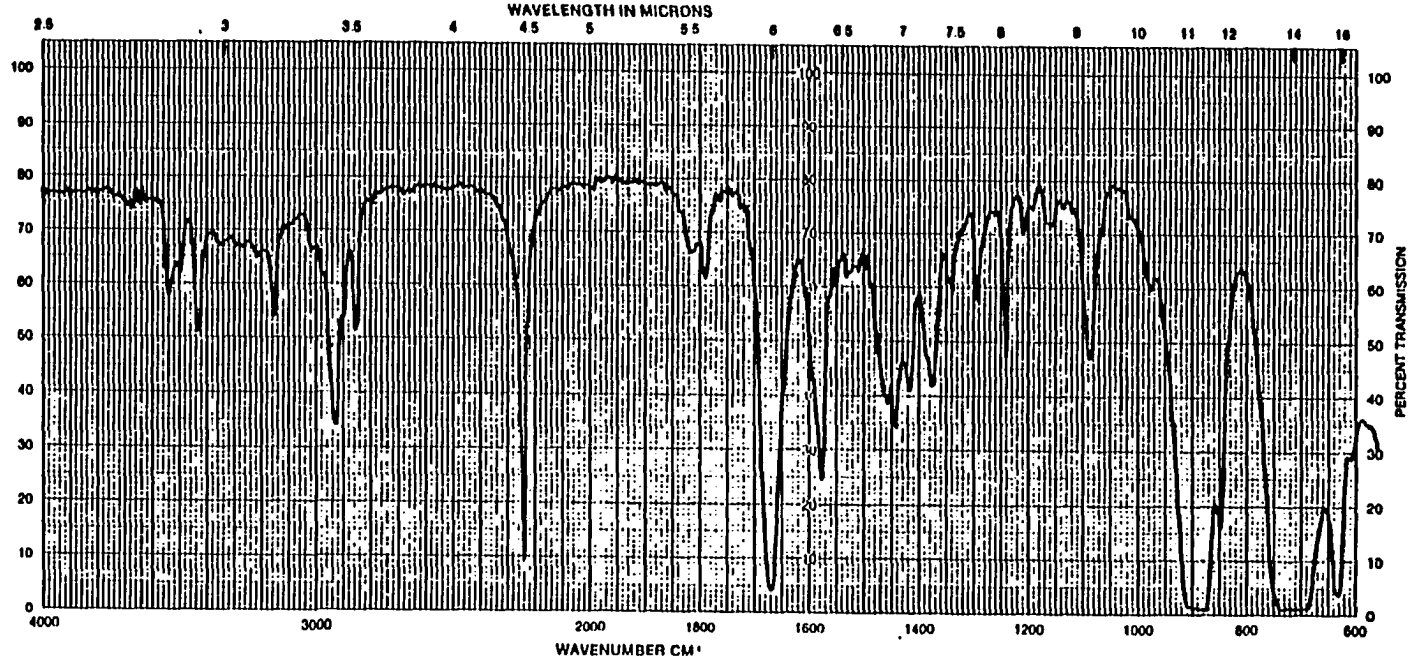

Figure 37. Continued

Figure 38. N-(7-exo-Bicyclo[4.1.0]heptyl)-N-nitrosourea (19')

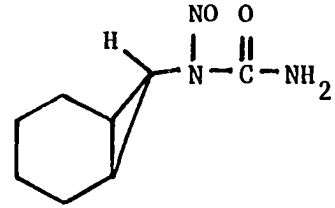

19'

page 134: ^{1}H NMR in $CDCl_3$

page 135: ^{13}C NMR in $CDCl_3$

page 136: IR in $CDCl_3$

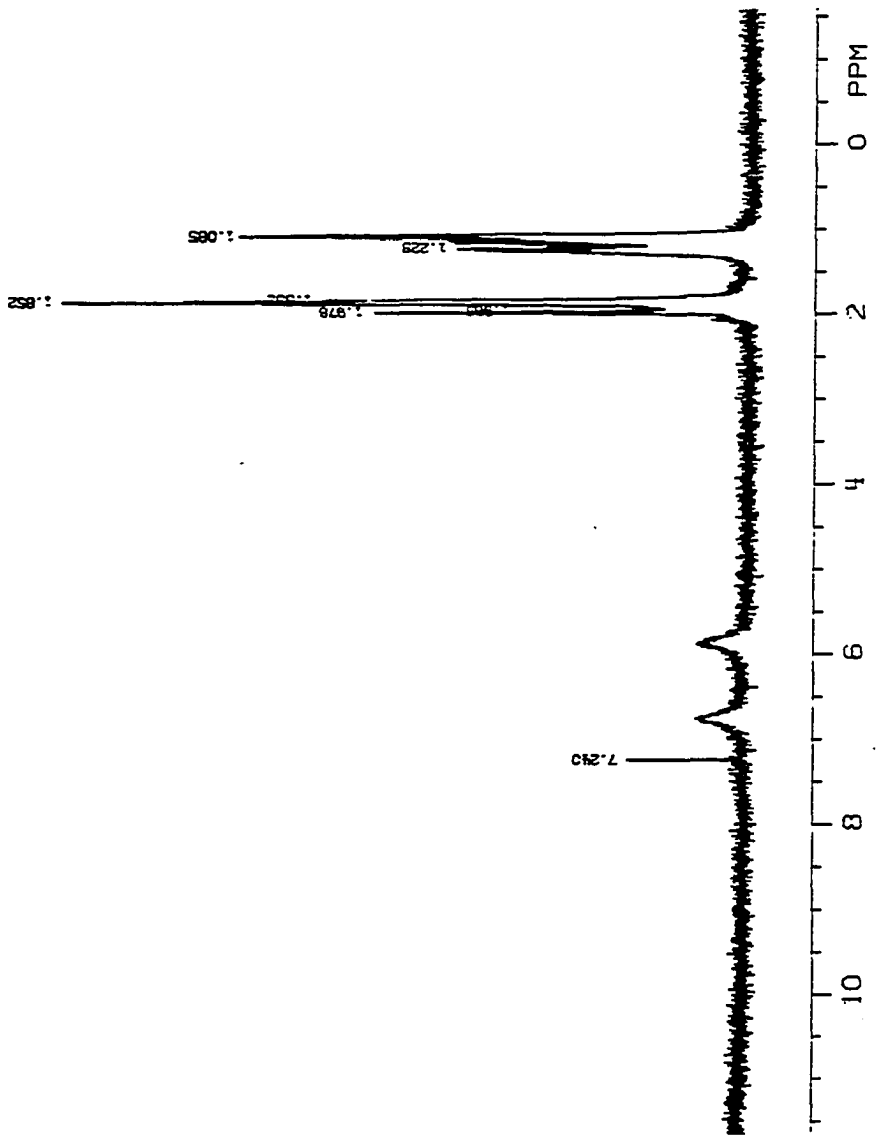
1.085
1.229
1.852
1.978
7.243
0 PPM
2
4
6
8
10

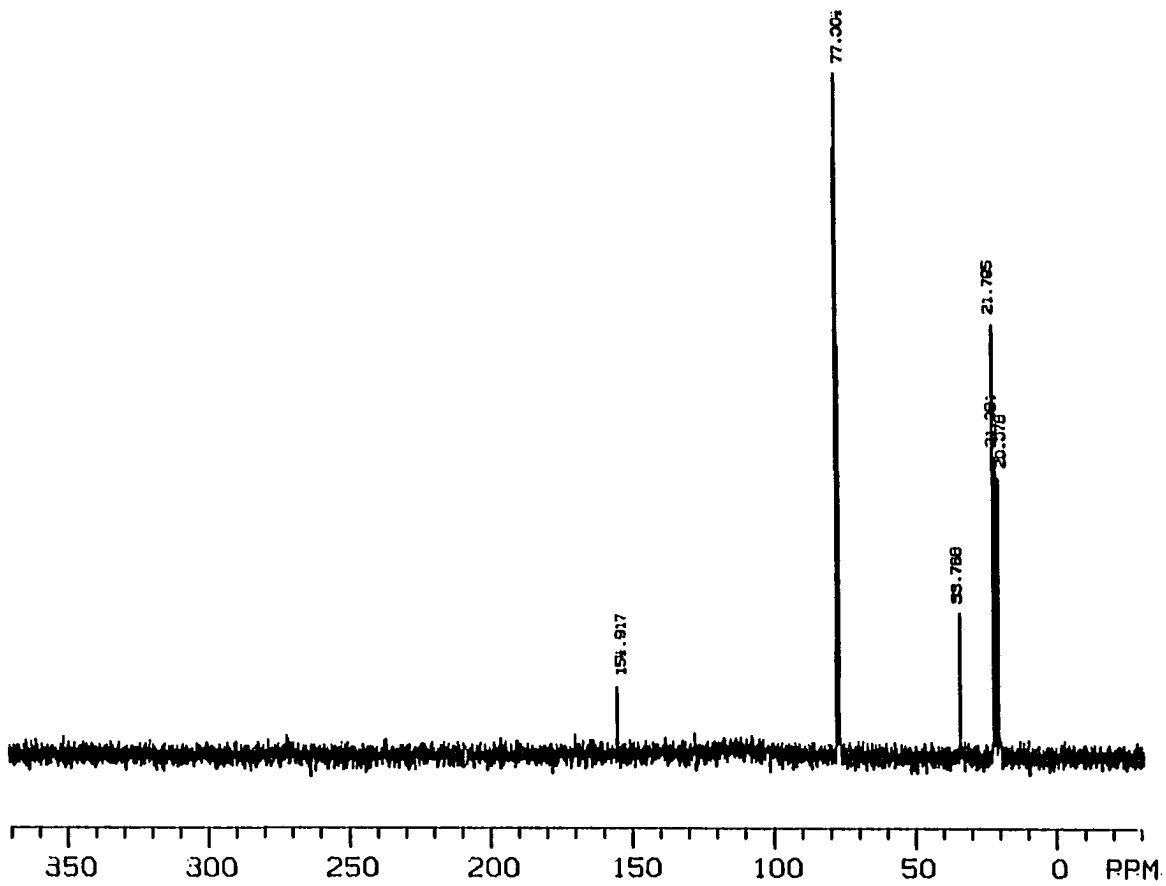

Figure 38 (continued)

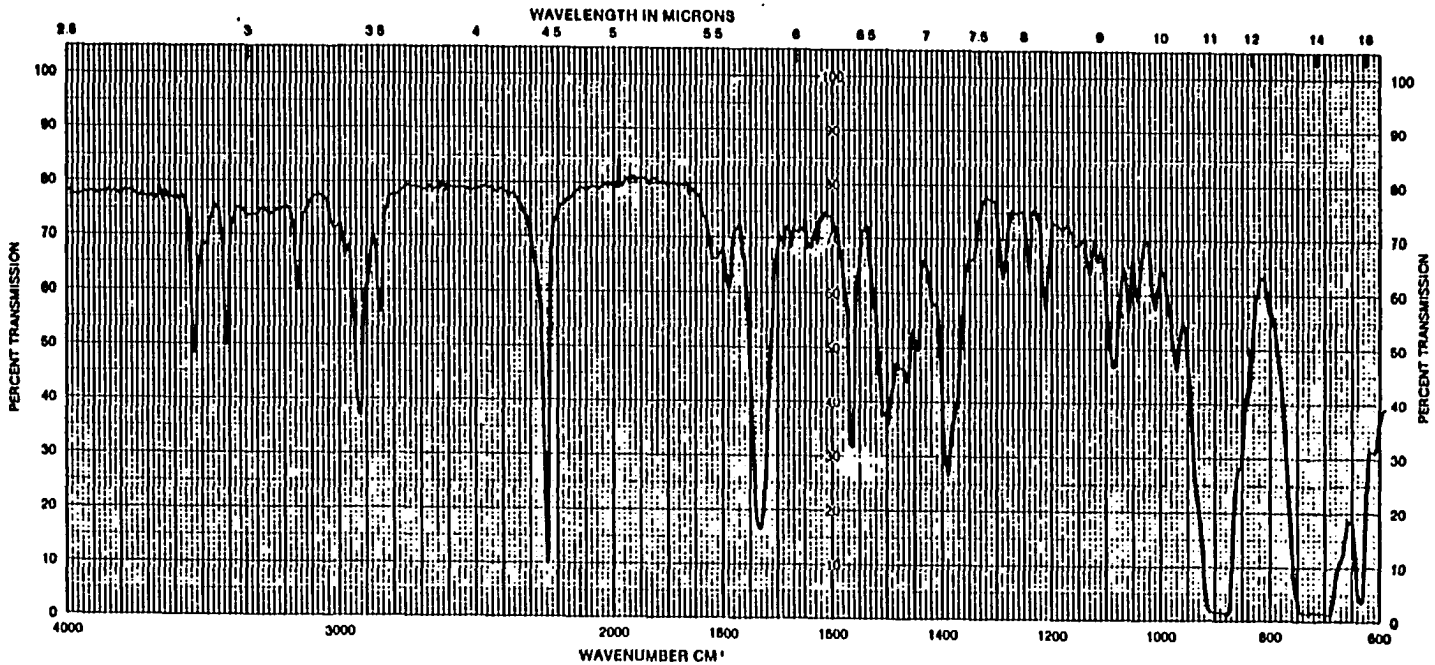

Figure 38. Continued

Figure 39. anti-7-t-Butoxy-bicyclo[4.1.0]heptane (33)
~~

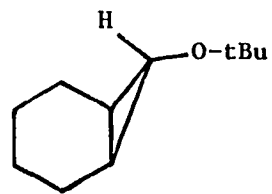

33
~~

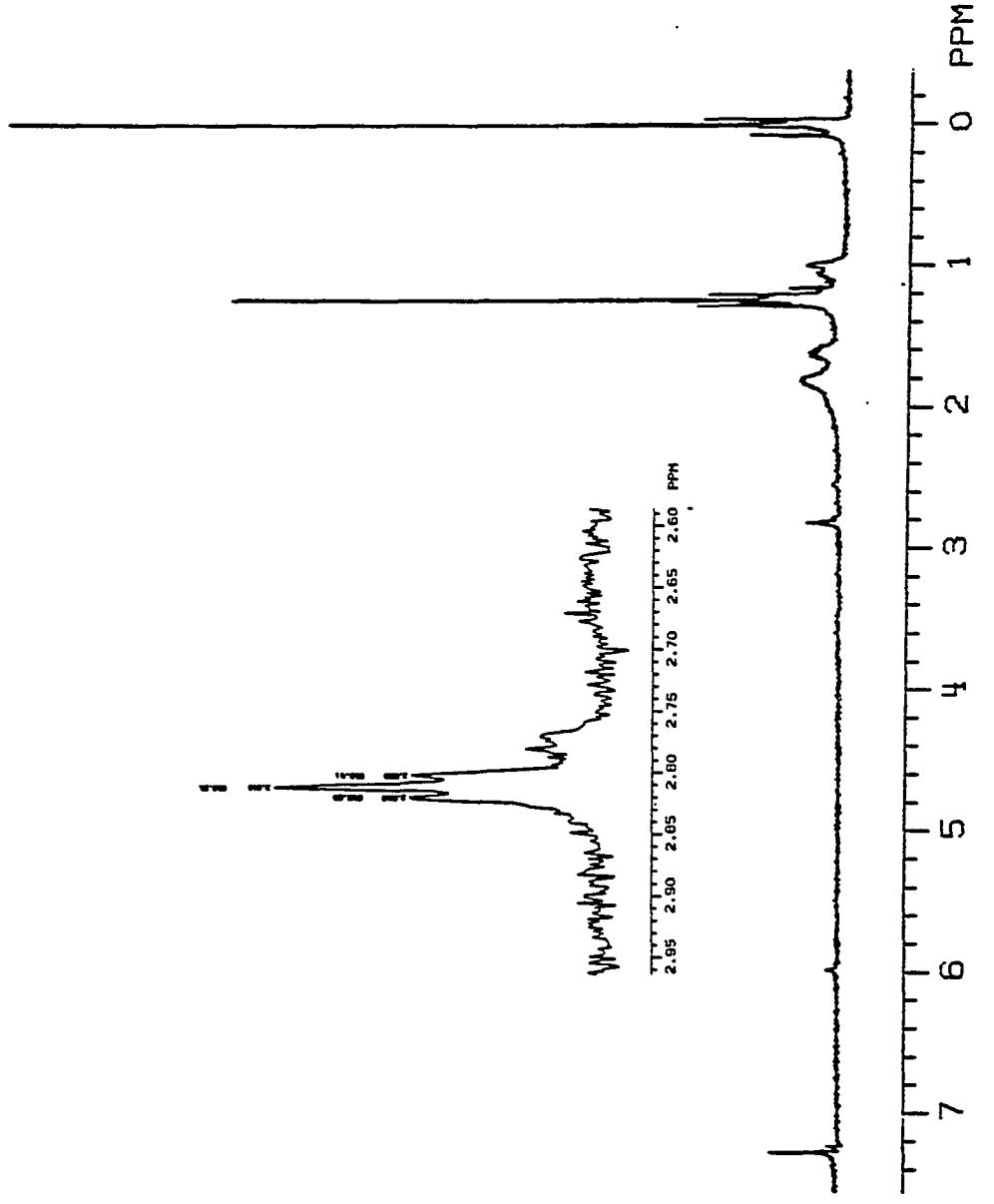
PPM
0
1
2
3
4
5
6
7
2.95
2.90
2.85
2.80
2.75
2.70
2.65
2.60
PPM

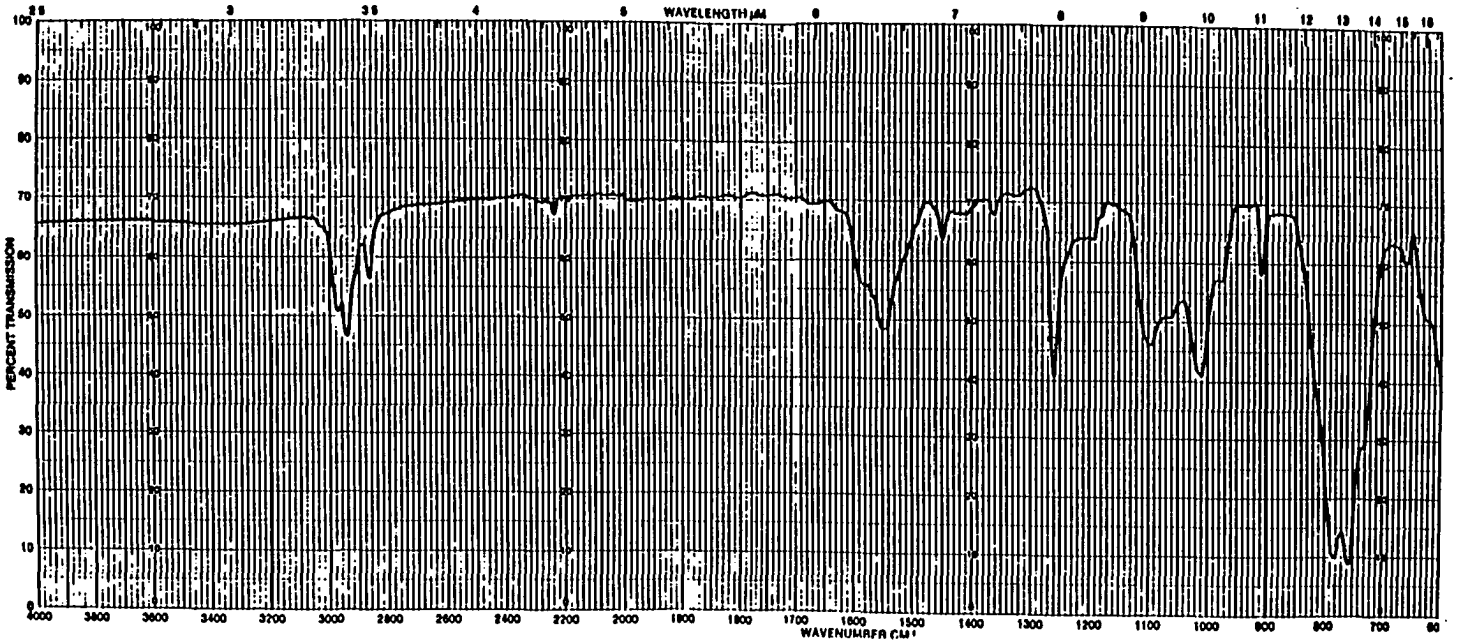

Figure 39. Continued

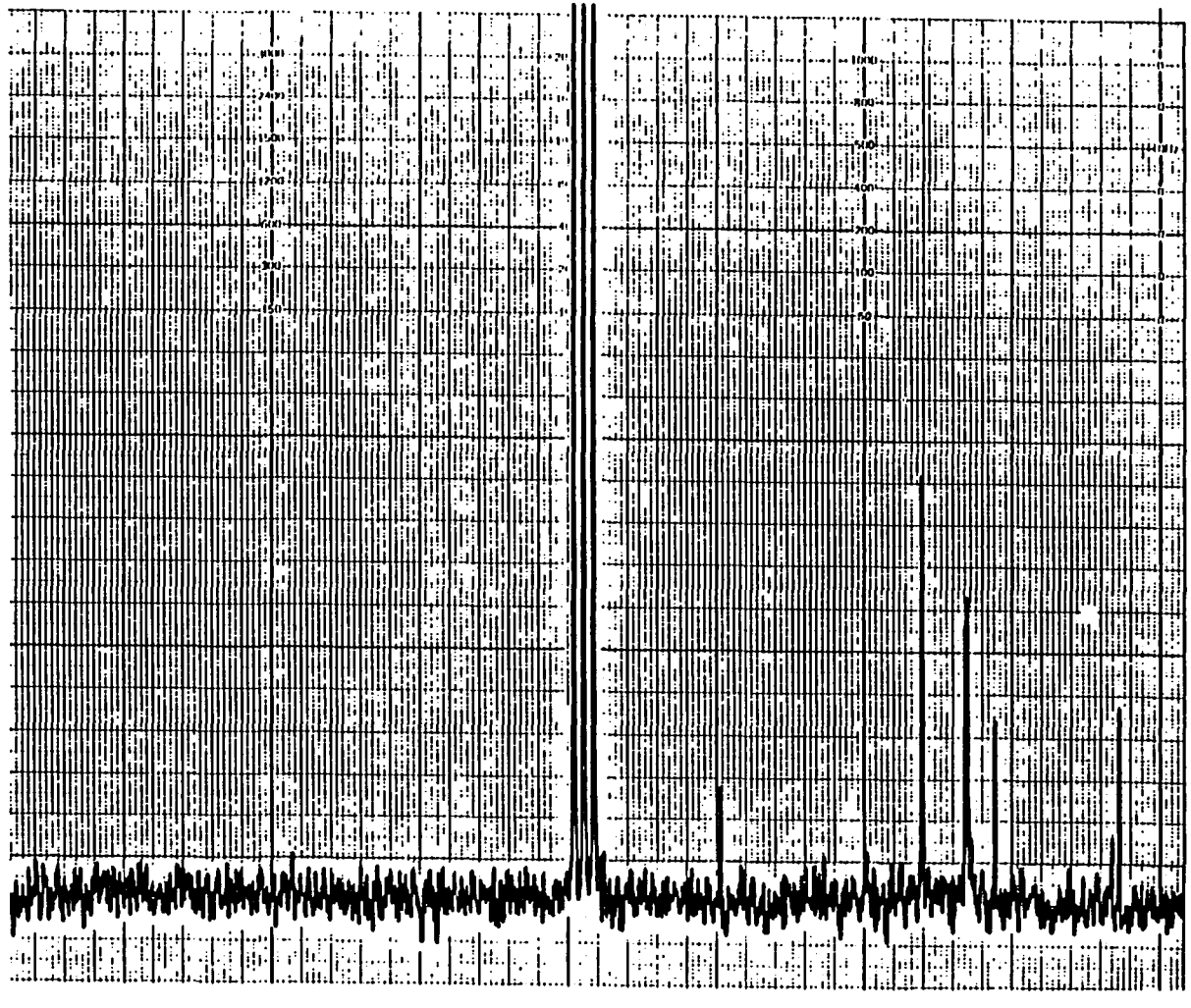

Figure 39. Continued

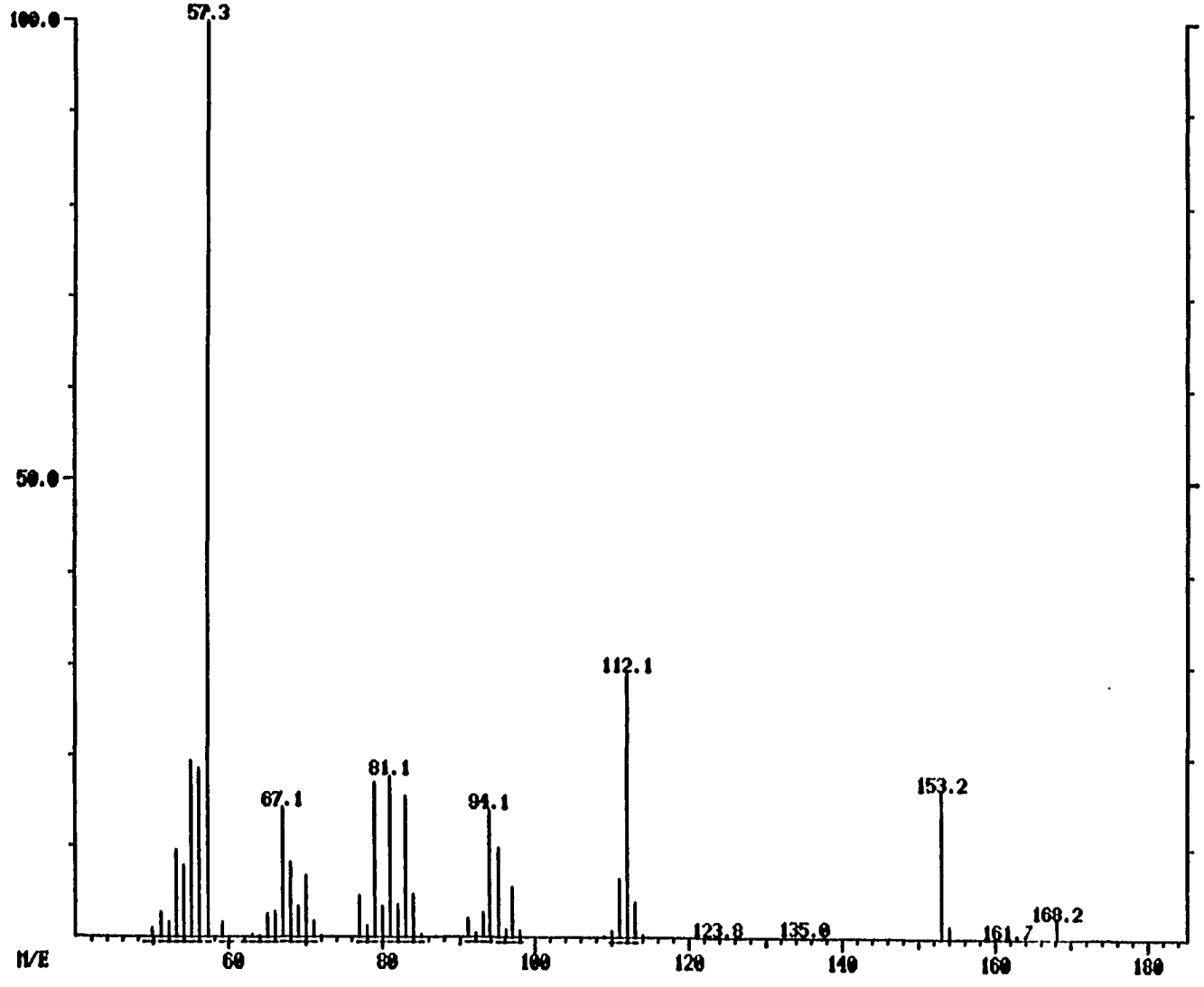

Figure 39. Continued

CHAPTER II. FORMATION OF NITRILE YLIDES FROM THE REACTION OF NORCARANYLIDENE WITH NITRILES

Introduction

Nitrile ylides, commonly generated from the photolysis of 2H-azirines, can be viewed as a class of 1,3-dipoles containing a central nitrogen atom and a π bond orthogonal to the 4π allylic system. They have been trapped with a wide variety of dipolarophiles to form five-membered heterocyclic rings. Huisgen (52) has argued that the bent geometric form (43) of a nitrile ylide would be less stable than the linear form (44), since allyl resonance would be at a maximum with the linear arrangement.

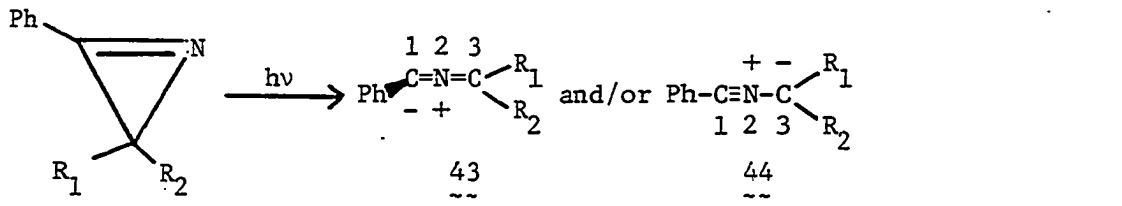

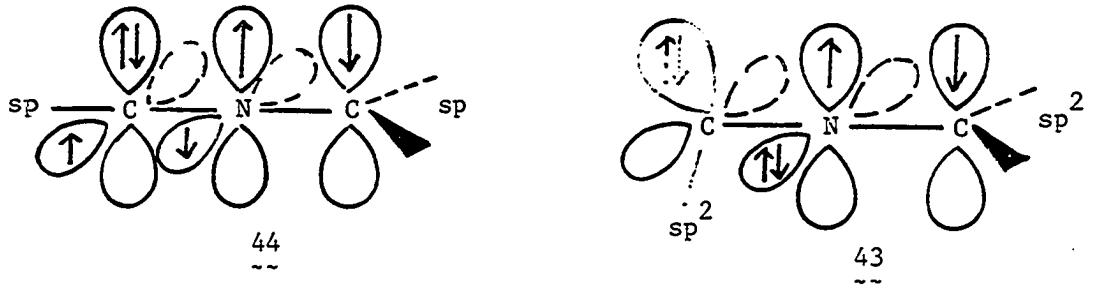

However, ab initio LCAO-MO-SCF calculations by Salem et al., cited in (53) indicated that the bent nitrile ylide geometry is favored over the linear. According to Salem's calculations, the ground state singlet geometry of the nitrile ylide has an HCN angle of 156.7° and is ~18 Kcal/mol more stable than the linear form. A similar conclusion was

reached by Houk and Caramella, cited in (53). Their calculations showed that the bent nitrile ylide geometry is favored over the linear, but otherwise optimized, geometry by 11.1 Kcal/mol. Moreover, Houk's calculations showed that the bent nitrile ylide HOMO is heavily localized at C-1, which should ordinarily be the nucleophilic terminus of the molecule. Protonation of the nitrile ylide was known to occur at the C-1 carbon atom (53). Therefore they believed that all the known reactions of simple nitrile ylides could be accounted for by a bent geometry. On the other hand, nitrile ylides with electron withdrawing groups at C_3 should favor the planar structure, with C_3 as the nucleophilic end. A case in point appears to be bis(trifluoromethyl)benzonitrile ylide (54). A more dubious case is benzonitrile cyclopropylide (45), which gives only a 5% yield of 46 (55). The nonplanarity preferred by cyclopropyl may induce linearity at C_1, wherefore protonation occurs at C_3.

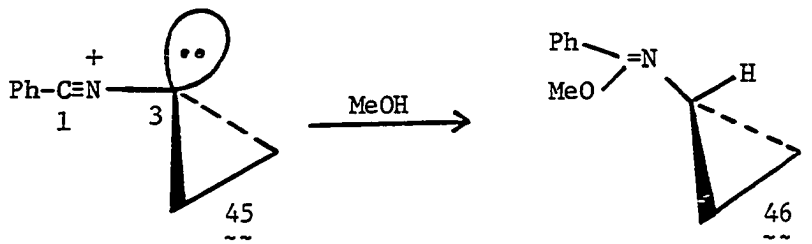

From the work of Huisgen (52), Padwa (56) and Orhovats et al. (57), nitrile ylides are known to add readily to electron deficient olefins. Houk et al. (58a) and Caramella and Houk (58b) used frontier molecular orbital theory to explain the regioselectivity of most 1,3-dipolar cycloadditions. With nitrile ylides as 1,3-dipoles, the dipole HOMO and dipolarphile LUMO interaction is

primarily responsible for stabilizing the transition state. The favored cycloadduct is that formed by the union of the atoms with the largest coefficients in the dipole HOMO and dipolarophile LUMO. An electron-deficient olefin has the largest coefficient on the unsubstituted carbon in the LUMO. In the HOMO of the bent nitrile ylide, the electron density at the disubstituted carbon (C_1) is greater than at the tri-substituted carbon atom (C_3) (59). On this basis, all the regiochemical data found in the photoaddition of 2H-azirines with a variety of dipolarophiles was explained (60).

It has been reported (61-64) that laser flash photolysis of 9-diazofluorene (47) in CH_3CN solution generates the nitrile ylide derived from the reaction of fluorenylidene with acetonitrile. In 1982, Griller et al. (65) demonstrated the formation of nitrile ylides by the interaction of fluorenylidene with nitrile solvents (acetonitrile, pivalonitrile and benzonitrile). In these solvents, they observed the buildup of transients at 400 nm, concurrent with the decay of the fluorenylidene signal at 470 nm. They concluded that the absorption of 470 nm was due to ^{3}Fl, while that at 400 nm was due to ylides formed by the reaction of fluorenylidene with nitriles. They further confirmed that they were nitrile ylides by olefin quenching experiments. Fumaronitrile quenched the acetonitrile ylide with $k_q = (5.7 \pm 0.4) \times 10^7\ M^{-1}s^{-1}$. At the same time, work from Schuster's laboratory agreed well with their band assignments (62).

In contrast to the observation of the ylide 48 by Griller et al. (65) in acetonitrile, Turro et al. (66) reported in 1983 that the ylide

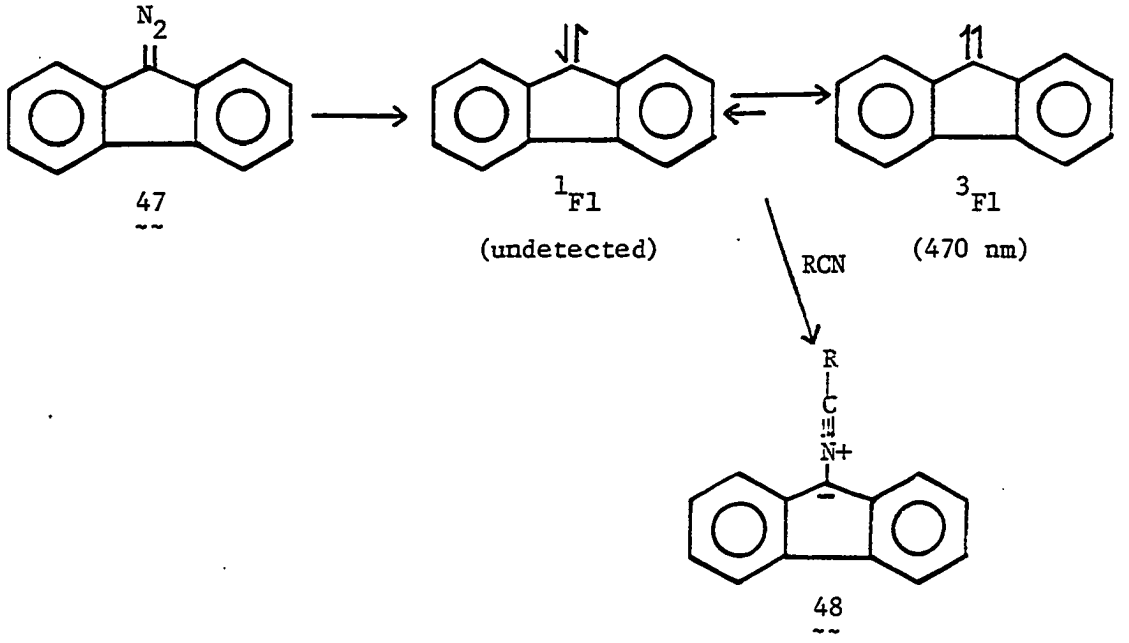

absorption obtained from azirine 49 was not observed upon pulsed laser photolysis in isooctane solutions at 25°C. On the other hand, the

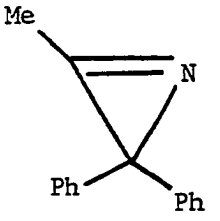

formation of diphenylcarbene was found in a detectable yield. These findings indicated that the rate constant for reaction of acetonitrile with diphenylcarbene was significantly smaller than that of acetonitrile with fluorenylidene. Moreover, Zupancic et al. (11) recently reported that ylide 48 (R = CH_3) didn't fragment to fluorenylidene rapidly

($k_{frag.} < 10^3\ s^{-1}$). Therefore, a conclusion can be made that the rates of ylide formation and dissociation will depend strongly on the nature of the carbene, and similarly may depend on the properties of the nitriles. Since the relatively stable fluorenylidene is formed rather slowly from its nitrile ylide, it may be anticipated that the much less stable norcaranylidene would be formed more slowly from a parallel ylide source.

Grasse et al. (67) reported another investigation of fluorenylidene by nanosecond laser spectroscopy in 1983. Irradiation of azirine 50 in acetonitrile gave a transient product whose absorption spectrum showed a maximum at ca. 400 nm. The similarity of this spectrum to the one obtained from the reaction of fluorenylidene with acetonitrile suggested that a common product was formed in these two reactions. In the presence of dimethylmaleic anhydride as a trapping agent, the azirine was converted to adduct 51, which was the product anticipated to result from dipolar addition of acetonitrile ylide 52 to the anhydride (Scheme XIII). Even more interesting was the trapping of 52 by methanol. While no reversion to Fl occurred, the imine product, 54, indicated that C_3 of the ylide was the nucleophilic center, in accord with an expectedly linear structure for 52.

Kende et al. (68) reported evidence for the intermediacy of ylide 59 in the thermolysis of 55 in methacrylonitrile (MAN). Compounds 56 and 57 were obtained in an approximately 1:1 ratio via either thermolysis or photolysis of 55 in MAN. Prolonged heating of 56 in refluxing MAN led simply to recovery of 56 in excellent yield, which ruled out the

Scheme XIII

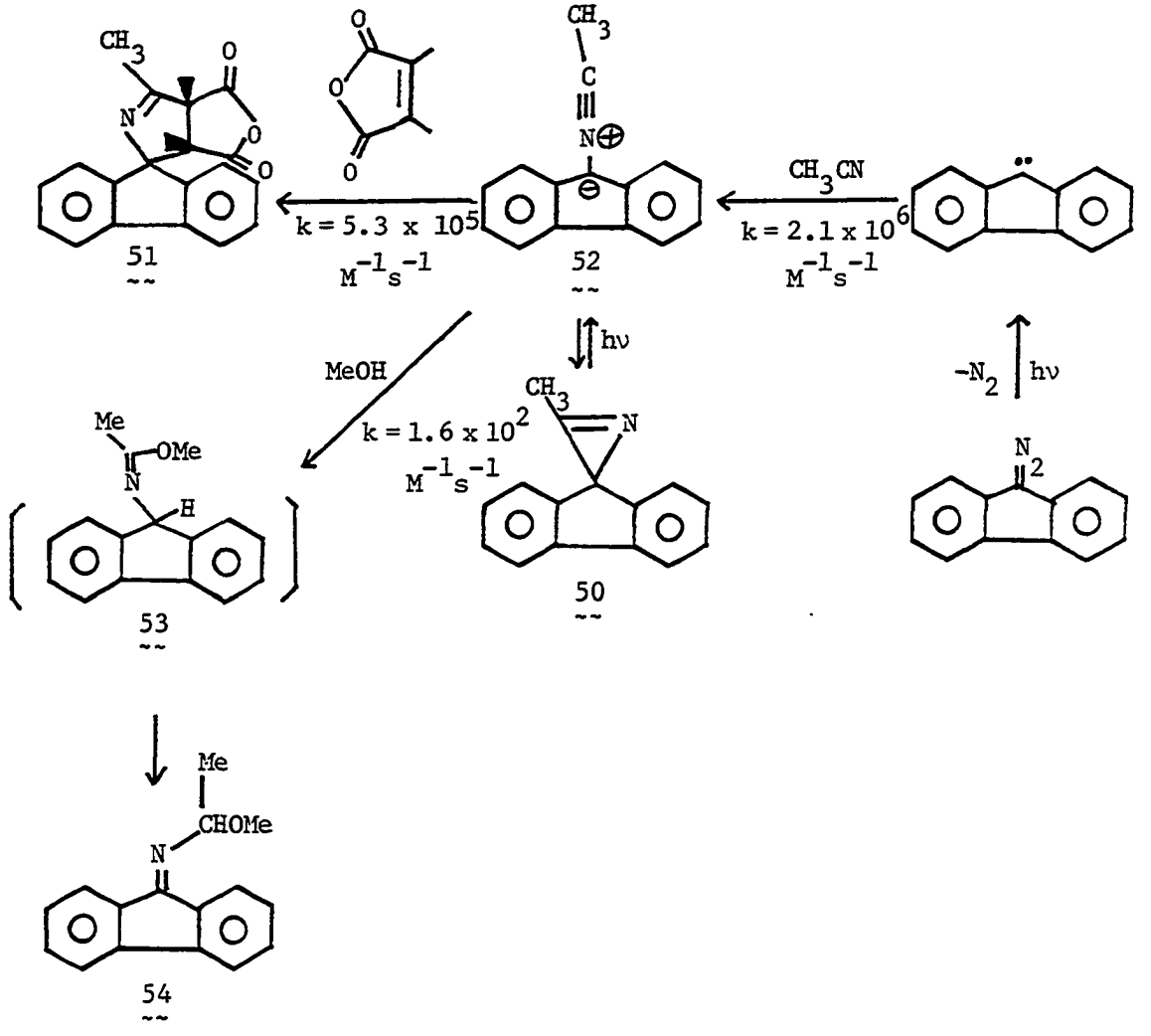

possibility that 57 was a secondary product. Their proposed mechanism, which features the reversible formation of 58 from 59, and is in accord with the kinetic observations, is shown in Scheme XIV. However, a kinetically equivalent alternative would be for 59 to competitively give rise to both 56 and 57 ($k_{56}/k_{57} \approx 0.2$), without reversion of 59 to 58.

Scheme XIV

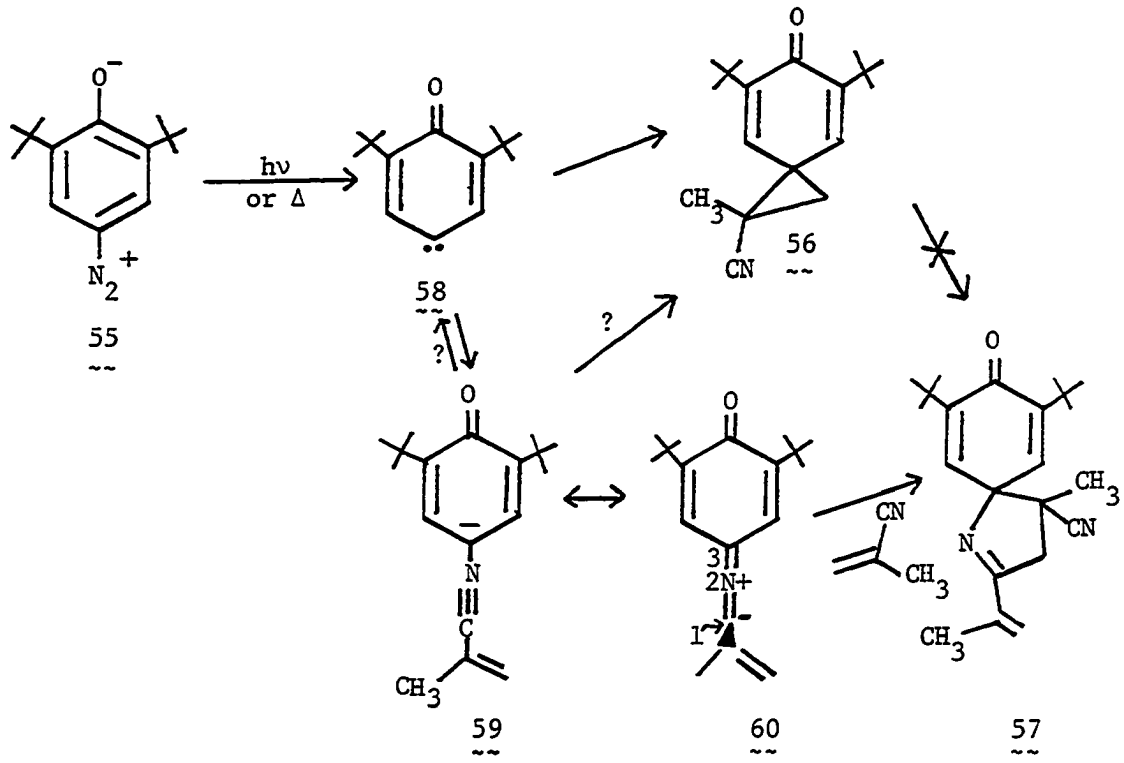

In view of the fluorenylidene ylide results, it would be surprising if the conversion of 59 to 58 were actually operative, particularly since MAN reacts with nitrile ylides at least 100 times faster than MeOH (vide infra) (11).

The regiochemistry of the addition of 59 to MAN to give 57 seems consistent with the bent formulation, 60, as that structure affords a HOMO with the large lobe at C_1 (58).

Barcus et al. (69) reported that photolysis of 61 (λ = 350 nm, Rayonet reactor) in acetonitrile containing acrylonitrile gave cyclopropanes 62Z and 62E, as well as heterocycles 62Z and 63E. The ratio of cyclopropanes/pyrroline was sensitive to the concentration of acrylonitrile: high concentration favored carbene addition, while

Scheme XV

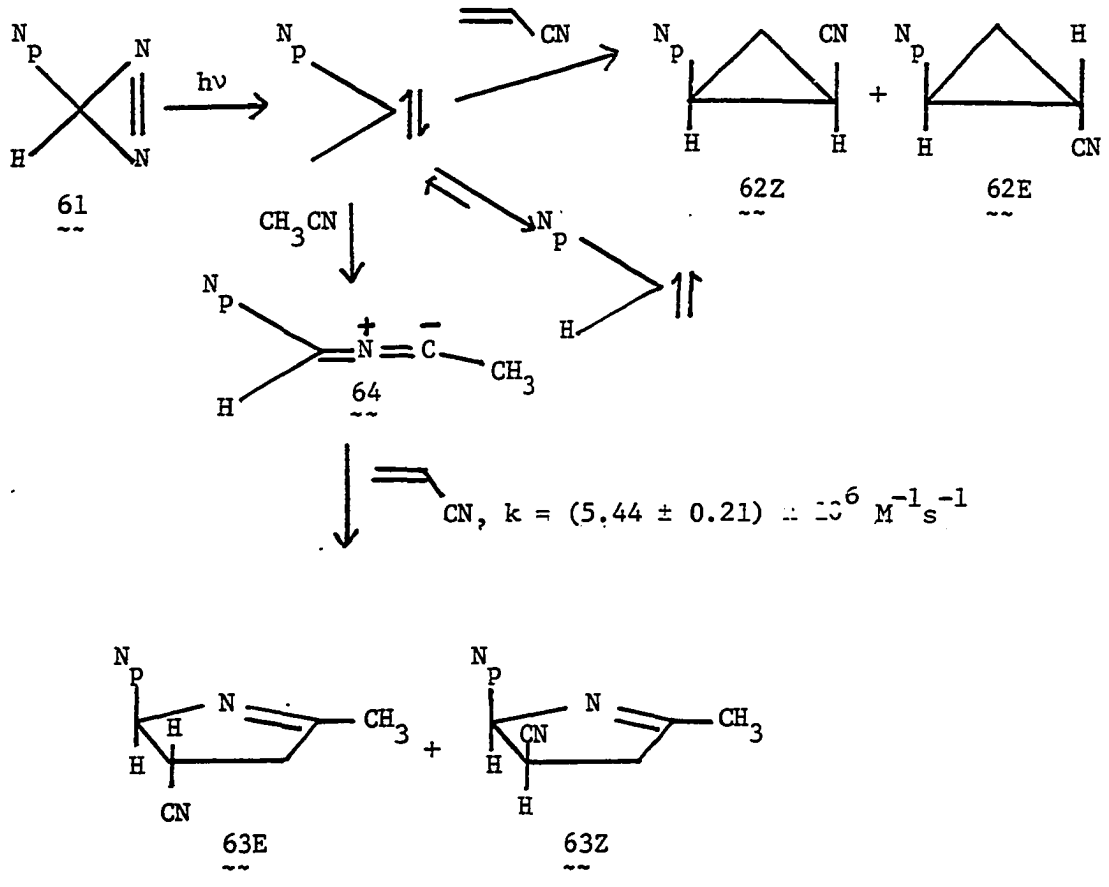

dilution increased the yield of ylide products. As was the case for 59, the regiochemistry of the cycloaddition of 64 with acrylonitrile supports a bent structure for 64.

In 1984, Janulis et al. (70) reported the isolation of the first stable nitrile ylide from 1-adamantylnitrile as the precursor. The 1-adamantyl nitrilium-N-tetrakis(trifluoromethyl)-cyclopentadienylide (65) had the x-ray structure shown in Figure 40. The central ylidic system is very close to linear, with only 4° bends at the nitrilium carbon and

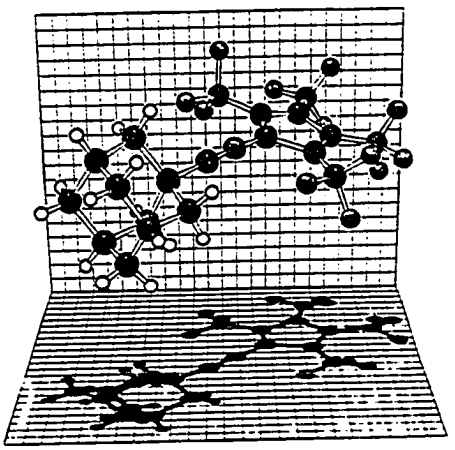

Figure 40. KANVAS drawing of nitrile ylide 65

nitrogen centers. The ^{1}HNMR showed resonances at δ2.27 and 1.83, while the IR absorption at 2210 cm^{-1} (C≡N) was consistent with the ylidic structure.

MINDO/3 calculations on 66 indicated that the linear structure was indeed preferred, and also suggested that the charge separation in this system was much like that in an idealized resonance structure for nitrilium ylides. The unique cyclopentadienyl carbon had a calculated charge of -0.16, while that on nitrogen was 0.36 and C_1 was -0.12.

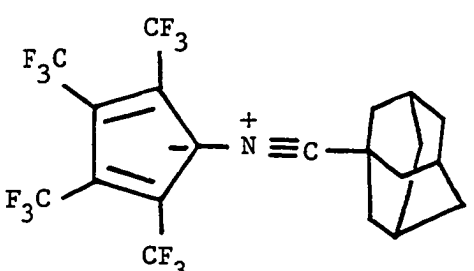

65

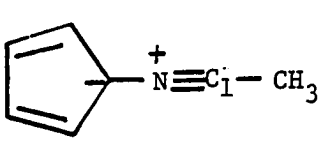

66

More recently, Turro et al. (71) reported that pulsed excimer laser photolysis of diazomethane or diazirine in acetonitrile produced a transiet absorption with λ_{max} = 280 nm ($\tau = 10^{-8}$ sec in the absence of a trap). This transient was assigned as methyl nitrile ylide, 67, which was formed by the addition of singlet methylene to acetonitrile. Ylide 67 reacted with acrylonitrile with k = (5.6 ± 0.2) x 10^6 $M^{-1}s^{-1}$ (compare k = 5.4 x 10^6 $M^{-1}s^{-1}$ for reaction of 64 with acrylonitrile). Trapping of 67 with methyl propiolate gave two regioisomeric cycloadducts, 68 and 69, in a 1:1 ratio. This is surprising, because regioisomer 68 would have been expected to be preferred (54).

Our interest in nitrile ylide chemistry originated with our discovery of reversed stereochemistry in the reaction of carbene 11 with CH_3CN/CH_3OH (21). In the absence of acetonitrile, carbene 11 reacted with methanol through the alcohol ylide (72) route to give only exo-isomer 13 [equation (19)]. This ylide mechanism was further supported by secondary deuterium isotope effects observed when the experiments were carried out in MeOH/MeOD (21).

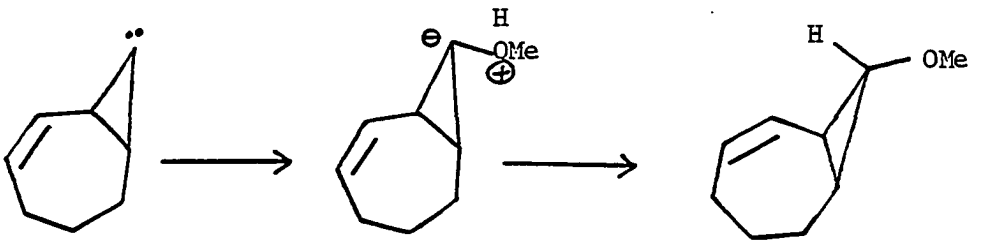

11 12 13 (19)

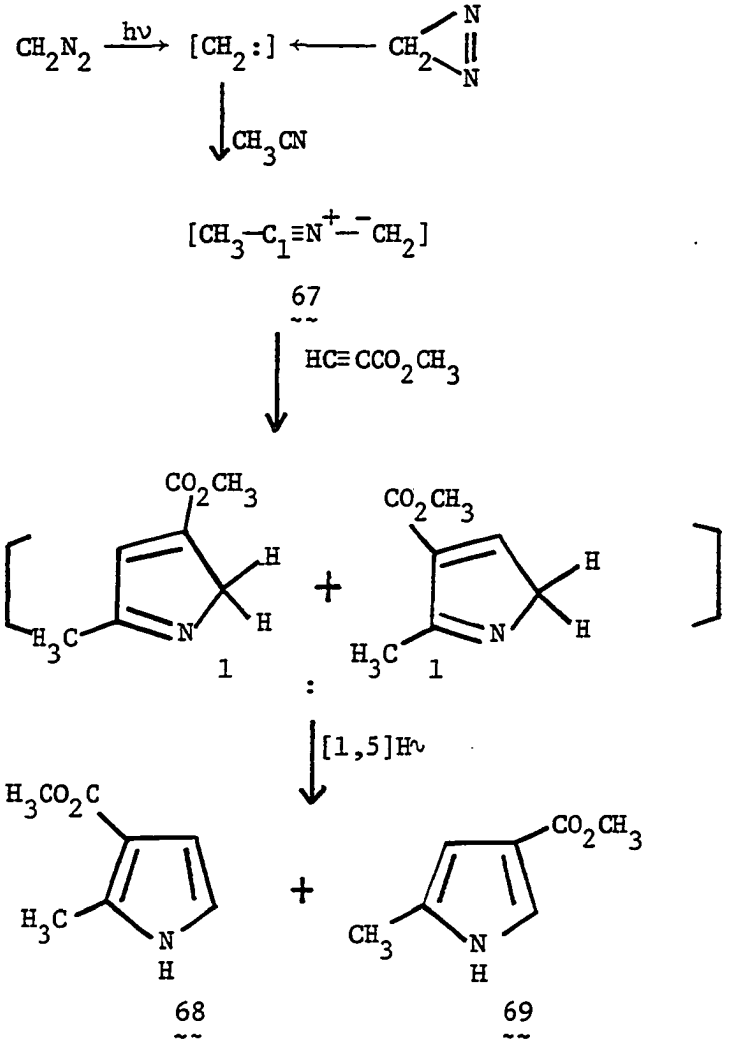

However, when the reaction was conducted in CH_3CN/CH_3OH, a new product, with the identical fragmentation pattern as 13, was observed in the GC-MS. This new product was assigned as the epimer of 13, namely endo-isomer 70. The structure of 70 was further confirmed by independent synthesis. We have proposed the mechanism shown in Scheme XVI, in which the nitrile ylide 71 was suggested as the intermediate responsible for the formation of 70.

Scheme XVI

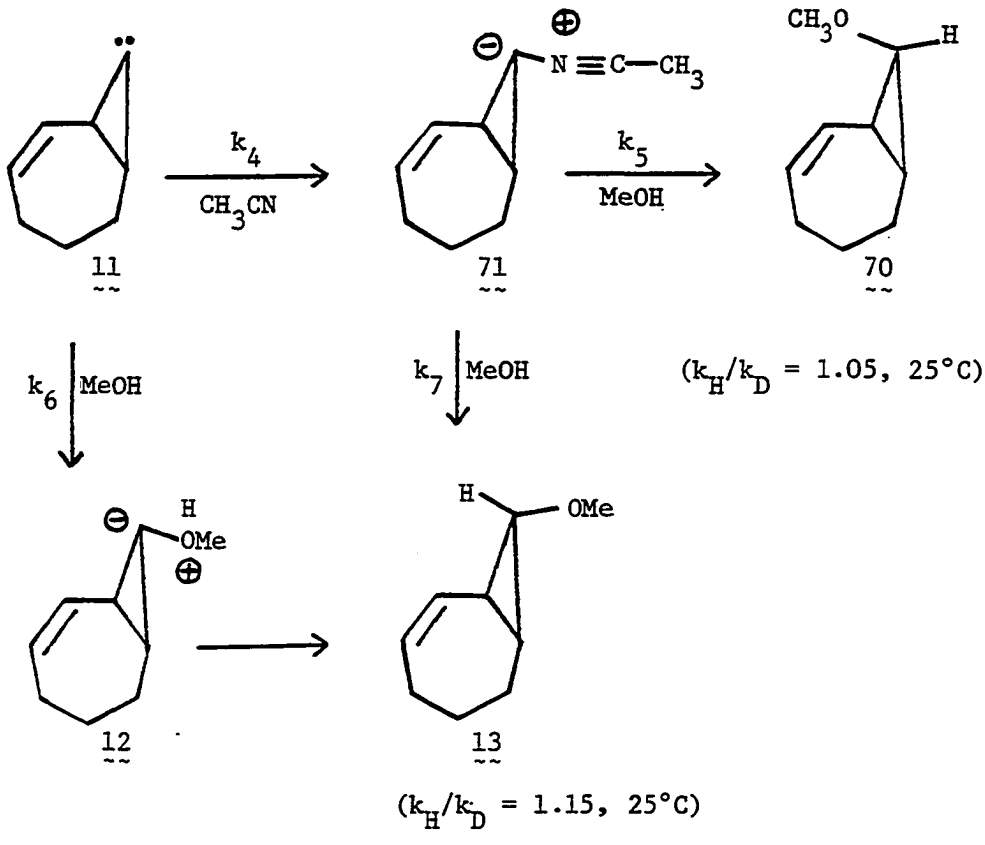

Kinetic studies indicated that $k_7/k_5 = 0.15$. Also, the competitive rate constants k_4 and k_6 were found to have the ratio 1.18:1 (compare F1, where CH_3CN is ca. 400 times less reactive than CH_3OH). To our knowledge, this is the first example in carbene ylide chemistry of a stereochemical reversal caused by adding a second solvent.

In order to study further the formation and reaction of nitrile ylides formed from cyclopropylidenes, we selected norcaranylidene, 20', as our substrate for two reasons: (1) the lack of the possibility of

Skattebol rearrangement of 20' should facilitate the studies; and (2) the synthesis of the diazo-precursor for 20' is quite simple.

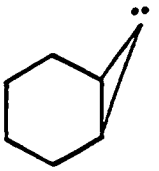

20'

Results and Discussion

The initial experiment was carried out in 3:1 (v/v) CH_3CN/CH_3OH by dissolving nitrosourea 19' in the presence of sodium methoxide. As expected, both 25 and 31 were afforded in a 16:1 ratio [equation (20)]. Independent syntheses of 25 and 31, effected by treating cyclohexene with methyl lithium/lithium iodide complex, followed by reaction with α,α-dichloromethyl methyl ether (43), confirmed the structural assignments.

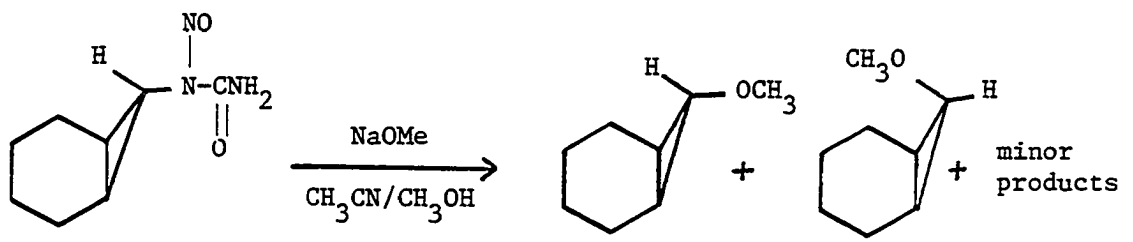

19' 25 31 (20)

Since a nitrile ylide has been suggested to be an intermediate in the reaction between acetonitrile and carbene 11, the unsaturated analog of norcaranylidene 20', we also presumed that an analogous ylide was involved in the reaction of 20' with acetonitrile. However, an alternative

Scheme XVII

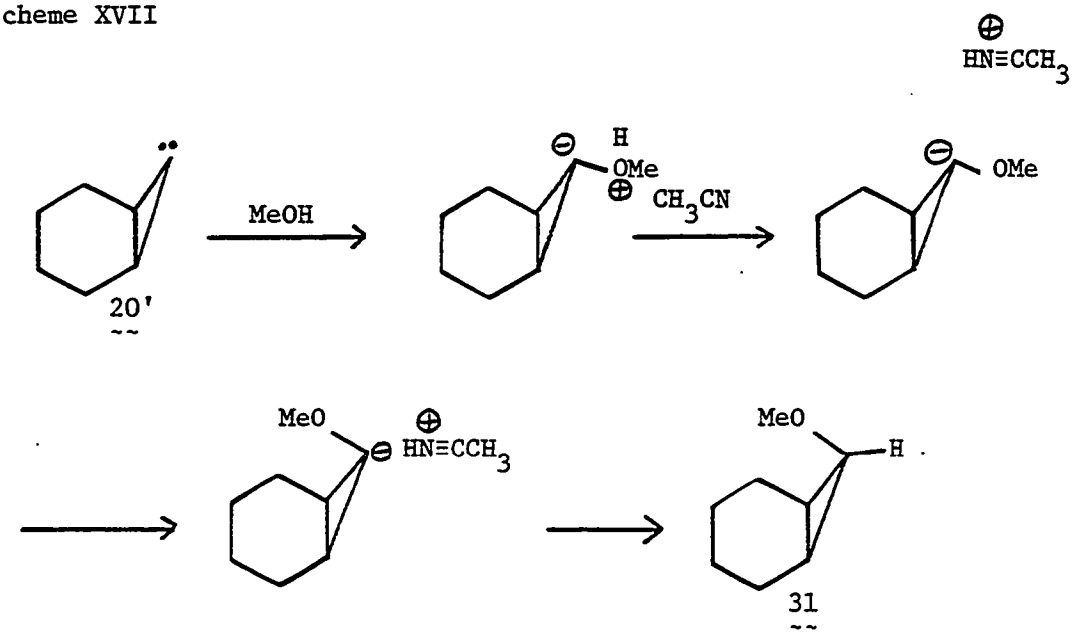

possibility was that acetonitrile merely behaved as a base which deprotonated the ylide, as shown in Scheme XVII. This concept was probed by conducting the reaction in methanol/diisopropylethylamine (1:3 by volume). In this experiment, diisopropylethylamine could behave as a hindered base, but was not expected to form an ylide with carbene 20'. The result was that no 31 was observed, thereby eliminating from consideration the mechanism shown in Scheme XVII. The same results were obtained when the reaction was done in MeOH/THF (1:3 by volume).

It is well-established from the work of Kende et al. (68) and Grasse et al. (67) that nitrile ylides can be captured through 1,3-dipole cycloadditions. Therefore, we conducted a trapping experiment in a 10:1 (v/v) CH_3CN/MAN mixture. The crude product showed two pairs of peaks in the GC-MS. Chemical ionization (CI) mass spectra was used to identify these peaks.

The first pair of products (minor, m/e 161) were seen to be two isomeric adducts from 20' and MAN (cf. 73a, 73), while the second pair of products (major, m/e 189) were assigned as two (of the four possible) isomeric adducts 75a from trapping of the diazocompound 72 by MAN (the regiochemistry is expected to be as in 75a based on frontier orbital theory (58). In fact, no obvious ylide trapping products were obtained, although the minor products could have been (cf. 73a), especially considering that compound 31 was also a product from the CH_3OH/MAN mixture (see below). Increasing the concentration of acetonitrile

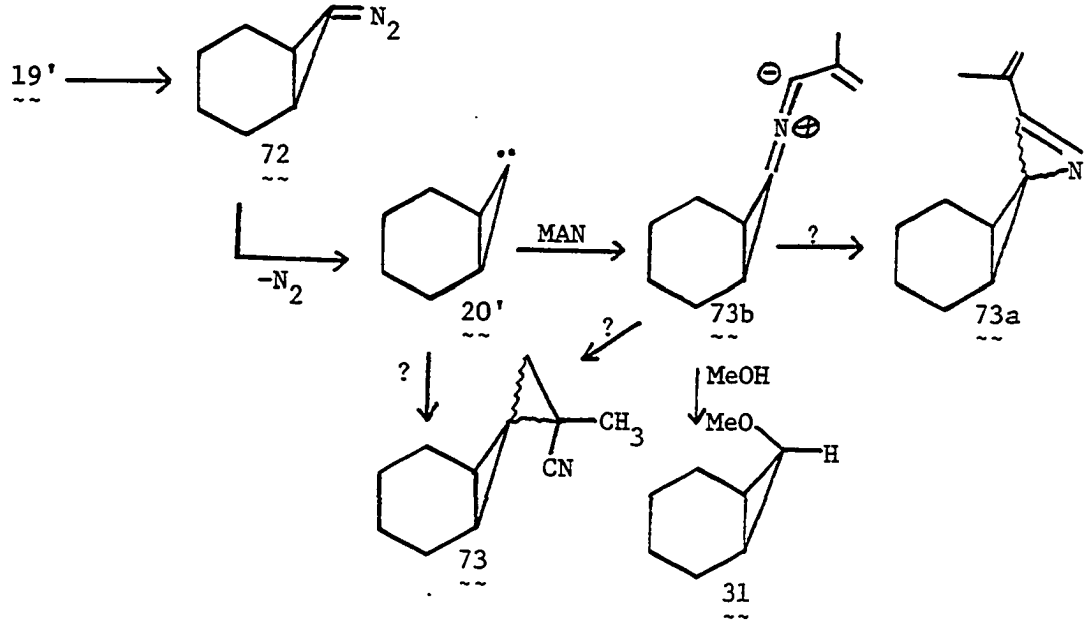

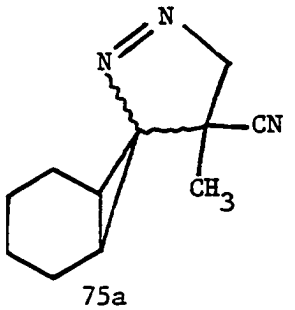

75a

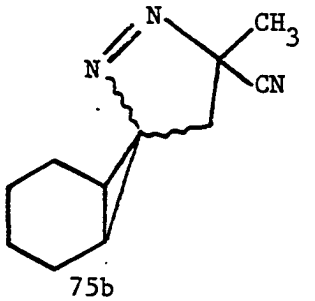

75b

(CH_3CN/MAN = 50:1, v/v) gave similar results. This finding indicated that MAN is a better ylide-former than acetonitrile. The experimental data are shown in Tables 55 and 56.

Table 55. The product ratios of 25/31 as a function of $[CH_3OH]/[CH_3CN]$ at 25°C

(v/v) $\frac{CH_3OH}{CH_3CN}$	$\frac{[MeOH]}{[CH_3CN]}$	% 25	% 31	25/31
1:1	1.28	25.1	0.79	31.8
1:3	0.43	20.3	1.28	15.8
1:7	0.18	21.8	2.45	8.9
1:12	0.13	13.4	1.66	8.0

Table 56. The product ratios of 25/31 as a function of $[CH_3OH]/[MAN]$ at 25°C

(v/v) $\frac{CH_3OH}{MAN}$	$\frac{[MeOH]}{[MAN]}$	% 25	% 31	25/31
3:1	6.21	2.69	1.51	1.78
1:1	2.07	1.85	1.55	1.19
1:3	0.69	1.06	1.07	0.99
1:7	0.29	0.82	0.95	0.86

Scheme XVIII

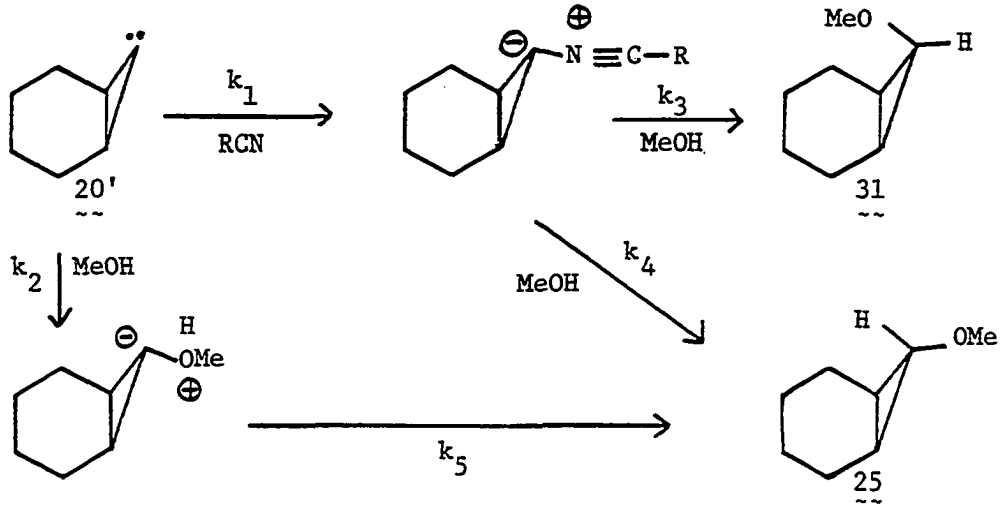

$$\frac{25}{31} = \frac{k_4}{k_3} + \frac{k_2(k_3 + k_4)}{k_1 k_3} \cdot \frac{[MeOH]}{[RCN]} \qquad (21)$$

Equation (21) was derived based on Scheme XVIII. Kinetic analysis (Figures 41 and 42) showed that the ratio of k_2/k_1 = 3.48 ± 0.55 in acetonitrile (compare to 0.85 for carbene 11) and 0.08 ± 0.01 in methacrylonitrile. The low reactivity of 20' toward MeOH in CH_3OH/MAN accounted for the low yield of 25 as the product. Apparently ylide 73b from 20' and MAN rearranged to minor products (cf. 73a or 73) in addition to collapsing with CH_3OH to give 25 and 31. But the major effect of MAN was to capture the diazo precursor 72. On the other hand, acetonitrile is a relatively poor ylide-former, so that 31 was produced in low yield compared to 25 resulting from direct capture of 20' by MeOH.

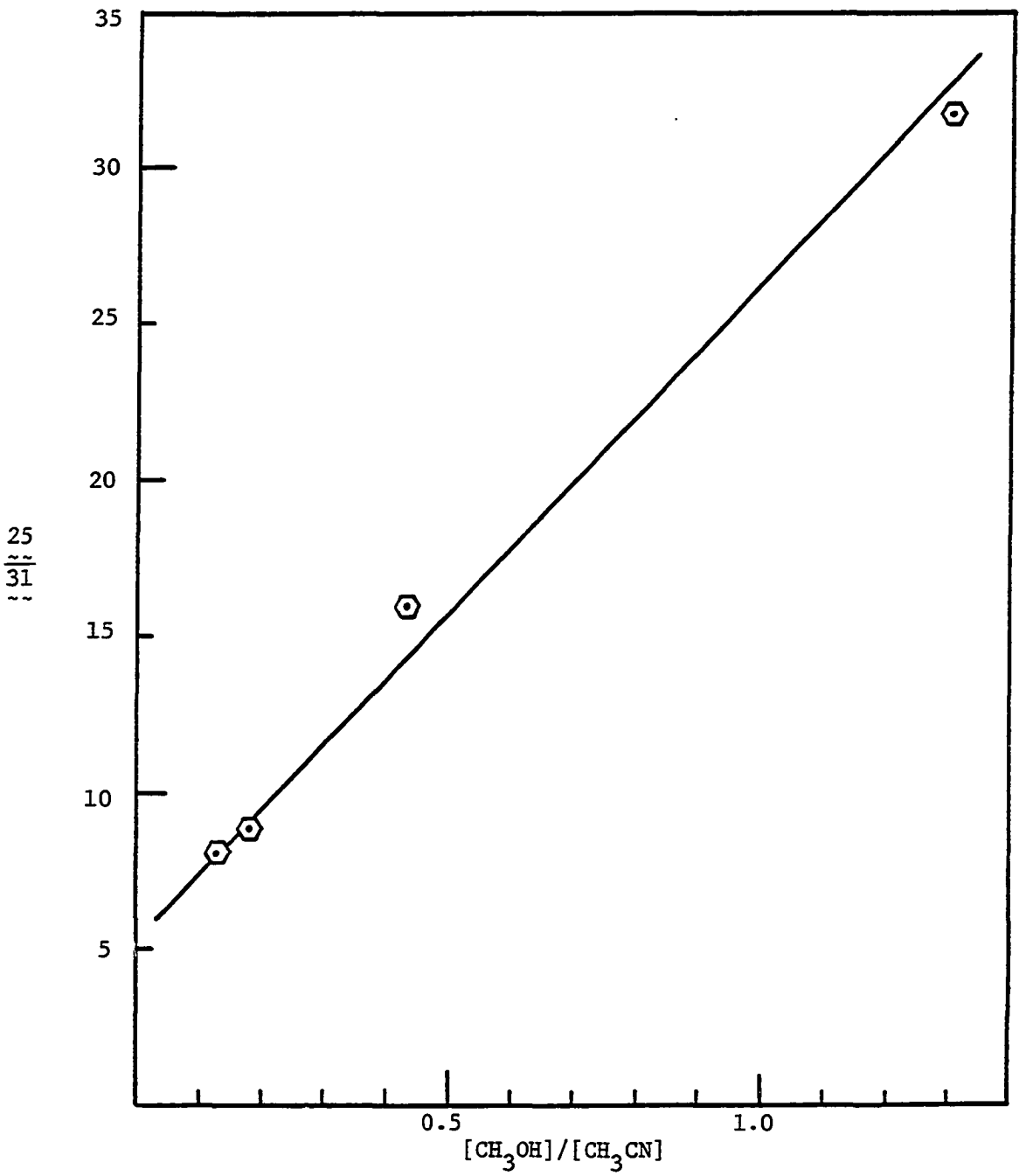

Figure 41. Plot of 25/31 vs. $[CH_3OH]/[CH_3CN]$. r = 0.997, int. = 5.25 ± 0.51, slope = 21.68 ± 1.70

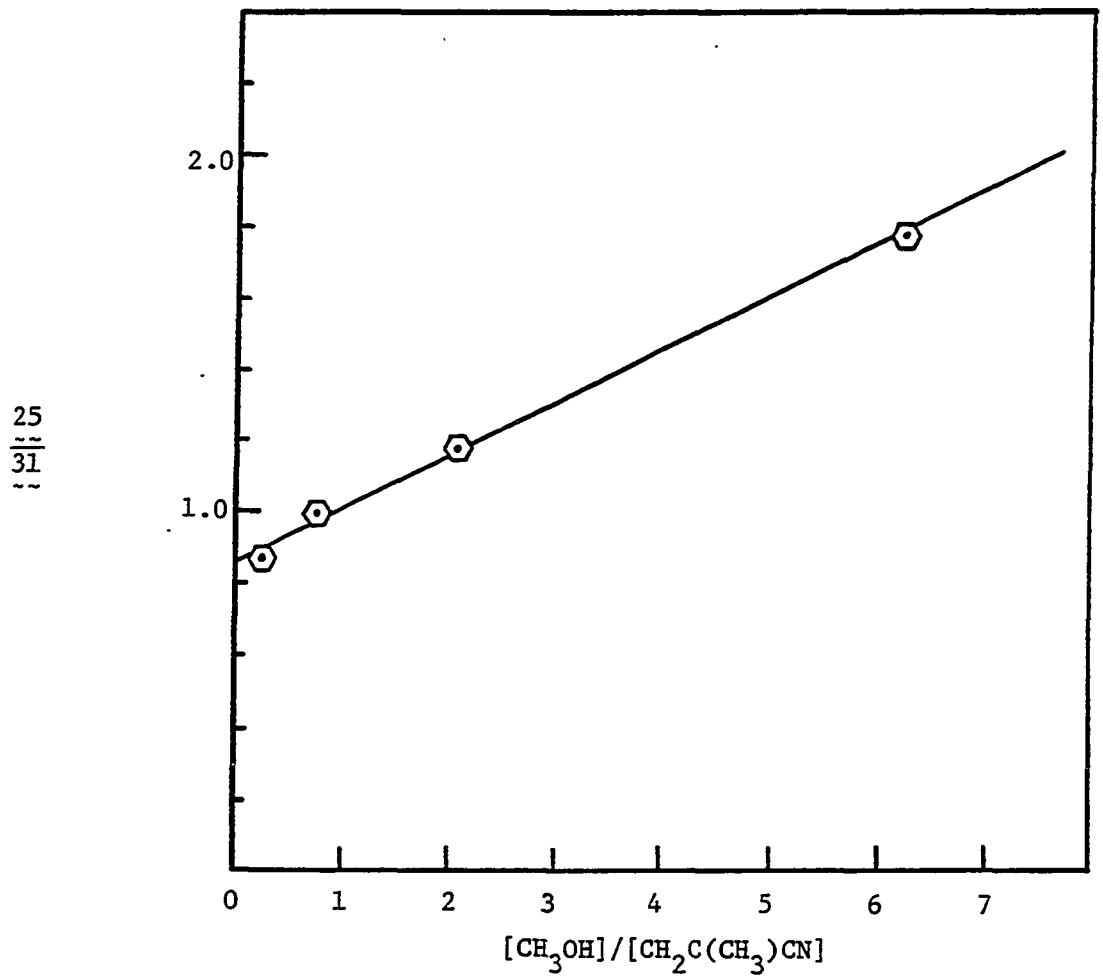

Figure 42. Plot of 25/31 vs. $[CH_3OH]/[CH_2C(CH_3)CN]$. r = 0.997, int. = 0.85 ± 0.03, slope = 0.15 ± 0.01

Benzonitrile, 76, was then considered as a possibly better ylide-forming nitrile, since the aromatic ring would be expected to stabilize the charge in the ylide structure. Unfortunately, 73 (minor product) and 75 (major product) were the only products observed when the reaction was carried out in 10:1 (v/v) C_6H_5CN/MAN.

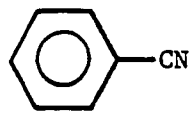

76

However, when the reaction was conducted in CH_3OH/benzonitrile, substantial amounts of 25 and 31 were formed, and no ylide-adducts were observed. Kinetic analysis based on equation (21) revealed that k_2/k_1 = 0.0007 ± 0.0001, meaning that almost all of 25 and 31 were formed via the reaction of methanol with nitrile ylide 77. Table 57 and Figure 43 show the kinetic results in CH_3OH/C_6H_5CN.

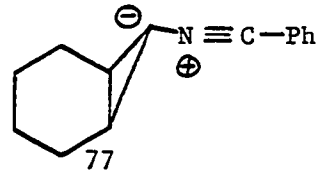

77

Maleic anhydride was chosen as the next dipolarophile. When nitrosourea 19' was dissolved in 25:1 (wt/wt) acetonitrile/maleic anhydride, and NaOMe added, the major product observed (GC-MS) had the correct mass for carbene adduct 78. We also generated carbene 20' in the presence of fumaronitrile, ethyl vinyl ether, and 2,3-dimethylmaleic anhydride, but none of them afforded detectable nitrile ylide cycloaddition products.

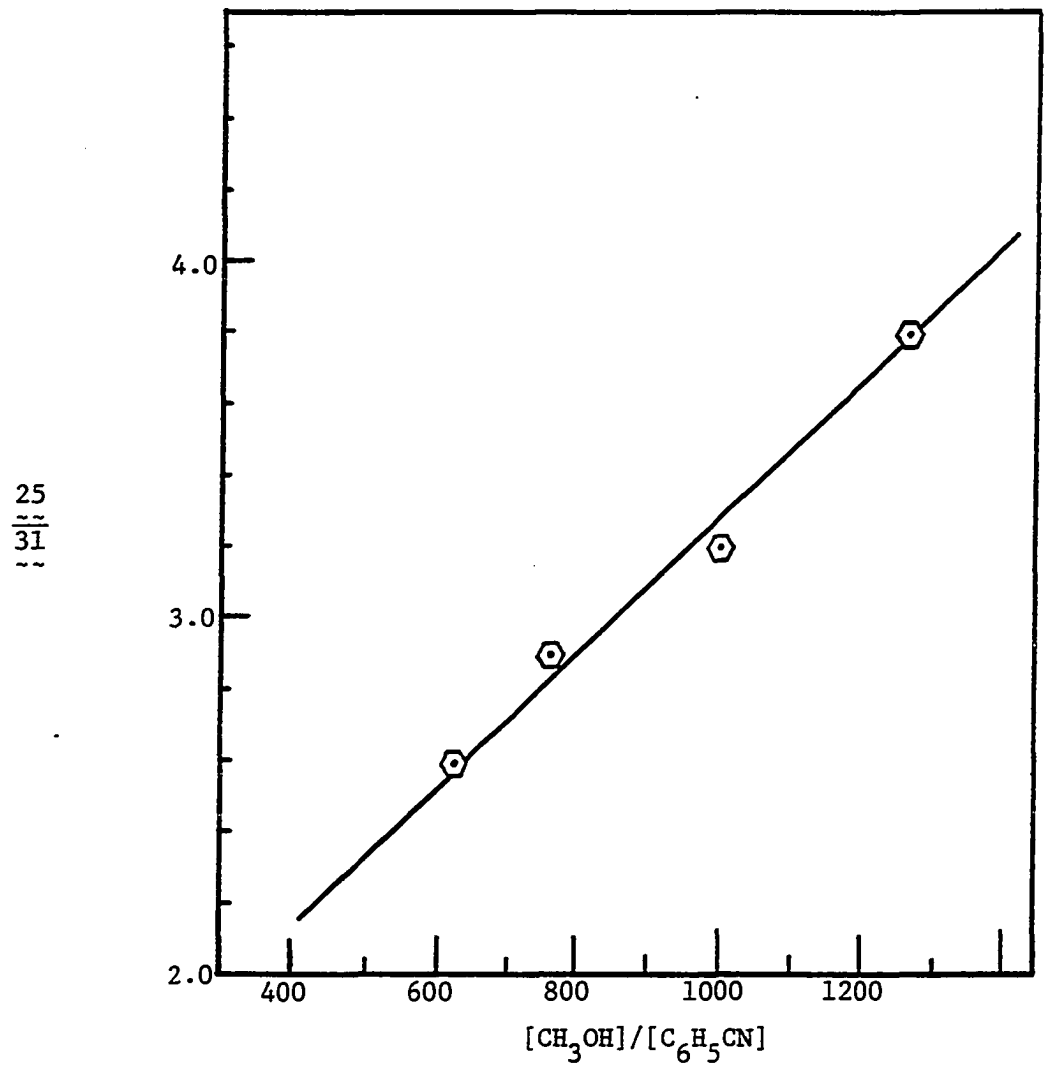

Figure 43. Plot of 25/31 vs. $[CH_3OH]/[C_6H_5CN]$. r = 0.990, int. = 1.48 ± 0.16, slope = 0.0018 ± 0.0002

Table 57. The product ratios of 25/31 as a function of $[CH_3OH]/[C_6H_5CN]$ at 25°C

(v/v) $\frac{CH_3OH}{C_6H_5CN}$ [a]	$\frac{[CH_3OH]}{[C_6H_5CN]}$	% 25	% 31	25/31
500:1	1261	36.4	9.6	3.8
400:1	1009	44.1	13.6	3.2
300:1	757	54.6	18.4	2.9
250:1	630	34.1	13.0	2.6

[a]The reason that such small amounts of benzonitrile were used is that its GC retention time is very close to that for 25 and 31.

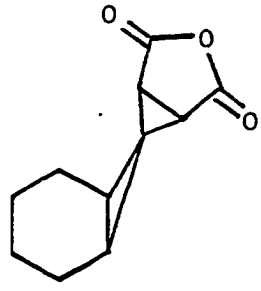

78

Finally, we found that acrylonitrile performed very well as both ylide precursor and ylide trap. When 25:1 (v/v) CH_3CN/CH_2CHCN was used, two major isomeric products were formed in ∿1:1 ratio. GC-MS (CI) analysis indicated that adduct 79 (m/e 200) was a possible structure; the regiochemistry shown for 79 is that expected based on frontier molecular orbital theory (56, 58, 73).

Attempts were then made to isolate 79 in order to gain spectroscopic evidence for the structure(s). The isomeric adducts were collected as a

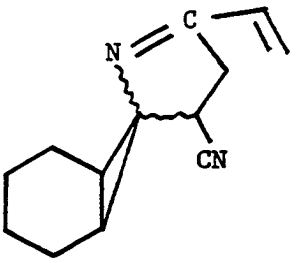

79

colorless oil by preparative gas chromatography at 160°C on a SE-30 column. GC-FT-IR showed two identical spectra for two isomers, each of which contained a —C≡N group. UV spectra showed an absorption at 227 nm ($\varepsilon_{apparent}$ = 1560 in CH_3CN, this might not be correct in view of polymer formation), which is in accord with an imine group (>C=N) in conjugation with a double bond. The ^1H NMR spectra indicated the presence of an α,β-unsaturated imine moiety in 79. However, the integrated area of the aliphatic hydrogens compared to that of the olefinic hydrogens was much larger than expected. This might be due to polymerization which may have occurred during collection from the preparative GC. Some improved collecting techniques are now being employed. So far all the spectroscopic findings are consistent with the structures of two stereoisomers 79, rather than regioisomers 80. For example, it was suggested that 80 should rearrange to the more stable isomer 81, which should exhibit a strong N-H absorption in the IR and an absorption at or above 300 nm in the UV spectra (74).

Attempts were also made to convert 79 to alcohols or ketones, from which solids for x-ray crystallography might be obtainable. The first approach was to hydrolyze the imine portion with 10% HCl to ketone 82. However, no desired products were observed. This might be due to

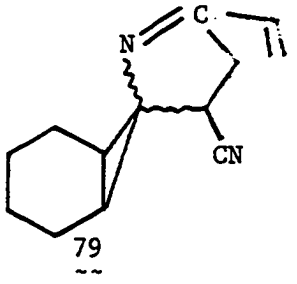

79

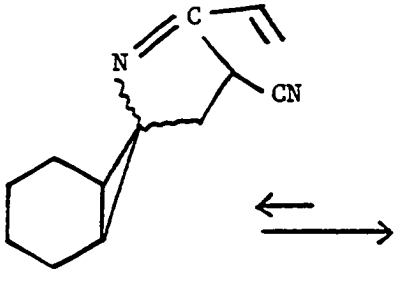

80

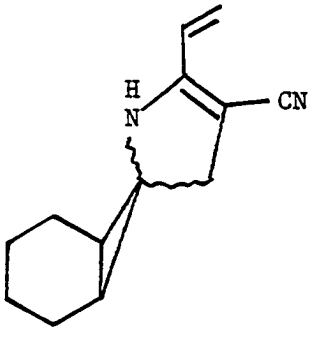

81

instability of the resulting enone under the acidic conditions. Reductive amination of 79 with $NaCNBH_3$/MeOH or H_2 (1 atm or 50 psi)/PtO_2, ethyl acetate led to only the recovery of starting materials.

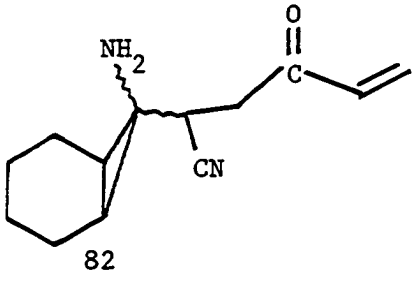

82

The next trial was to convert the olefin moiety of 79 to a primary alcohol by hydroboration/oxidation. Borane-Me_2S complex led only to

recovered starting material. When 9-BBN was used, no alcohols were detected, but the starting material was consumed. Ozonolysis of 79 at -78°C in methanol followed by quenching with dimethyl sulfide was also tried, but no meaningful products could be isolated. Further efforts are still pending.

As a further probe of mechanism, we investigated the effect of conducting the reaction of 19' in the presence of both acrylonitrile and MeOH. If MeOH and acrylonitrile competitively intercepted ylide 83 to afford 31 (and 25) and 79, respectively, then certain kinetic relationships (vide infra) should be observable. When the reaction was in fact conducted

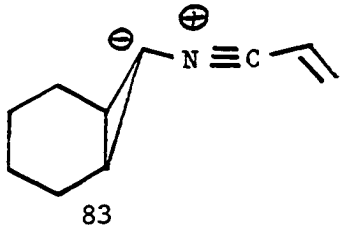

83

in a mixture of CH_3OH/CH_2CHCN (1:1, v/v), 31 and 25 were formed in a 1.28:1 ratio, and 79 was the major product [equation (22)].

If the nitrile ylide 83 is indeed a common source of both 31 and 79 (and also the only source of these two products), then the kinetic relationship suggested by equation (23), namely $79/31 = k_{10}/k_9 \cdot [CH_2CHCN]/[MeOH]$, must hold. Therefore, experiments were carried out in CH_3OH/CH_2CHCN at different volume ratios at room temperature. Table 58 and Figure 44 show the results.

From the slope of Figure 44, the value of k_{10}/k_9 was found to be 423 ± 35, which at first glance appears to be smaller than expected (ylides

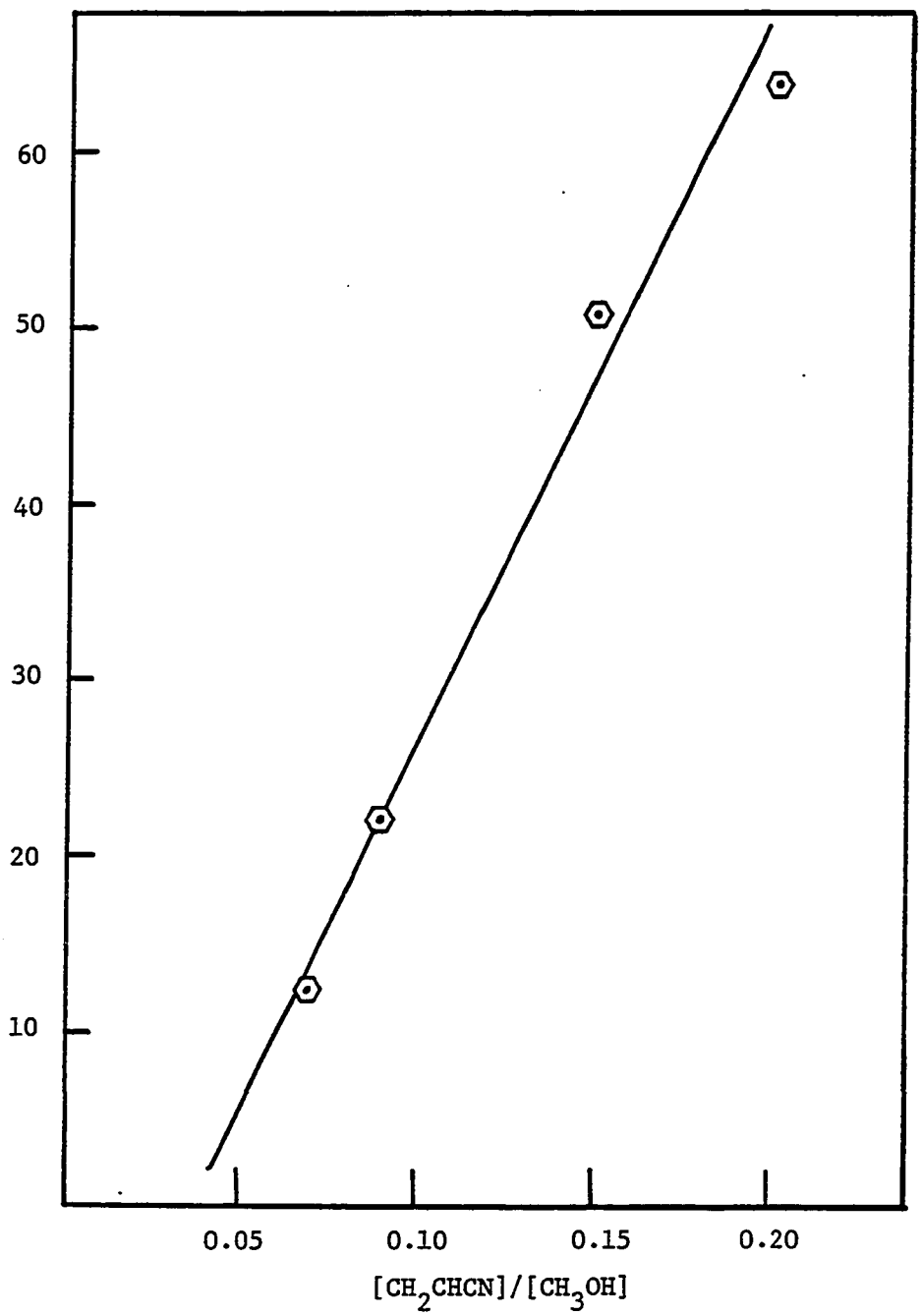

$\frac{79}{31}$

Figure 44. Plot of 79/31 vs. $[CH_2CHCN]/[CH_3OH]$. r = 0.990, int. = -16.6 ± 2.8, slope = 423.47 ± 35.71

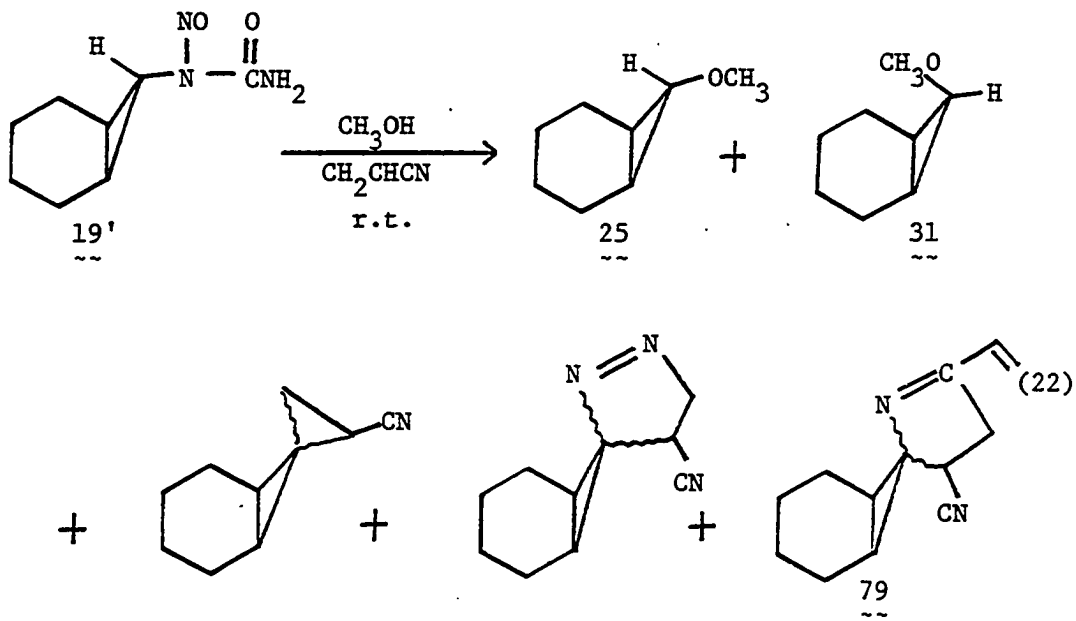

19' 25 31 79

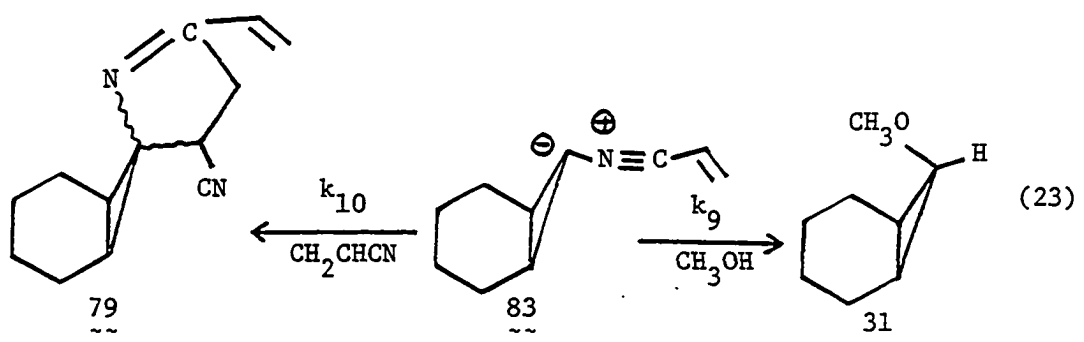

79 83 31

Table 58. Product ratios of 79/31 as a function of $[CH_2CHCN]/[CH_3OH]$ at room temperature.

(v/v) $\frac{CH_2CHCN}{CH_3OH}$	$\frac{[CH_2CHCN]}{[CH_3OH]}$	$\frac{79}{31}$ (by % yield)
1.3	0.20	62.3
1:4	0.15	50.6
1:7	0.09	21.6
1:9	0.07	11.9

52 and 64 reacted with acrylonitrile with $k \sim 4 \times 10^6$ $M^{-1}s^{-1}$ (65,67); the fluorenylidene nitrile ylide (52) reacted with MeOH at $k \sim 10^2$ $M^{-1}s^{-1}$ (11), so that the value of k_{10}/k_9 might be naively predicted to be $\sim 4 \times 10^4$). However, the vinyl group of 83 makes it more stable than does the Me groups of 52 and 64. This may effect both k_{10} and k_9 in an unknown way, making predictions of k_{10}/k_9 from existing data on other systems impossible. Furthermore, the charge at C_3 of 52 is delocalized, while that of 83 is localized, and this may greatly effect the rate of reaction with MeOH (k_9).

Next, we compare the relative reactivities of norcaranylidene (20') toward $MeOH/CH_2CHCN$ (Scheme XVIII and equation (21)). Table 59 and Figure 45 show the results.

From Figure 45, the ratio of k_4/k_3 was 0.767 ± 0.003, and the ratio of k_2/k_1 was 0.0040 ± 0.0002. The relatively low reactivity of 20' with MeOH, and the low yields of 25 and 31 in the reaction, indicated that

Table 59. The product ratios of 25/31 as a function of $[CH_3OH]/[CH_2CHCN]$ at 25°C

(v/v) $\frac{CH_3OH}{CH_2CHCN}$	$\frac{[CH_3OH]}{[CH_2CHCN]}$	% 25	% 31	25/31
1:1	1.64	0.88	1.13	0.78
4:1	6.56	1.90	2.36	0.81
7:1	11.48	3.13	3.71	0.85
9:1	14.76	3.32	3.83	0.87

ylide 83 was formed very fast and was primarily trapped by another molecule of acrylonitrile rather than by MeOH (as borne out by the large k_{10}/k_9).

We can also compare the relative reactivities of 20' to its unsaturated 7-membered-ring analog, 11, in mixtures of methanol and acetonitrile. Previous studies of 11 showed that methanol attack on ylide 71 occurred predominantly from the endo side to form 70 (k_4/k_3 = 0.15, k_2/k_1 = 0.85, for a scheme analogous to Scheme XVIII in CH_3CN). However, for ylide 84 the lack of a double bond in the 6-membered ring might increase the chance for exo-attack of methanol due to the absence of electronic repulsion between π electrons of the ylidic system and π-electrons of the double bond (in 71). In fact, exo attack occurred significantly more often for all the nitrile ylides formed from 20' and nitrile solvents relative to 71. Table 60 shows the ratios of rate constants k_4/k_3 and k_2/k_1 for 20' in different nitriles.

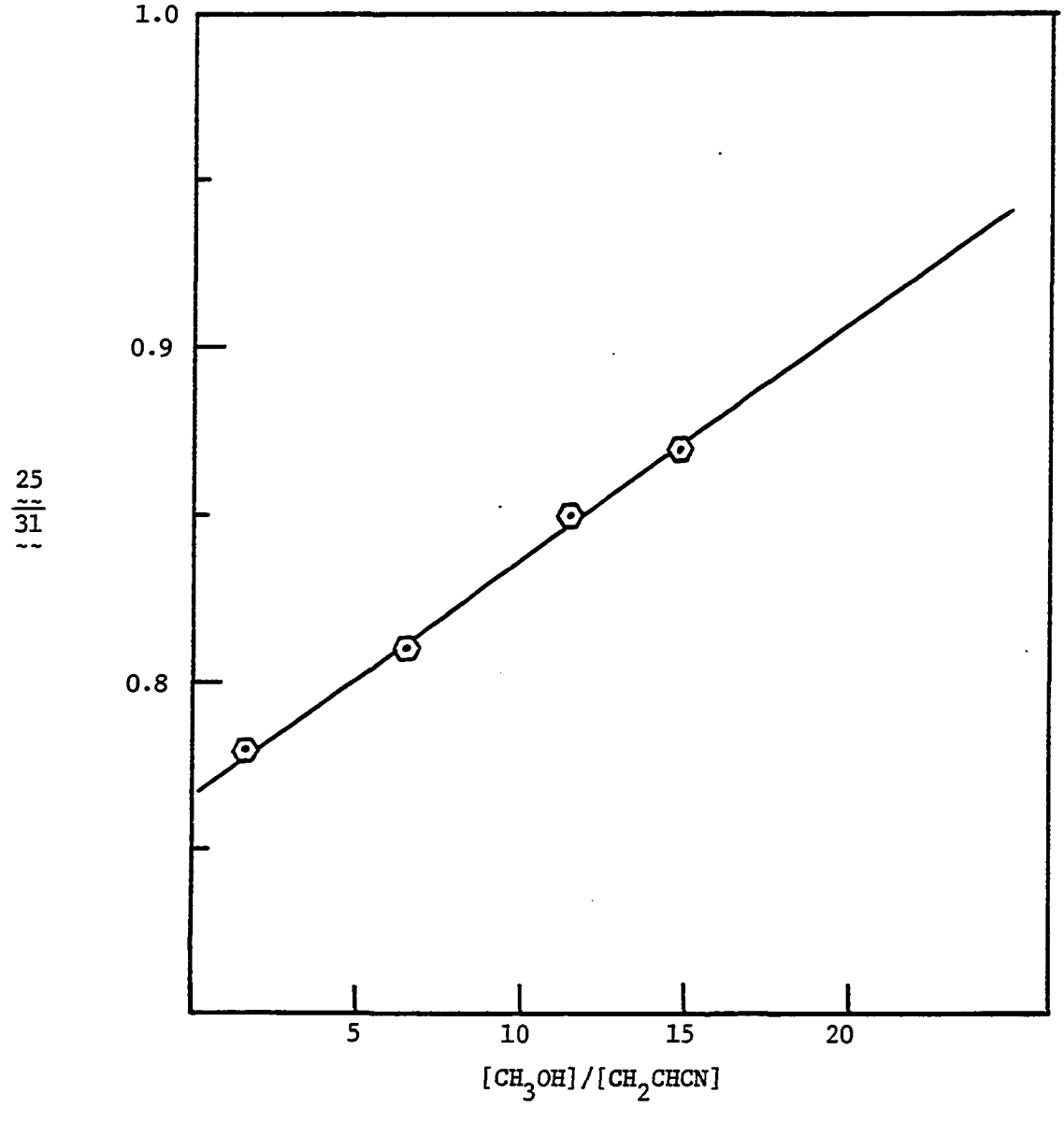

Figure 45. Plot of 25/31 vs. $[CH_3OH]/[CH_2CHCN]$. r = 0.998, int. = 0.767 ± 0.003, slope = 0.0070 ± 0.0003

Table 60. Rate constant ratios from the reaction of 19' in methanol and nitriles at 25°C

Nitrile	$\frac{k_4}{k_3}$ [a]	$\frac{k_2}{k_1}$ [b]	$\frac{k_1}{k_2}$
C_6H_5CN	1.48 ± 0.16	0.0007 ± 0.0001	1400 ± 200
CH_2CHCN	0.767 ± 0.003	0.0040 ± 0.002	250 ± 13
$CH_2C(CH_3)CN$	0.85 ± 0.03	0.08 ± 0.01	13 ± 2
CH_3CN	5.23 ± 0.51	3.48 ± 0.55	0.29 ± 0.05

[a] $\frac{k_4}{k_3} = \frac{\text{rate constant for exo MeOH attack to 25}}{\text{rate constant for endo MeOH attack to 31}}$.

[b] $\frac{k_2}{k_1} = \frac{\text{rate constant for MeOH attack on carbene 20'}}{\text{rate constant for RCN attack on carbene 20'}}$.

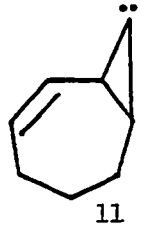

11

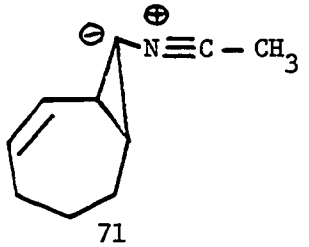

71

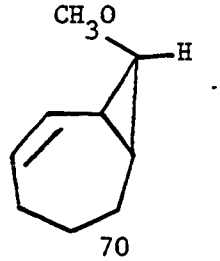

70

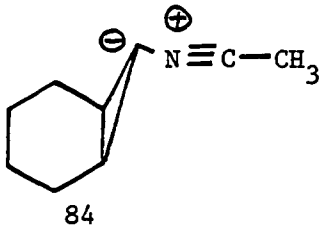

84

In summary, several conclusions may be offered:

(i) Both norcaranylidene 20' and carbene 11 react with methanol to give the exo-methoxy insertion product by an oxygen-ylide mechanism. However, when nitriles are present in the methanol, an epimeric methanol insertion product was formed via a nitrile ylide intermediate, one of which was captured by a dipolarophile as a [3 + 2] cycloadduct. Dipolarophiles also served to capture the diazo precursor to 20'.

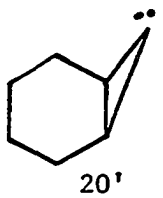

20'

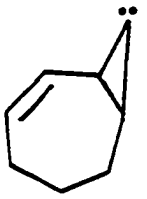

11

(ii) In the case of 11, possibly due to the electronic repulsions, exo-attack on the acetonitrile ylide by methanol was relatively less favored. But for 20', exo-attack on the nitrile ylides by MeOH was more facile to predominant.

(iii) Except in acetonitrile, MeOH reacted with norcaranylidene more slowly than did the nitriles. In acrylonitrile and MAN, the resulting ylides may either rearrange to products or be trapped to form an adduct. But, in benzonitrile, the resulting ylide reacts with MeOH readily to give substantial amounts of 25 and 31.

(iv) The structures of the two isomeric trapping adducts of ylide 83 with acrylonitrile appear to be stereoisomers rather than regioisomers. They have idential IR and mass spectra. Moreover, the fact that methanol

could attack ylide 83 from both the exo- and endo-sides (k_4/k_3 = 0.77) strongly suggests that a stereoisomeric formulation for the 2 isomers 79 is quite reasonable. Further investigation is in progress at the present time.

Experimental

General

For the general consideration, see the experimental section of Chapter I.

Reactions and syntheses

Preparation of 8-methoxybicyclo[5.1.0]oct-2-ene (13 and 70) (Figure 46) Compounds 13 and 70 were prepared according to the procedure of Schöllkopf and Paust (43), with some slight modifications. The first step was to prepare a methyllithium-lithium iodide complex. A 25 ml 3-necked round bottom flask, equipped with a magnetic stirring bar and a nitrogen inlet, was charged with 0.27 g (2 mmole) of anhydrous lithium iodide powder, and 3 ml of dry ether. Then 2.83 ml (3.6 mmole) of a 1.27 M methyllithium/ether solution was syringed dropwise into the suspension of lithium iodide. The resulting cloudy solution was stirred for one hour at room temperature under nitrogen, and then kept under nitrogen.

A 50 ml 3-necked round bottom flask equipped with a magnetic stirring bar and a nitrogen inlet was charged with 3.46 ml (32 mmole) of 1,3-cycloheptadiene (21) and 0.15 ml (1.62 mmole) of α,α-dichloromethyl methyl ether. Then the methyllithium/lithium iodide in ether solution was

syringed in dropwise. After another 1.5 hours of stirring at room temperature under nitrogen, the reaction mixture was cooled to 0°C and quenched with 1 ml of water. The mixture was then diluted with water and extracted with ether. The ether layer was washed with water, 10% sodium bisulfite solution (to remove I_2), water and saturated NaCl (aq), dried over anhydrous $MgSO_4$ and filtered. GC analysis indicated that both 13 and 70 were formed. Purification via preparative gas chromatography afforded 13 and 70 as a colorless liquid mixture (75).

GC-MS: P^+ at m/e 138.0.

^1H NMR ($CDCl_3$): δ 5.4 ∿ 5.9 (m), δ 3.19 (s), δ 3.17 (s), δ 2.95 (t, 6.6 Hz), δ 2.71 (t, 3 Hz), δ 0.9 ∿ 2.2 (m).

GC-FT-IR (neat) for 13: 3020, 2950, 2820, 1700, 1450, 1240, 1120, 1060 cm^{-1}

GC-FT-IR (neat) for 70: 3010, 2940, 1450, 1420, 1200, 1140, 1060 cm^{-1}.

Reaction of 19' in RCN/MeOH or RCN/R'CN at 25°C To a solution of 5 mg of 19' in ∿0.3 ml of RCN/MeOH or RCN/R'CN in a desired ratio was added 11 mg of sodium methoxide, and the resulting solution stirred for five minutes at 25°C. Then the mixture was analyzed by GC-MS spectra. In $C_6H_5CN/CH_2C(CH_3)CN$, two pairs of products were obtained (Figure 47). Chemical ionization (CI) mass spectra was used to identify these peaks.

Isolation of 79 from reaction of 19' in acrylonitrile (Figure 48) To a solution of 100 mg of 19' in 10 ml of distilled acrylonitrile at room temperature was added 200 mg of sodium methoxide, and the resulting solution stirred until the color changed from bright yellow to pale yellow.

Ether was then added, and the sodium methoxide filtered off. Purification through preparative gas chromatography (SE-30 column) at 160°C gave 79 as a colorless oil.

HRMS: Calculated for $C_{13}H_{15}N_2$ ($M^{\cdot+}$ - H) - m/e 199.12352

found for $C_{13}H_{15}N_2$ - m/e 199.12352

^{1}H NMR ($CDCl_3$); δ 6.22 (H_A,d), δ 6.06 (H_B,d), δ 5.64 (H_C, doubly doublet, J_{AC} = 18 Hz, J_{BC} = 11.7 Hz), δ 2.4 ∿ 2.8 (m), δ 1.6 ∿ 2.0 (m), δ 1.0 ∿ 1.6 (m).

GC-FT-IR (neat): 3010, 220, 1450, 1360 cm^{-1}.

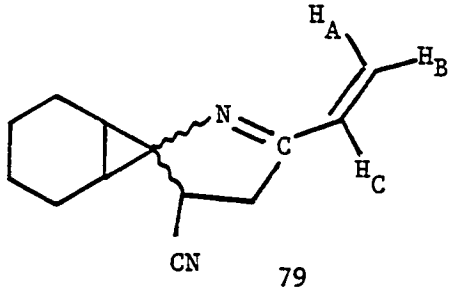

79

Figure 46. 8-Methoxybicyclo[5.1.0]oct-2-ene (13 and 70)

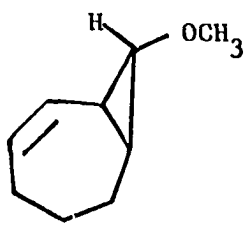

13

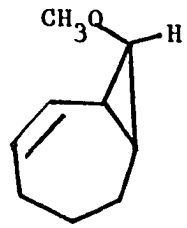

70

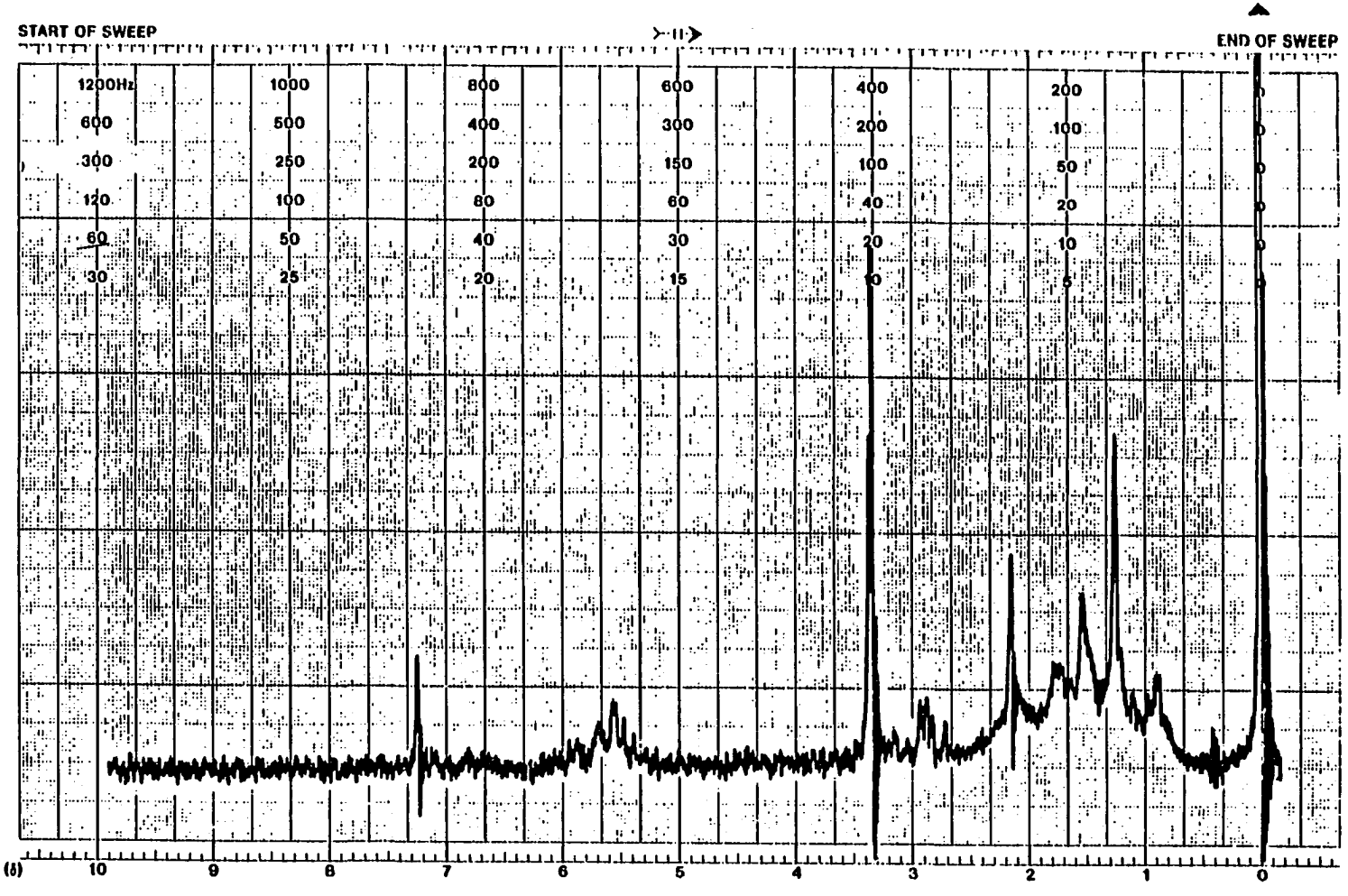
START OF SWEEP
END OF SWEEP
1200Hz
600
300
120
60
30
1000
500
250
100
50
25
800
400
200
80
40
20
600
300
150
60
30
15
400
200
100
40
20
10
200
100
50
20
10
5
(δ)
10
9
8
7
6
5
4
3
2
1
0

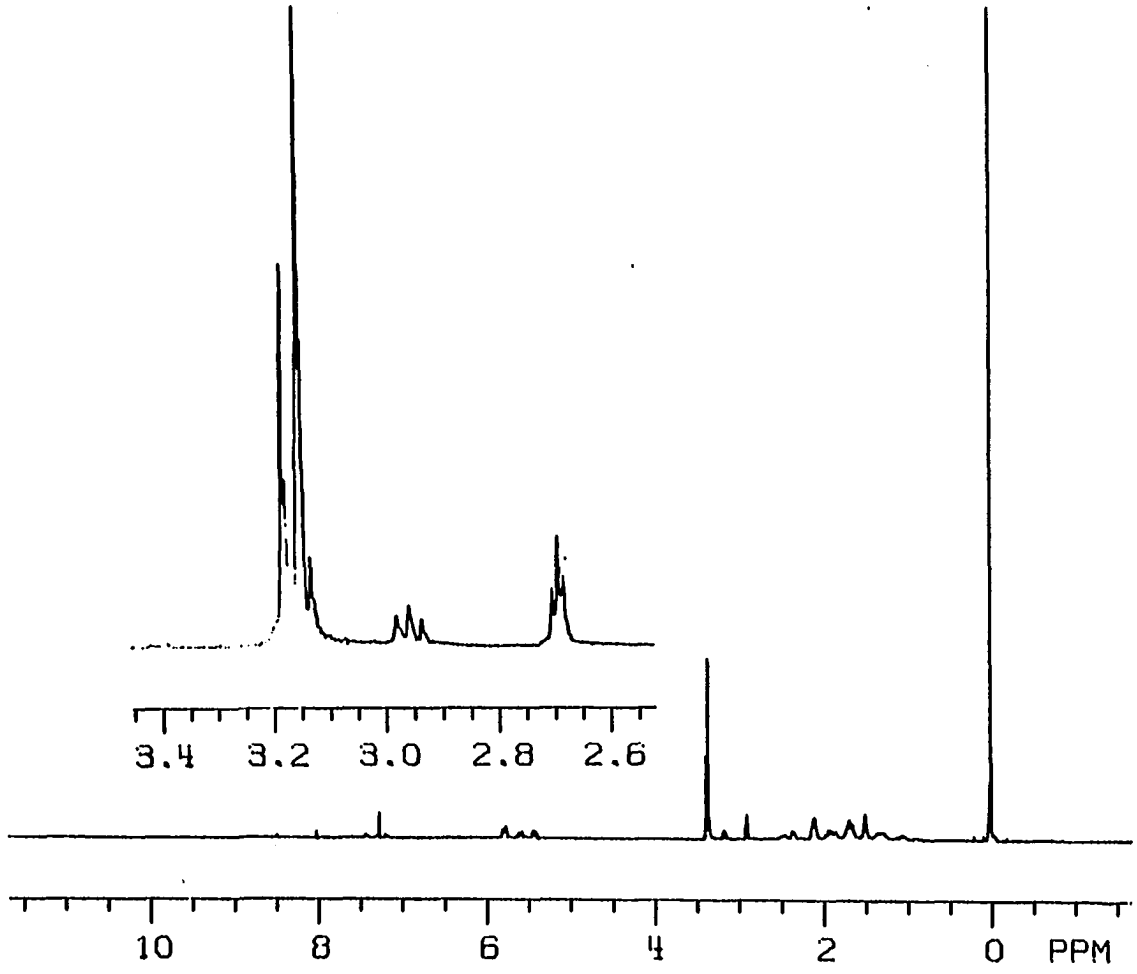

Figur 46. Continued

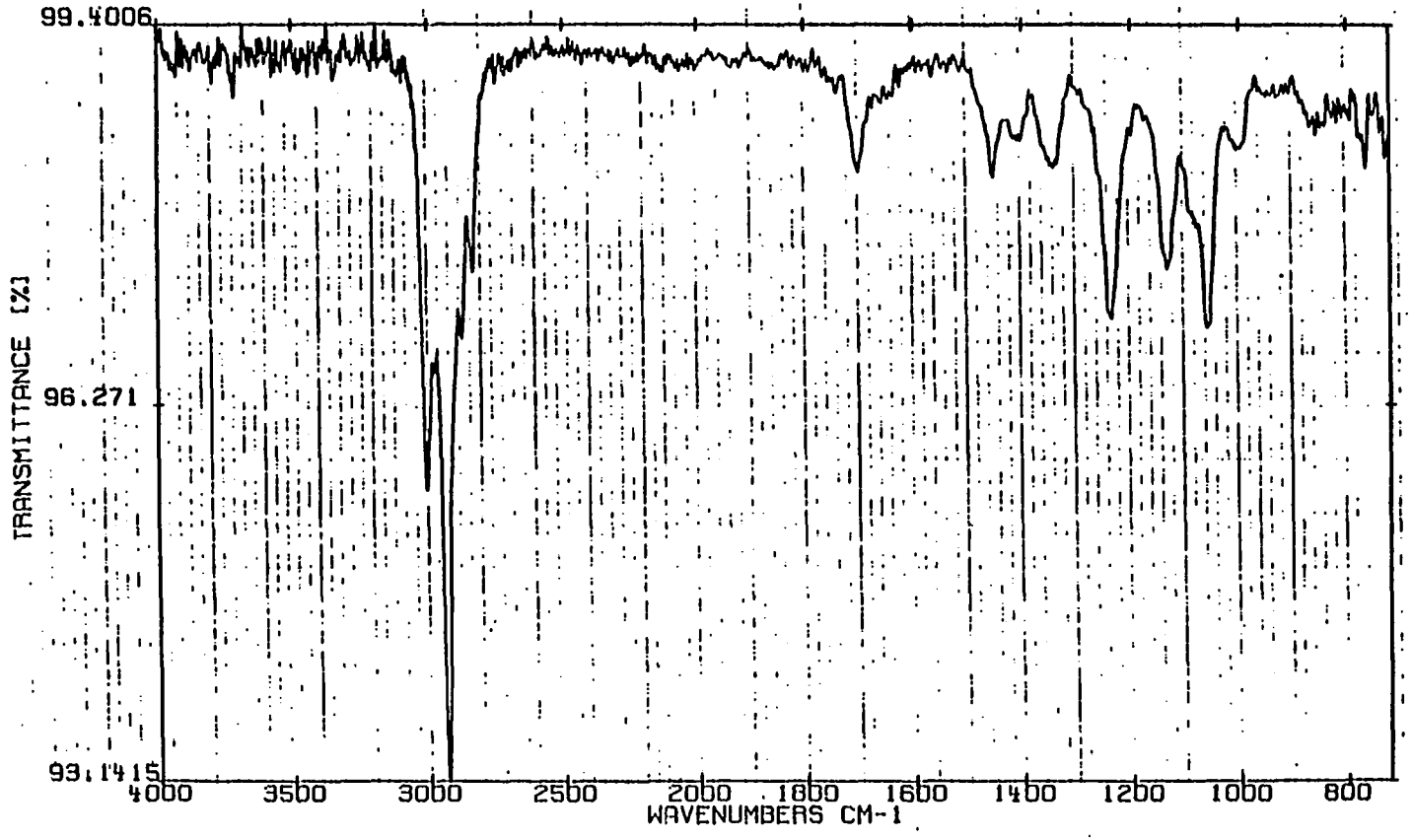

Figure 46. Continued

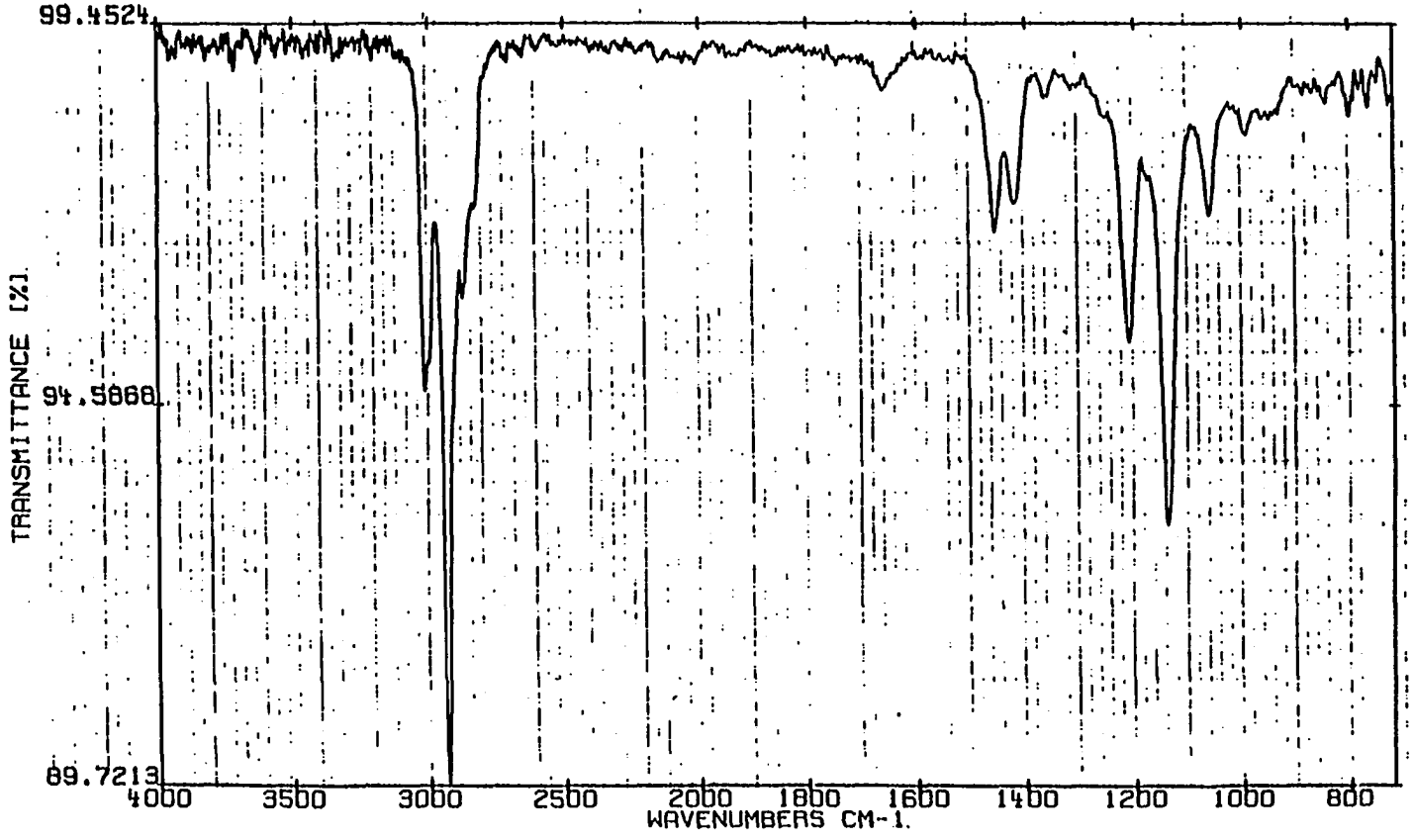

Figure 46. Continued

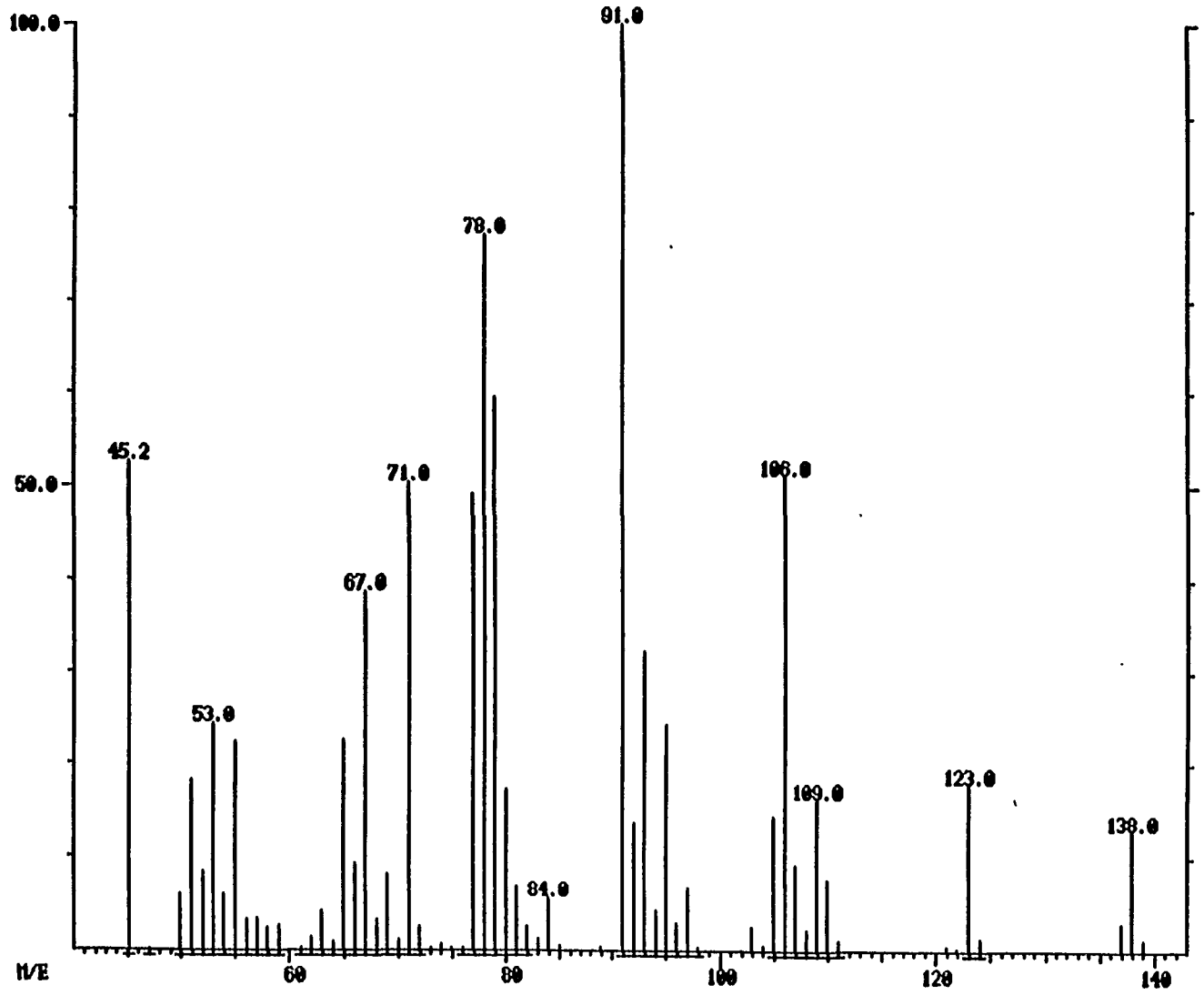

Figure 46. Continued

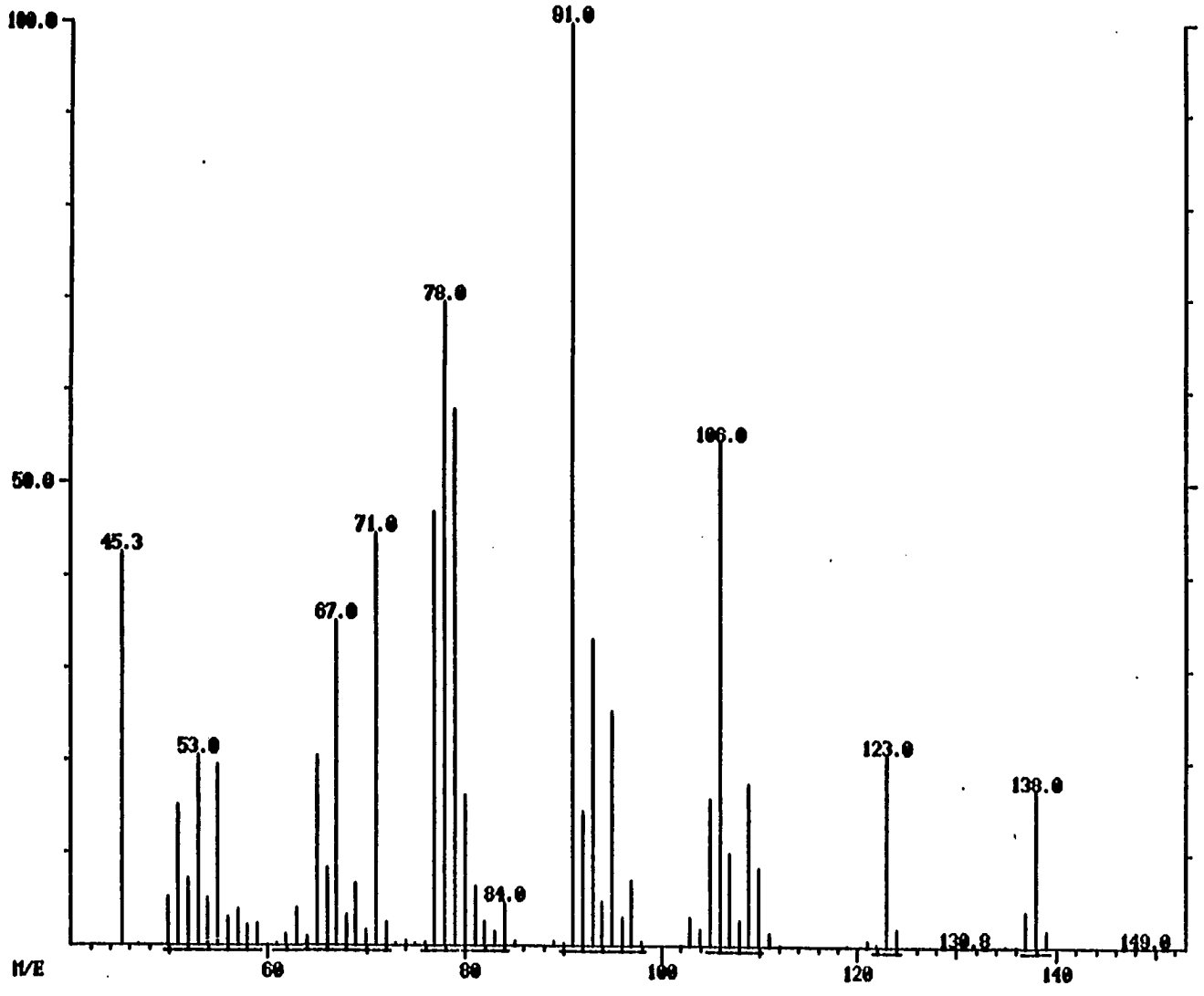

Figure 46. Continued

Figure 47. Products from reaction of 19' in $C_6H_5CN/CH_2C(CH_3)CN$

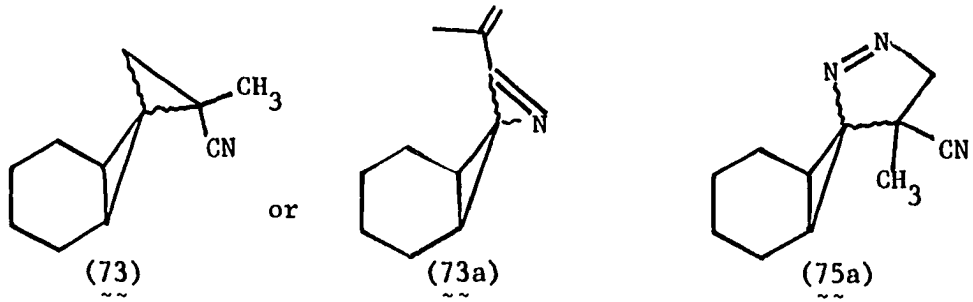

(73) or (73a) (75a)

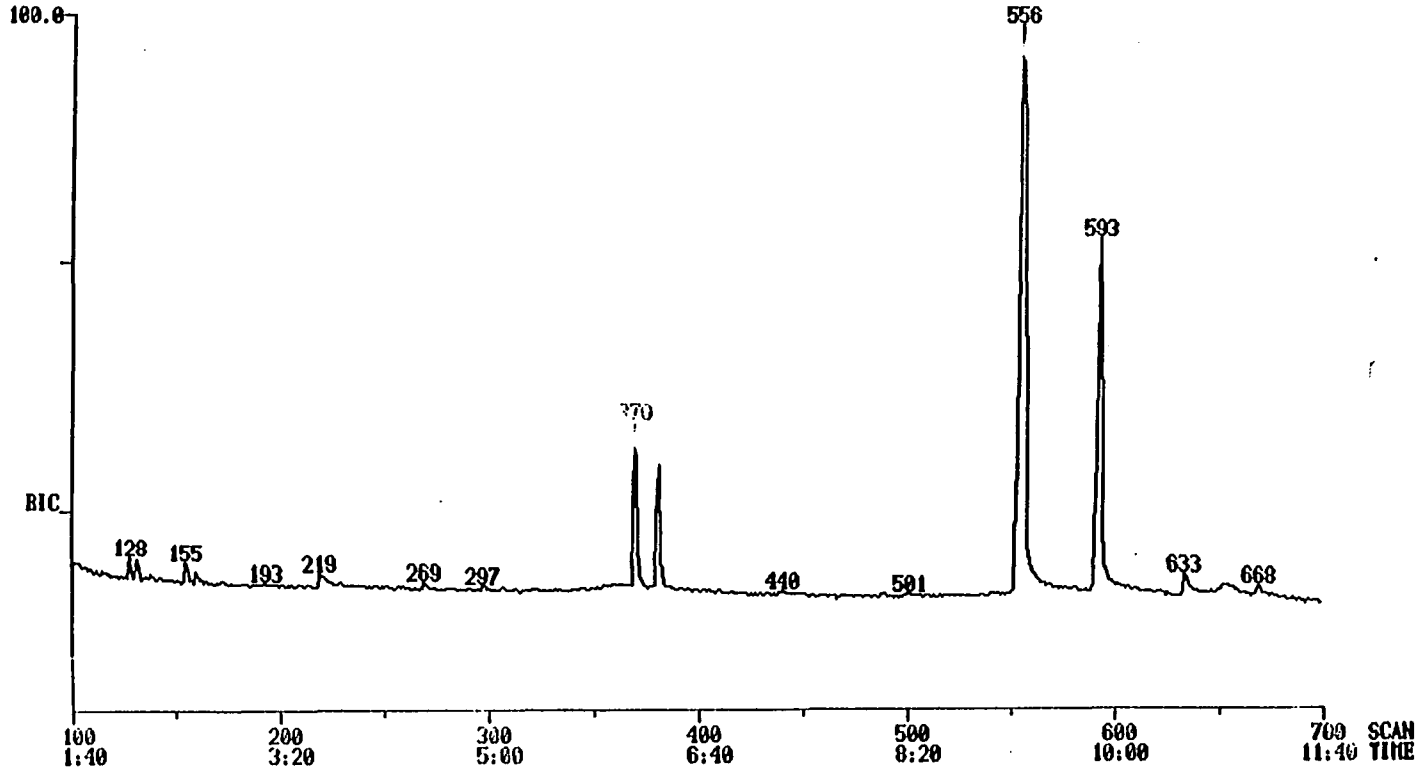
100.0
BIC
128
155
193
219
269
297
370
440
501
556
593
633
668
100
1:40
200
3:20
300
5:00
400
6:40
500
8:20
600
10:00
700
11:40
SCAN
TIME

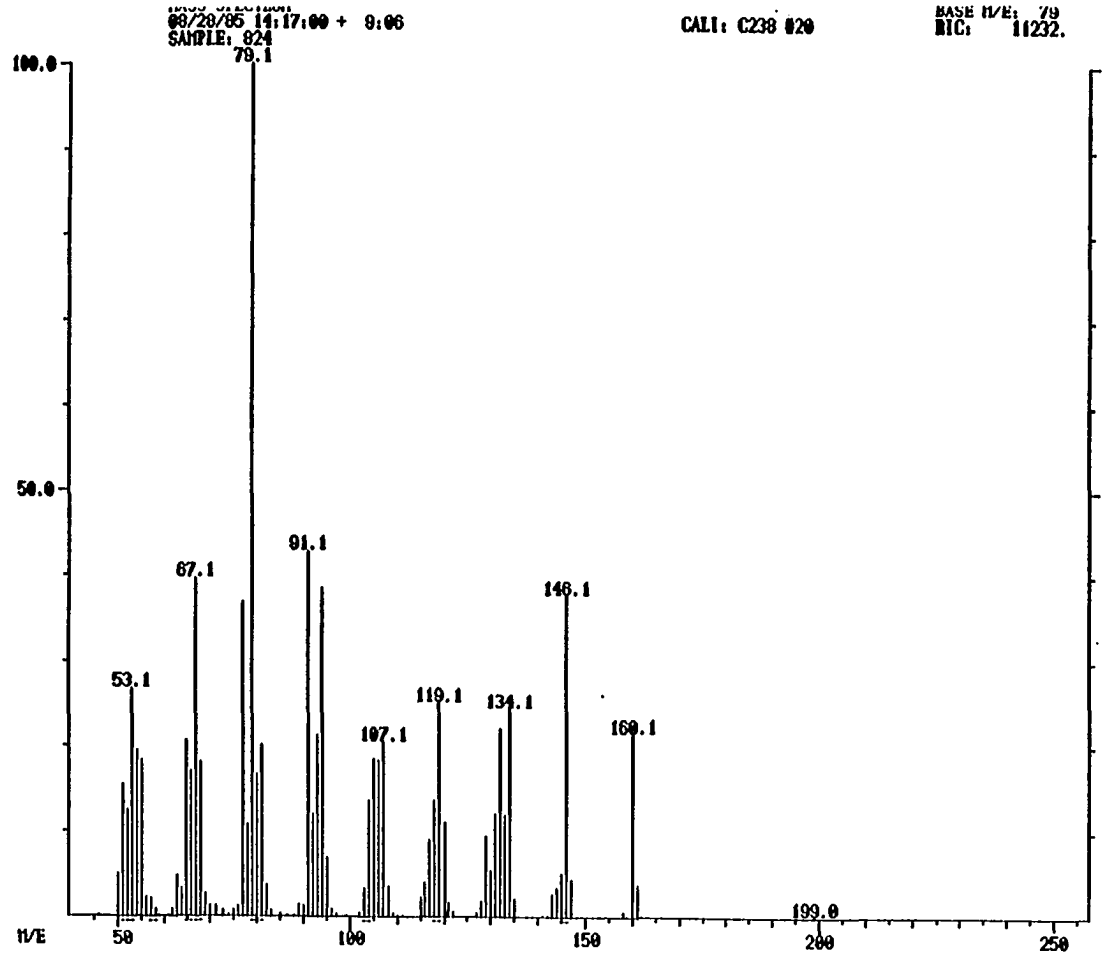

Figure 47. Continued

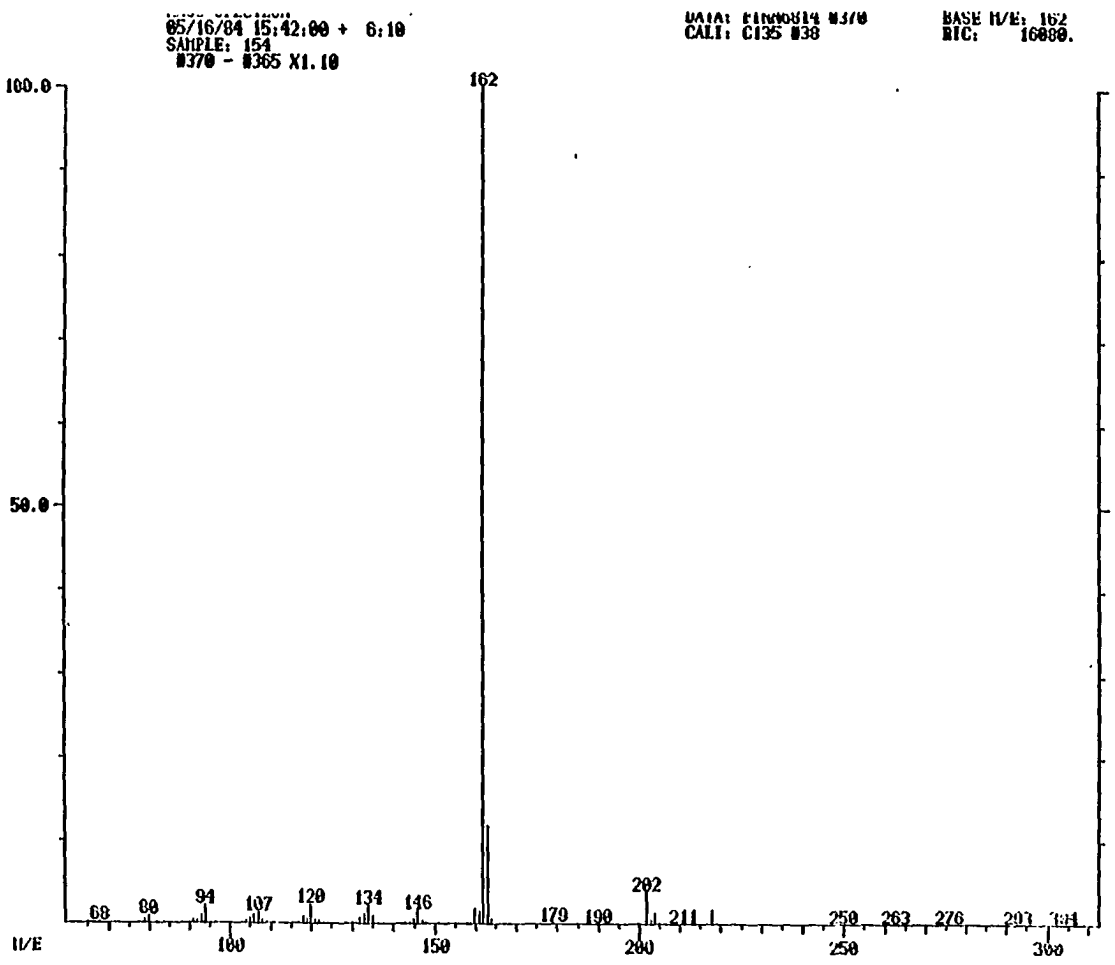

Figure 47. Continued

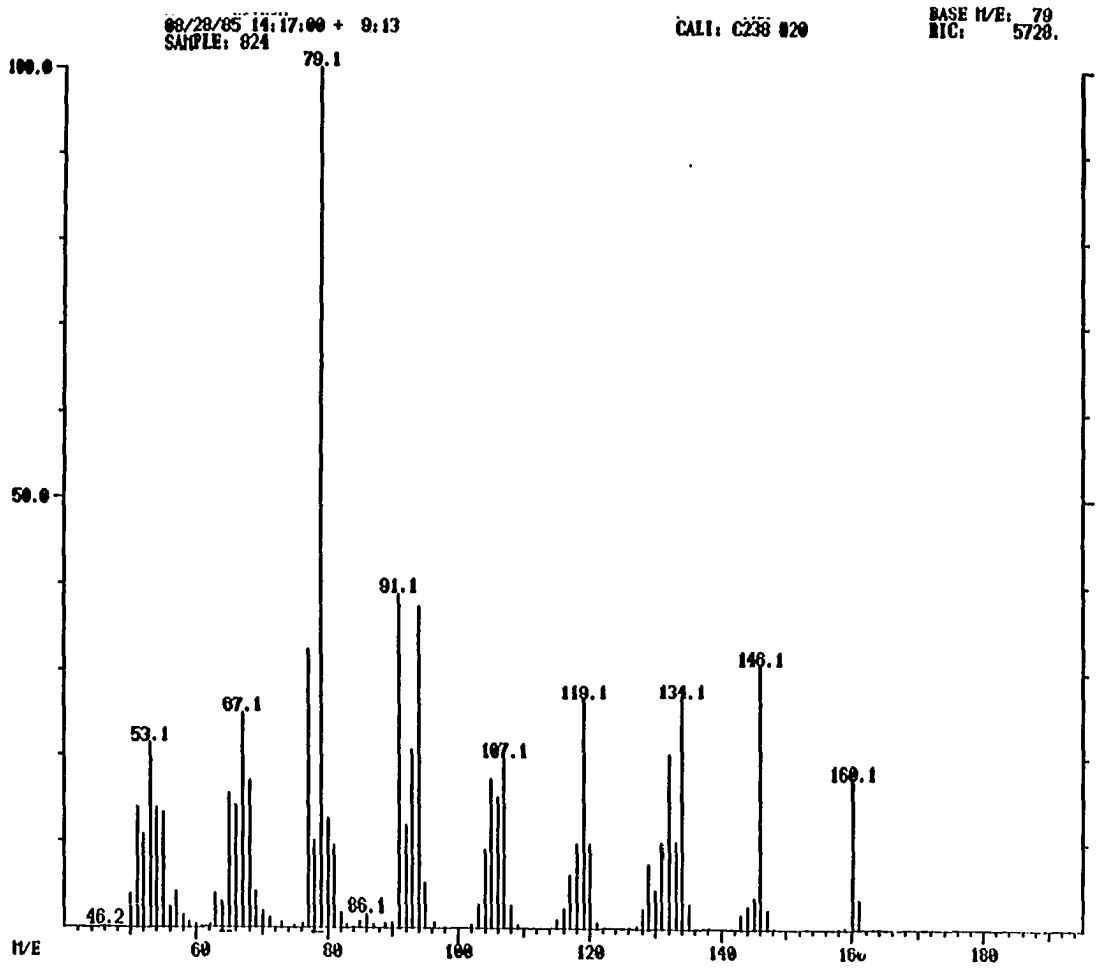

Figure 47. Continued

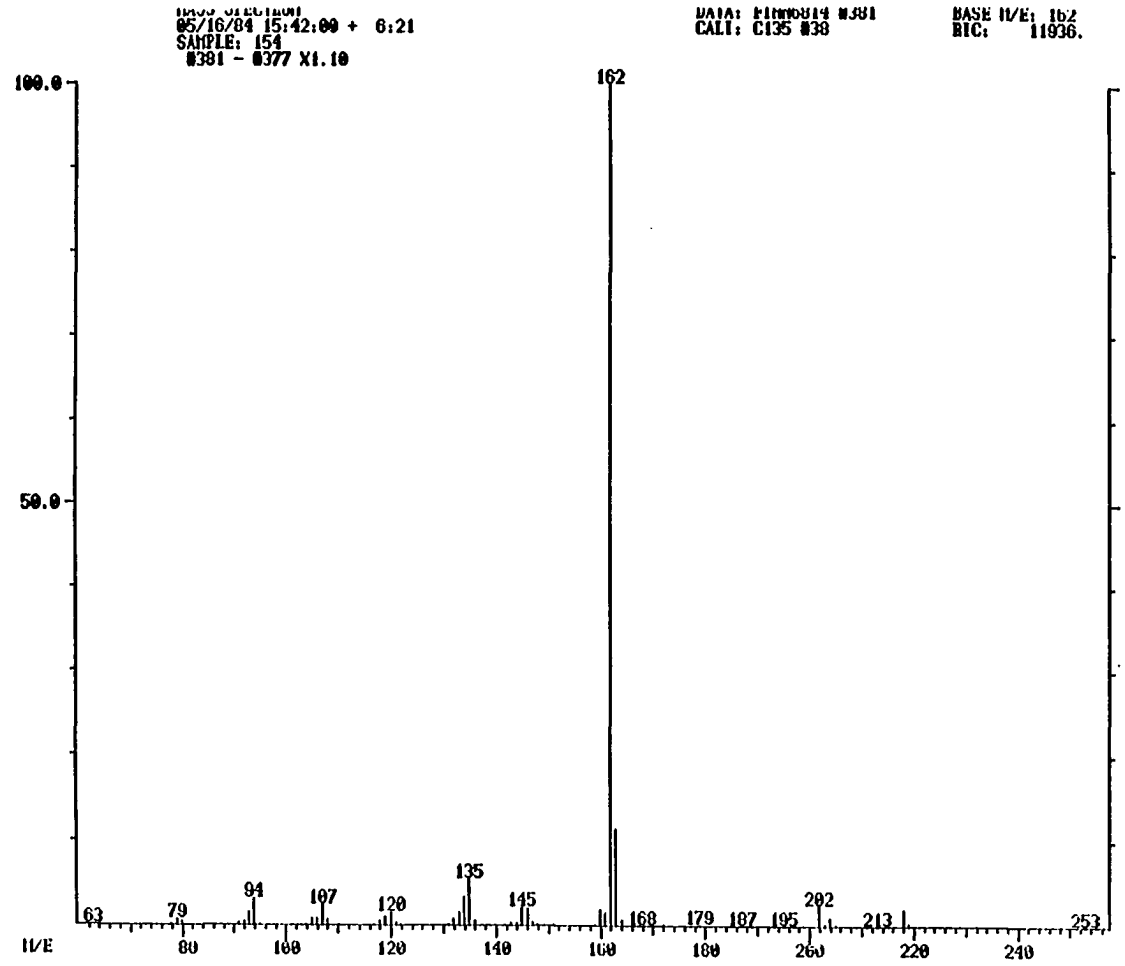

Figure 47. Continued

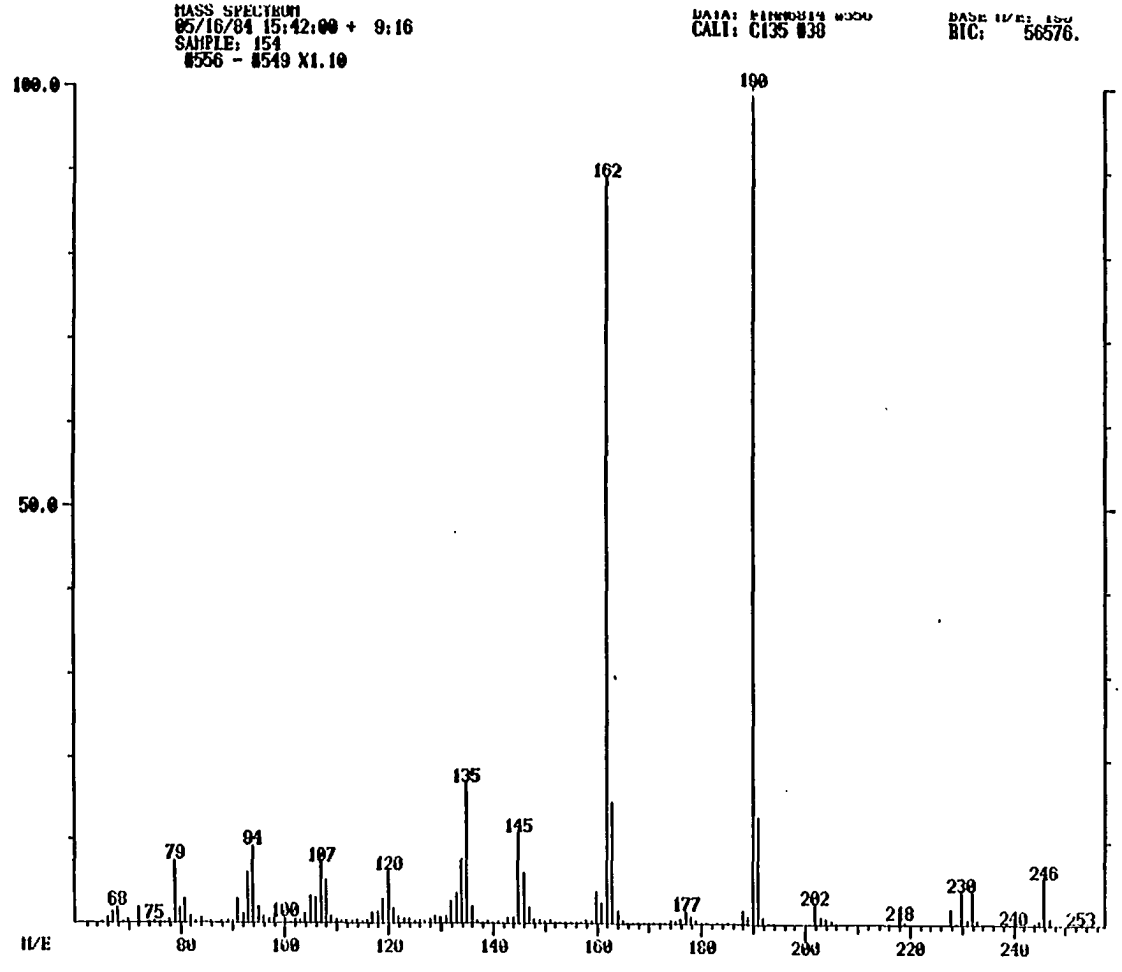

Figure 47. Continued

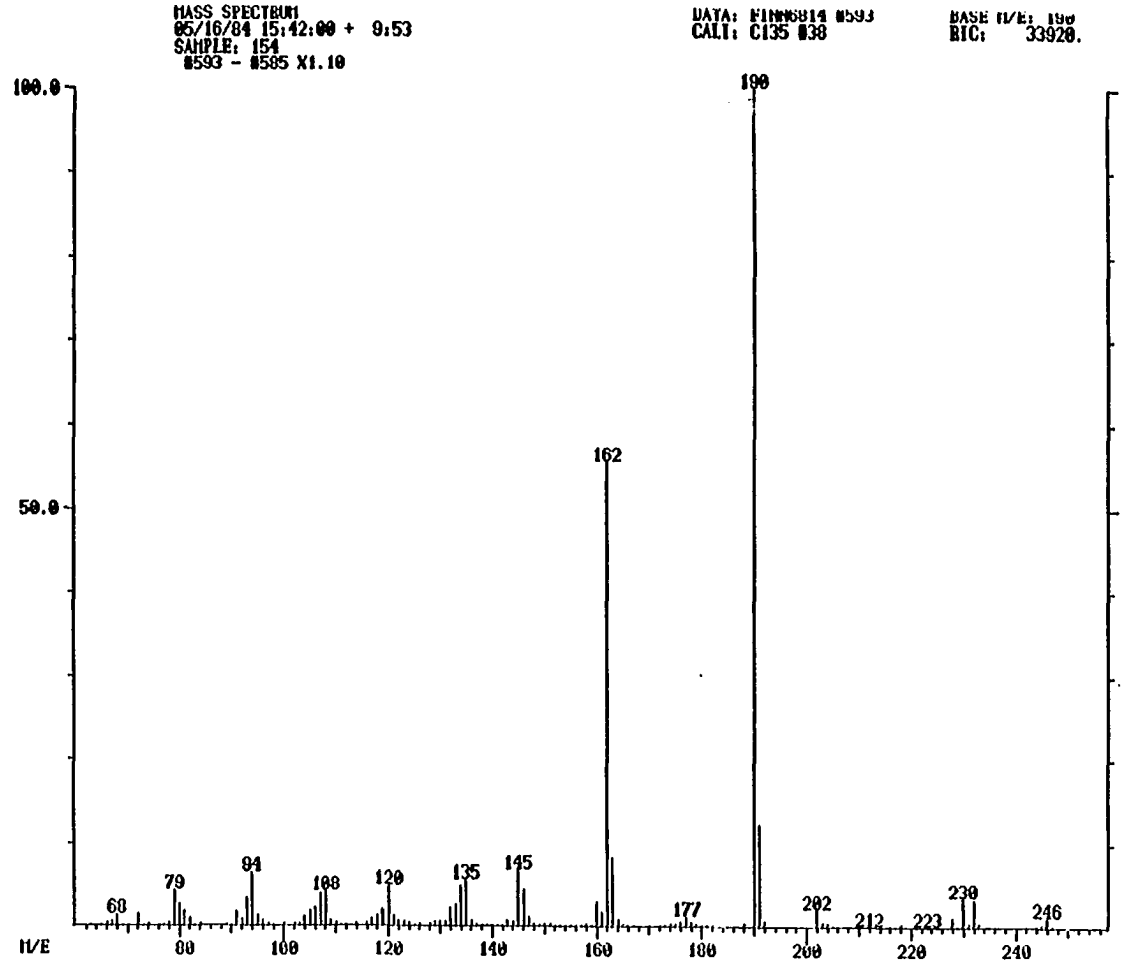

Figure 47. Continued

Figure 48. Nitrile ylide adducts 79

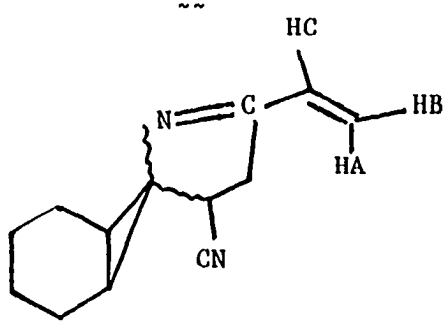

79

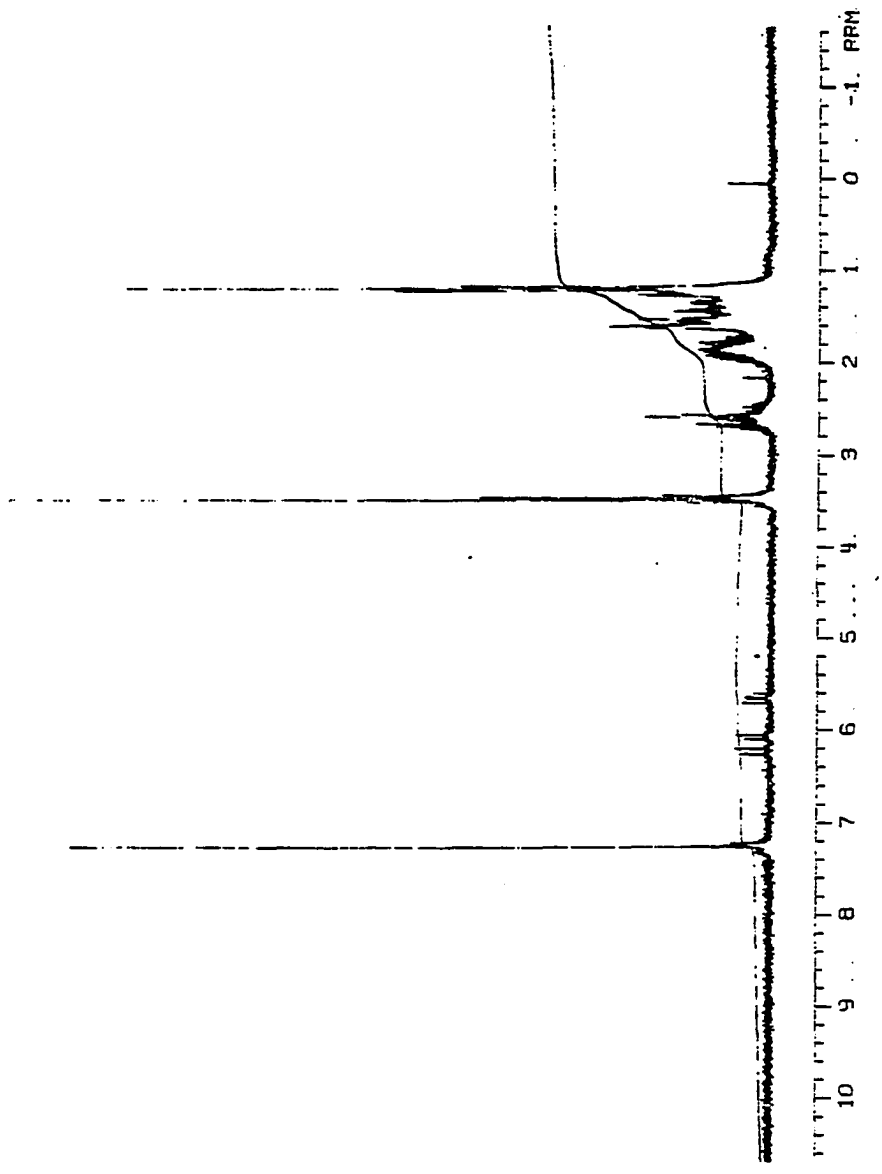
10
9
8
7
6
5
4
3
2
1
0
-1. PPM

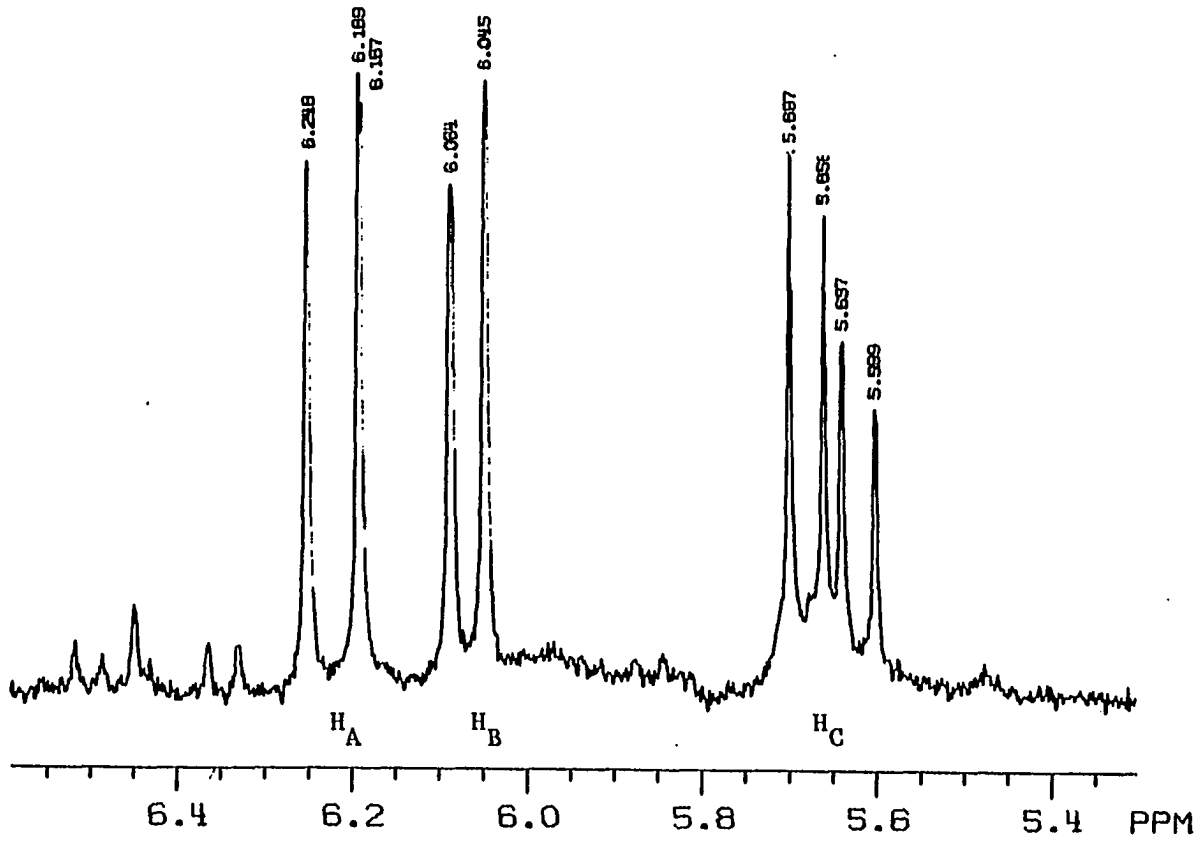

Figure 48. Continued

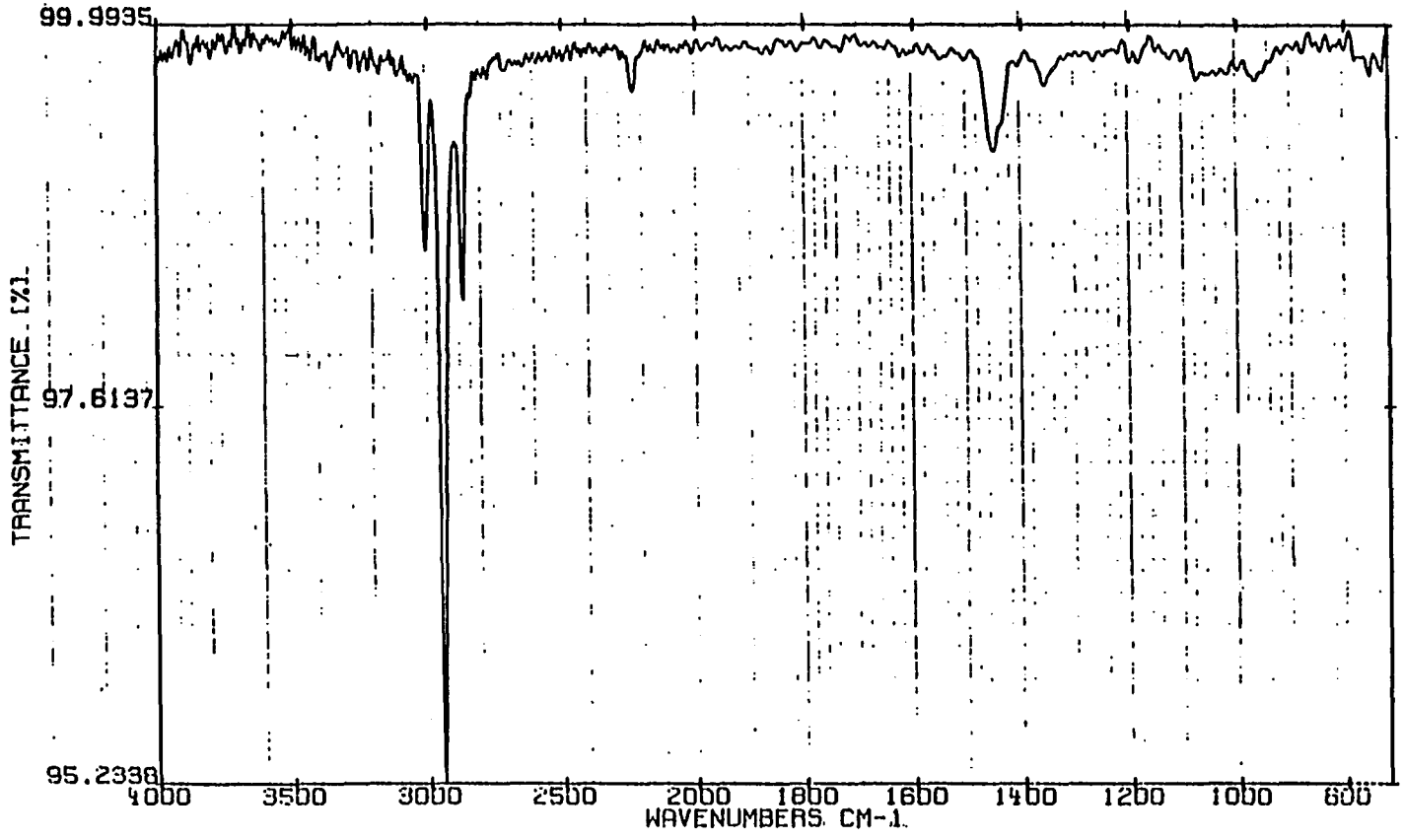

Figure 48. Continued

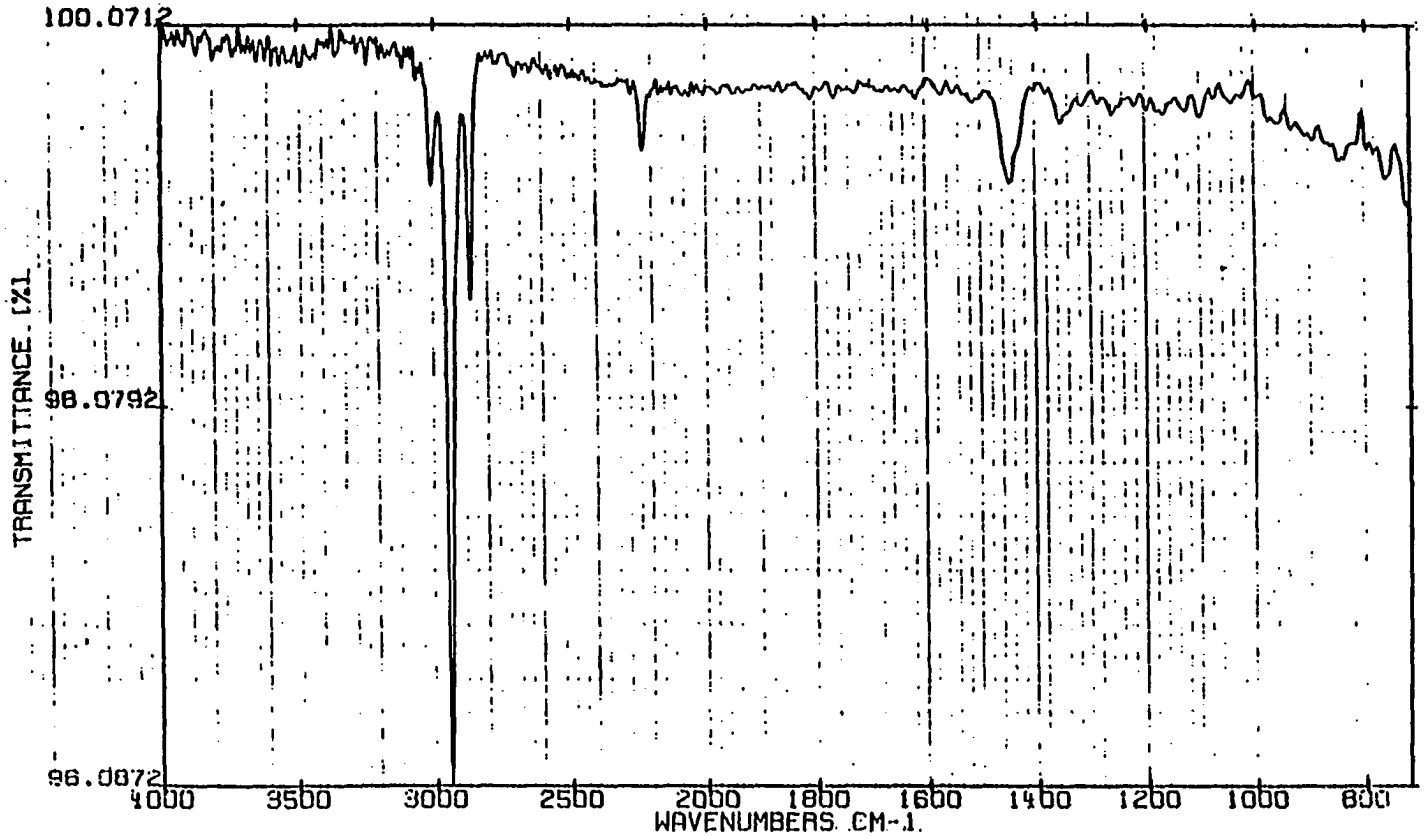

Figure 48. Continued

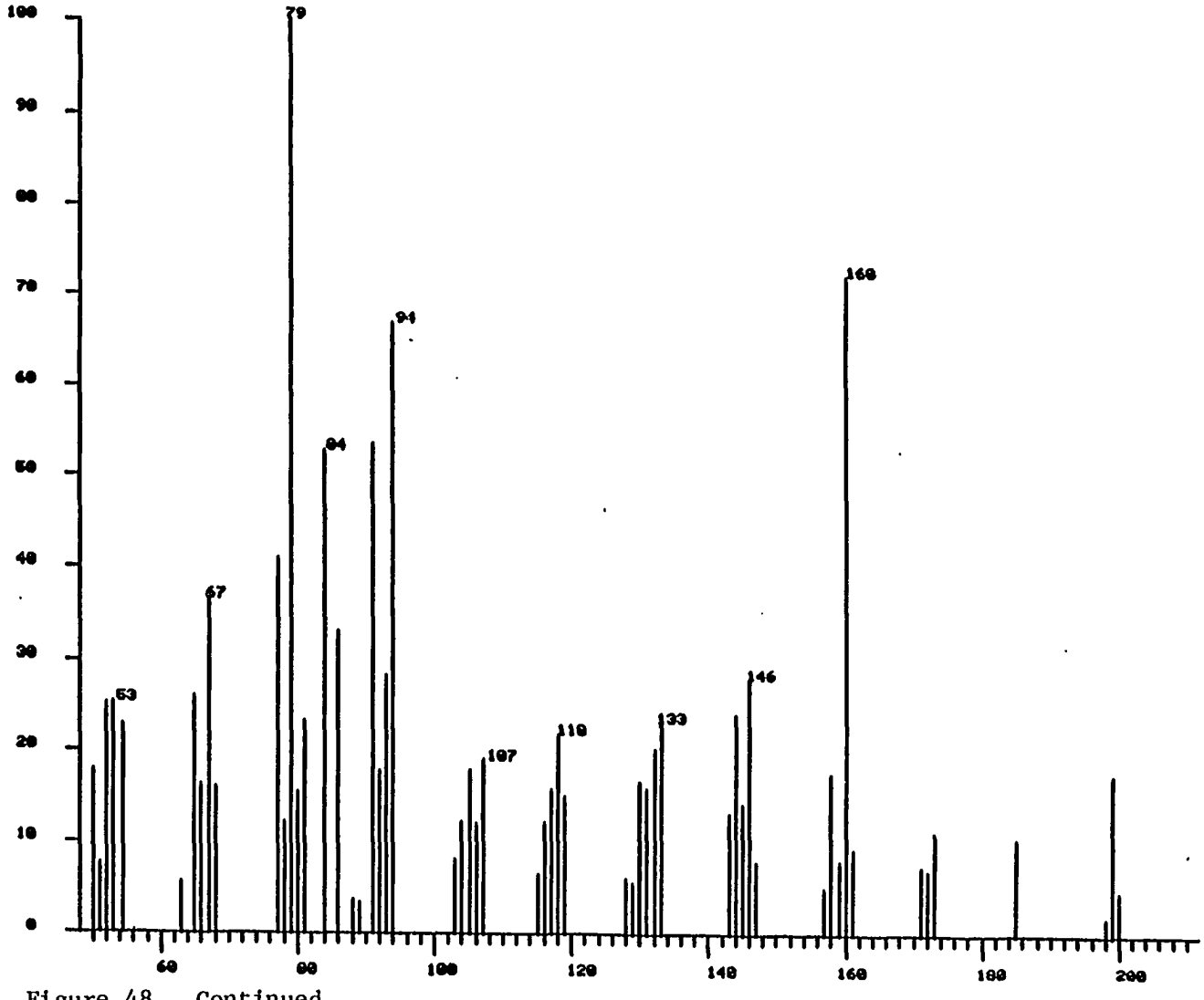

Figure 48. Continued

CHAPTER III. PYROLYSIS OF ANTI-7-BROMO-SYN-7-TRIMETHYLSTANNYLBICYCLO[4.1.0]HEPTANE IN METHANOL AND t-BUTANOL

Introduction

In 1975, Seyferth and Lambert (76) reported that heating α-bromotrimethylstannylcyclopropanes (85) in solution provided a possible route to cyclopropylidenes (86). They pyrolyzed 87-anti and 87-syn separately in refluxing cyclooctene solution and obtained the cyclopropanation product 88 from each. They also studied the pyrolysis of a 4:1 mixture of 87-anti and 87-syn in cyclohexene solution at 170°C, and obtained a 33% isolated yield of 89. When a 4:1 mixture of 87-anti and 87-syn was pyrolyzed in chlorobenzene solution in the presence of triethylsilane at 125°C, compounds 90-anti, 90-syn and allene dimer 91 were afforded in

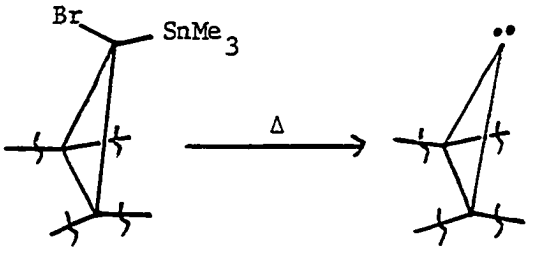

85 86

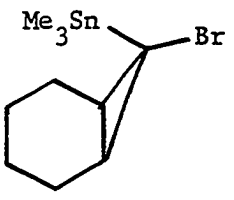

87-anti

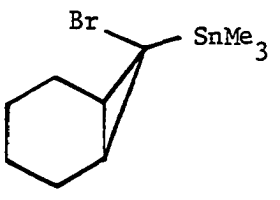

87-syn

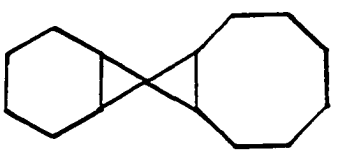

88

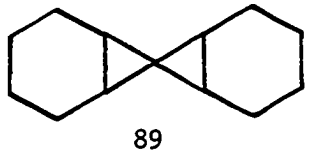

89

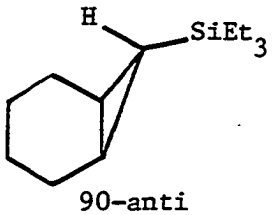

90-anti

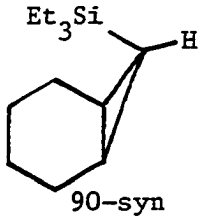

90-syn

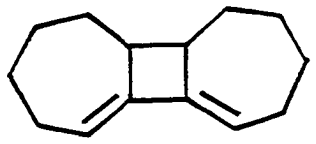

91

24%, 25% and 12% isolated yields, respectively. Seyferth and Lambert (76) suggested the intermediacy of a carbene in these divalent carbon transfer reactions, but at the same time concluded that alternative mechanisms were possible.

To further investigate the possible formation of cyclopropylidene intermediates from organotin precursors, Warner and Herold (77) investigated the solution chemistry of the epimers of 87. They pyrolyzed a 0.04 M benzene solution of either 87-anti or 87-syn at 160°C, and found 91 as the major product [equations (24) and (25)]. In the presence of DPIBF, 92 was formed in a 30% isolated yield. These findings verified that products 91 and 92 originated from allene intermediate 93.

When they carried out the pyrolysis of 87-syn and 87-anti in cyclohexene at 160°C, the products found were those shown in equations

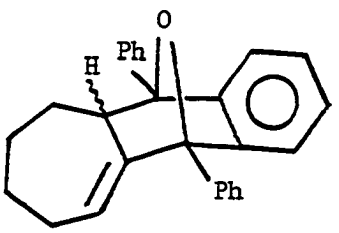

92

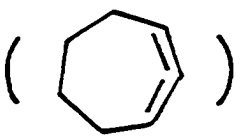

93

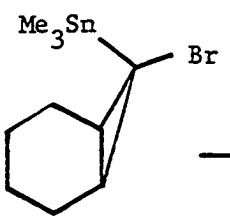

87-anti

$$\xrightarrow[C_6D_6]{160^\circ C} Me_3SnBr\ (100\%) + \underset{\sim\sim}{91}\ (78\%) \qquad (24)$$

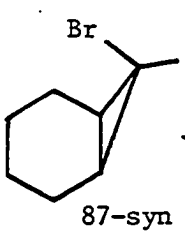

87-syn

$$\xrightarrow[C_6D_6]{160^\circ C} Me_3SnBr\ (100\%) + \underset{\sim\sim}{91}\ (77\%) + \underset{\sim\sim}{94}\ (9\%) + \underset{\sim\sim}{95}\ (1\%) \qquad (25)$$

(26) and (27). Epimer 87-anti was found to be 20 times more reactive than 87-syn, which was in accord with Seyferth and Lamberts' results (76).

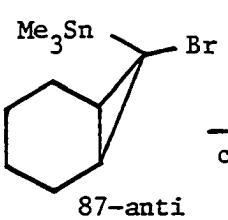

87-anti

$$\xrightarrow[\text{cyclohexene}]{160^\circ C} Me_3SnBr\ (98\%) + \underset{\sim\sim}{89}\ (53\%) + \underset{\sim\sim}{91}\ (16\%) \qquad (26)$$

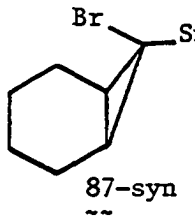

87-syn

$$\xrightarrow[\text{cyclohexene}]{160^\circ C} Me_3SnBr + \underset{\sim\sim}{89} + \underset{\sim\sim}{91} + \underset{\sim\sim}{94} \qquad (27)$$

95% 18% 58% 4.5%

Warner and Herold (77) suggested that compound 87-anti produced mainly compounds arising from the trapping of either ion pair 96 or norcaranylidene 20', but 87-syn produced most compounds from the trapping of either ion pair 97 or allene 93. To test this, they conducted the

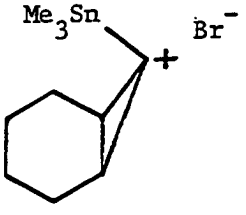

96

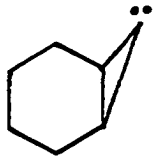

20'

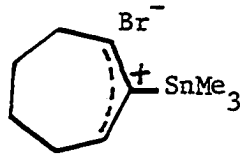

97

93

thermolyses in benzene/methanol solvent mixtures. The products were as shown in equations (28) and (30). Product 98 must have resulted from the trapping of ion pair 96. Additionally, 98 could be the precursor to 25 via acid cleavage of the trimethyltin group of 98. Therefore triethylamine was used as an acid scavenger, with the results shown in equations (29) and (31). As shown in equation (29), a very substantial amount (15%) of 98 was now formed, at the expense of 25. Moreover, the kinetic deuterium isotope effect for 25 was observed to be 2.40 at 160°C in the presence of 1.1 equivalents of triethylamine. This surprisingly high value seemed consistent with a component of the reaction involving

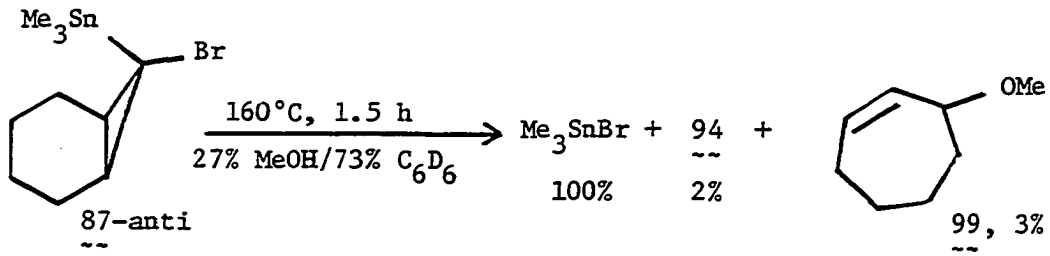
Me3Sn
Br
160°C, 1.5 h
27% MeOH/73% C6D6
Me3SnBr + 94 +
100% 2%
OMe
87-anti
99, 3%

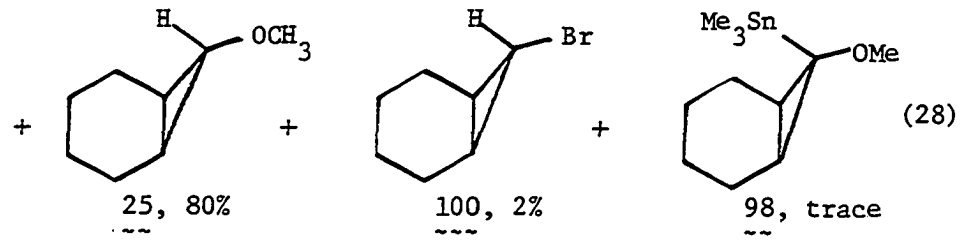
H
OCH3
H
Br
Me3Sn
OMe
25, 80%
100, 2%
98, trace

(28)

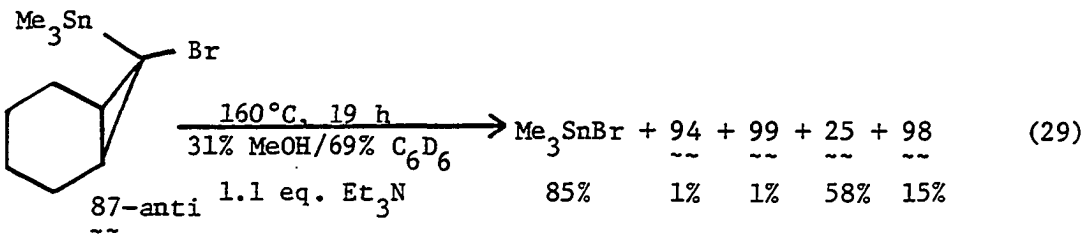
Me3Sn
Br
160°C, 19 h
31% MeOH/69% C6D6
1.1 eq. Et3N
87-anti
Me3SnBr + 94 + 99 + 25 + 98
85% 1% 1% 58% 15%

(29)

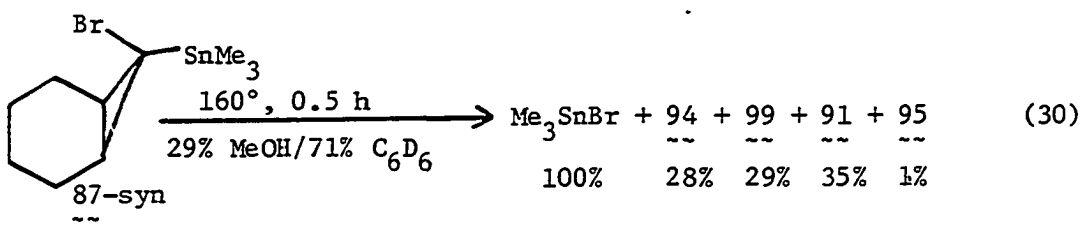
Br
SnMe3
160°, 0.5 h
29% MeOH/71% C6D6
87-syn
Me3SnBr + 94 + 99 + 91 + 95
100% 28% 29% 35% 1%

(30)

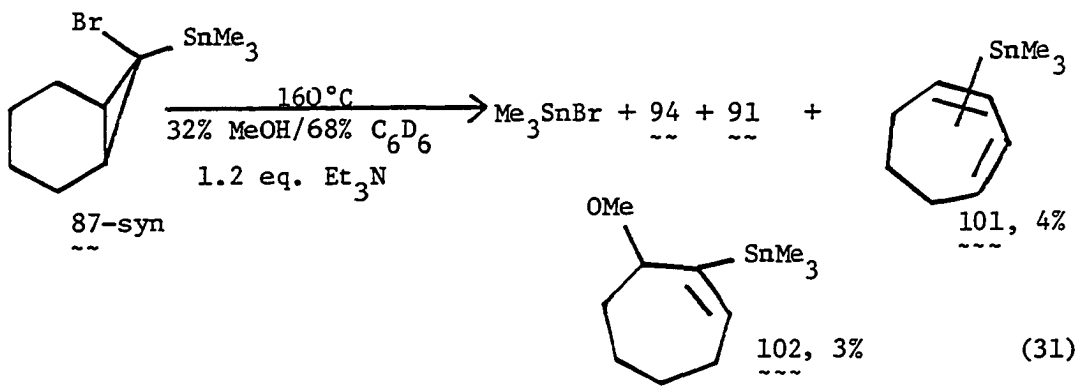
Br
SnMe3
160°C
32% MeOH/68% C6D6
1.2 eq. Et3N
87-syn
Me3SnBr + 94 + 91 +
SnMe3
101, 4%
OMe
SnMe3
102, 3%

(31)

cleavage of 98 to 25 (primary isotope effect expected; perhaps >3), even in the presence of Et_3N.

Summarizing their studies of the solution-phase pyrolysis reactions of 87-anti and 87-syn, Warner and Herold (78) concluded that the major reaction pathway of 87-syn was a cationic ring-opening reaction, concommitant with C-Br bond heterolysis, to yield a cationic species (97), which was trappable by methanol (Scheme XIX). However, the major reaction pathway of 87-anti was C-Br bond heterolysis, leading to the generation of a cyclopropyl cationic species (96), which would lose trimethyltin bromide to give norcaranylidene 20' which was trappable by either methanol of cyclohexene (Scheme XX).

Although the mechanism of the thermal decomposition of the two epimers of 87 had been largely clarified by the studies of Warner and Herold, some questions still remained:

(i) Significant quantities of 98 were observed only in the presence of Et_3N. Did 98 not survive the reaction conditions in the absence of Et_3N, or was it not formed at all? Was 98 transformed to 25 in the absence of Et_3N?

(ii) The kinetic deuterium isotope effect found for 25 at 160°C was 2.40. However, according to the ylide mechanism [equation (32)], a secondary isotope effect was expected. What explanation is there for this discrepancy? These questions will be addressed in this chapter.

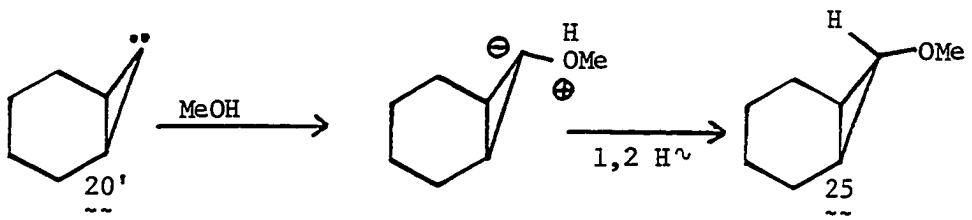

(32)

Scheme XIX

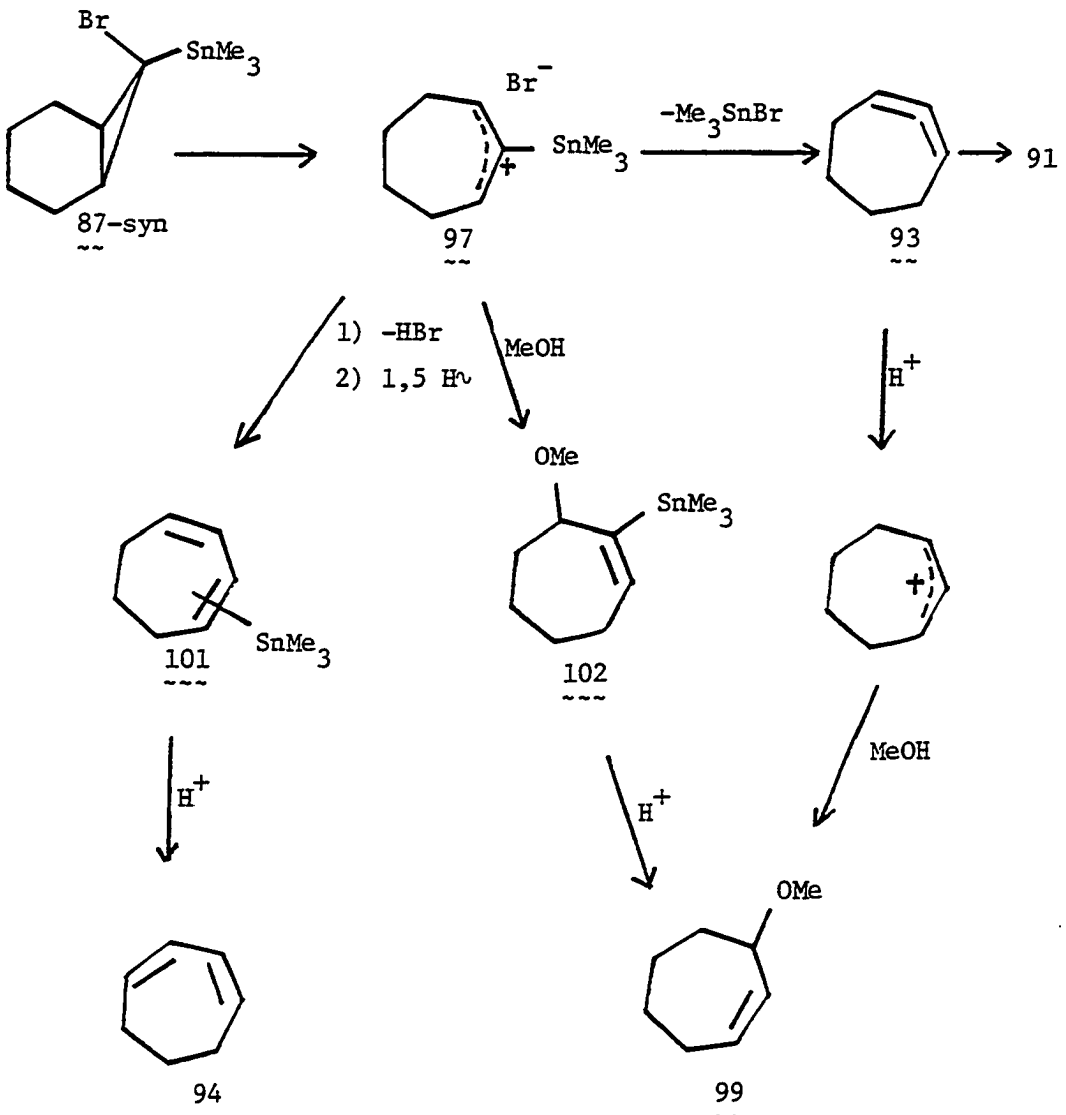
Br
SnMe3
87-syn
Br⁻
SnMe3
97
-Me3SnBr
93
91
1) -HBr
2) 1,5 Hν
MeOH
H+
OMe
SnMe3
101
SnMe3
102
H+
MeOH
H+
OMe
94
99

Scheme XX

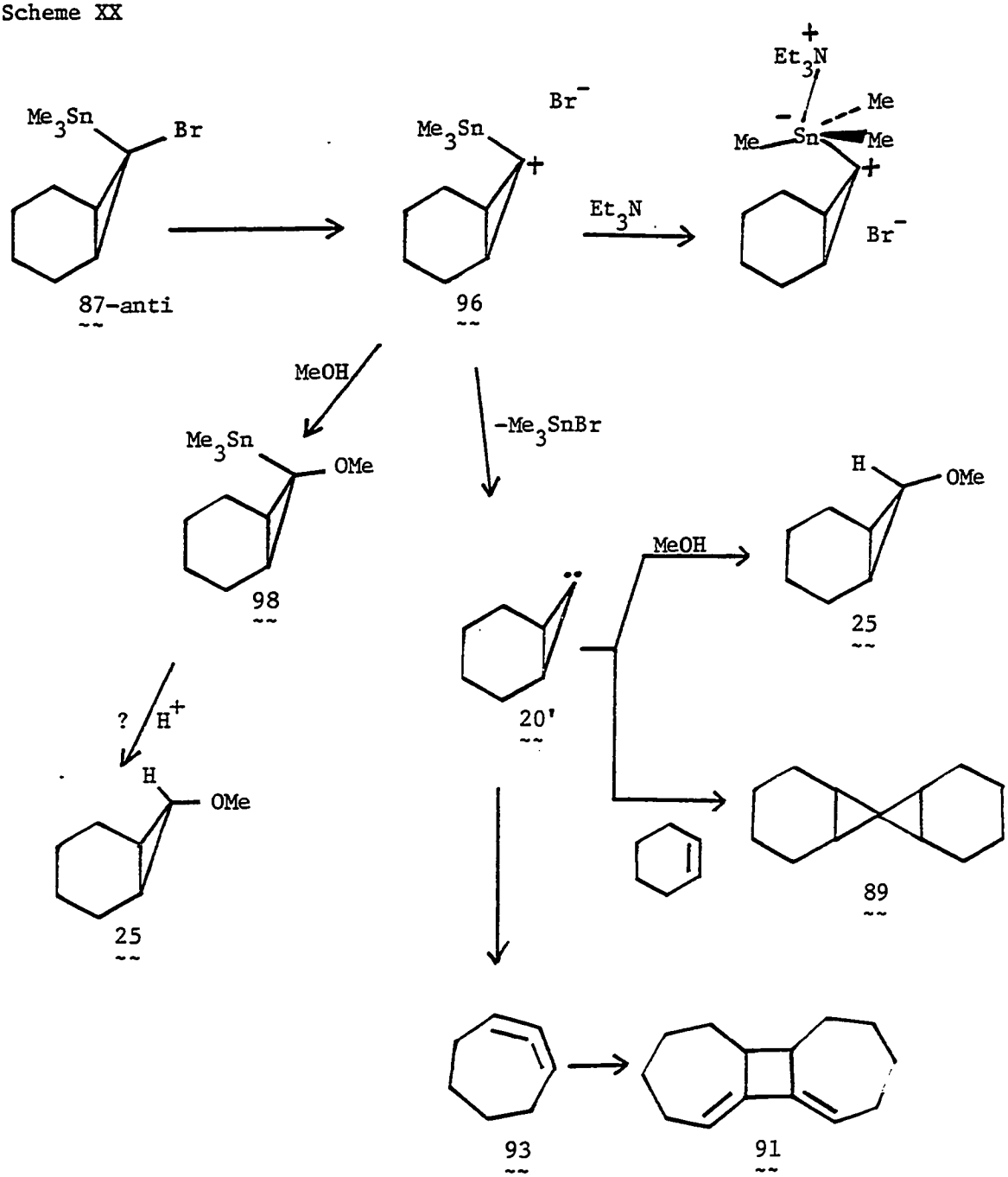
Me3Sn
Br
87-anti
Br⁻
Me3Sn
96
Et3N
Et3N
Me
Me
Sn
Me
Br⁻
MeOH
Me3Sn
OMe
98
-Me3SnBr
20'
MeOH
H
OMe
25
? H+
H
OMe
25
89
93
91

Results and Discussion

As a starting point, we carried out the reaction of 87-anti in 20% (1:1) MeOH/MeOD/80% C_6H_6 in the presence of 0.88 equivalents of triethylamine at 160°C. The sample was equally distributed to a set of NMR tubes, sealed, and heated simultaneously in a preheated oil bath. The time-resolved products were then analyzed by gas chromatography with appropriate corrections for the known response factors. Table 61 lists the time-resolved product distribution under these conditions. The value of k_H/k_D was obtained from GC-MS analysis, using equation (33), where the % D incorporations were determined by comparison with the fully deuterated and partially deuterated MS results.

$$\frac{k_H}{k_D} = \frac{100-\%\ D_{incor.}}{\%\ D_{incor.}} \cdot \frac{[MeOD]}{[MeOH]} \qquad (33)$$

Table 61. Time-resolved product distribution from 87-anti in 80% methanolic[a] benzene at 160°C in the presence of 0.88 equivalents of triethylamine

Time (h)	(starting material) 87-anti (%)	98 (%)	25 (%)	$\frac{k_H}{k_D}$ (25)
1	65.5	11.6	12.0	2.80
3	9.5	14.8	18.0	3.04
5.5	1.0	11.5	28.5	3.23
22	trace	6.3	31.5	3.62

[a]The 20% methanol portion of the solvent was an 1:1 (v/v) mixture of MeOH/MeOD.

As shown in Table 61, the production of 25 and 98 was non-linear. Indeed, 98 was slowly, although apparently not quantitatively, converted to 25 (Figure 49). Moreover, all the k_H/k_D values correspond to primary isotope effects. The increase in K_H/k_D with time is consistent with the protolysis of 98 to 25. These results belie the hypothesis that 25 was formed only via the carbene pathway when triethylamine was used as an acid scavenger. However, it remained clear that a large percentage of 25 was formed via carbene 20'. We next turned to experiments without triethylamine.

In the absence of triethylamine, the reaction rate increased (Table 62), which was consistent with Warner and Herold's finding that triethylamine functioned as a rate inhibitor. And compound 25 was found to be produced linearly (Figure 50) with smaller values of k_H/k_D. However, with 1.1 equivalents of triethylamine was used, the reaction was again slower (Table 63), and production of 25 and 98 was nonlinear (Figure 51).

From these results, the possibility that compound 98 was cleaved by acid to give 25 in the absence of triethylamine became doubtful due to the rather smaller value of k_H/k_D observed in the absence of triethylamine. A control experiment then showed that compound 25 was formed quantitatively from 98, with k_H/k_D = 4.10, in the presence of 2.4 equivalents of triethylamine [equation (34)]. A reasonable explanation is that triethylamine reacted with 98 to form a complex (cf., Scheme XXI) which subsequently gave 25 with a primary deuterium isotope effect. A crucial experiment was to then carry out the pyrolysis of 98 without triethylamine.

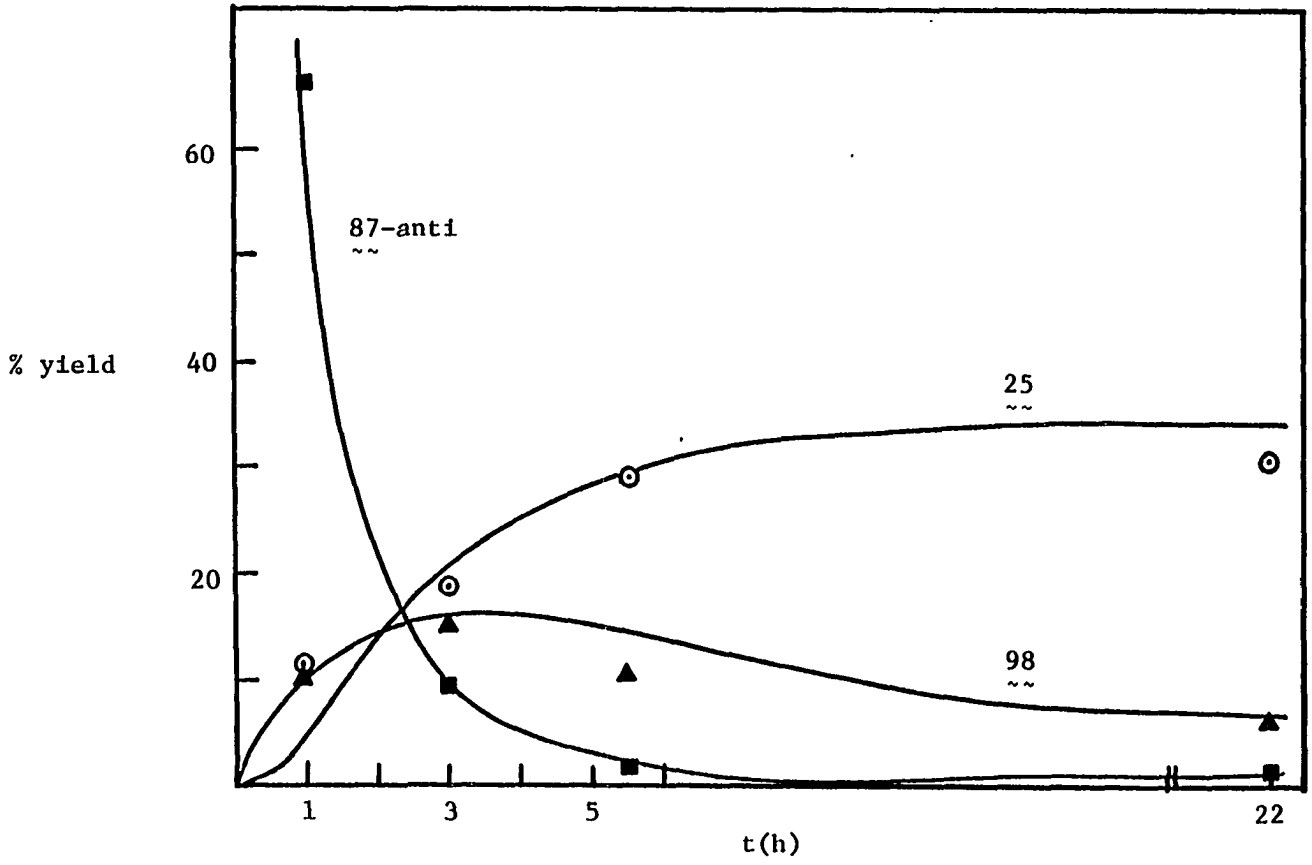

Figure 49. Concentration-time curves for 87-anti, 25 and 98 in the pyrolysis of 87-anti

Table 62. Time-resolved product distribution from 87-anti in 80% methanolic[a] benzene at 160°C in the absence of triethylamine

Time (h)	87-anti (%)	25 (%)	$\frac{k_H}{k_D}$ (25)
1	52.1	47.9	1.63
2	15.0	71.3	2.00
2.5	13.0	75.5	1.78
3	trace	94.1	1.89

[a]The 20% methanol portion of the solvent was an 1:1 (v/v) mixture of MeOH/MeOD.

Table 63. Time-resolved product distribution from 87-anti in 80% methanolic[a] benzene at 160°C in the presence of 1.1 equivalents of triethylamine

Time (h)	87-anti (%)	98 (%)	25 (%)	$\frac{k_H}{k_D}$ (25)
0.5	87.0	4.8	trace	--
2	66.5	9.2	5.6	2.52
3	58.8	21.8	15.0	2.73
17	10.2	43.5	46.2	2.82

[a]The 20% methanol portion of the solvent was an 1:1 (v/v) mixture of MeOH/MeOD.

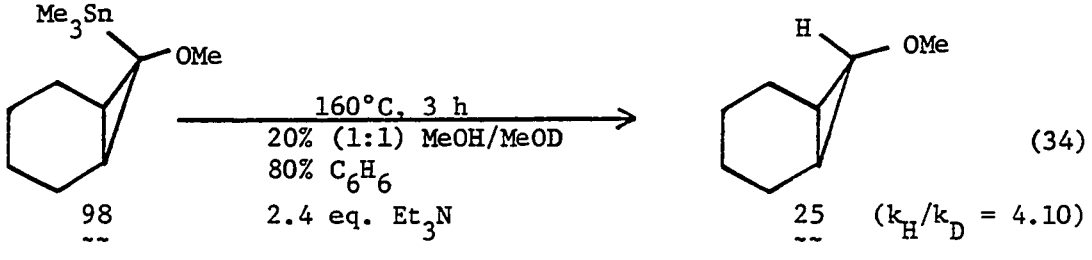

98 25 (k_H/k_D = 4.10) (34)

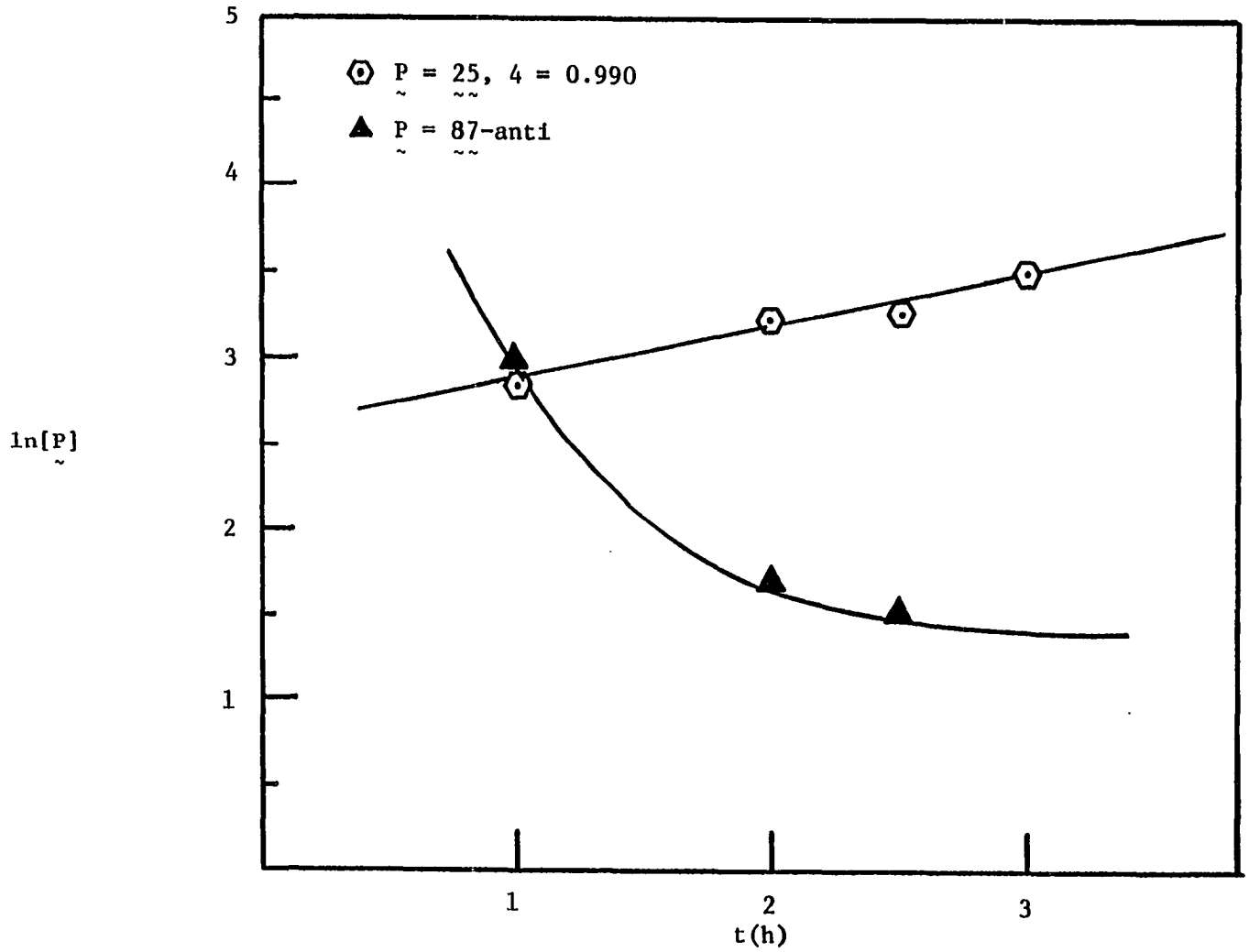

Figure 50. Concentration-time curves for 87-anti and 25 in the pyrolysis of 87-anti in the absence of triethylamine ([P] as % yield)

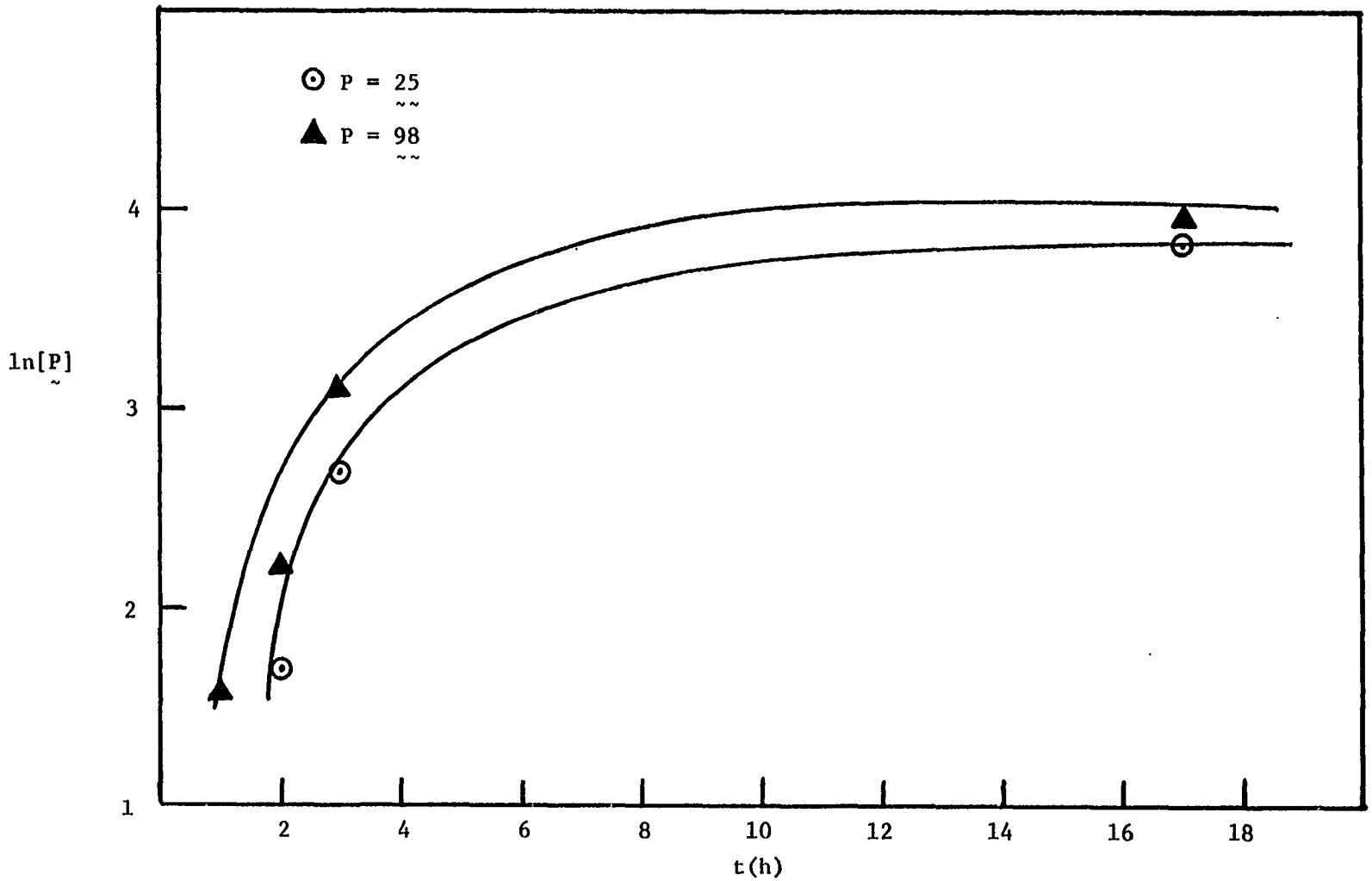

Figure 51. Concentration-time curves for 25 and 98 in the pyrolysis of 87-anti in the presence of 1.1 equivalents of triethylamine ([P] as % yield)

Compound 98 was prepared by conducting a large scale pyrolysis of 87-anti in methanolic benzene solution in the presence of triethylamine, followed by purification via thin-layer chromatograph (44). When 98 was pyrolyzed at 160°C for five hours, 25 was formed in 10% yield with k_H/k_D = 1.50 [equation (35)]. This finding strongly supports the notion that the formation of 25 from 87-anti in the absence of triethylamine occurs via carbene 20', which probably reacts with MeOH via the ylide mechanism. However, the isotope effect value, which is larger than observed at room temperature, needs to be addressed (see below). When triethylamine was present, k_H/k_D was intermediate between that expected for 20', and that observed for the protolysis of 98. The small amount of 25 formed from 98 in the absence of triethylamine exhibited an isotope effect consistent with it arising via 20' [equation (36)]. As a whole, the results suggested that 98 was not formed at all in the absence of triethylamine. Scheme XXI shows a mechanism which fits all the data in hand. The initial ion pair, 96 (or possibly the Br^- should be shown as attached to the tin, making tin pentacoordinate, whereby the process yielding 103 involves nucleophilic substitution at tin) could be captured by triethylamine, if present, or proceed to carbene 20'; 96 doesn't yield 98. The presumably more stable (relative to 96) 103 might then suffer methanol attack to give 98. Other pathways open to 103 might include return to 87-anti (inhibitor effect), or (possibly) extrusion of the tin moiety to give carbene 20'.

Since pyrolysis of 87-anti provided a method to study the kinetic deuterium isotope effect for 25 at high temperatures, we then carried out

Scheme XXI

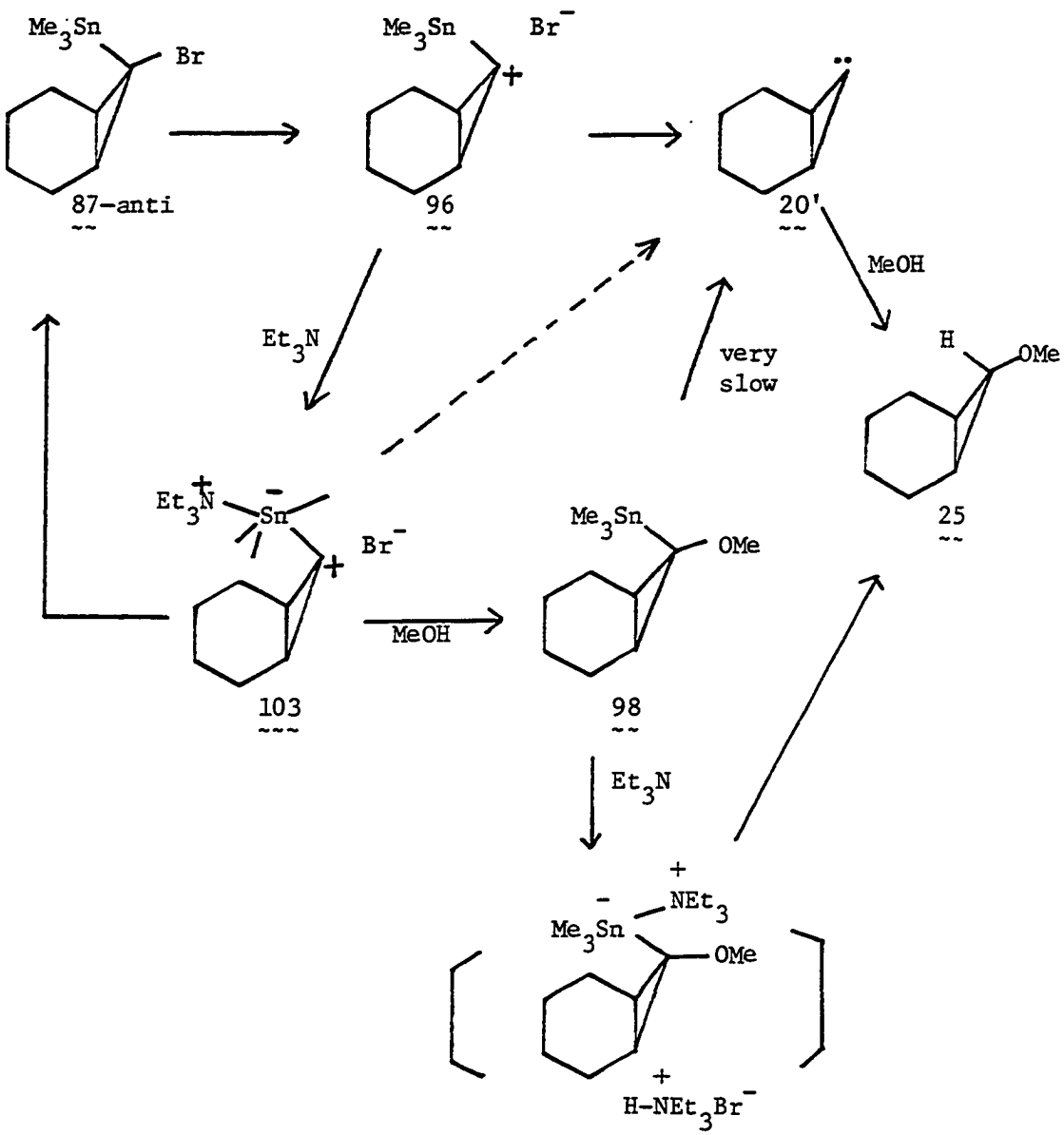
Me3Sn
Br
87-anti
Me3Sn
Br−
96
20'
MeOH
Et3N
very
slow
H
OMe
25
Et3N
Sn
Br−
103
MeOH
Me3Sn
OMe
98
Et3N
NEt3
Me3Sn
OMe
H-NEt3Br−

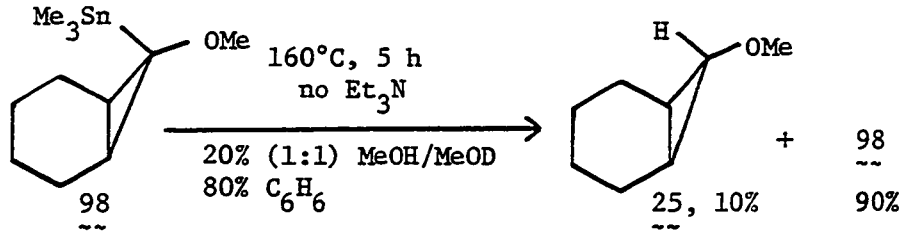

(35)

$(k_H/k_D = 1.50)$

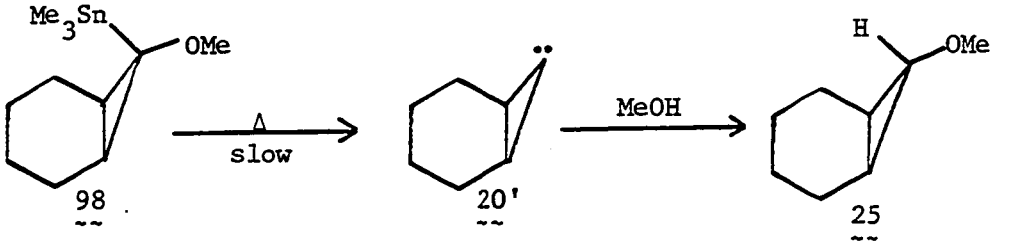

(36)

the pyrolysis within the temperature range 120° to 160°C in the absence of triethylamine (the reaction was too slow if the temperature was lower than 120°C). Table 64 lists the kinetic deuterium isotope effects within the temperature range -78° to 160°C. The data at temperatures below 120°C were obtained from NaOMe-initiated decomposition of nitrosourea 19' in methanol.

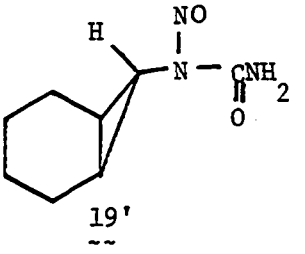

Although the k_H/k_D values shown in Table 64 are roughly within the region of secondary isotope effects, they don't show a smooth temperature-dependent trend. This is clearly illustrated in Figure 52. In fact, the

Table 64. Kinetic deuterium isotope effects for 25 at different temperatures

T (°C)	$10^3/T$ (K^{-1})	k_H/k_D	ln k_H/k_D
-78	5.13	1.40	0.34
0	3.66	1.27	0.24
10	3.53	1.23	0.21
25	3.36	1.04	0.04
40	3.19	1.32	0.28
65	2.96	1.55	0.44
120	2.54	1.68	0.52
135	2.45	1.58	0.46
160	2.31	1.83[a]	0.60

[a]This number is the average of the four values in Table 62.

data indicate possibly two mechanism changes: one on going from high to room temperature, and the other on going from ambient to the low temperature. Why might this occur?

In the first place, we previously demonstrated that k_H/k_D for insertion of 11 into MeOH changed from secondary to primary upon going from ambient temperature to -78°C, while that for 14 remained unchanged (and secondary). Since we observe only the product-forming isotope

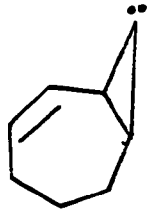

11

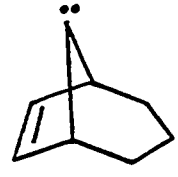

14

effect, there are only a limited number of ways such a change could occur. At the outset, we can rule out a protonation mechanism, since (a) protonation of 11 would lead to a cyclopropyl cation which would suffer ring-opening, and (b) 14 is expected to react via protonation (or direct insertion), and its isotope effect doesn't change significantly with temperature. The ylide mechanism affords the following features:

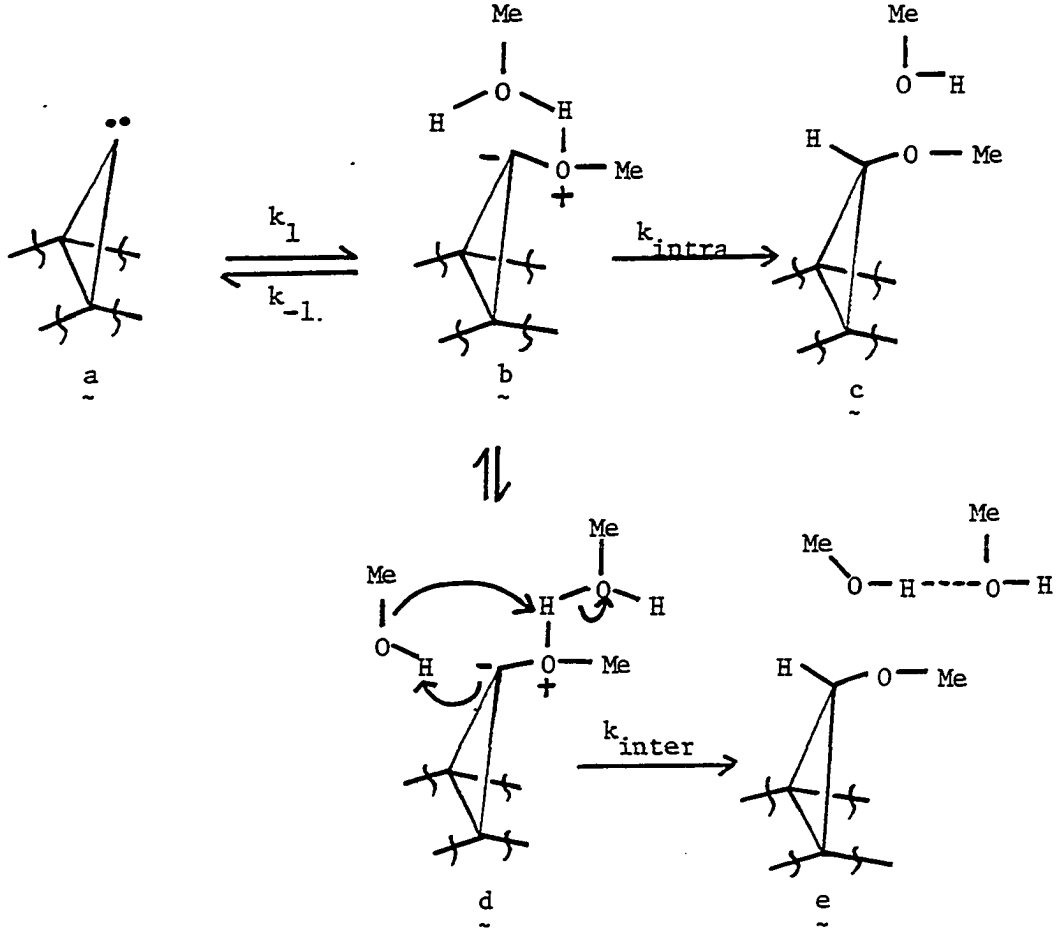

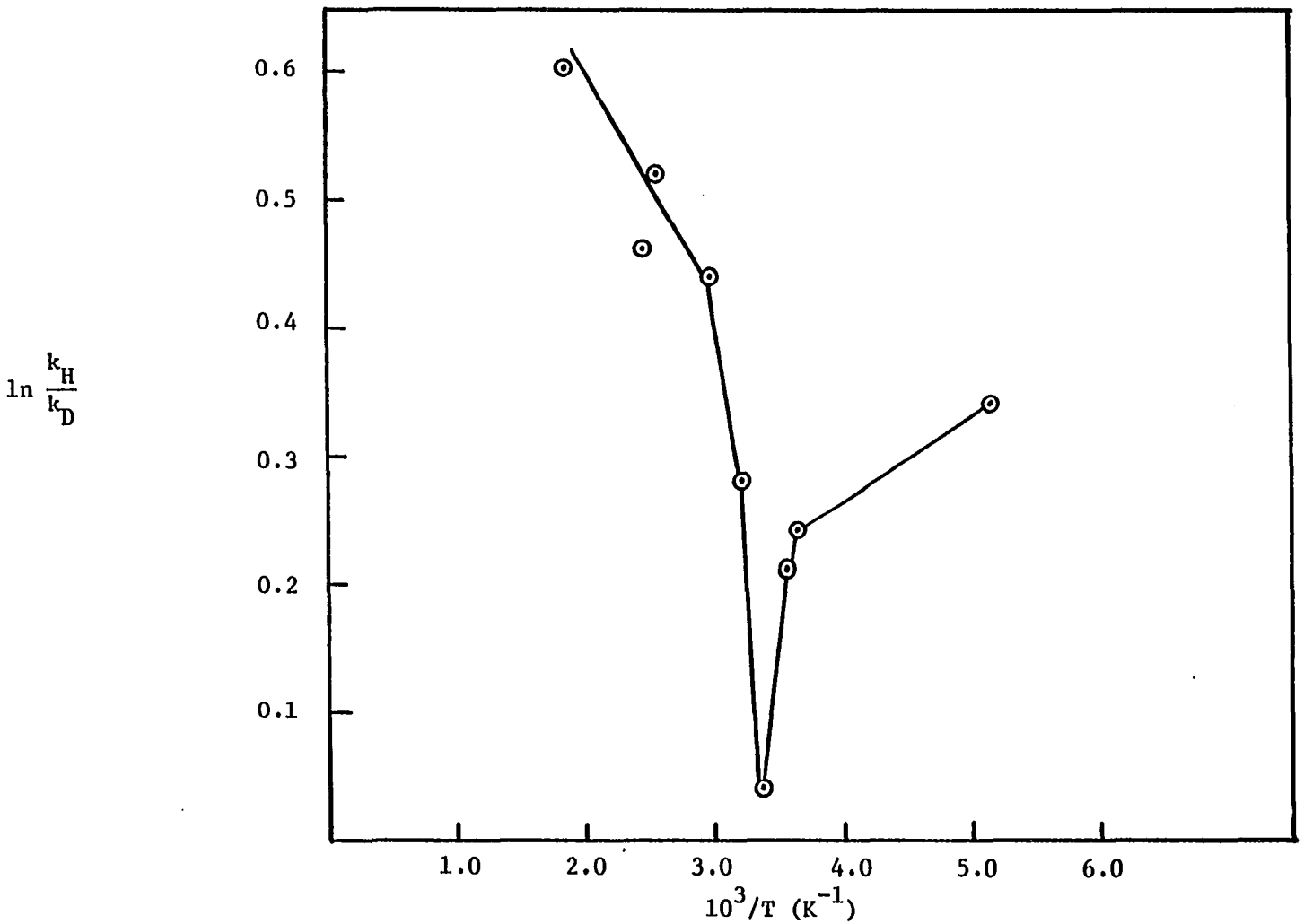

Figure 52. Plot of ln k_H/k_D vs. 1/T for 25

(1) at some temperature, the formation of ylide b from a may be rate-determining (normally at ambient temperature); such a step should have an associated secondary isotope effect (perhaps inverse, since the steric environment around MeOH becomes more congested as b is formed). But since we measure only the product isotope effect, two subsequent situations may be recognized:

(a) proton transfer from the ylide occurs intramolecularly ($k_{intra} > k_{-1}$, e.g., b to c). As the schematic drawing implies, the proton or deuteron to be transferred in this situation is determined in the ylide-forming step. Therefore, only a secondary isotope effect will be observed (ambient temperatures).

(b) proton transfer to the cyclopropyl carbon occurs intermolecularly ($k_{inter} > k_{-1}$, e.g., d to e). In this situation the product-forming step is subject to a primary isotope effect, so the trend would be to higher k_H/k_D as this mechanism becomes operative.

(2) at some temperature, the ylide formation may become reversible (k_{intra} or $k_{inter} < k_{-1}$). When this occurs, one expects a primary isotope effect via either the intra- or intermolecular protonation pathways.

Now, then, does situation (1b) apply at higher temperatures and (2) at low temperatures, or vice-versa?

Let us examine the latter possibility. If we substitute t-BuOH for MeOH, we would expect that ylide reversibility should occur more readily; i.e., b would be relatively less stable if Me were replaced by t-Bu, so it would tend to revert to a faster. Thus a larger k_H/k_D should be seen

upon raising the temperature when utilizing t-BuOH. On the other hand, if (1b) intercedes at higher temperature, t-BuOH should be less effective, as it is less acidic. Such an event would then predict a lower k_H/k_D as the temperature is raised. As will be demonstrated below, the latter is indeed the case.

One other important line of evidence exists. In the case of 11 (21), the ratio of products from 11 and 14 as a function of temperature did not increase linearly as the temperature was lowered. In effect, there were two temperature regimes. At low temperature, more product from 14 was found than expected because the formation of ylide was reversible, thus "giving 14 more of a chance to form" at low temperature than at room temperature. The same result was obtained for the partitioning of 20' into 25 and 26 (cf. Chapter I). Thus situation (2) must hold at low temperature.

Thus we conclude that the isotope effect data is most consistent with two mechanism changes: mechanism (2) above being operative at low temperature, mechanism (1a) operative at ambient temperature, and mechanism (1b) taking over at elevated temperature.

As alluded to above, we next studied the pyrolysis of 87-anti in t-butanol under different conditions. In the presence of 0.47 equivalents of triethylamine, the reaction was conducted in 20% (1:1) t-BuOH/t-BuOD/ 80% benzene at 160°C. No tin-containing product 104 was observed. But the k_H/k_D values of 33 were nevertheless large (primary isotope effect). Table 65 shows the results.

Table 65. Time-resolved product distribution from 87-anti in 80% t-butanolic[a] benzene at 160°C in the presence of 0.47 equivalents of triethylamine

t (h)	87-anti (%)	33 (%)	k_H/k_D (33)
2	42.6	13.9	--
4	27.0	42.7	2.97
18	trace	96.6	3.61

[a]The 20% t-butanol portion of the solvent was a 1:1 (v/v) mixture of t-BuOH/t-BuOD.

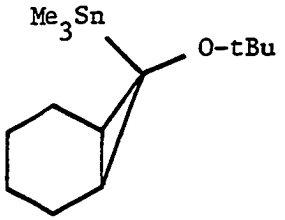

104

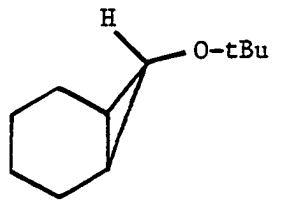

33

When 1.1 equivalents of triethylamine were used, the rate of disappearance of 87-anti was also inhibited (Table 66). Now rather larger primary isotope effects were found. Since no 104 was detected in the presence of triethylamine, the reason for the large k_H/k_D value was unclear. One could argue that 104 was formed, but, being too unstable, immediately reacted with triethylamine to give 33.

As expected, in the absence of triethylamine, the k_H/k_D value for 33 became smaller (1.74 at t = 5 hr, 160°C). However, the crossover path to 26 from ylide 105 (Scheme XXII) makes the analysis of the isotope effect data more complicated. Normally, k_H/k_D is calculated from the

Table 66. Time-resolved product distribution from 87-anti in 80% t-butanolic[a] benzene at 160°C in the presence of 1.1 equivalents of triethylamine

t (h)	87-anti (%)	33 (%)	k_H/k_D (33)
1.5	79.8	4.7	--
2.5	76.8	5.9	--
7.0	70.5	9.2	4.25
16.0	65.2	13.1	5.00

[a]The 20% t-butanol portion of the solvent was an 1:1 (v/v) mixture of t-BuOH/t-BuOD.

Scheme XXII

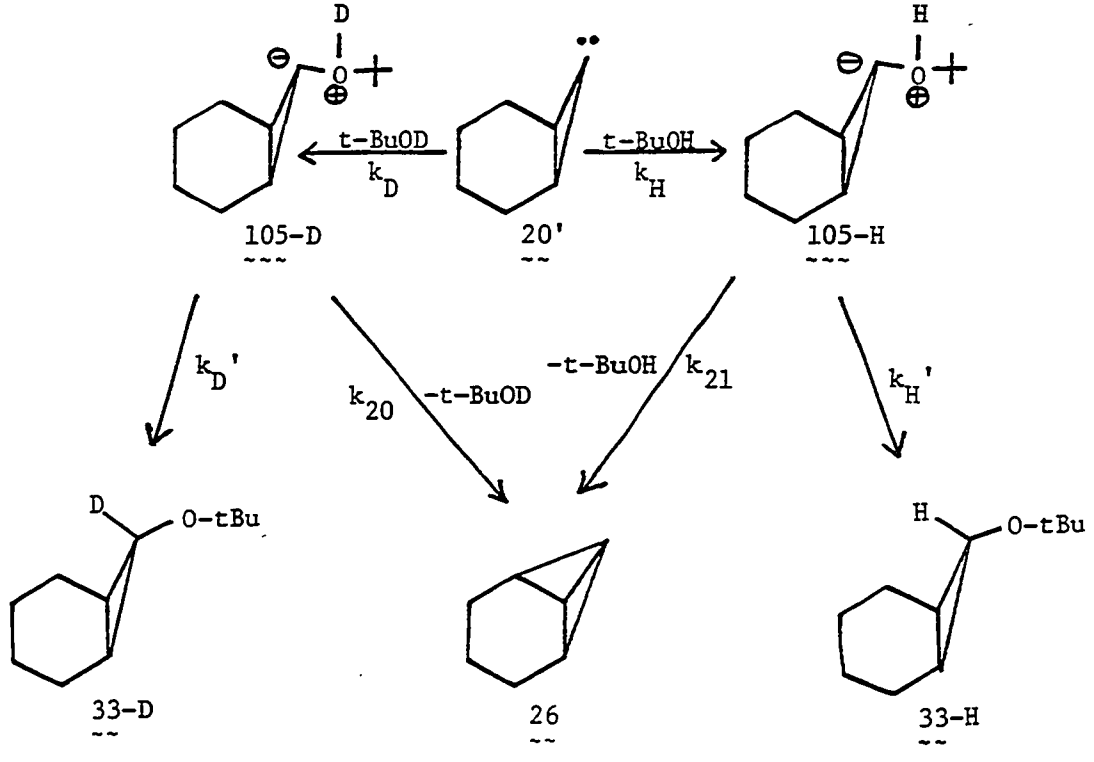

$$\frac{33\text{-H}}{33\text{-D}} = \frac{k_H k_H'}{k_D k_D'} \cdot \frac{k_D' + k_{20}}{k_H' + k_{21}} \cdot \frac{[t\text{-BuOH}]}{[t\text{-BuOD}]}$$

$$= \frac{k_H}{k_D} \cdot \frac{k_H'k_D' + k_H'k_{20}}{k_H'k_D' + k_D'k_{21}} \cdot \frac{[t\text{-BuOH}]}{[t\text{-BuOD}]} \qquad (37)$$

product isotope ratios (e.g. 33-H/33-D). In this case, equation (37) could be derived based on Scheme XXII.

The term $(k_H'k_D' + k_H'k_{20})/(k_H'k_D' + K_D'k_{21})$ could change as a function of temperature, thereby affecting the apparent value of k_H/k_D (Table 67 and Figure 53). A further analysis of equation (37) reveals an approach which would be very valuable:

$$\text{let } \frac{k_{20}}{k_D'} = a \qquad \text{and} \qquad \frac{k_{21}}{k_H'} = b$$

then

$$\frac{33\text{-H}}{33\text{-D}} = \frac{k_H}{k_D} \cdot \frac{k_H'}{k_D'} \cdot \frac{k_D'}{k_H'} \cdot \frac{1 + a}{1 + b} \cdot \frac{[t\text{-BuOH}]}{[t\text{-BuOD}]}$$

$$= \frac{k_H}{k_D} \cdot \frac{1 + a}{1 + b} \cdot \frac{[t\text{-BuOH}]}{[t\text{-BuOD}]} \qquad (38)$$

Values of b are already known (cf., Chapter I), and those for a can be determined via studies in pure t-BuOD (except at high temperatures, where 26 is not formed), admixed with benzene. The results would then give a value for the isotope effects for the carbene collapse itself, which must be secondary.

Table 67. Kinetic deuterium isotope effects for 33 at different temperatures

T (°C)	$10^3/T$ (K^{-1})	$(k_H/k_D)^a_{apparent}$	$\ln(k_H/k_D)^a_{apparent}$
-78	5.13	1.82	0.60
-50	4.48	1.58	0.46
-23	4.00	1.56	0.44
0	3.66	1.28	0.25
10	3.53	1.02	0.02
25	3.36	0.98	-0.02
40	3.19	0.92	-0.08
55	3.05	0.85	-0.16
75	2.87	0.72	-0.33
120	2.54	2.19	0.78
135	2.45	1.78	0.58
160	2.31	1.83[b]	0.60

[a]These are the "complex" k_H/k_D's corresponding to $(k_H/k_D)(1 + a/1 + b)$, equation (38).

[b]This number is the average value of two runs.

To get values of a in equation (38), experiments were then conducted in t-BuOD at different temperatures. Tables 68 and 69 list the results.

In accord with equation (39), the activation parameters were obtained by plotting ln k_H/k_D vs. 1/T. Table 70 and Figure 54 show the results: $\Delta\Delta H^{\neq}$ = 1.48 ± 0.09 Kcal/mol. (or 0.43 ± 0.03 Kcal/mol.), $\Delta\Delta S^{\neq}$ = -5.17 ± 0.29 e.u. (or -1.63 ± 0.11 e.u.), where $\Delta\Delta H^{\neq} = \Delta H_D^{\neq} - \Delta H_H^{\neq}$, $\Delta\Delta S^{\neq} = \Delta S_H^{\neq} - \Delta S_D^{\neq}$. Thus the inverse nature of the ylide-forming step isotope effect is entropic in origin.

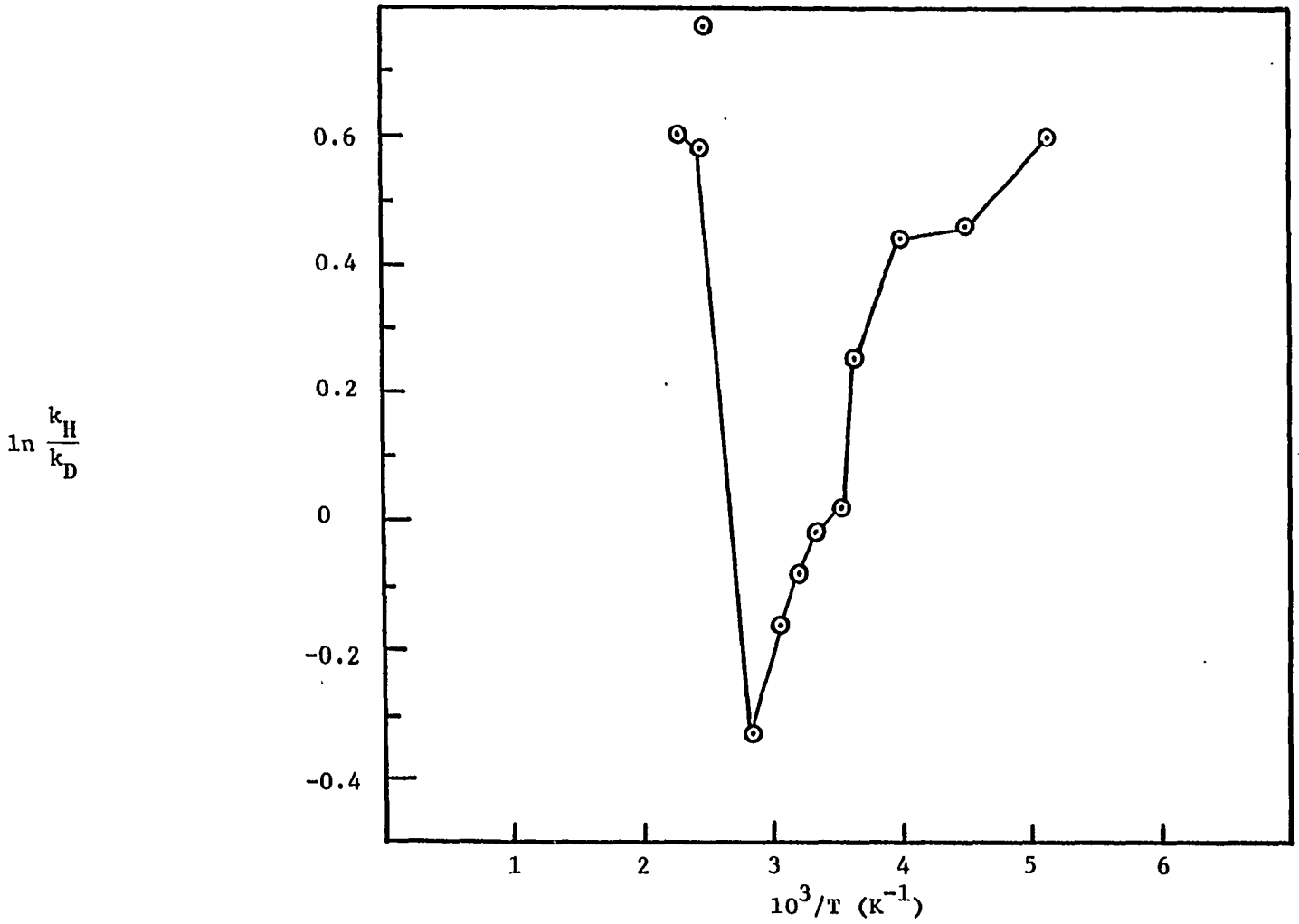

Figure 53. Plot of ln k_H/k_D vs. 1/T for 33

Table 68. Product distribution as a function of t-butanol-D concentration and temperature, S.M. = 0.027 mmole, [t-BuOK]/[S.M.] = 7:1, total solvent volume = 0.4 ml, benzene cosolvent

T (°C)	% t-BuOD	$\frac{1}{[\text{t-BuOD}]}$ (M^{-1})	% 26	% 33-D	$\frac{26}{33\text{-D}}$
25	25	0.38	34.1	17.9	1.91
25	40	0.24	39.1	24.5	1.60
25	50	0.19	39.7	26.5	1.50
32	25	0.38	42.1	20.6	2.04
32	40	0.24	22.6	13.1	1.72
32	50	0.19	36.6	24.9	1.46
42	25	0.38	51.4	18.0	2.85
42	40	0.24	42.1	19.6	2.15
42	50	0.19	25.3	14.4	1.75

Table 69. The data of a,b and k_H/k_D at different temperatures

T (°C)	$\frac{33\text{-H}}{33\text{-D}}$	$a = \frac{k_{20}}{k_D'}$	$b = \frac{k_{21}}{k_H'}$	$\frac{k_H}{k_D}$
25	0.98[a]	1.08 ± 0.01	0.89[b] (0.94 ± 0.04)[c]	0.89 (0.91)
32	0.96[a]	0.93 ± 0.17	0.70[b] (0.80 ± 0.15)[c]	0.84 (0.90)
42	0.89[a]	0.69 ± 0.18	0.50[b] (0.66 ± 0.05)[d]	0.78 (0.87)

[a]Values are interpolated from Table 67.

[b]Values are obtained from Table 27 by NLLSQ analysis.

[c]Values are obtained from Table 19 by linear least-square analyses.

[d]Value is interpolated from the data at 25°, 32°, 37°C on Table 19.

Table 70. Deuterium isotope effects for 33 vs. T (K)

T (°C)	$10^3/T$ (K^{-1})	k_H/k_D	ln k_H/k_D
25	3.35	0.89 (0.91)	-0.12 (-0.09)
32	3.28	0.84 (0.90)	-0.17 (-0.11)
42	3.17	0.78 (0.87)	-0.25 (-0.13)

$$\ln \frac{k_H}{k_D} = \frac{1}{T} \cdot \frac{\Delta\Delta H^{\neq}}{R} + \frac{\Delta\Delta S^{\neq}}{R} \qquad (39)$$

Since norcaranylidene insertion product 26 was formed in both methanol and t-butanol below 75°C (see Chapter I), but was not found in the 135-160°C thermolyses of 87-anti, the question arose as to what could happen to 26 were it formed at 160°C. To this end, 26 was pyrolyzed in 30% methanol/70% benzene at 160°C for four hours. 1,3-Cycloheptadiene, 94, was formed in 41% yield, along with three other unidentified products with p^+ and m/e 126 (but neither 25 nor 99), which were observed in the GC-MS analysis. Scheme XXIII suggests reasonable structures for the compounds with m/e 126.

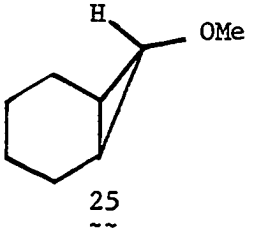

25

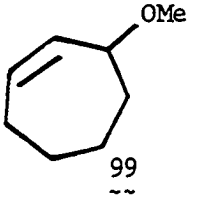

99

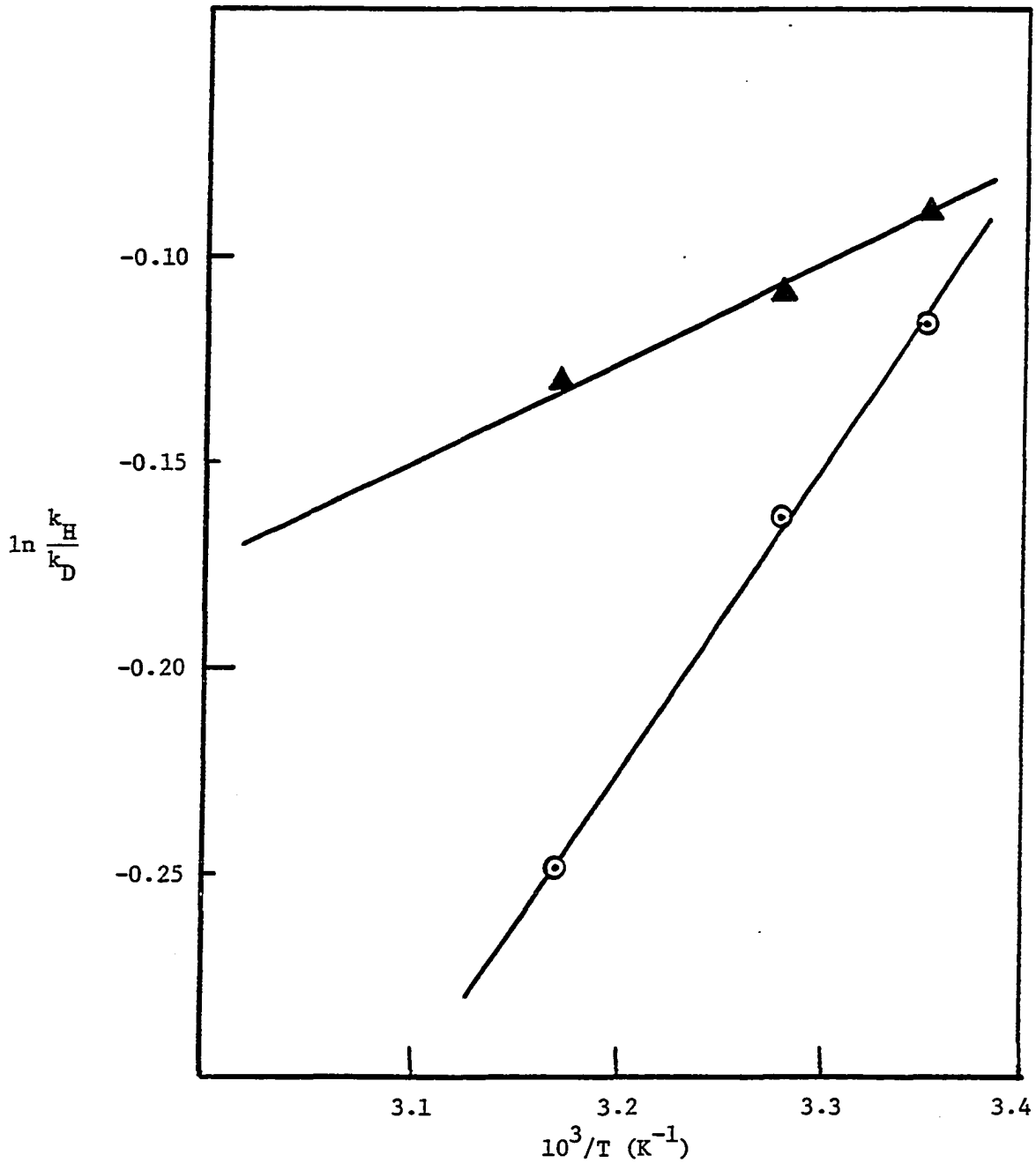

Figure 54. Plot of ln k_H/k_D vs. 1/T for 33.

⊙ r = 0.998, int. = -2.61 ± 0.15, slope = 746.36 ± 46.21

▲ r = 0.992, int. = -0.82 ± 0.05, slope = 217.7 ± 15.1

Scheme XXIII

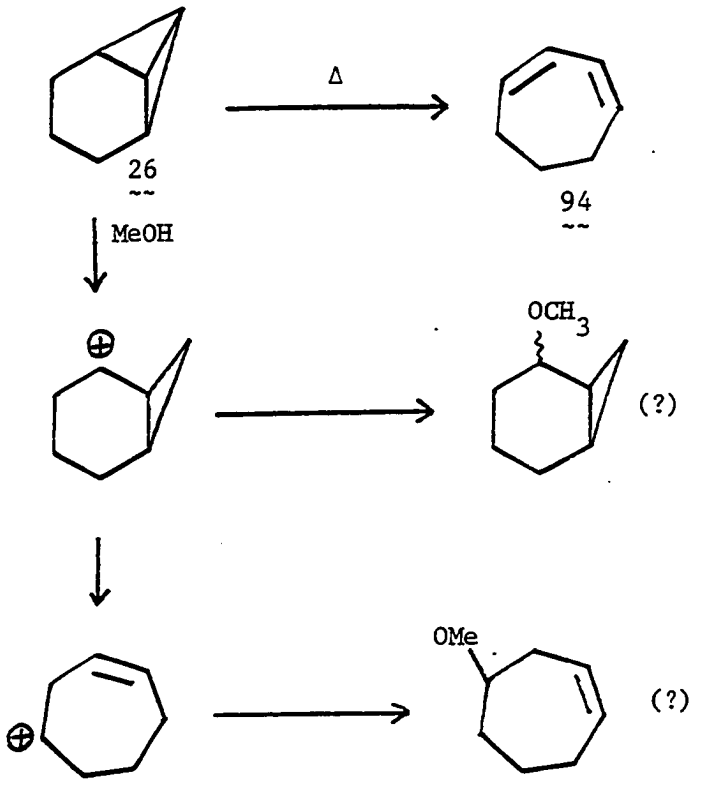

Since 87-anti yielded almost solely carbene 20' in methanolic benzene, there was no reason to think it did otherwise in benzene or cyclohexene (i.e., if methanol didn't intercept 96, cyclohexene and benzene certainly wouldn't). We became interested in the nature of the transition state between carbene 20' and allene 93. No experimental

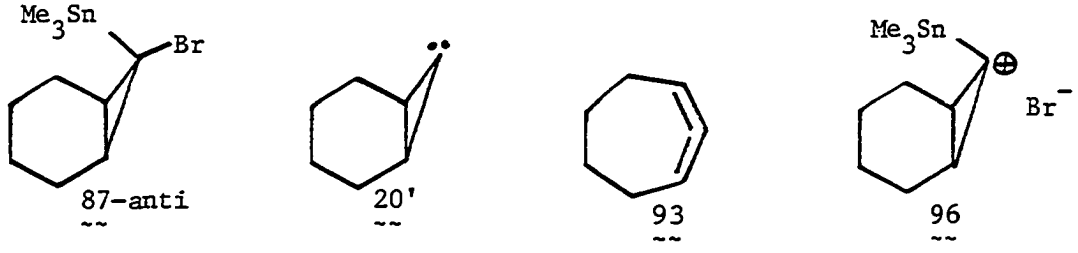

study designed to shed light on the electronic demands exerted by the carbenic carbon in the cyclopropylidene to allene ring-opening has been undertaken.

We intend to probe the effects of substituents on the transition state for ring-opening in the following systems:

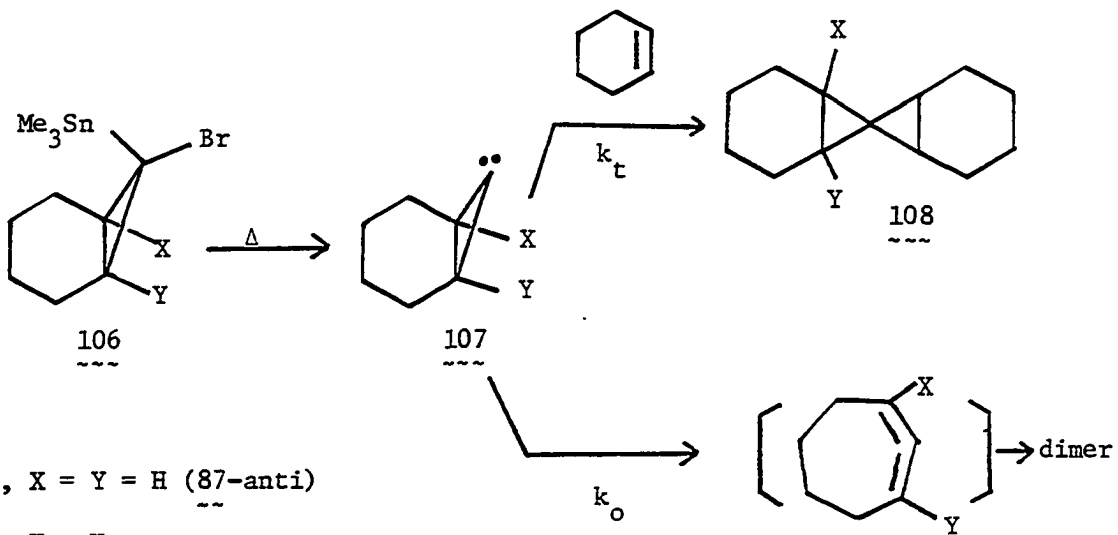

a, X = Y = H (87-anti)

b, X = H

Y = Ar (p-subst. Ph)

The ratio of olefin adduct 108 to allene dimer can be viewed as the partitioning of carbene 107 between cycloaddition and ring-opening. By measuring the product ratios at different [cyclohexene] (79), k_o/k_t would be derived. The preliminary results for 87-anti showed that at 162 ± 2°C, $k_o/k_t \simeq 3$ (where [cyclohexene] = 10 M) (80). Further studies are pending.

Compounds 106b (Y = Ph, p-Cl-Ph, An) were prepared according to equation (40).

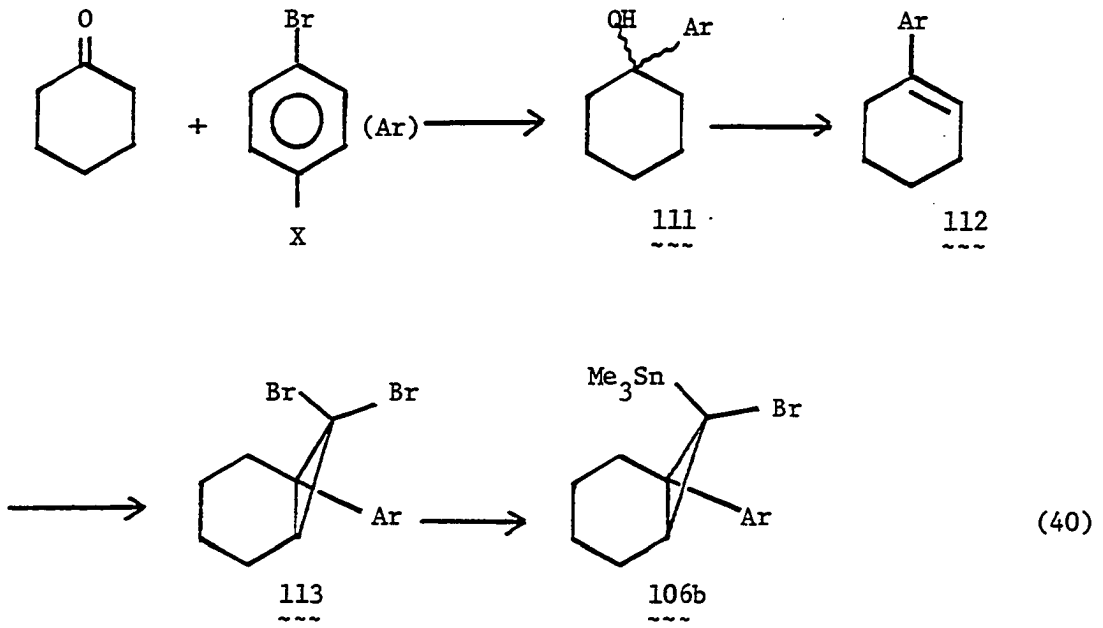

(40)

Compound 111 was made by reaction of cyclohexanone with the p-substituted bromobenzene in the presence of Li in THF at 0°C. Dehydration of 111 was effected by treating 111 with thionyl chloride in pyridine at 0°C. Di-romocarbene addition to 112 was achieved by using bromoform and potassium t-butoxide in hexanes. Stannylation involved treating 113 with n-BuLi, followed by quenching with trimethyltin chloride. Only one isomer (114) was obtained. Its stereochemistry was further confirmed by converting 114 to monobromide 115 with n-BuLi and quenching with MeOH. The coupling between the cyclopropyl hydrogens on 115 was 1.5 Hz, which is consistent with the structure shown for 115.

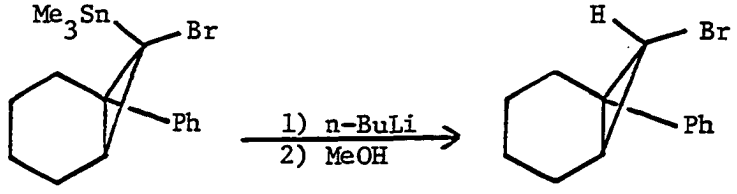

114 115

Experimental

General

For general considerations, see the experimental section of Chapter I.

Reactions and Syntheses

Pyrolysis of 87-anti in methanolic benzene in the presence of triethylamine. Compound 87-anti was prepared according to Seyferth et al. (81) by a slight modification (44), followed by purification via preparative thin layer chromatography on silica gel (hexanes).

A 45 mg sample of 87-anti was dissolved in 0.32 ml of benzene and 0.08 ml of 1:1 methanol/methanol-O-d, along with 18 µl (0.88 eq) of triethylamine and 8 µl of mesitylene (used as an internal standard in GC analysis). Then the solution was evenly distributed among four NMR tubes. After each tube was flushed with nitrogen for one minute, it was sealed and was then fully immersed in a preheated oil bath (160°C), and heated. After a certain period (1, 3, 5½ and 22 hr), the tube was cooled, opened, and the products analyzed on a Varian 3700 gas chromatograph. Compounds 25 and 98 were identified by comparison of their GC retention times

and GC-MS spectra with those of authentic samples. The corrected GC yield was obtained based on the peak areas and the response factors relative to the internal standard.

Pyrolysis of 98 in methanolic benzene in the presence of triethylamine Compound 98 was prepared by carrying out a large scale pyrolysis of 87-anti in 80% methanol/20% benzene, in the presence of 1.1 equivalents of triethylamine at 160°C (44). Then the pyrolysates were subjected to purification via preparative TLC on silica gel to afford 98 as a colorless oil.

A 4 mg sample of 98 was dissolved in 0.08 ml of benzene and 0.02 ml of 1:1 CH_3OH/CH_3OD, along with 4 µl (2.4 eq) of triethylamine. The sample was then pyrolyzed in a sealed NMR tube at 160°C for three hours. GC-MS analysis indicated that no starting material was left and 25 was formed as the sole product.

The kinetic isotope effects were determined via GC-MS analysis and the % D incorporations were calculated from the relative intensities of (P-1), P, (P+1) ... peaks by comparison with the MS results for the fully deuterated 25, according to equation (41).

$$\%\ D_{incor.} = \frac{(P+1)^D + P^D + (P-1)^D + (P-2)^D}{(P+1)^D + P^D + (P-1)^D + (P-2)^D + P^H + (P+1)^H + (P+2)^H + (P-1)^H} \quad (41)$$

Then,

$$\frac{k_H}{k_D} = \frac{\%\ H \text{ in } 25}{\%\ D \text{ in } 25} \times \frac{[MeOD]}{[MeOH]}$$

Table 71. GC-MS data for fully and partially deuterated samples of 25, at 18 eV

Solvent	Int. of m/e 125	Int. of m/e 126	Int. of m/e 127	Int. of m/e 127
	1.62	7.63	100.00	8.90
CH_3OD	$(P-1)^H$	P^H	$(P+1)^H$	$(P+2)^H$
(1:1)	11.70	100.00	25.08	2.05
CH_3OH/CH_3OD	$(P-2)^D$	$(P-1)^D$	P^D	$(P+1)^D$

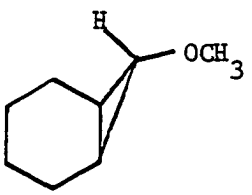

25

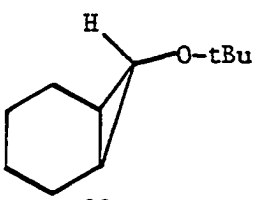

33

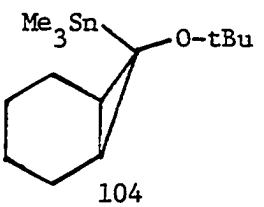

104

Pyrolysis of 87-anti in t-butanolic benzene in the presence of triethylamine A 26 mg sample of 87-anti was dissolved in 0.24 ml of benzene and 0.06 ml of t-BuOH/t-BuOD, along with 7.5 µl (0.47 eq) of triethylamine and 5 µl of 1,4-di-t-butylbenzene solution (100 mg/ml benzene, used as an internal standard in GC analysis). The solution was equally distributed among three NMR tubes. The pyrolysates were analyzed by gas chromatography. Compound 33 was formed as the major product (by comparison of its GC retention time and GC-MS spectra with those of an authentic sample), and no 104 was detected. Table 72 lists the GC-MS data for fully and partially deuterated samples of 33 at 18 eV.

Table 72. GC-MS data for fully and partially deuterated samples (4 hr) of 33, at 18 eV

Solvent	Int. of m/e 152	Int. of m/e 153	Int. of m/e 154	Int. of m/e 155
t-BuOD	0.59	8.54	100.00	10.07
(1:1) t-BuOH/t-BuOD	2.44	100.00	35.88	3.12

Reaction of nitrosourea 19' in CH_3OH/CH_3OD or t-BuOH/t-BuOD; kinetic isotope effects A 5 mg sample of 19' was dissolved in 0.16 ml of benzene and 0.04 ml of 1:1 t-BuOH/t-BuOD (or CH_3OH/CH_3OD) in the presence of 22 mg of potassium t-butoxide (or 11 mg of sodium methoxide) at various reaction temperatures (Table 73). Then the reaction mixture was swirled until the color changed from yellow to colorless. This process took from 3 to 5 minutes. GC-MS analysis provided the data for the calculation of the kinetic isotope effects. Table 73 shows the solvents and baths used for controlling the reaction temperatures.

Preparation of 1-p-subst-phenyl (X = H, Cl, OCH_3) cyclohexanol (111) (82) (Figures 55-57) A mixture of cyclohexanone (9.8 g) and bromobenzene (18.05 g, 1.15 eq) was added dropwise to a suspension of Li metal (1.05 g, 1.5 eq) in 80 ml of dry THF (freshly distilled from LAH). The reaction was highly exothermic and the rate of addition was adjusted to maintain the reaction temperature below 0°C. The reaction was complete in two hours. Water was then added, and the reaction mixture extracted

Table 73. Solvents and baths used for kinetic isotope effects studies in methanol and t-butanol

T (°C)	Conditions	Bath
-78	80% (1:1) CH_3OH/CH_3OD	2-propanol/CO_2
	20% toluene (m.p. -95°C)	
-78	20% (1:1) t-BuOH/t-BuOD	
	80% pentanes (m.p. -130°C)	2-propanol/CO
-50	20% (1:1) t-BuOH/t-BuOD	
	80% pentanes (m.p. -130°C)	acetonitrile /CO_2
-23	20% (1:1) t-BuOH/t-BuOD	
	80% pentanes (m.p.) -130°C)	carbon tetrachloride/CO_2
0-25	20% 1:1) t-BuOH/t-BuOD	oil bath with thermocouple
	80% toluene	
>25	80% (1:1) t-BuOH/t-BuOD	oil bath with thermocouple
	20% benzene	
>10	80% (1:1) CH_3OH/CH_3OD	oil bath with thermocouple
	20% benzene	

with ether. Evaporation of solvents gave the crude products as yellow oils. Vacuum distillation afforded pure 111 in ∿40% yield.

X = H, B.P. 116-118°C/1.7 mmHg

HRMS: calculated for $C_{12}H_{16}O$ - m/e 176.12012

found for $C_{12}H_{16}O$ - m/e 176.12044

^{1}HNMR (CCl_4): δ 7.2 ∿ 7.5 (m), δ 1.5 ∿ 2.2 (m).

IR (neat): 3400, 3100, 3040, 2940, 2875, 1590, 1440, 1350, 1210, 1150 cm^{-1}.

X = OCH_3, B.P. 148 ∿ 150°C/1.7 mmHG

HRMS: Calculated for $C_{13}H_{16}O$ ($M^{+\cdot}$ - H_2O) - m/e 188.12011

found for $CH_{13}H_{16}O$ - m/e 188.12052

^1H NMR (CCl_4): δ 6.8 ∿ 7.6 (AA'XX', two distorted doublets), δ 3.8 (s), δ 1.4 ∿ 2.0 (m).

IR (neat): 3450, 2940, 2870, 1610, 1510, 1490, 1450, 1300, 1250, 1180, 1110, 1040 cm^{-1}.

X = Cl, B.P. 142 ∿ 145°C/1.65 mmHg

HRMS: Calculated for $C_{12}H_{15}OCl$ - m/e 210.08115

found for $C_{12}H_{15}OCl$ - m/e 210.08056

^1H NMR (CCl_4): δ 7.3 ∿ 7.7 (m), δ 1.3 ∿ 2.1 (m).

IR (neat): 3440, 3040, 2940, 2860, 1600, 1490, 1450, 1400, 1250, 1150 cm^{-1}.

Preparation of p-subst-phenyl (X = H, OCH_3) cyclohexene (112) (83) (Figures 58-59) Thionyl chloride (3.25 g, 1.2 eq) was added to a well-stirred, ice-cooled solution of 111 (X = H) in 40 ml of pyridine. The temperature never exceeded 20°C during the addition. The color turned from clear to golden yellow. The stirring was then stopped and the reaction mixture allowed to stand overnight. Next the liquid phase was forced through a filter onto ice, leaving the pyridinium hydrochloride behind. Then the mixture was diluted with ether, washed with 10% HCl (aq), sat. NaCl (aq), and dried over anhydrous Na_2SO_4. Evaporation of

solvent gave the crude products. Vacuum distillation afforded 112 (X = H) as a colorless oil, b.p. 106-108°C/1.65 mmHg.

HRMS: calculated for $C_{12}H_{14}$ - m/e 158.10955

found for $C_{12}H_{14}$ - m/e 158.10924.

^{1}HNMR (CCl_4): δ 7.2 ∿ 7.5 (m), δ 6.1 ∿ 6.2 (m), δ 2.1 ∿ 2.5 (m), δ 1.6 ∿ 1.9 (m), δ 1.2 ∿ 1.4 (m), δ 0.8 ∿ 1.1 (m).

IR (neat): 3100, 3080, 3050, 2955, 2880, 2860, 1600, 1500, 1455, 1350, 1140 cm^{-1}.

Preparation of 1-phenyl-7,7-dibromobicylco[4.1.0]heptane (113)

(Figure 60) A 100 ml 3-necked round bottom flask was equipped with an addition funnel, a magnetic stirring bar, and a nitrogen inlet, and was flushed with nitrogen and dried. Then it was charged with 2.2 g (1.2 eq) of commercial potassium t-butoxide, followed by 25 ml of hexanes. A solution of 2.6 g (17 mmole) of 112 (X = H) and 4.16 g (17 mmole) of bromoform in 20 ml of hexanes was next placed in the addition funnel. The flask and its contents were cooled to -78°C, and the solution was added dropwise over one hour to the stirred potassium t-butoxide suspension. The resulting mixture was allowed to warm to room temperature while being stirred overnight under nitrogen. Water was then added, the reaction mixture extracted with ether, then washed with sat. NaCl (aq), and dried over $MgSO_4$. Vacuum distillation (1.6 mmHg) gave 3.10 g of 113 as a pale-yellow oil (60% yield), b.p. 162 ∿ 164°C.

HRMS: Calculated for $C_{13}H_{14}Br_2$ - m/e 329.94417

found for $C_{13}H_{14}Br_2$ - m/e 329.94496

^{1}H NMR (CCl_4): δ 7.40 (s), δ 2.10 ∿ 2.40 (m), δ 1.30 ∿ 1.70 (m).

IR (neat): 3080, 3040, 1600, 1495, 1450, 1340, 1235, 1130, 1080 cm^{-1}.

Preparation of 1-phenyl-anti-7-bromo-syn-7-trimethylstannyl-bicyclo[4.1.0]heptane (114) (Figure 61) A 100 ml 3-necked round bottom flask, equipped with a magnetic stirring bar, an addition funnel, and a nitrogen inlet, was flushed with nitrogen and dried, and then charged with a solution of 1.0 g (3 mmole) of 113 in 40 ml of dry THF. A solution of 0.65 g (3.3 mmole) of trimethyltin chloride in 20 ml of dry THF was placed in the addition funnel. The flask was next cooled to -95° to -100°C with a "Skelly B" hexane slush bath. Then 1.68 ml (3.6 mmole) of 2M n-butyllithium/hexanes solution was slowly syringed down the inside of the flask. After the resulting solution had been stirred for fifteen minutes, the trimethyltin chloride solution was added dropwise at -95° to -100°C. The resulting reaction mixture was stirred under nitrogen while it was allowed to warm to room temperature over a 3 hour period, after which 15 ml of a saturated ammonium chloride solution was slowly added as a quench. Water was then added, and the mixture extracted with ether. The ether layer was washed with water, saturated NaCl (aq) and dried over anhydrous Na_2SO_4. Evaporation of solvent gave 1.23 g of colorless liquid. Purification via column chromatography on silica gel (pentanes) afforded 114 in pure form.

HRMS: Calculated for $C_{15}H_{20}SnBr$ ($M^{+\cdot}$ - CH_3) - m/e 398.97703

found for $C_{15}H_{20}SnBr$ - m/e 398.97820

^{1}HNMR (CCl_4): δ 7.30 (s), δ 1.7 ∿ 2.2 (m), δ 1.3 ∿ 1.6 (m), δ 0.4 (s).

IR (neat): 3070, 3040, 2940, 2860, 1605, 1495, 1450, 1185, 1070, 1020 cm^{-1}.

Treatment of 114 with n-butyllithium at -100°C A 50 ml 3-necked round bottom flask, equipped with a magnetic stirring bar and a nitrogen inlet, was flushed with nitrogen and dried, and then charged with a solution of 350 mg (0.85 mmole) of 114 in 20 ml of dry THF, and cooled to -95° to -100°C. Next, 1.25 ml (3 eq) of 2 M n-butyllithium/hexanes was slowly syringed down the inside of the flask. After the resulting solution had been stirred for fifteen minutes, 0.3 ml of methanol was added as a quench at -95° to -100°C. The reaction mixture was then slowly warmed up, water added, and extracted with ether. The ether extracts were washed with water, saturated NaCl (aq), and dried over anhydrous $MgSO_4$. Removal of solvent afforded a colorless liquid as the product. ^{1}HNMR showed a doublet (J = 1.5 Hz) at δ 2.96 for the C-7 cyclopropyl hydrogen, which is consistent with structure 115.

Figure 55. Phenylcyclohexanol (111, X = H)

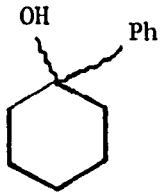

111

page 241: ^{1}H NMR in CCl_4

page 242: IR (neat)

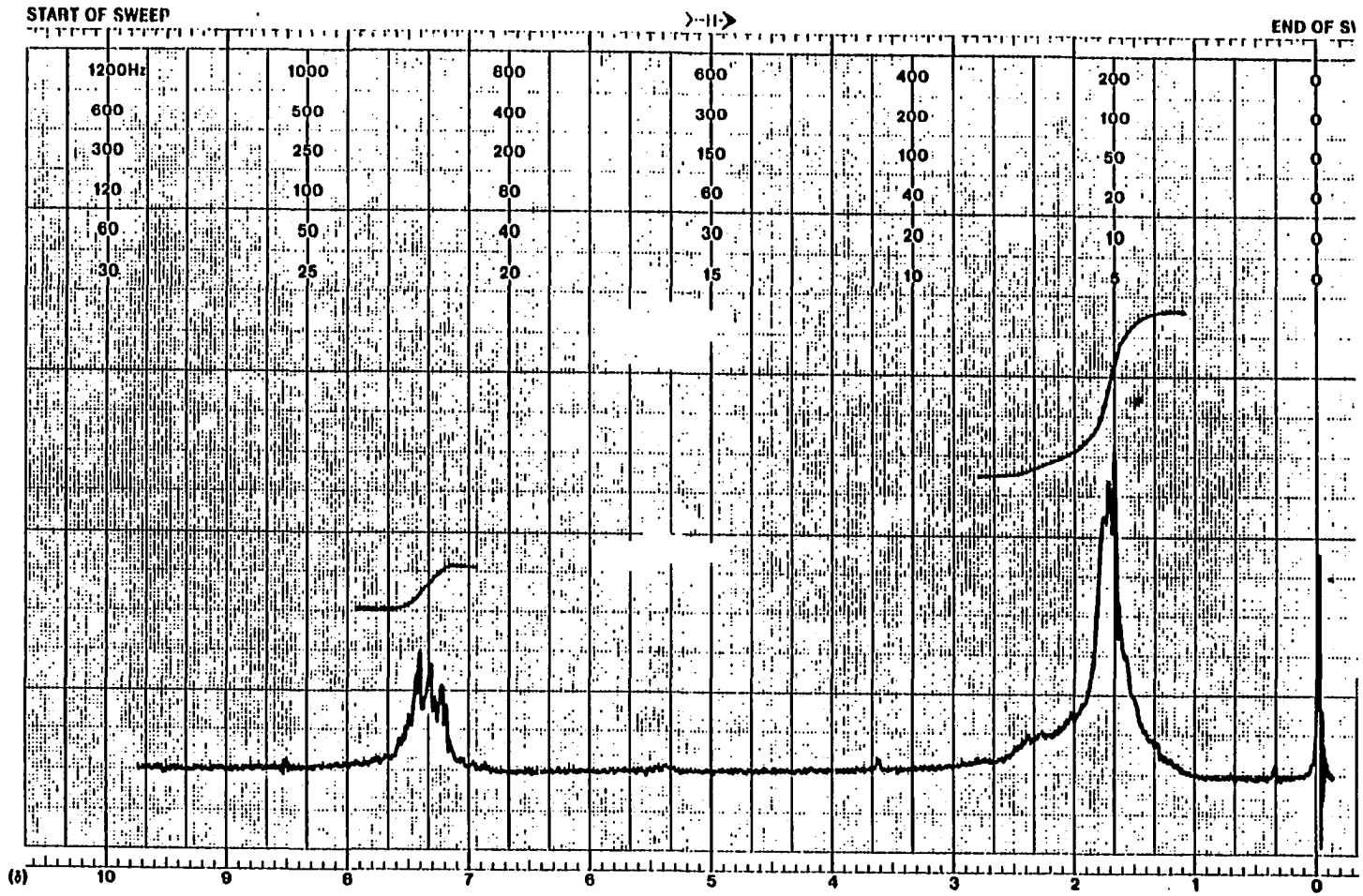
START OF SWEEP
END OF SI
1200Hz
600
300
120
60
30
1000
500
250
100
50
25
800
400
200
80
40
20
600
300
150
60
30
15
400
200
100
40
20
10
200
100
50
20
10
5
0
0
0
0
0
0
(δ)
10
9
8
7
6
5
4
3
2
1
0

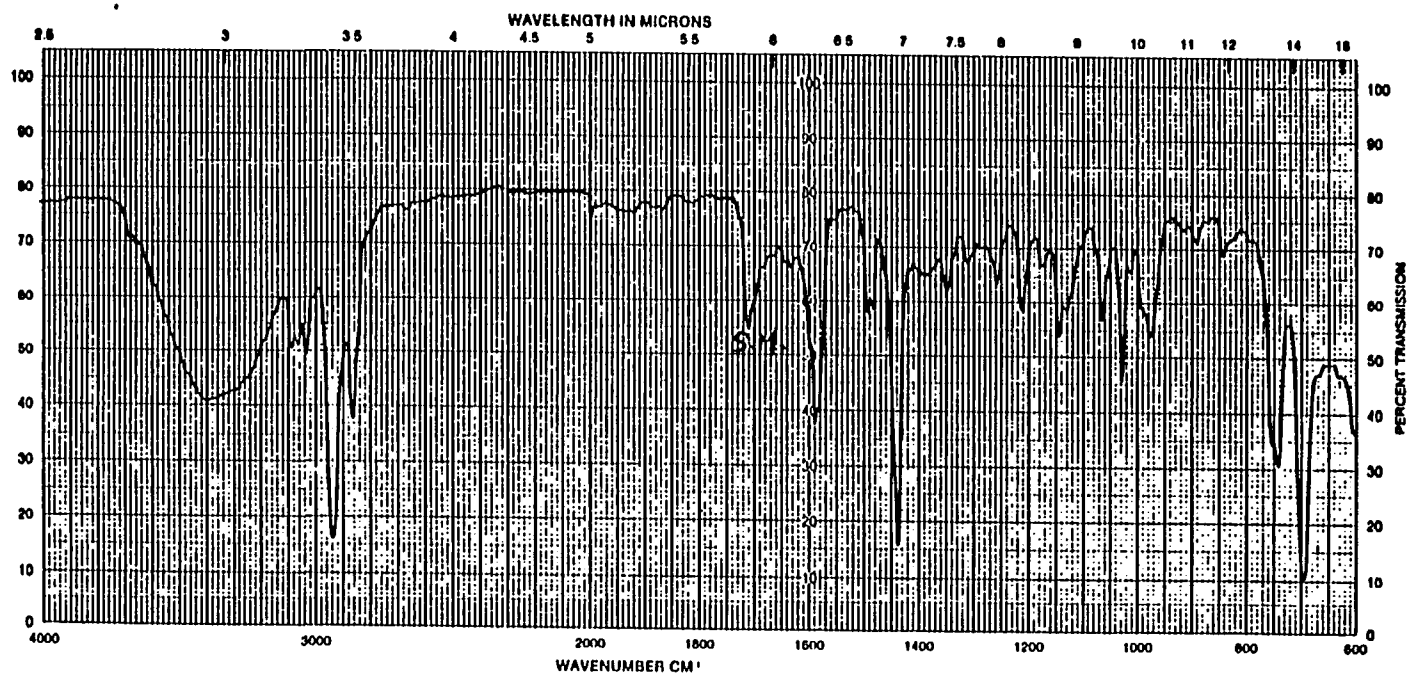

Figure 55. Continued

Figure 56. p-Methoxyphenylcyclohexanol (111, X = OCH_3)

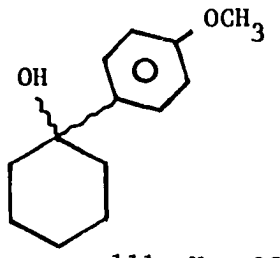

111, X = OCH_3

page 244: ^1H NMR in CCl_4

page 245: IR (neat)

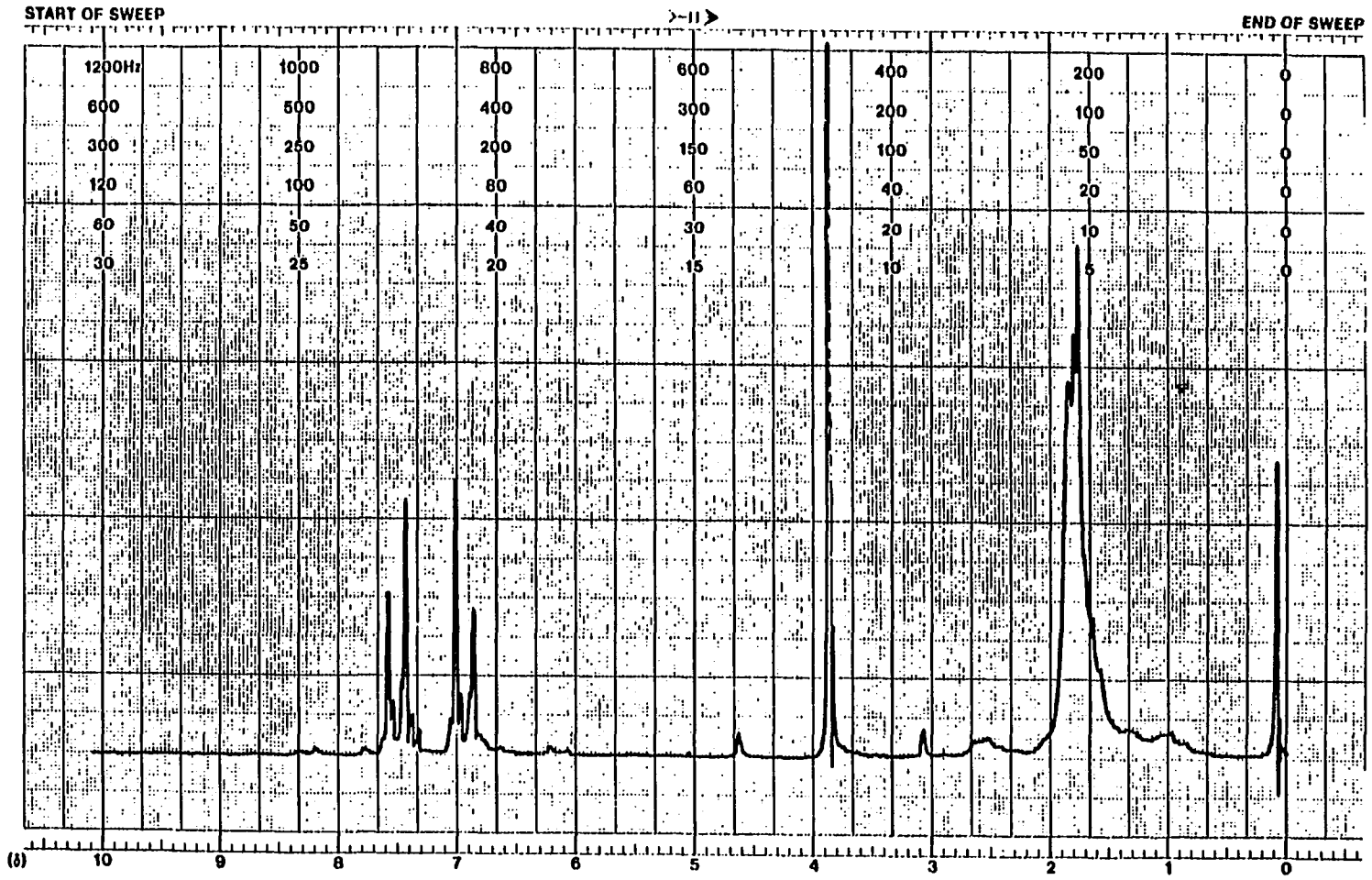
START OF SWEEP
END OF SWEEP
1200Hz
600
300
120
60
30
1000
500
250
100
50
25
800
400
200
80
40
20
600
300
150
60
30
15
400
200
100
40
20
10
200
100
50
20
10
5
0
0
0
0
0
0
(δ)
10
9
8
7
6
5
4
3
2
1
0

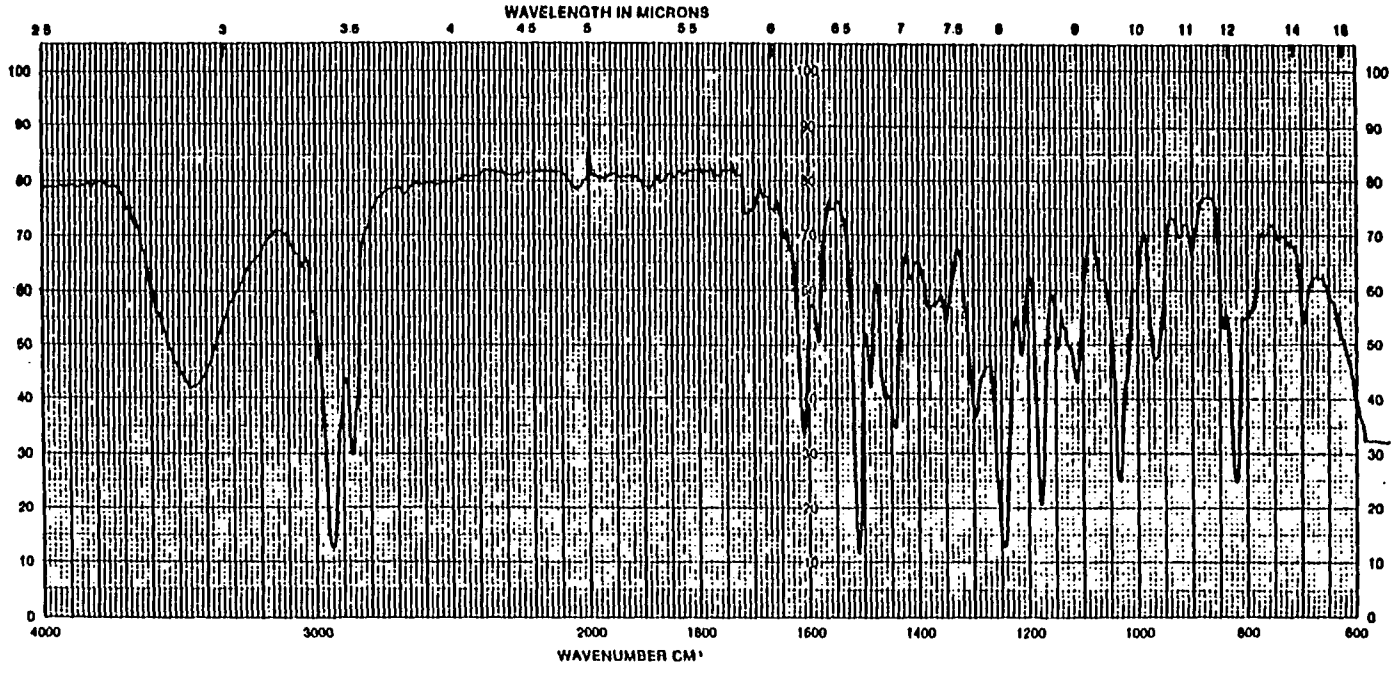

Figure 56. Continued

Figure 57. p-Chlorophenylcyclohexanol (111, X = Cl)

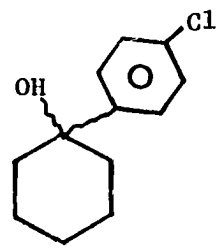

111, X = Cl

page 247: ^{1}H NMR in $CDCl_3$

page 248: IR (neat)

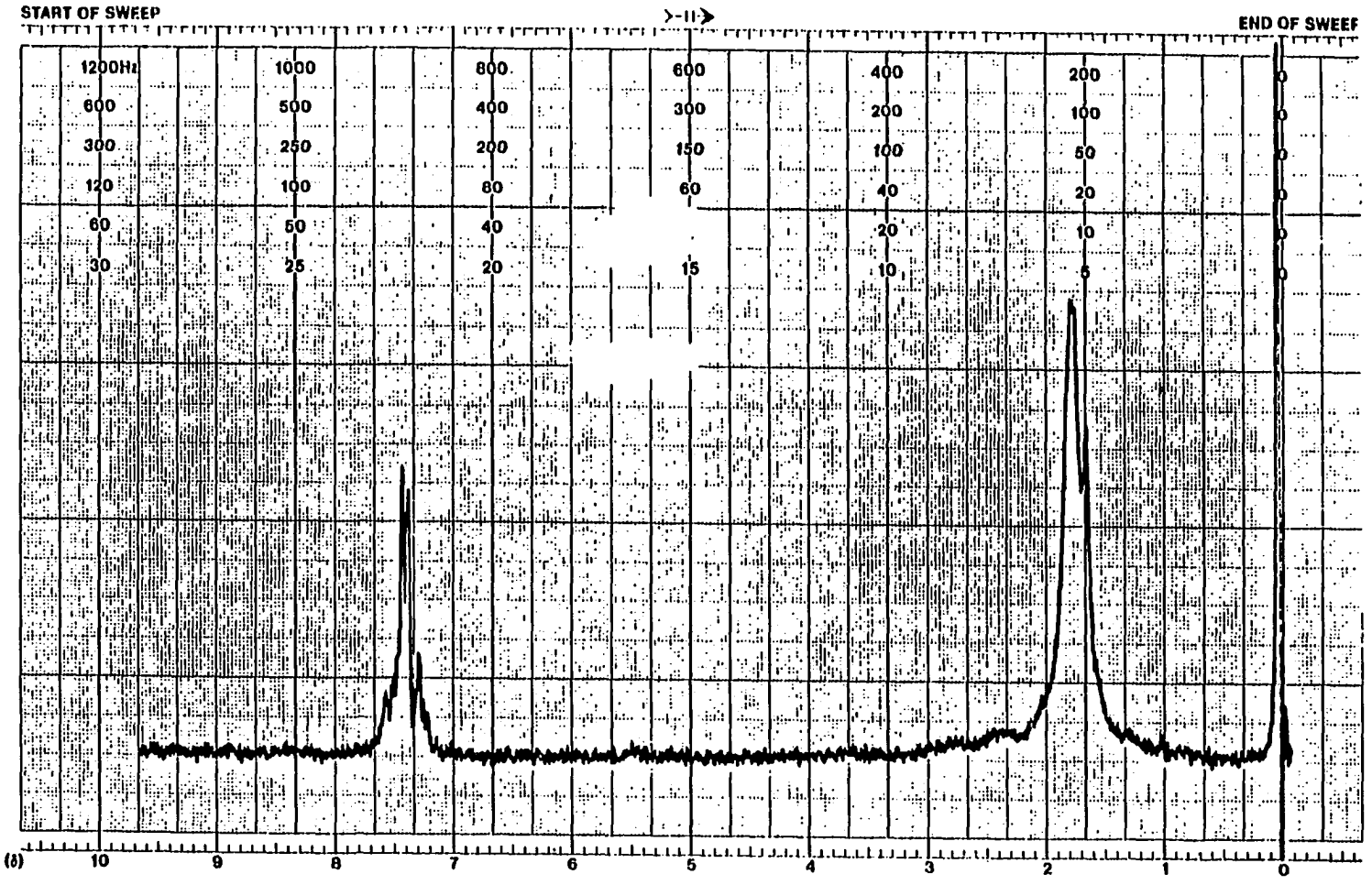
START OF SWEEP
END OF SWEEP
1200Hz
600
300
120
60
30
1000
500
250
100
50
25
800
400
200
80
40
20
600
300
150
60
15
400
200
100
40
20
10
200
100
50
20
10
5
(δ)
10
9
8
7
6
5
4
3
2
1
0

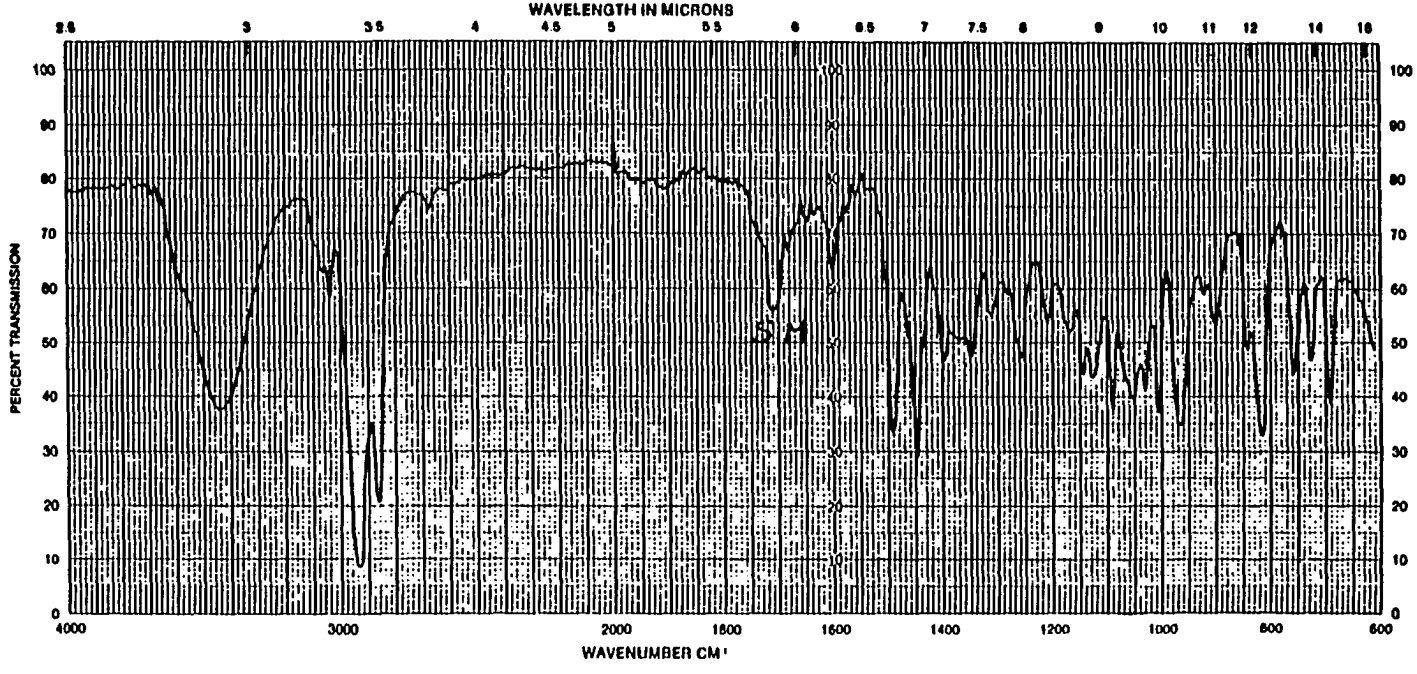

Figure 57. Continued

Figure 58. Phenylcyclohexene (112, X = H)

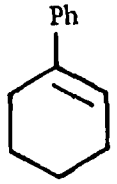

112

page 250: ^{1}H NMR in CCl_4

page 251: IR (neat)

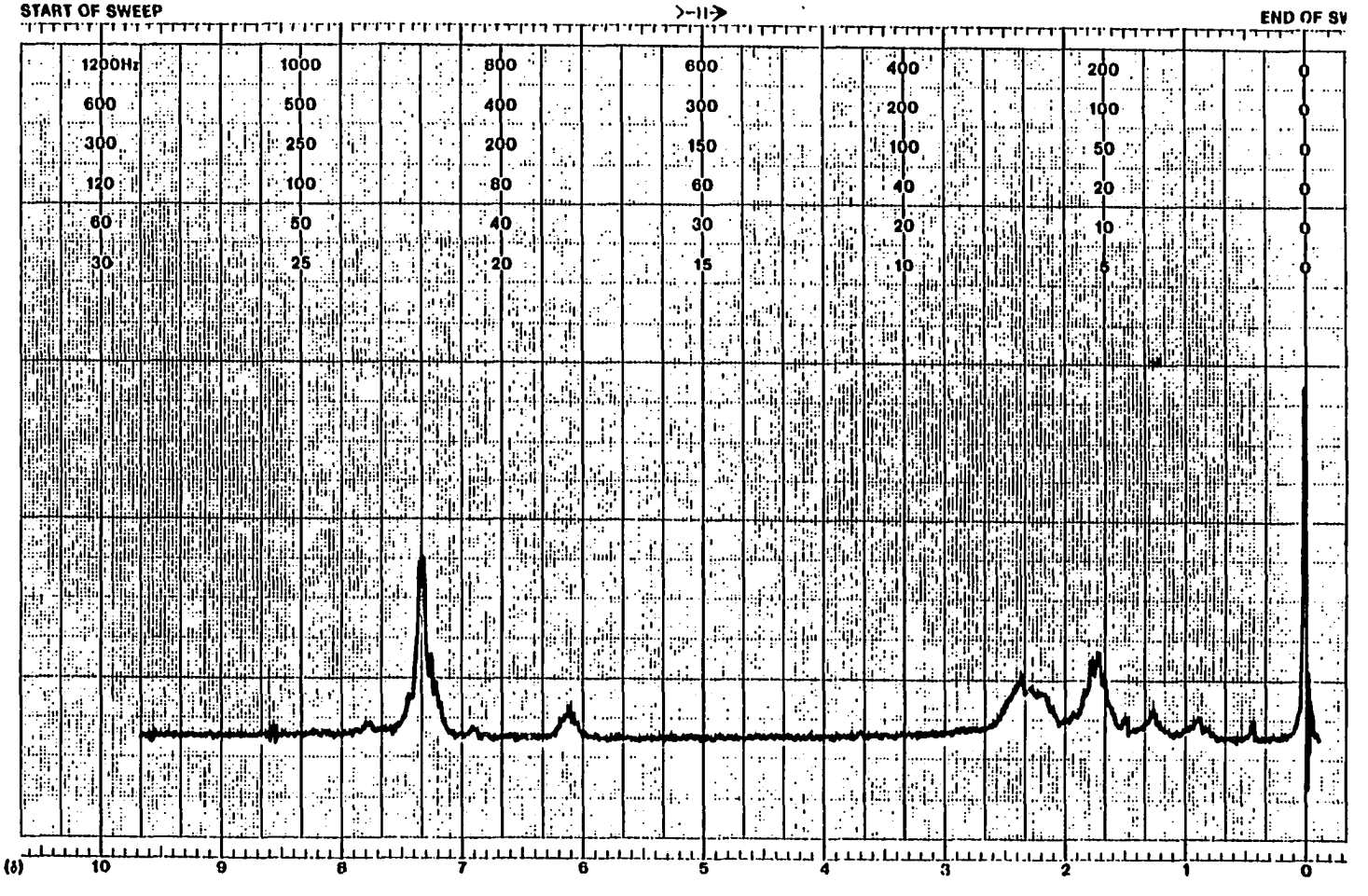
START OF SWEEP
END OF SV
1200Hz
600
300
120
60
30
1000
500
250
100
50
25
800
400
200
80
40
20
600
300
150
60
30
15
400
200
100
40
20
10
200
100
50
20
10
5
0
0
0
0
0
0
(δ)
10
9
8
7
6
5
4
3
2
1
0

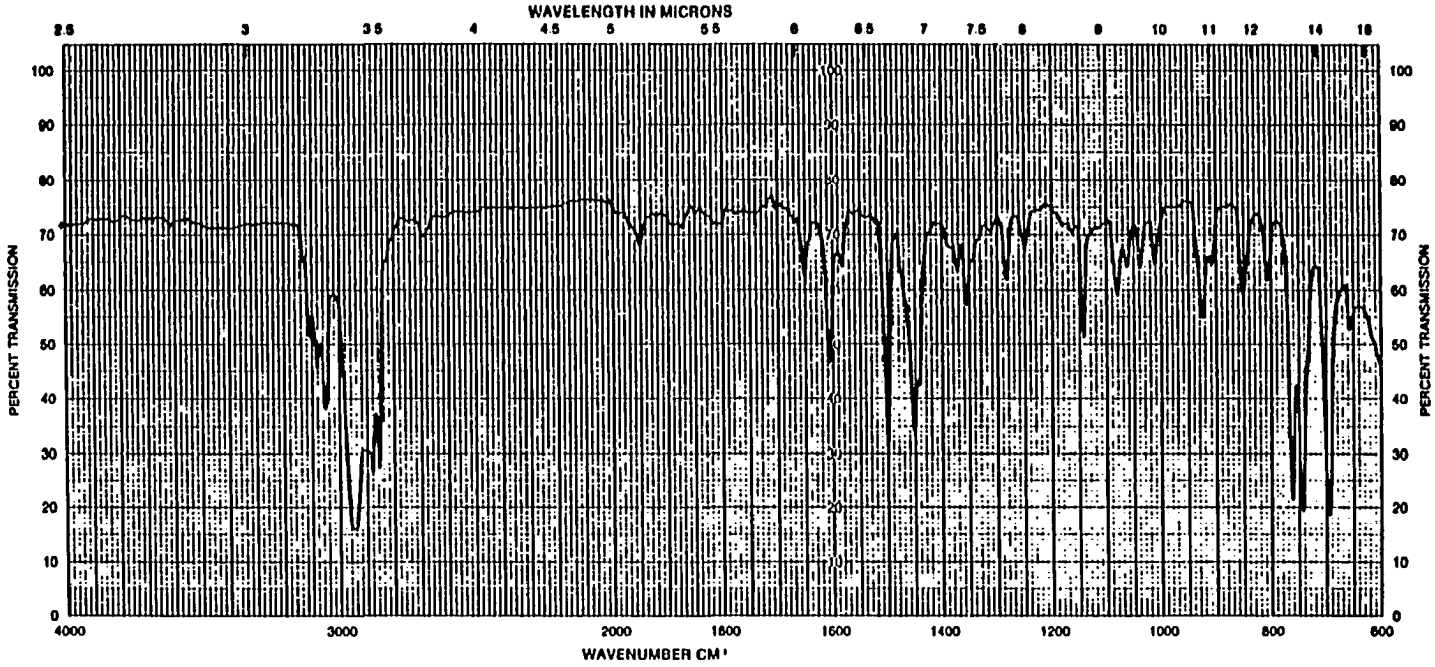

Figure 58. Continued

Figure 59. Anisylcyclohexene (112, X = OCH_3)

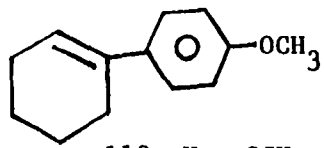

112, X = OCH_3

page 253: ^1H NMR in CCl_4

page 254: IR (neat)

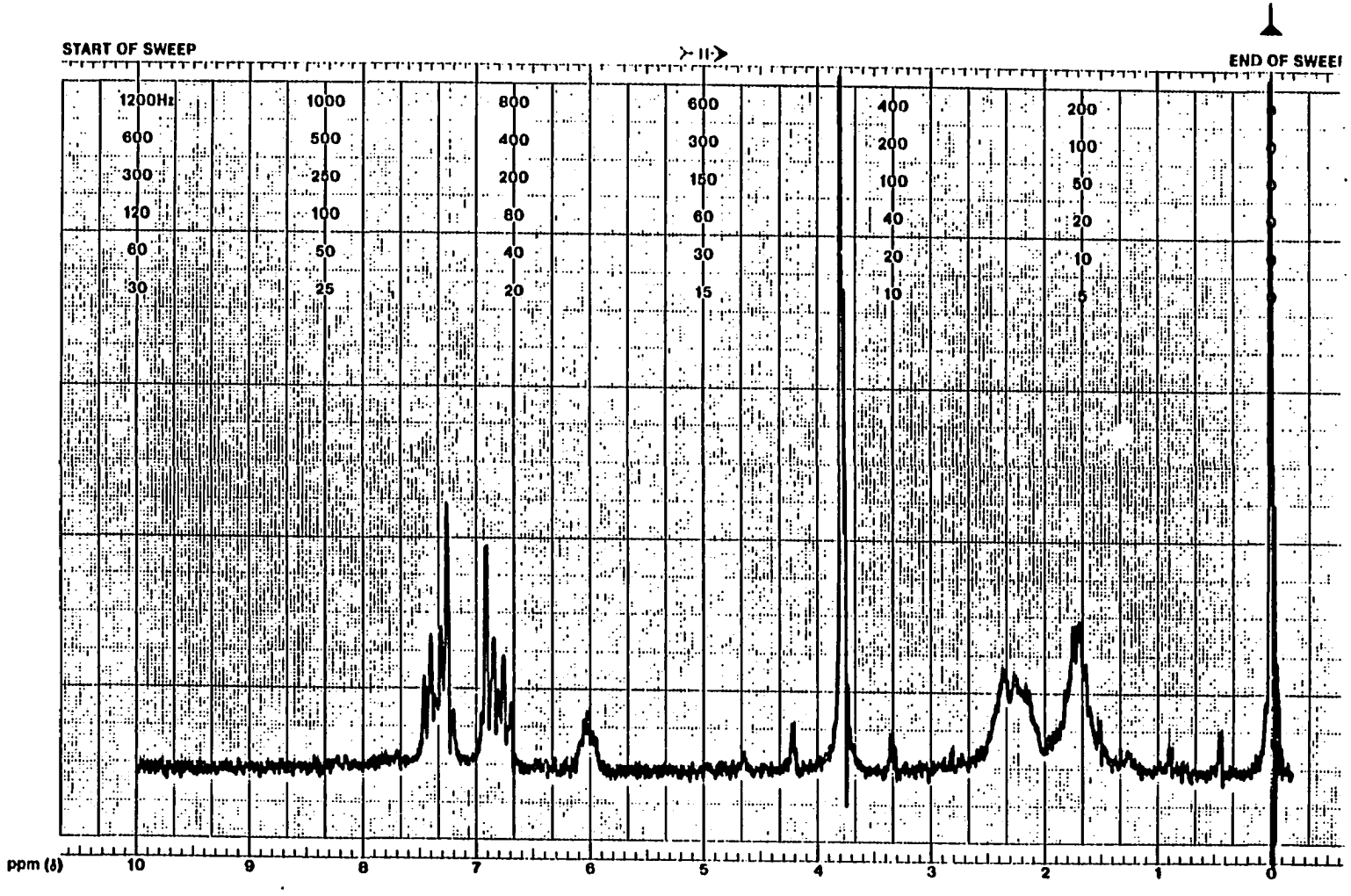
START OF SWEEP
END OF SWEEI
1200Hz
600
300
120
60
30
1000
500
250
100
50
25
800
400
200
80
40
20
600
300
150
60
30
15
400
200
100
40
20
10
200
100
50
20
10
5
ppm (δ)
10
9
8
7
6
5
4
3
2
1
0

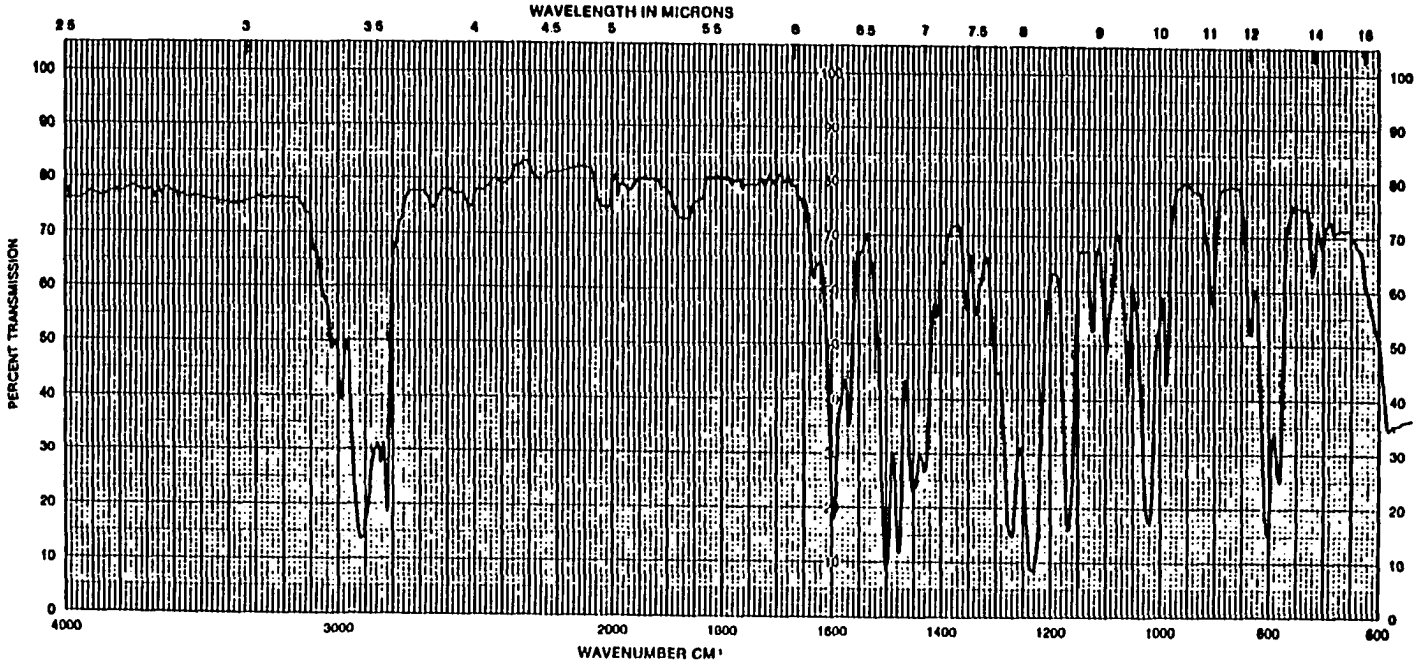

Figure 59. Continued

Figure 60. 1-Phenyl-7,7-dibromobicyclo[4.1.0]heptane (113, X = H)

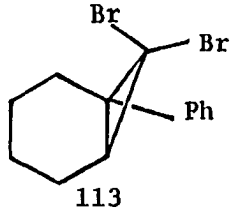

113

page 256: ^{1}H NMR in CCl_4

page 257: IR (neat)

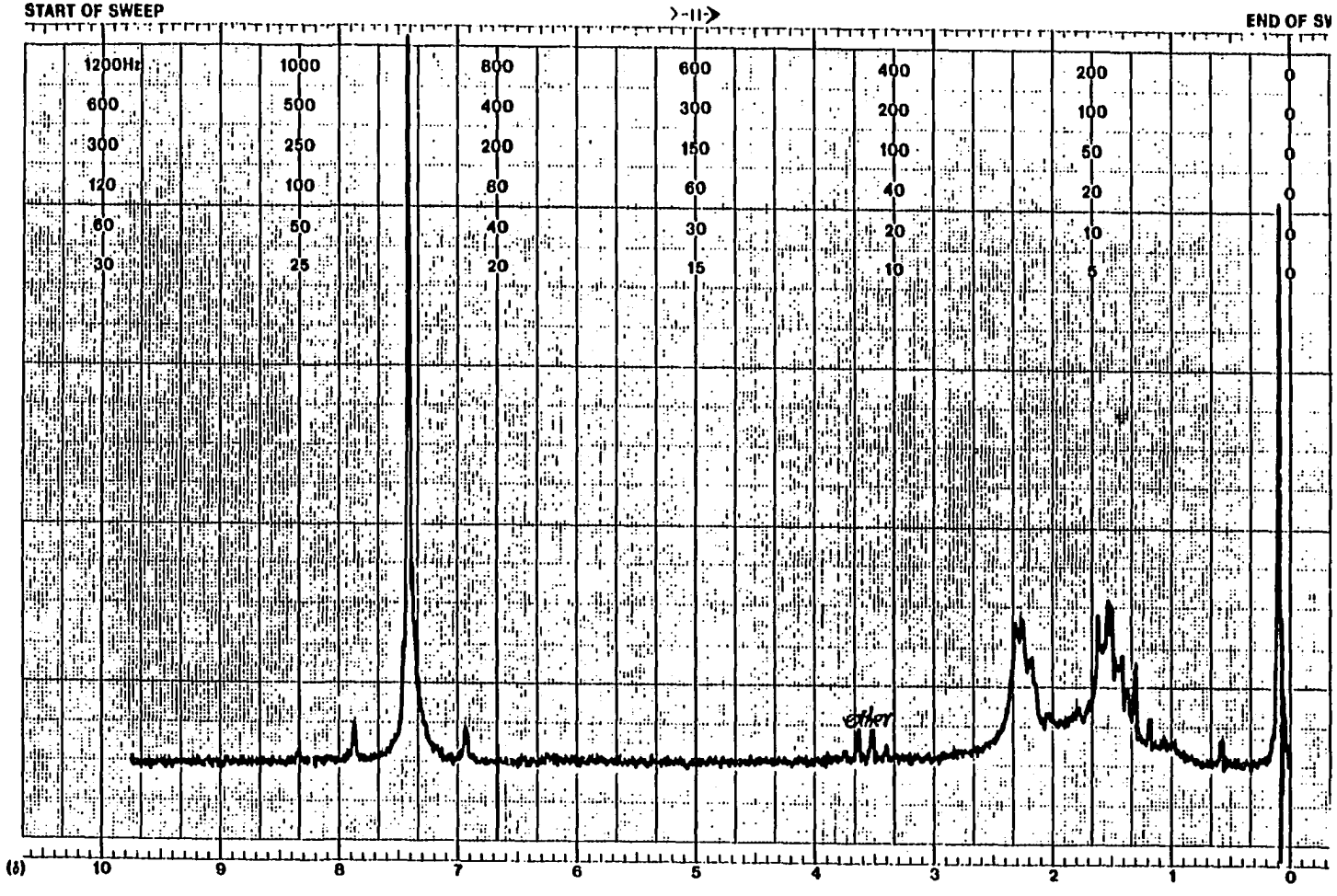
START OF SWEEP
END OF SW
1200Hz
600
300
120
60
30
1000
500
250
100
50
25
800
400
200
80
40
20
600
300
150
60
30
15
400
200
100
40
20
10
200
100
50
20
10
5
0
0
0
0
0
0
Ether
(δ)
10
9
8
7
6
5
4
3
2
1
0

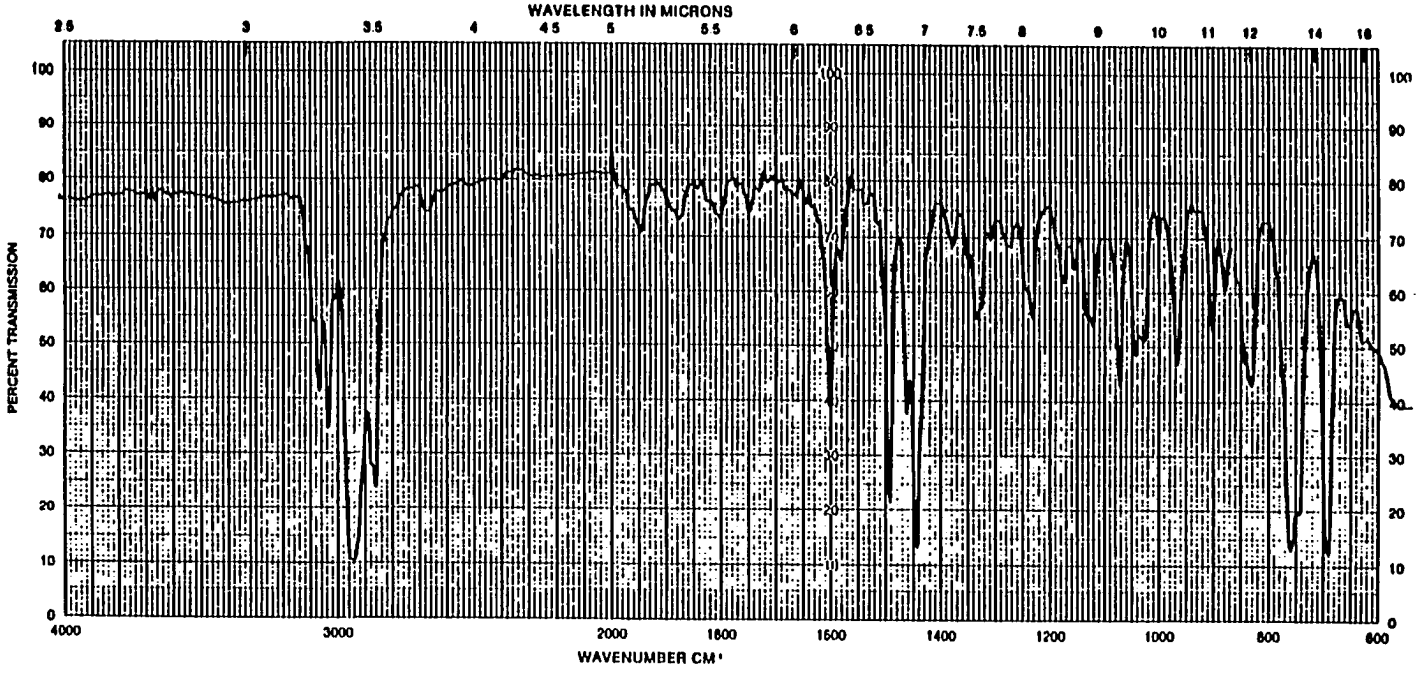

Figure 60. Continued

Figure 61. 1-Phenyl-anti-7-bromo-syn-7-trimethylstannyl-bicyclo[4.1.0]heptane (114)

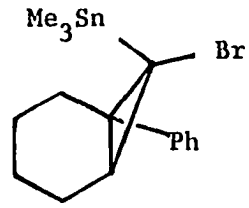

114

page 259: ^{1}H NMR in $CDCl_4$ (60 MHz)

page 260: ^{1}H NMR in $CDCl_3$ (300 MHz)

page 261: IR (neat)

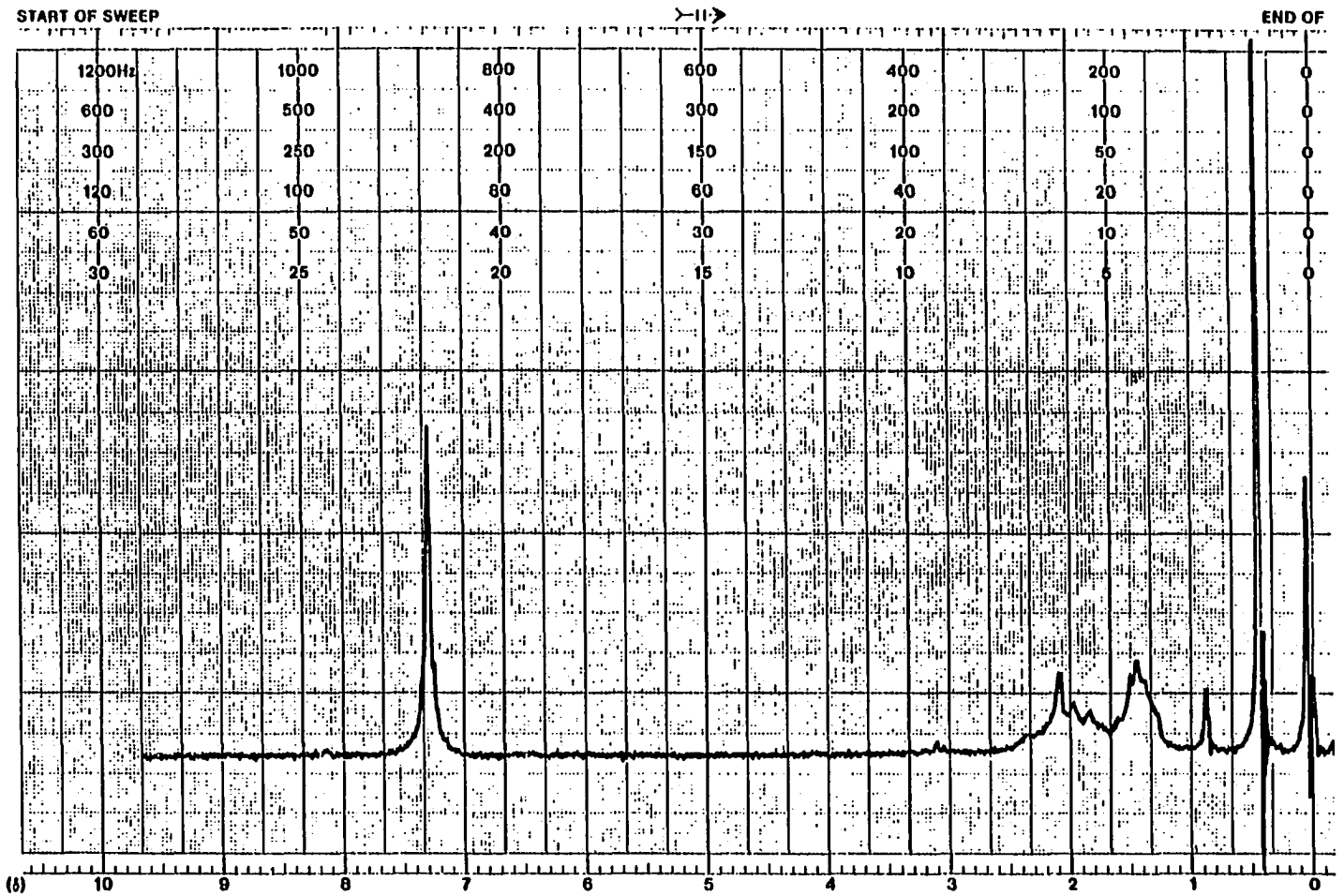
START OF SWEEP
END OF
1200Hz
600
300
120
60
30
1000
500
250
100
50
25
800
400
200
80
40
20
600
300
150
60
30
15
400
200
100
40
20
10
200
100
50
20
10
5
0
0
0
0
0
0
(δ)
10
9
8
7
6
5
4
3
2
1
0

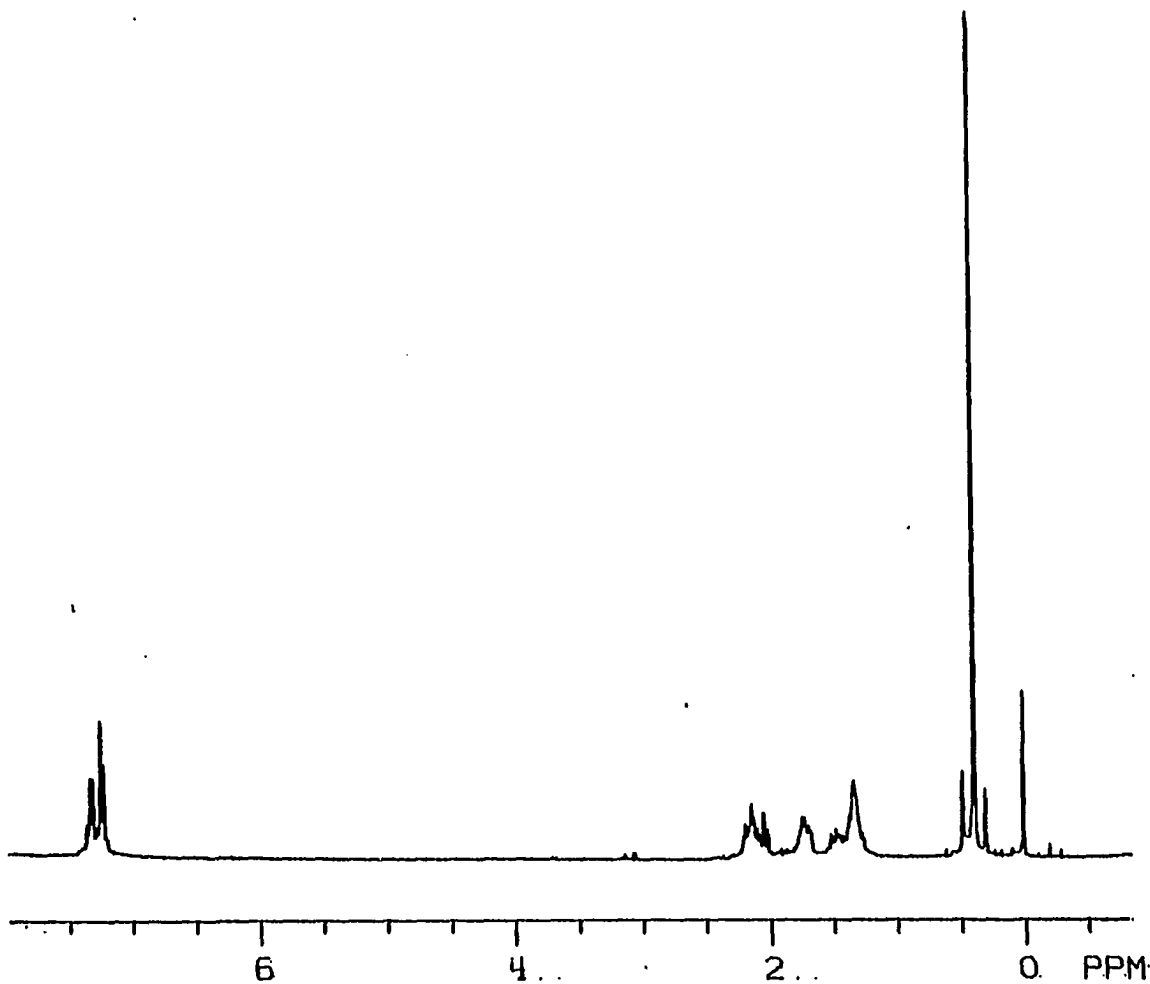

Figure 61. Continued

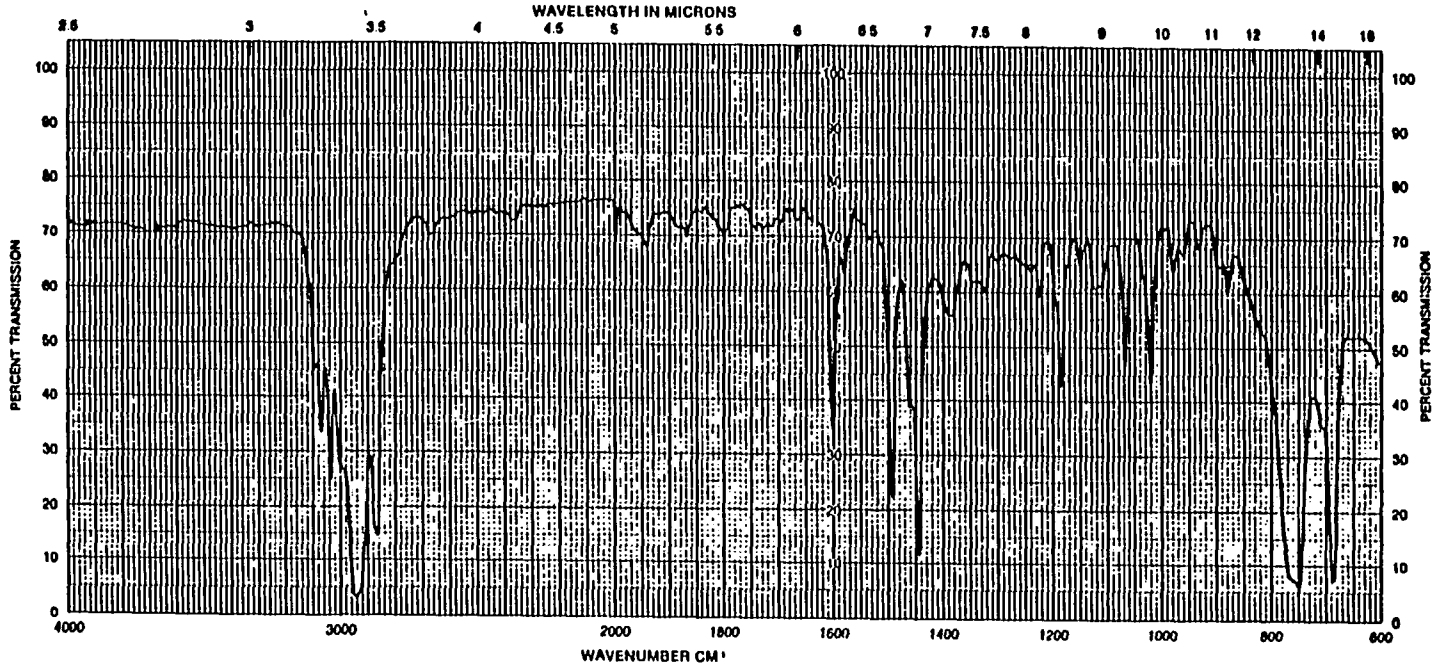

Figure 61. Continued

REFERENCES

1. Kirmse, W. "Carbene Chemistry", 2nd ed.; Academic Press: New York, 1971.

2. a) Jones, M., Jr. "Carbenes", Wiley: New York, 1973.
b) Bethell, D. Adv. Phys. Org. Chem., 1969, 7, 153.

3. a) Bethell, D.; Howard, R. D. J. Chem. Soc. (B), 1969, 745.
b) Bethell, D.; Whittaker, D.; Callister, J. D. J. Chem. Soc., 1965 2466.

4. Bethell, D.; Newall, A. R.; Whittaker, D. J. Chem. Soc. (B), 1971, 23.

5. Kirmse, W. Annalen, 1963, 9, 666.

6. Bethell, D.; Newall, A. R.; Stevens, G.; Whittaker, D. J. Chem. Soc. (B), 1969, 749.

7. Griller, D.; Liu, M. T. H.; Scaiano, J. C. J. Am. Chem. Soc., 1982, 104, 5549.

8. Tomioka, H.; Izawa, Y. J. Am. Chem. Soc., 1977, 99, 6128.

9. Tomioka, H.; Miwa, T.; Sazuki, S.; Izawa, Y. Bull. Chem. Soc. Jpn., 1980, 53, 753.

10. Griller, D.; Nazran, A. S.; Scaiano, J. C. J. Am. Chem. Soc., 1984, 106, 198.

11. Zupancic, J. J.; Garsse, P. B.; Lapin, S. C.; Schuster, G. B. Tetrahedron, 1985, 41, 1471.

12. Liu, M. T. H.; Subramanian, R. J. Chem. Soc., Chem. Commun., 1984, 1062.

13. For a review of diazirine thermolysis and photolysis. See: Liu, M. T. H. Chem. Soc. Rev., 1982, 11, 127.

14. Tomioka, H.; Hayashi, N.; Izawa, Y.; Liu, M. T. H. Tetrahedron Lett., 1984, 4413.

15. Tomioka, H. J. Am. Chem. Soc., 1979, 101, 256.

16. Tomioka, H.; Griffin, G. W.; Nishiyama, K. J. Am. Chem. Soc., 1979, 101, 6009.

17. Tomioka, H.; Suzuiki, S.; Izawa, Y. J. Am. Chem. Soc., 1982, 104, 3156.

18. Eisenthal, K. B.; Turro, N. J.; Sitzmann, E. V.; Gould, I. R.; Hefferon, G.; Langan, J.; Cha, Y. Tetrahedron, 1985, 41, 1543.

19. Turro, N. J.; Cha, Y.; Gould, I. R. Tetrahedron Lett., 1985, 5951.

20. Landeck, H.; Wolff, H.; Gotz, R. J. J. Phys. Chem., 1977, 81, 718.

21. Chu, I.-S. M.S. Thesis, Iowa State University, Ames, Iowa. 1983.

22. Warner, P. M.; Chu, I.-S. J. Am. Chem. Soc., 1984, 106, 5366.

23. Gilbert, B. C.; Griller, D.; Nazran, A. S. J. Org. Chem., 1985, 50 4738.

24. Nazran, A. S.; Griller, D. J. Chem. Soc., Chem. Commun., 1983, 850.

25. Nazran, A. S.; Griller, D. J. Am. Chem. Soc., 1984, 106, 543.

26. Nazran, A. S.; Gabe, E. J.; Lepage, Y.; Northcott, D. J.; Park, J. M.; Griller, D. J. Am. Chem. Soc., 1983, 105, 2912.

27. Nazran, A. S.; Gabe, E. J.; Lepage, Y.; Northcott, D. J.; Park, J. M.; Griller, D. J. Phys. Chem., 1984, 88, 5251.

28. Metcalfe, J.; Halevi, E. A. J. Chem. Soc., Perkin Trans. 2, 1977, 364.

29. Hoffman, R.; Zeiss, G. D.; Van Dine, G. W. J. Am. Chem. Soc., 1968, 90, 1485.

30. Bethell, D.; Stevens, G.; Tickle, P. J. Chem. Soc., Chem. Commun., 1970, 792.

31. For a review, see: Griller, D.; Nazran, A. S.; Scaiano, J. C. Acc. Chem. Res., 1984, 17, 283.

32. Kirmse, W.; Jendralla, H. Chem. Ber., 1978, 1857.

33. Zayas, J.; Plantz, M. S. Tetrahedron Lett., 1985, 26, 2853.

34. Moore, W. R.; Ward, H. R., Merritt, R. F. J. Am. Chem. Soc., 1961, 83, 2019.

35. Reinarz, R. B.; Fonken, F. J. Tetrahedron Lett., 1973, 4013.

36. Paquette, L. A.; Taylor, R. T. J. Am. Chem. Soc., 1977, 99, 5708.

37. Paquette, L. A.; Zon, G.; Taylor, R. T. J. Org. Chem., 1974, 39 2677.

38. Moore, W. R.; Ward, H. R. J. Org. Chem., 1962, 27, 4179.

39. Marquis, E. T.; Gardner, P. D. J. Chem. Soc., Chem. Commun., 1966 726.

40. Inoue, Y.; Hagiwara, S.; Daino, Y., Hakushi, T. J. Chem. Soc., Chem. Commun., 1985, 1307.

41. Wiberg, K. B.; Szeimies, G. Tetrahedron Lett., 1968, 1235.

42. Greenberg, A.; Liebman, J. F. "Strained Organic Molecules", Academic Press: New York, 1978, p 70.

43. Schöllkopf, U.; Paust, J. Chem. Ber., 1965, 2221.

44. Herold, R. D. Ph.D. Dissertation, Iowa State University, Ames, Iowa, 1984.

45. Coggeshall, N. D.; Saier, E. L. J. Am. Chem. Soc., 1951, 73, 5414.

46. Wilson, G. M. J. Am. Chem. Soc., 1964, 86, 127.

47. Berson, J. A.; Hand, E. S. J. Am. Chem. Soc., 1964, 86, 1978.

48. Schaeffer, J. P.; Endres, L. "Organic Syntheses", Wiley-Interscience: New York, 1973; Collect. Vol. 5, p 285.

49. Hine, J.; Brown, J. A.; Zalkow, L. H.; Gardner, W. E.; Hine, M. J. Am. Chem. Soc., 1955, 77, 594.

50. Weisz, A.; Mandelbaum, A. J. Org. Chem., 1984, 49, 2649.

51. Chow, Y. L.; Lee, A. C. H. Canadian J. Chem., 1967, 45, 311.

52. Huisgen, R. Angew. Chem. Int. Ed. Engl., 1963, 2, 633.

53. Padwa, A.; Carlson, P. H. J. "Reactive Intermediates", 2, Abramovitch, R. A. (Ed.); Plenum Press: New York, 1982; p 78.

54. a) Bruger, K.; Thenn, W.; Müller, E. Angew. Chem., Int. Ed. Engl., 1973, 12, 155.
b) Burger, K.; Einhellig, K. Chem. Ber., 1973, 106, 3421.
c) Burger, K.; Einhellig, K.; Süss, G.; Gieren, A. Angew. Chem. Int. Ed. Engl., 1973, 12, 56.

55. Padwa, A.; Rasmussen, J. K. J. Am. Chem. Soc., 1975, 97, 5912.

56. Padwa, A. Acc. Chem. Res., 1976, 9, 371.

57. Orhovats, A.; Heimgartner, H.; Schmid, H.; Heinzelmann, W. Helv. Chim. Acta, 1975, 58, 2662.

58. a) Houk, K. N.; Sims, J.; Duke, R. E.; Strozier, R. W.; George, J. K. J. Am. Chem. Soc., 1973, 95, 7301.
b) Caramella, P.; Houk, K. N. J. Am. Chem. Soc., 1976, 98, 6397.

59. Padwa, A.; Smolanoff, J. J. Chem. Soc., Chem. Commun., 1973, 342.

60. Padwa, A., Rosenthal, R.; Dent, W.; Filho, P. J. Org. Chem., 1984, 49, 3174.

61. Zupancic, J. J.; Schuster, G. B. J. Am. Chem. Soc., 1981, 103, 2423.

62. Brauer, B. E.; Grasse, P. B.; Kaufmann, K. J.; Schuster, G. B. J. Am. Chem. Soc., 1982, 104, 6814.

63. Wong, P. C.; Griller, D.; Scaiano, J. C. J. Am. Chem. Soc., 1981, 103, 5034.

64. Wong, P. C.; Griller, D.; Scaiano, J. C. J. Am. Chem. Soc., 1982, 104, 663.

65. Griller, D.; Montgomery, C. R.; Scaiano, J. C. J. Am. Chem. Soc., 1982, 104, 6813.

66. Turro, N. J.; Hrovat, D. A.; Gould, I. R.; Padwa, A.; Dent, W.; Rosenthal, R. J. Angew. Chem. Int. Ed. Engl., 1983, 22. 625.

67. Grasse, P. B.; Brauer, B. E.; Zupancic, J. J.; Kaufmann, K. J.; Schuster, G. B. J. Am. Chem. Soc., 1983, 105, 6833.

68. Kende, A. S.; Hebeisen, P.; Sanfilippo, P. J.; Toder, B. H. J. Am. Chem. Soc., 1982, 104, 4244.

69. Barcus, R. L.; Wright, B. B.; Platz, M. S.; Scaiano, J. C. Tetrahedron Lett., 1983, 24, 3955.

70. Janulis, E. P., Jr.; Wilson, S. R.; Arduengo, III., A. J. Tetrahedron Lett., 1984, 25, 405.

71. Turro, N. J.; Cha, Y.; Gould, I. R.; Padwa, A.; Gasdasha, J. R.; Tomas, M. J. Org. Chem., 1985, 50, 4415.

72. Friedrich, K.; Jansen, U.; Kirmse, W. Tetrahedron Lett., 1985, 26, 193.

73. Padwa, A. Ed.; "1,3-Dipolar Cycloaddition Chemistry", Wiley-Interscience: New York, 1984, Vol. 1 and 2.

74. Eschenmoser, A., Eidenössische Technische Hochschule, Zürich, Switzerland, private communication, 1985.

75. Kirmse, W.; Richarz, U. Chem. Ber., 1978, 111, 1883.

76. Seyferth, D.; Lambert, R. L. Jr. J. Organomet. Chem., 1975, 91, 31.

77. Warner, P. M.; Herold, R. D. Tetrahedron Lett., 1984, 25, 4897.

78. Warner, P. M.; Herold, R. D. J. Org. Chem., 1983, 48, 5411.

79. Jones, W. M.; Walbrick, J. M. J. Org. Chem., 1969, 34, 2217.

80. Warner, P. M.; Herold, R. D. Dept. of Chem., Iowa State University, unpublished results.

81 Seyferth, D.; Lambert, R. L., Jr.; Massol, M. J. Organomet. Chem., 1975, 88, 255.

82. Pearce, P. J.; Richards, D. H.; Scilly, N. F. J. Chem. Soc., Chem. Commun., 1970, 1160.

83. Newman, M. S.; Arkell, A.; Fukunaga, T. J. Am. Chem. Soc., 1960, 82, 2498.

ACKNOWLEDGEMENTS

I would like to express my sincere gratitude to Professor Philip M. Warner, without whose patience, encouragement, and guidance this thesis would not have been possible.

I am grateful to the members of the research group. Many interesting discussions and unforgettable friendships will remain in my memory. I would also like to thank Professor James H. Espenson for assisting with the analysis of kinetic data.

Special thanks are due my parents for their everlasting and unchangeable love. I am indebted to my husband Chen-Wen for his love and patient understanding. My daughter Victoria, born during the course of this work, has been a source of much pleasure, providing an exciting supplement to my graduate studies.